A HYDROGEOLOGICAL AND HYDROGEOCHEMICAL STUDY OF THE EVOLUTION OF GROUNDWATER IN A FRACTURED GRANITE, HOLYROOD NEWFOUNDLAND

NICOLAS J. SARGENT

A HYDROGEOLOGICAL AND HYDROGEOCHEMICAL STUDY OF THE EVOLUTION OF GROUNDWATER IN A FRACTURED GRANITE, HOLYROOD NEWFOUNDLAND

by

Nicolas J. Sargent

A thesis submitted to the school of Graduate
Studies in partial fulfilment of the
requirements for the degree of Master of Science

Department of Earth Sciences
Memorial University of Newfoundland
April 1994

St.John's Newfoundland

ISBN 0-612-01917-9

ABSTRACT

An extensive set of hydrogeological and geochemical data has been collected from a 150 m deep borehole in the near coastal discharge area of the Holyrood Granite, Newfoundland. Because of the selected location of the borehole, over the underlying saltwater wedge, it was possible to intersect flow paths that are believed to have extended considerably deeper within the aquifer than the depth of the borehole.

The physical data indicate that the geometric average of the hydraulic conductivity over the length of the borehole is approximately 4×10^{-9} m/s and that the open fractures, controlling most of the flow in the aquifer are approximately vertical and parallel to the coast. Fractures of this nature have been postulated by others to have resulted from isostatic post glacial rebound. The hydraulic conductivity (measured at approximately 2 m intervals along the entire length of the borehole) shows a decrease of approximately three orders of magnitude with depth. Based on the hydraulic conductivity measurements made in the study borehole, known hydraulic gradients and probable flow-path length, it is believed that water samples collected may have had residence times of the order of 1000 a.

Inspection of aqueous chemical data reveals that some parameters have a strong correlation with depth while other analytes have a strong inverse correlation with hydraulic conductivity. In general the water quality reflects the effect of low-temperature weathering of an alumino-silicate rich granite. However, the water samples collected were all relatively rich in chloride. Though there is no direct evidence of the source or sources of chloride in the study area, evidence from other granitic terrains indicate that the likely sources of chloride in the groundwater are from the rock mass (possibly from fluid inclusions) and from seawater.

Study and analysis of fracture plane mineralogy using X-ray diffraction (XRD) and scanning electron microscopy (SEM) has provided evidence for a suite of minerals which may control the groundwater chemistry. Thermodynamic speciation calculations using the water analysis data indicates minerals including calcite, amorphous silica, kaolinite, and some varieties of feldspar may be precipitating. Subsequent mass balance modelling using the groundwater analyses could not identify a groundwater evolutionary scheme that was consistent with the speciation calculations unless both a seawater source of chloride and a rock source of chloride were invoked. However, the results indicated that the percentage of seawater mixed with the groundwater decreased with depth, while the fraction of chloride added from the hypothetical rock source increased with depth. This, together with the inverse correlation of dissolved silica with hydraulic conductivity, probably reflects the increasing importance of rock-water interaction with depth, in-turn reflecting increasing aquifer residence times at increasing depths.

Oxygen and hydrogen isotope data collected during the study indicate that both isotope systems show a strong correlation with depth and both are increasingly enriched in their light isotopes with depth. The decrease in ^{18}O and ^{2}H abundance with depth is consistent with the expected differences in altitudes of recharge between the deepest groundwater samples collected (believed to have been recharged at approximately 170 m above sea level), and the shallowest groundwater samples collected (believed to have been recharged at 60 m above sea level). This evidence indicates that flow through the aquifer (although it occurs in discontinuous fractures) is, on a large scale, roughly equivalent to well ordered porous granular flow.

The interpretation of the isotope data together with the results of mass balance modelling suggests an internally consistent evolutionary scenario. It is proposed that the modelled decline of the saltwater component with depth reflects the addition of marine aerosols that provide chloride to recharging waters in quantities that decrease with increasing distance inland.

The increase in the modelled rock-derived chloride source with depth is consistent with the increasing degree of low-temperature rock-water mass exchange with increasing depth, itself resulting from increased aquifer residence time with depth.

ACKNOWLEDGEMENTS

Many people have helped me to complete this tome and my other graduate studies. Their help is sincerely appreciated. I hope that I have included all of those who provided assistance in completing analyses, provided advice or who gave a ready ear. I apologise to those I have missed and express my thanks.

The field work would have not have been completed if it had not have been for the diligence and expertise of Frank Mooney. Frank operated the drill and made the drilling enjoyable. Frank also provided assistance with other aspects of the field work. I am most grateful to him for both his help and his friendship. I thank the Jones family of Seal Cove (especially Lemont Jones) who were kind enough to make sure that I was still in the land of the living as did Wes Morgan (who was also the rig watchman) and his family while I was conducting borehole testing after the drilling was completed.

Dr.John Gale provided the drilling and field testing equipment and partial funding for the field work, Dr.John Welhan provided partial funding for the field work and subsequent analytical work. A further $6,000 disbursement from the Newfoundland and Labrador Department of the Environment, arranged by Jim Robinson, Provincial Hydrogeologist, assisted in the funding of the project. The funding is appreciated. The Province of Newfoundland and Labrador were kind enough to award me a "Special Scholarship for Students to Pursue Graduate Studies Related to Resource Development". I thank the Province for this award.

My thanks are extended to the many people who helped conduct analyses on the water samples. The ICP-MS analyses were performed by Dr.Simon Jackson and Dr.Henry Longerich and their staff. They also provided extensive advice regarding the quality of analyses. Gert Andrews performed the AA analyses. Dr. Roger

Mason provided help with the use of the Rigaku machine. Caroline Emerson provided training and assistance in the use of the SEM. Dr. Ali Aksu and Helen Gillespie provided help in interpretation of the clay minerals. Other staff within the Department helped by loaning equipment and chemicals and their efforts are appreciated.

Thanks are due to David Van Everdingen (now Dr.David), a fellow graduate student, who provided advice and friendship throughout my graduate studies. The use of a stereonet plotting program (see Chapter 2) which he co-wrote, transformed the task of plotting and interpreting over 800 fracture plane orientations from being a daunting project into a relatively easy one.

Thanks are also due to those Professors in the Faculty of Engineering who gave the many courses that were a requirement of this course. I would also like to thank the technical staff of the Engineering machine shop who fabricated (usually at short notice) many items required for the field project.

Mr.George Trainor of Newfoundland Light and Power (now Newfoundland Power) coordinated the use of the Light and Power Land where the borehole was located. The cooperation of Mr.George Trainor, and the staff of the Seal Cove Power station, helped make the field work pleasant but fortunately not electrifying. The cooperation of Newfoundland Light and Power and their employees is sincerely appreciated.

Several professors, not directly involved with my studies were kind enough to proof lengthy chapters of this thesis. I thank Dr.Peter Cawood and Dr.Toby Rivers for giving the considerable time necessary to proof and provide critical comment on Chapters 2 and 7 respectively.

This thesis would not be in its present form without the meticulous proofing of my graduate advisor Dr.John Welhan, now of Idaho State University. John also provided considerable personal support at some fairly rough times during the graduate process. He has also managed to imbue me with a sense of how science is done. I cannot satisfactorily express my appreciation of his efforts, especially as much of the proof reading was conducted after he had left Memorial and was busy starting a new position at Idaho State University.

Dr.Peter Howard, now of the University of Regina, was a friend with knowledge of the machinations of the University and his friendship and advice was invaluable.

Finally most people will not realise that my wife Wendy has been an equal partner in the completion of this project and has shared in both the highs and the lows of the graduate course. Wendy provided support, love and friendship through a tough process. Our children, Aiden, Chloe and Timo have also been affected by my graduate studies and I thank them for suffering a sometimes cranky Dad.

TABLE OF CONTENTS

CHAPTER 1: INTRODUCTION 1

1.1 BACKGROUND 1

1.2 OBJECTIVE AND SCOPE 9
1.2.1 Objective 9
1.2.2 Approach 10
1.2.3 Scope 12

1.3 PHYSICAL SETTING 12
1.3.1 Geology 12
1.3.2 Hydrogeology 20

1.4 STUDY SITE 23

1.5 CONCLUSIONS 26

2.1 INTRODUCTION 27

2.2 GEOLOGICAL DESCRIPTION OF THE CORE 27
2.2.1 Method 27
2.2.2 Core Description 28
2.2.3 Fracture Minerals Logged 30

2.3 DESCRIPTION OF FRACTURE ORIENTATIONS 32
2.3.1 Method 32
2.3.2 Method of Interpretation of Fracture Data 37

2.4 FRACTURE DATA PRESENTATION 43
2.4.1 Fractures Differentiated by Depth Intervals 43
2.4.2 Fracture Differentiated by Fill Material 46
2.4.3 Fractures Differentiated by Rock Type 53
2.4.4 Fracture Orientations in intervals sampled for groundwater 62

2.5 CONCLUSIONS AND INTERPRETATIONS 67

CHAPTER 3: HYDRAULIC CONDUCTIVITY TESTING 70

3.1 INTRODUCTION 70

3.2 METHODS OF HYDRAULIC CONDUCTIVITY AND HEAD TESTING 70
3.2.1 Description of the Straddle Packer Tool 70
3.2.2 Hydrostatic Head measurements 71
3.2.3 Falling (or rising) head test 73
3.2.4 Constant head tests 79
3.2.5 Falling head test while measuring the test cavity pressure 83
3.2.6 Comparison of Hydraulic Conductivity Testing methods 84

3.3 OVERVIEW OF HYDRAULIC CONDUCTIVITY AND HEAD MEASUREMENT RESULTS 84

3.4 CONCLUSIONS 90

CHAPTER 4: GEOCHEMICAL METHODS AND DATA QUALITY 93

4.1 DATA COLLECTED 93
4.1.1 Sampling methods 93
4.1.2 Analytical Methods 97
4.1.3 Quality of non isotope analyses 98
4.1.4 Quality of Isotope analyses 111
4.1.5 Quality of pH and Eh measurements 113
4.1.6 Efficacy of sample interval flushing 115

4.2 CONCLUSIONS 119

CHAPTER 5: GEOCHEMICAL TRENDS AT NSCRV 121

5.1 OVERVIEW OF WATERS AT NSCRV 121
5.1.1 Variations of single chemical parameters with depth and permeability. 121
5.1.2 Description of variations of bulk groundwater chemistry with depth: Piper 124
5.1.3 Description of variations of groundwater chemistry with depth: Mineral stability diagrams. 127

5.2 CONCLUSIONS 132

CHAPTER 6: INTERPRETATION OF AQUEOUS ISOTOPE DATA 134

6.1 DISCUSSION 134

6.2 CONCLUSIONS 142

CHAPTER 7: ANALYSIS OF FRACTURE MINERALOGY 143

7.1 ANALYSIS OF FRACTURE MINERALOGY 143

7.2 SAMPLE COLLECTION AND ANALYSIS 144
7.2.1 Analysis of Fracture flakes by SEM 144
7.2.2 Analysis of Fracture Minerals by XRD. 145

7.3 METHODS OF DATA INTERPRETATION 145
7.3.1 Interpretation of SEM/EDM data. 145
7.3.2 Method of Interpreting XRD data 148

7.4 RESULTS 148

7.5 ELEMENTS IDENTIFIED. 163

7.6 CONCLUSIONS 168

CHAPTER 8: HYDROGEOCHEMICAL MODELLING 170

8.1 INTRODUCTION 170

8.2 DATA AND THERMODYNAMIC DATABASE QUALITY 174
8.2.1 Groundwater Data Quality 174
8.2.2 Thermodynamic Data 176

8.3 HYDROGEOCHEMICAL MODELLING 180
8.3.1 Speciation Calculations 180
8.3.2 Mass Balance calculations 186

8.4 TEST OF MASS BALANCE MIXING HYPOTHESIS USING OXYGEN AND HYDROGEN ISOTOPE DATA 192

8.5 TEST OF GEOCHEMICAL MODELLING RESULTS USING CHLORIDE DATA 196
8.5.1 Discussion 203

8.6 CONCLUSIONS 206

CHAPTER 9: CONCLUSIONS & INTERPRETATIONS 207

9.1 SUMMARY OF RESULTS 207

9.2 FUTURE WORK 211

LIST OF FIGURES

Figure 1.1 Location Map 11
Figure 1.2 Local Geological Setting 14
Figure 1.3 Flow net of the Holyrood Aquifer 24
Figure 2.1 Synopsis of Core Log 29
Figure 2.2 Core orientation device 34
Figure 2.3 Angles measured to orientate planar features 36
Figure 2.4 Blind zone and borehole orientation 40
Figure 2.5 Number of open fractures per metre 42
Figure 2.6 Pole plots of fracture orientations; depth differentiated 44
Figure 2.7 Pole plots of fracture orientations; mineral differentiated 47
Figure 2.8 Pole plots of fracture orientations; rock type differentiated 54
Figure 2.9 Pole plots of fracture orientations in andesite, mineral differentiated. 56
Figure 2.10 Pole plots of fracture orientations in green granite (mineral differentiated) 59
Figure 2.11 Pole plots of fracture orientations in pink-granite (mineral differentiated) 61
Figure 2.12 Poles to all open fractures sampled 63
Figure 2.13 Poles to open fractures in sample intervals 64
Figure 3.1 Hydraulic conductivity testing configuration 72
Figure 3.2 Formation pressure build-up curves from selected test intervals 74
Figure 3.3 Comparison of result of calculating formation head from constant head test information, or deriving it from shut in tests 82
Figure 3.4 Comparison of results of differing conductivity testing methods 85
Figure 3.5 Summary of hydraulic data from NSCRV 88
Figure 3.6 Line fit to hydraulic Conductivity 89
Figure 3.7 Fractures logged as open versus interval flux 91
Figure 4.1 ICP-MS vs AA analyses 101
Figure 4.2 ICP-MS vs HPLC analyses 103
Figure 4.3 Variations in pH with sample interval flushing 114
Figure 4.4 Effects of sample interval flushing on specific element concentrations 116
Figure 5.1 Correlation of analyte concentrations with both depth and log hydraulic conductivity 123
Figure 5.2 Piper diagram showing analytical results from NSCRV 126
Figure 5.3 Mineral stability diagrams constructed for comparison of thermodynamic data 128
Figure 5.4 Stability diagrams for the NSCRV waters sampled 130
Figure 6.1 Isotope Data for NSCRV plotted against MWL 135
Figure 6.2 Evapotranspiration diagram for Seal Cove 139

Figure 7.1a ED spectrum for calcite from 53.97 m 153
Figure 7.1b XRD spectrum of calcite from 72.48 m 154
Figure 7.2 SEM photograph of Chlorite from 147.31 m (NSCRV 7lge) 155
Figure 7.3 SEM photograph of Dickite from 136.53 m (NSCRV 16A) 159
Figure 7.4 XRD trace for Montmorillonite/Saponite from 148.31 m 162
Figure 7.5a) ED spectrum of quartz from 71.80 m (NSCRV 14lge) 164
Figure 7.5b) XRD trace of quartz from 139.69 m 165
Figure 7.6 SEM photograph of Octahedral crystal, high in iron, from 29.48 m (NSCRV 5A) 167
Figure 8.1 Modelled fractions of chloride concentrations versus physical parameters 200

LIST OF TABLES

Table 2.1 Synopsis of fracture orientation data 39
Table 2.2 Synopsis of mineral differentiated fracture orientation data 50
Table 3.1 Composite table detailing hydraulic conductivity results 76
Table 4.1 Relative analytical errors estimated by comparing different methods of analysis 105
Table 4.2 Compilation showing the average relative differences and the 95% confidence interval (2σ) for the analysis, by ICP-MS, of 20 different elements, at a variety of concentrations in USGS water standards. 106
Table 4.3 Results of all laboratory ^{18}O analyses 112
Table 4.4. $\delta^{18}O$ values selected as being representative of virgin formation water at NSCRV 119
Table 5.1 Results of statistical test to determine the statistical significance of the correlation of hydraulic conductivity or depth with concentration of an element 122
Table 6.1 Synopsis of Weather data at NSCRV. 138
Table 7.1 Table showing minerals identified by microprobe and XRD 150
Table 7.2 Selection criteria for minerals analyzed by electron microprobe 152
Table 7.3 Selected chlorite compositions, calculated from ED microprobe data 156
Table 7.4 Selected calculated Halloysite compositions 158
Table 7.5 Selected calculated Illite compositions 161
Table 8.1 Comparison of Geochemical Modelling Codes 179
Table 8.2 Minerals approaching saturation derived from speciation calculations 181
Table 8.3 Selected Results of Mass Balance Modelling 188
Table 8.4 Hypothetical mixing of end members of differing isotopic compositions 195
Table 8.5 Results of calculating contributions of end members to chloride budget 201

APPENDICES

APPENDIX A	Core Log
APPENDIX B	Fracture Data
APPENDIX C	Geochemical Analyses
APPENDIX D	Thermodynamic Data Base Review
APPENDIX E	HELGTHEM thermodynamic Data Base Used with PHREEQE
APPENDIX F	Results of Mass Balance Calculations
APPENDIX G	Method of Mass Balance Calculation

CHAPTER 1: INTRODUCTION

1.1 BACKGROUND

The flow processes occurring in fractured crystalline media are distinctly different from those found in porous intergranular media. The hydrogeochemistry of groundwater in fractured crystalline rocks is dominated by the processes occurring during flow and transport through a virtually impermeable rock mass whose porosity is likely to be dominantly intergranular or microcrystalline, but in which a relatively few fractures act as principal flow pathways.

From point of recharge to point of discharge water in an 'intergranular' aquifer (i.e. an aquifer with only intergranular porosity as opposed to water in a fractured aquifer, having intergranular and fracture porosity) normally displays relatively gradual changes in its physical and hydrogeochemical properties. The chemical composition reflects an increasing aquifer residence time with increasing distance from the recharge point. The progressive change in chemical properties seen in the waters of non-fractured porous aquifers is a consequence of the necessity of any discrete packet of water, at a point within the aquifer, having had to arrive there by passage through the intergranular pore spaces, along tortuous pathways. The travel of water via intergranular pathways ensures a progressive increase in the degree of rock-water interaction, at successive points along a flow path. Fractured crystalline aquifers, on the other hand, apparently do not confine a packet of water to move only via intergranular (or intercrystalline) pathways. A fractured crystalline medium is comprised of:

a) a crystalline rock mass, usually of extremely low hydraulic conductivity material with values reported from 10^{-13} to 10^{-16} m/s by Nordstrom et al. (1985) for the Stripa Granite. Though relatively unconductive the crystalline rock mass will still have porosity, resulting from blind fractures, microcracks and intercrystal cracks and voids,

b) an interconnected web of fractures which are the main conduits for groundwater flow through the rock-mass. The average hydraulic conductivity of the bulk fractured rock-mass is orders of magnitude higher than that of the crystalline media. However, the principal flow paths, provided by the interconnected fractures, only account for a fraction of a percent of the total porosity of the rock-mass.

Norton and Knapp (1977) defined three different types of porosity in fractured media; flow porosity (interconnected fractures), diffusional porosity (such as voids and micro-cracks, between crystals, and fluid inclusions), and the residual porosity comprised of blind fractures and other unconnected voids. The velocity of groundwater through the fractured media is many orders of magnitude higher in the flow porosity, where crack widths range from 10 to 1000 μm (Neretnieks 1980) and through which solutes travel principally by advection. Solutes in the diffusion porosity can only diffuse through an essentially static solvent phase (Gascoyne et al. 1987), in cracks ranging from 0.01 to 10 μm (Neretnieks 1980). As a result of the increased rock-water interaction resulting from long residence times in the diffusion porosity, the concentrations of solutes in the micro-crack fluids will be many times greater than the concentration of solutes in the fluids of the flow porosity.

Knapp (1975) estimated that a fractured crystalline rock-mass has as little as 1-2% porosity of which ~1% is flow porosity (or effective porosity), ~5% is diffusion porosity and 94% is residual porosity. For the Stripa Granite Nordstrom et al. (1985) determined the total porosity averaged 0.46% with flow porosity in the order of 10^{-5} to 10^{-4} or 2 to 20 ‰ of the total porosity.

The overall hydraulic nature of the fractured crystalline rock-mass is controlled by the geometry of the fracture network. Above a certain minimum volume of the rock-mass (known as the representative elementary volume or REV), the average hydraulic conductivity of the total volume will be relatively uniform. At volumes below the REV the hydraulic conductivity fluctuations calculated for successively smaller volumes will vary over orders of magnitude. The variations will be damped considerably as the REV is approached. The concept of REV is used widely (i.e. Cacas et al. 1990). When modelling flow through a fractured aquifer the scale of the aquifer (as opposed to the REV) may justify approximating the real system with an equivalent porous media.

Because of the dual nature of porosity in fractured crystalline media, a sample of water and solute mass, collected at a point within the fractured crystalline aquifer is in fact the result of the mixing of two fractions:

i) The fracture component derived from water, and its dissolved solutes, flowing along fractures within the flow porosity and;

ii)The intercrystalline component, derived from water and its dissolved solutes which is contained in intercrystalline spaces (diffusional porosity).

The mixing of these components would be expected to occur locally in the crystalline media and the fractures, but would also be expected to occur during sample collection from any discrete volume of aquifer which contained both flow and diffusional porosity.

In the shallow parts of a fractured aquifer (where the fracture apertures and the fracture permeability tend to be large) the fracture component of water mass in a fluid sample will be many times larger than the intercrystalline component in the sample with the intercrystalline component an insignificant contributor to the mass of water collected. However, the **solute** mass contributed by the intercrystalline fluids, will be disproportionately large. Conversely the fracture component of the solute mass will be a much less significant contributor to the total solute mass of the sample collected. Furthermore, it can be theorised that the relative proportions of solute contributed by the fracture and intergranular components will change with depth since fracture porosity is a function of depth. At some depth the proportions of solute and solvent contributed to the volume by the flow and diffusional porosity will be in the same proportions as the intergranular to fracture space. At this point the fracture system would be indiscernible from the intergranular microcracks. This may be considered to be a boundary condition.

The manner in which minerals dissolve has been extensively studied. From this information the expected chemical evolution of water in contact with some selected minerals has been deduced. Feldspars are significant contributors to the solvent load of groundwaters and a large amount of effort has been expended in the study of their dissolution mechanisms. Quartz and the micas are relatively poor contributors to the total dissolved solids (TDS) in groundwaters; the dark micas and amphiboles are thought to be major contributors of chlorine (Edmunds et al. 1984, 1985; Kamineni, 1987).

Rates for feldspar leaching have been calculated by Busenberg and Clemency (1976). A mathematical model was proposed by Paces (1973) for the solution process. Both solution models postulated the formation of a thin (<50 μm) surface layer on the feldspars, the subsequent equilibrium of which was proposed as acting as a rate controlling step in the dissolution of the feldspars. The surface layer was cited as a cause for the initial parabolic dissolution rate of the feldspars, wherein solute is released at a rate proportional to the square root of time.

Holdren and Berner (1979), after exhaustive scanning electron microscope work, questioned the presence of the rate controlling layer and possibly the parabolic step believing it to be an artifact of mineral preparation. Nevertheless they generally agreed with the solution rates determined by Busenberg and Clemency (1976) for the linear phase of feldspar dissolution. The linear phase accounts for the bulk of the dissolution process, with the exception of the first few months. Helgeson (1968) has studied mineral solution from the perspectives of both mass balance and thermodynamic principles, with a view to describing evolutionary pathways for solutions in contact with mineral assemblages. Using this approach Helgeson (1969) developed activity diagrams for the system:

$K_2O-Al_2O_5-SiO_2-H_2O$

at 25°C (Gibbsite-Kaolinite-K-Feldspar-Mica) and pathways of evolution for dissolving either or both of K-Feldspar and Albite. The work of Helgeson corroborated the mass balance calculations of Garrels and MacKenzie (1967) who derived the same information for the Sierra Nevada granites.

Several groups have published results and interpretations of observed hydrogeochemistry in granite terrains. However, a satisfactory source for the salinity (halides) of the groundwater has still not been found. Edmunds et al. (1984, 1985) attributed the salinity in the groundwaters of the Carnmellis Granite to chloride produced from the weathering of biotite micas. Nordstrom et al. (1985) proposed that the salinity observed in the Stripa Granite (Sweden) could have been entirely derived from gradual leaching and leaking of fluid inclusions in the granite. However this theory has been refuted by Fontes et al. (1989) on the grounds both of lack of mass balance for the system, and the simplifying assumptions made by Nordstrom et al. (1985) Frape et al. (1984), working on the Canadian Shield, admit that a satisfactory source of salinity in the highly saline deep groundwaters of the shield has yet to be found; however they cite remnant Palaeozoic marine transgressions and remnant, highly saline, Permian connate waters derived from evaporites as possible sources of salinity.

The interpretation of groundwater evolution through geochemical modelling requires a variety of input data such as rock mineralogy, fracture minerals in contact with the flow system, groundwater chemistry, and the composition of end-members (which may mix) in the system. A valid thermodynamic data base for both the dissolved and the solid components is also needed. How the data are used depends on the approach to modelling.

In the inverse approach (Plummer, 1984), a non-thermodynamic mass balance is computed for the observed changes in groundwater chemistry. The mass balance approach can allow for precipitation or dissolution of minerals likely to be available in the flow system; it can also be used to model mixing of end-members, or to apply redox and isotopic constraints to the reactions. The results of these mass balance calculations may or may not be thermodynamically plausible and they must be checked for thermodynamic validity or compared with the calculated saturation states of the minerals of interest in the groundwater. An alternate approach is to model the forward problem and attempt to mimic the known groundwater composition (or predict an unknown groundwater composition) by theoretical addition (or removal) of species to the groundwater. The groundwater modelling process is described by Plummer et al. (1983) and Plummer (1984). The latter paper notes the problems of geochemical modelling in fractured systems which may result from an inability to model the rapid mixing of geochemically different waters.

1.2 OBJECTIVE AND SCOPE

Recent work in the Holyrood Aquifer has included a study of the relationship between stream-flow and groundwater flow by Schillereff (1991) and some limited interpretation of part of the data of this study by Button (1990).

1.2.1 Objective

As a continuation of the groundwater studies in the Holyrood Granite a project was devised which would allow a detailed hydrogeological investigation in a deep borehole in the discharge area of the Holyrood Aquifer. The detailed investigation was to provide an extensive set of physical-hydrogeological and geochemical data including:

i) punctual hydraulic conductivities (i.e those from intervals of approximately 2 m over the entire borehole length),

ii) a full core which was to provide information regarding fracture orientations and nature of minerals deposited in the fractures,

iii) the chemical and isotopic nature of the groundwater at different intervals in the borehole, to be determined by extensive sampling of intervals having higher hydraulic conductivities.

This data was used to develop a consistent hydrogeological/ hydrogeochemical model of processes in the Holyrood Aquifer.

It was hoped that a location would be selected which would provide artesian conditions throughout its length so that groundwater samples could be collected under optimum conditions with a minimum amount of degassing or other chemical changes.

1.2.2 Approach

The study requirements were met by the coring and detailed logging of fractures in a 150 m (drilled depth) hole, located in the north of the Seal Cove River Valley, at a site which will be referred to as NSCRV (Figure 1.1). After completing coring the hole was extensively packer tested to determine hydraulic conductivities over its length and to collect groundwater samples for analysis of the inorganic and the isotopic composition of the water. The location was selected, after preliminary numerical groundwater flow modelling, to maximise the possibility of intersecting artesian groundwater flow conditions.

Figure 1.1 Location Map

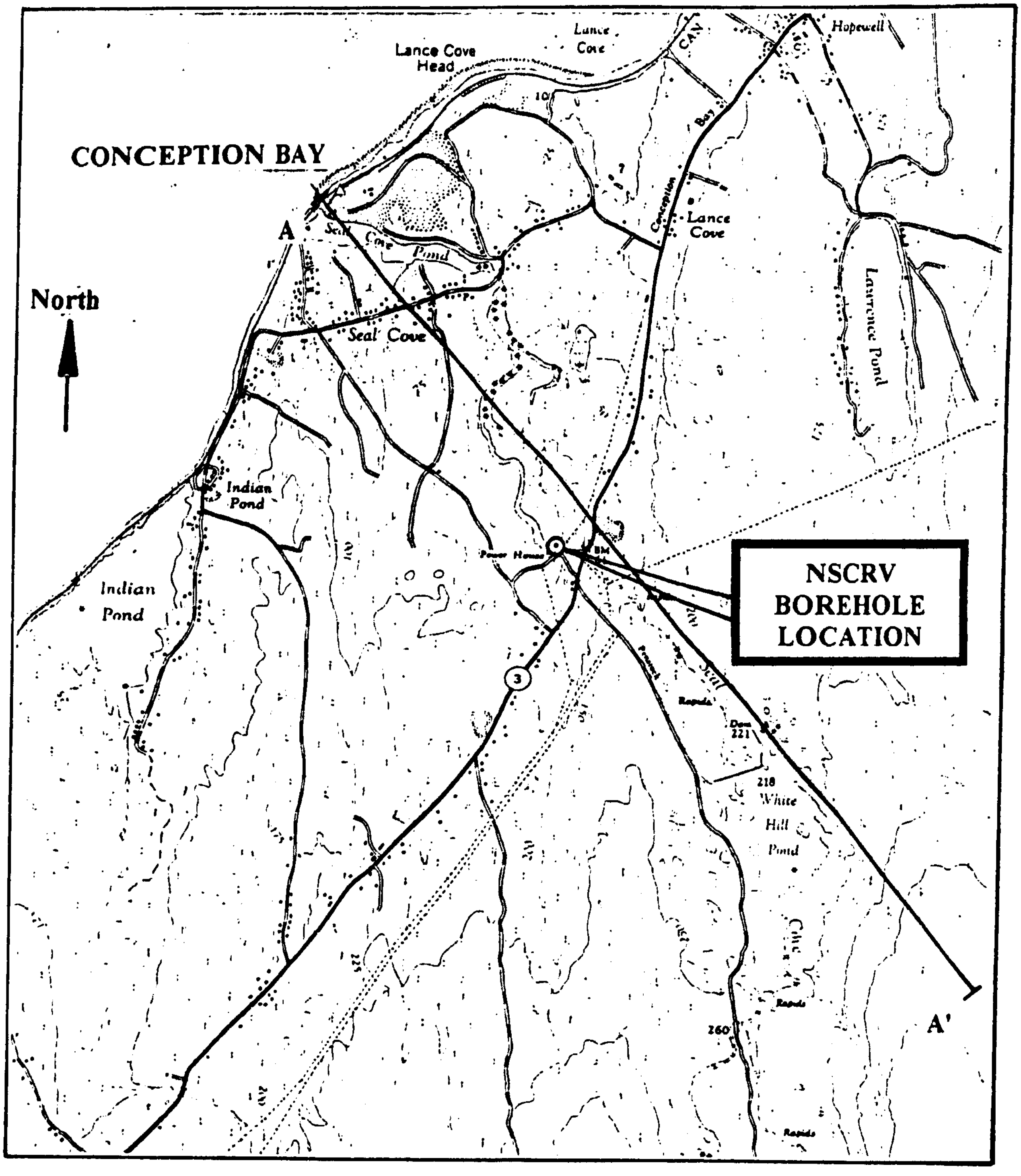

From 1963 Imperial 1:25,000 Map,"SEAL COVE" 1N/6h

1.2.3 Scope

By limited flow modelling and extensive hydrogeochemical modelling the following study attempts to integrate the data collected at NSCRV in terms of the flow paths, geochemical evolution of the groundwater in the Holyrood Granite, the probable source of solute and solvent, the nature of minerals likely to be precipitated from the groundwater, and the influence of the mineral composition, hydraulic nature and fracture mineralogy of the granite, on the hydrogeochemistry.

1.3 PHYSICAL SETTING

1.3.1 Geology

The study area lies in the Avalon Zone which is the most easterly tectonostratigraphic unit of the Appalachians, described by Williams et al. (1974). The Avalon Zone runs south, and is approximately coincidental with the eastern seaboard of the United States. It is typified by a sequence of late Proterozoic volcanic and associated sedimentary rocks. This sequence is overlain by shallow-water terrestrial sedimentary rocks of mid Palaeozoic age (Taylor et al. 1979). The sequence is everywhere found intruded by plutonic rocks ranging in age from Proterozoic to Carboniferous. In the study area the plutonic rocks are represented by the Pre-Cambrian Holyrood Plutonic series. The timing of emplacement of the granite, its mode of emplacement and the geological setting during emplacement have been the source of considerable debate in the literature, as has the probable age of the Holyrood Granite.

All major structural features in the area (faulting and fold axes) trend approximately north-northeast to south-southwest, and the Holyrood Granite is itself somewhat elongated in the main structural direction.

The local geological setting of the study area is shown in Figure 1.2, after King (1990). The Holyrood Granite is bounded on its eastern margin by the Topsail Fault, believed by Hughes (1971) and Hughes and Bruckner (1971) to have resulted from explosive emplacement of the granite, probably at levels as shallow as 2000 m, with subsequent caldera subsidence in an (compressional) island arc setting. Strong and Minatidis (1975) concur with Hughes and Bruckner on the level of emplacement of the granite but believe (from petrographic and relational evidence) that the area represents a tensional, basin-and-range rift setting as the petrochemistry of the Holyrood Plutonic Series closely matches that found in rocks of the Sierra Nevada which are believed to represent a continental rift environment (Strong and Minatidis, 1975).

The granite is bounded on its western side by the volcanics and pyroclastics of the Harbour Main Group. These Pre-Cambrian volcanics are in

Figure 1.2 Local Geological Setting

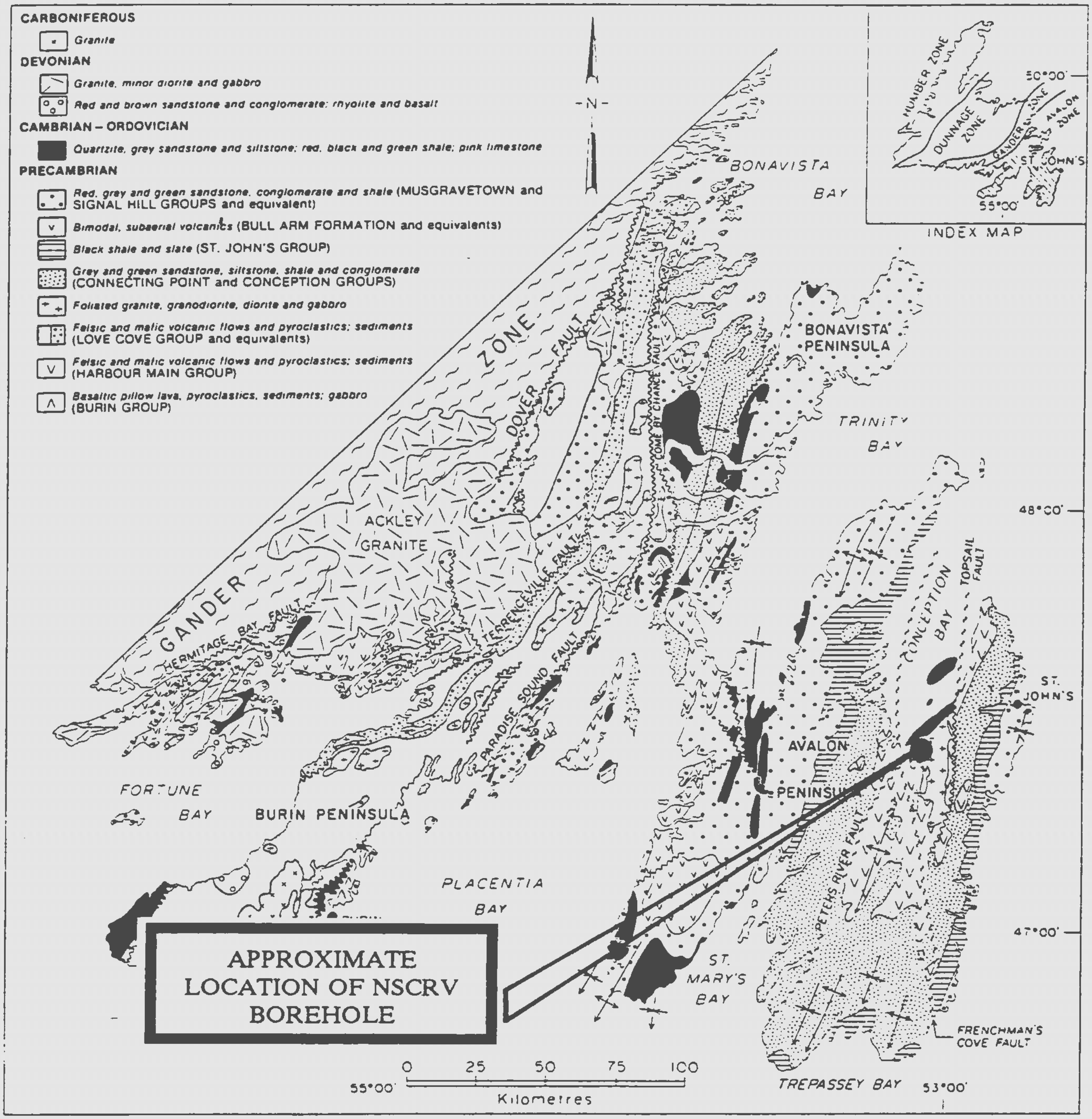

after King and O'Brien in press (from King 1990) faulted contact with Cambrian volcanics of the Adeyton Group, along a northerly extension of the Peter's River Fault, on the west side of the study area. The fault bounded block was originally referred to as the Holyrood Horst by McCartney (1969). Harbour Main volcanics have not been mapped in the immediate vicinity of the NSCRV borehole, but are found to the east along the Topsail Fault and also to the north of NSCRV.

The Harbour Main Group has been divided into three members, divided by faults (see King, 1990 for a synopsis of the faulted divisions comprising the Harbour Main Group). The divisions are:

i) The western block, (west of the Holyrood Horst) which includes the type locality of Avondale-Harbour Main, characterised by red, pink, and grey ignimbrites, locally intercalated with fluvial volcanogenic sedimentary rocks, and overlain by terrestrial, fissure-type flows of dark green to purplish, massive and amygdaloidal basalt (McCartney, 1967), previously described as green andesites by Hutchinson (1953).

ii) The central block (west of the Topsail Fault) includes felsic and mafic flows, pyroclastics and minor volcaniclastics. These volcanics are intruded by high-level granite, quartz monzonite, and granodiorite of the Holyrood Intrusive Suite. NSCRV lies in the central block.

iii) Volcanic and volcaniclastic rocks, dominated by pillow lavas and volcaniclastics, are found east of the Topsail Fault

Though the Harbour Main volcanics seen at NSCRV lay in the central block, they are believed to be representative of the western block unit of the Harbour Main volcanics. The andesite at the NSCRV location was apparently agmatitic in nature (Sederholm, 1967). Agmatite blocks of the green andesite, in the Holyrood Granite, are also to be found in the floor of the Kelligrews River Swimming Pool. These volcanics would appear to be members of the western block.

In the study area, and to the north of the NSCRV borehole location, the Holyrood Granite is unconformably overlain by sediments, predominantly shales and slates of the Conception Group which dip gently (approximately 10°) towards the ocean. A discontinuous basal conglomerate is identified in some areas (notably the bridge across the Manuels River on the Conception Bay highway) though it appears to be absent at the NSCRV location. Contours on the granite/ Lower Cambrian contact appear to reveal an undulating surface with the amplitude increasing and the wavelength decreasing along the contact surface from southwest to northeast. The axes of the undulations trend approximately down dip and are normal to the strike of the contact. The supposed geometry of the contact surface should, however, be viewed with some scepticism as the Pre- Cambrian/ Cambrian contact is poorly defined, due to sparse outcrop. Attempts by the author to map the contact in greater detail were unsuccessful (again due to lack of outcrop). However, the mapping did seem to confirm the undulating nature of the contact surface. The undulations are possibly a manifestation of a Pre- Cambrian/ Cambrian drainage system or Pre-Cambrian glaciation, the latter recently noted by Grant (1989) but, as noted by Grant, first mooted by Lawson (1890).

The Holyrood Plutonic series has been extensively described and classified. It was first divided into three members by McCartney (1967). It is comprised of:

i) Holyrood Granite: pale pink coarse grained and equigranular with minor aplite veining, composed of 35 to 45% quartz, 33 to 39% orthoclase, 10 to 18% plagioclase, and 4 to 6% chlorite as a pseudomorph of biotite. The granite is altered, with chlorite and epidote replacing biotite. Feldspars are cloudy, a result of sericite.

ii) Quartz Monzonite; of quartz monzonite and quartz diorite, mottled pink and green in colour, with less quartz than the Holyrood Granite, but with an increase in abundance of saussirized plagioclase.

iii) Gabbro; closely associated with the granite and quartz monzonite. It occurs only sporadically and varies from fine to medium grained. It is principally composed of hornblende and labradorite.

In the vicinity of NSCRV and in the NSCRV core itself, only the granite and the quartz monzonite members of the Holyrood Plutonic Series were identified. In this study they retain their field classifications of pink granite (Holyrood Granite) and green granite (Quartz Monzonite). No gabbro was recovered at NSCRV nor is it found in the immediate study area. The granite is not in the metallogenically specialized group of granites (Taylor et al. 1979). The only mineral deposit of interest occurring in the granite is a pyrophyllite, associated with late stage pneumatolytic activity of the granite. An active pyrophyllite mine occurs southwest of NSCRV, in the sheared region of the Topsail Fault.

On the basis of petrochemistry Strong and Minatidis (1975) have concluded that the Harbour Main volcanics and the Holyrood Plutonics are not comagmatic.

Their age is believed to be in the vicinity of 620 Ma (Krogh 1983); however, there remains considerable debate regarding this point.

The Quaternary geology of the area is as relevant to this study as the bedrock geology: Based on work presented in this study the Holyrood Granite is estimated to have an average hydraulic conductivity of 4.74 x 10^{-9} m/s, a flow porosity in the range of 2 to 20‰ and an estimated average hydraulic gradient of 0.03. Given the distance from the nearest groundwater divide to NSCRV of 3.5 km, and a flow path length of approximately 4.5 km, then the average retention time of groundwater in the granite is estimated to be 1560 a, with a possible range of from 156 to 15600 a (±an order of magnitude). Thus it is conceivable that the events of the Quaternary (from late Wisconsinan to Holocene) such as sea level and climate changes, and glaciation might have influenced the present groundwater quality in the Holyrood Granite. It is conceivable that the effects of Quaternary events may still be retained in the groundwater geochemistry.

Grant (1989) provides a synopsis of Quaternary events in the Atlantic provinces. These events shaped the contemporary landscape, though the genesis of many of the topographic features may date back to the Proterozoic (Bruckner 1979). The Atlantic region was glaciated during the Quaternary and three major ice centres were believed to have been developed in Newfoundland, with one centred on the

Avalon Peninsula. The glacial events have resulted in Quaternary glacial deposits, of varying thickness and coverage, over most of the island. Glacial tills sporadically blanket the bedrock of the study area.

Of three Quaternary glacial events, the final one culminated in a Late Wisconsinan stadial maximum between 13 and 11 ka. Climate warming occurred approximately 11 ka (MacPherson 1982). Associated with these glacial events were significant sea level changes. Henderson (1972) identified an intertidal platform at ~3-10 m above present sea level, on the Avalon, which is also identified in the head of Conception Bay. There is no record for the Avalon of Quaternary marine incursions higher than this level.

1.3.2 Hydrogeology

The area of the Holyrood Granite can be divided into three broad hydrostratigraphic units

i) A Surficial Hydrostratigraphic unit comprised of bogs and intermittent thin (probably 1-4 m) glacial tills,

ii) A Bedrock Hydrostratigraphic unit comprised of the fractured bedrock of the Holyrood Plutonic series and,

iii) the siliclastic rocks of the Conception Group.

There is probably some difference in the hydraulic properties of the Holyrood Plutonic Series and the Conception Group. These differences, however, are unlikely to be as great as the differences between the bedrock units and the surficial deposits.

In the surficial deposits groundwater flow will chiefly be controlled by intergranular movement of groundwater. In the bedrock units all significant flow will be controlled by movement along fractures. It is unlikely, given the age of the bedrock sedimentary deposits, that they have any significant amounts of intergranular porosity remaining. Likewise intercrystalline porosity in the Holyrood Plutonics is likely to be insignificant as far as large scale movement of water is concerned.

The true nature of the Holyrood Aquifer is not known. It can be hypothesised that, even with the thin cover of glacial and bog material, the aquifer is essentially unconfined. The various bogs, lakes and streams indicate the elevation of the water table and can be used to estimate regional hydraulic gradients in the aquifer which are believed to be in the range 0.02-0.03. Flow boundaries in the aquifer will be represented by the topographic divide at the head of the Seal Cove River Valley, the saltwater freshwater interface near the coast and some depth where the fractures become closed and hydraulic conductivity is reduced to essentially zero.

The hydraulic conductivity in the glacial materials is likely to be extremely variable but on a large scale is probably quite consistent with little significant variation in hydraulic conductivity with depth. Conversely the bedrock aquifer is likely to have relatively high hydraulic conductivities near surface (associated with a high degree of open fractures) and decreasing hydraulic conductivity with depth as open fractures gradually close as a result of overburden pressure.

The geochemical evolution of the groundwater as it flows through the aquifer will be strongly influenced by contact with the surficial and the bedrock hydrostratigraphic units. While flowing through the surficial units meteoric water with a P_{co2} of $10^{-3.5}$ and pH of about 5.7, is likely to show a sharp increase in P_{co2}, by as much as an order of magnitude. The change in P_{co2} will primarily be a result of contact with decaying organic matter. The increase in P_{co2} will result in a large reduction in pH. The changes in pH will make the meteoric water more aggressive and better able to dissolve rock material. The solution of rock material will start in the rock debris of the glacial tills and continue in the bedrock units. Associated with the solution of rock material will be a change to a basic pH and an increase in total dissolved solids.

In order that flow paths within the aquifer could be more readily understood a simple two dimensional flow net was constructed, using the finite difference method. The boundaries used are partially described above, the saltwater interface was estimated using the Ghyben-Herzberg method (see Freeze and Cherry, 1979) and a no flow boundary was arbitrarily placed horizontally at 1000 m below sea-level. The elevation of the free water surface above sea level was estimated along AA' (Figure 1.1) from surface water bodies, rivers, streams and bogs. The grid for the finite difference model had a 250 m spacing. Head values for points not falling on the grid were estimated using the method of Hunt (1983). The method of finite difference flow net construction is described in Freeze and Cherry (1979). All calculations and matrix inversions were performed using the features of Lotus 1-2-3 spreadsheet. The flow net is shown in Figure 1.3 and is provided to give the reader an idea of probable flow patterns in the aquifer. It should be noted that the model is uncalibrated and is used as a simple screening tool. It proved useful for selecting the borehole location.

1.4 STUDY SITE

The location selected for the drilling of the study borehole is in the Seal Cove River Valley, north of the Conception Bay Highway, and is referred to as the North Seal Cove River Valley Location (NSCRV). The location lies approximately

Figure 1.3 Flow net of the Holyrood Aquifer

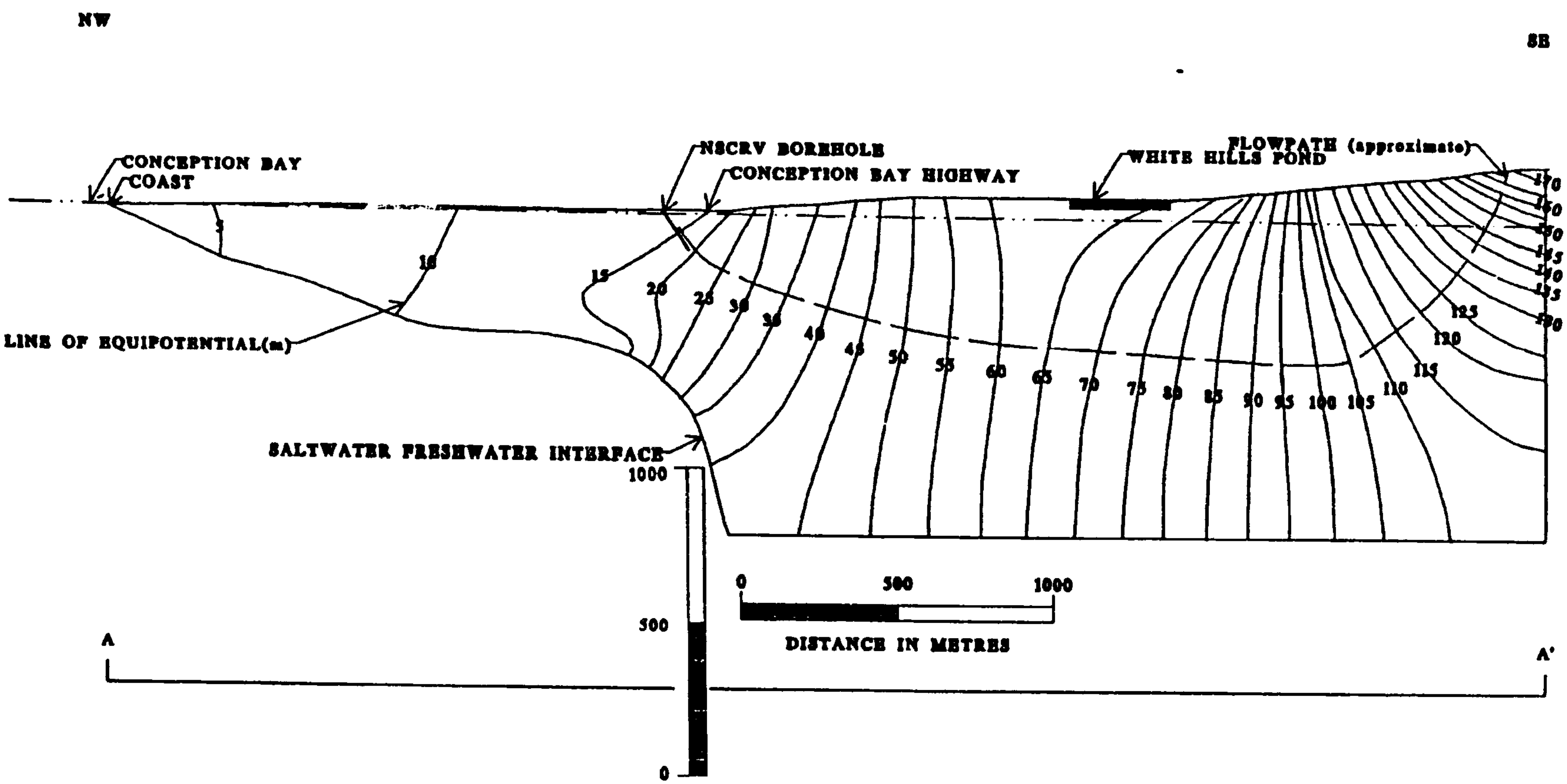

50 m east of the Newfoundland Power Seal Cove Power Station, at an elevation of about 12 m, a few metres east of a tributary of the Seal Cove River distributary.

All the outcrop mapped in the area is either Pre-Cambrian Harbour Main Volcanics or Holyrood Granite. No Basal Conglomerates or Lower Cambrian sediments were identified in the area. At the coastline no outcrop occurs in the Seal Cove Valley distributary. Sand and Gravel, often interspersed with large boulders,is being extracted along the coast at Seal Cove. Some of the gravel pits are an estimated 15 m below sea level, with no sign of bedrock. It appears that all the Pre-Cambrian and Cambrian sediments have been eroded by Pleistocene glaciation.

Bedrock is exposed in the Seal Cove River Valley, but generally at elevations greater than 19 m above sea level south of the highway, or at slightly lower elevations adjacent to the highway on its north side. A very small knob of possible outcrop (determined by matching fracture patterns) occurs about 50 m northeast of the power house at an elevation of approximately 10 m. The site selected was located as near to the knob of rock as possible. The borehole orientation was selected to maximise the possibility of intersecting successively older flow lines, based on the flow model.

1.5 CONCLUSIONS

For its intended purpose the hydrogeological setting of the NSCRV location is apparently ideal. Figure 1.3 indicates the strong possibility of upward gradients at the site, in part an effect of the wedging of freshwater over saltwater. The potential to intersect upward hydraulic gradients was an important consideration in site selection as the design of water sampling was predicated on artesian conditions bringing groundwater to surface; furthermore, the upward flexing of deep flow-lines provides the possibility of sampling waters that had evolved at greater depths than the total depth of the borehole.

CHAPTER 2: BOREHOLE GEOLOGY AND CORE DESCRIPTION

2.1 INTRODUCTION

A complete core was collected from B size (60 mm) hole, over an interval from 4.31 m to the total cored depth (TD) of 154.63 m. In general a triple tube coring arrangement (BQ) was used; however, interval 126.85 m to TD was cored using a double tube (BX) system. The triple tube system holds the core essentially motionless as the core barrel spins around it, allowing the recovery of undamaged and (for the purposes of measurement of planar features) accurately aligned core. The borehole orientation, determined purely from the orientation of the drill rig mast, is assumed to be at an azimuth of 135°, plunging at 68°, this direction was used in all calculations of fracture orientations. Orientated core was collected from 9.86 m to TD. Both the core description and the measurements to determine fracture orientations were made in the field.

2.2 GEOLOGICAL DESCRIPTION OF THE CORE

2.2.1 Method

The core was measured on recovery and, where required, broken segments carefully re-fitted, prior to scribing the core. The core was described for rock type and features, fracture fill or coating material.

2.2.2 Core Description

A detailed core log is contained in Appendix A. A synopsis of this information is provided on Figure 2.1. The core recovered at NSCRV is principally comprised of:

i) andesite presumably of the Harbour Main Volcanic Group (Hutchinson, 1953). The andesite is dark green and fine grained and usually highly fractured with most of the fracture surfaces filled or coated with chlorite.

ii) chloritised green granite, often agmatitic in nature. This is assumed to be the green mottled quartz monzonite described by McCartney (1967) and Bruckner (1979) who proposed that it had been formed by marginal hybridisation of the Harbour Main country rocks. The petrochemical nature of this rock is described in detail by Papezik (1970).

iii) pink, apparently unaltered granite. Described again by McCartney and Bruckner as containing 35-40% quartz, 35% microperthite, 15% oligoclase, and 5% biotite. With rare exceptions the feldspars are altered to sericite and epidote. The pink granite recovered at NSCRV was coarse grained, with relatively few fractures.

Figure 2.1 Synopsis of Core Log

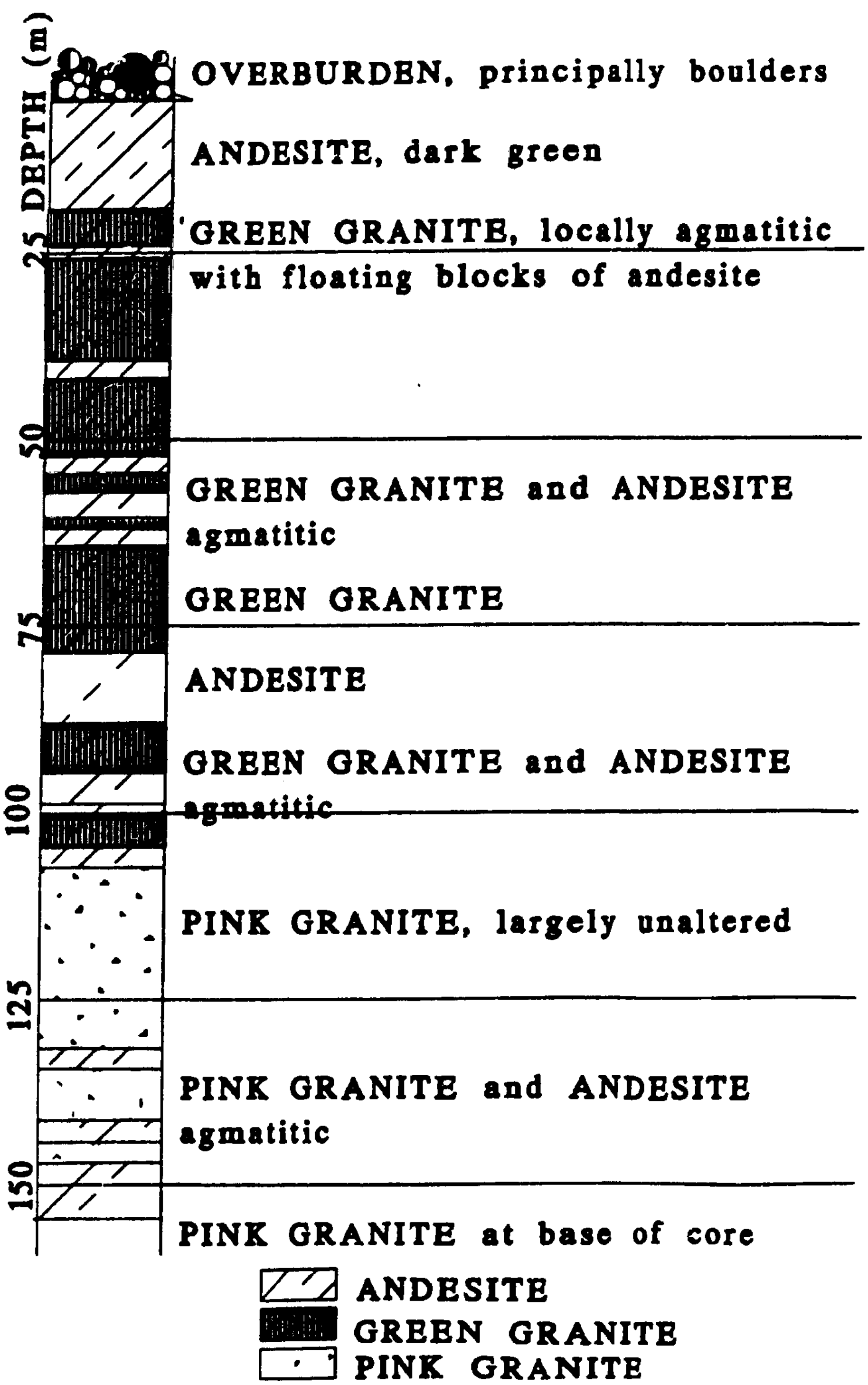

The core consists of andesite from the surface to a drilled depth of 20 m where predominantly green granite is found. After this point the granite is interspersed with andesite xenoliths of various sizes to a drilled depth of approximately 104 m. The andesite is presumed to represent roof blocks of country rock. From 104 m to 130 m the granite is predominantly pink and unaltered until it reverts back to chloritised green granite at 130 m and thence becomes agmatitic in nature with andesite xenoliths interspersed. Some further pink granite is found near the base of the cored interval before the lithology reverts to being essentially andesite, with only minor pink granite, from a depth of 141 m to TD.

Minor veins of pegmatite and aplite were also logged. Some breccia veins were noted, presumably a result of late stage gas streaming (Reynolds 1950) within the Holyrood Granite. Granite was also described as a vein filling material and was assumed to represent the initial intrusion of the material into the country rock.

2.2.3 Fracture Minerals Logged

Seven different minerals were identified in the core recovered from NSCRV. The descriptions provided below are from field descriptions. In part they have been corroborated by subsequent SEM/XRD work (Chapter 7) conducted on samples of fracture fill/coating minerals. However, some of the minerals have not been confirmed, and clay minerals identified by SEM/XRD were not detected in the field. Their occurrence and frequency is discussed in more detail in the section on fracture orientations.

Chlorite

Chlorite occurs throughout the NSCRV borehole and was the most common mineral. It was generally dark green in colour and flaky. Some slickensiding was found on chloritised surfaces.

Calcite

Calcite was observed both as fracture coatings and fillings, being white and varying from crystalline to amorphous.

Epidote

Epidote, amorphous and pistachio green in colour occurs as a fracture filling.

Quartz

Quartz occurred as both coatings and fracture fillings being white and cryptocrystalline.

Wolframite

The titanium bearing mineral wolframite was believed to have been observed as a fracture coating with a red coppery hue and a clinkery appearance. A sample from 139.69 m, logged as wolframite was .ater found to contain Ti during SEM work (Chapter 7). Wolframite can be found as pneumatolytic vein filling in a variety of settings around the world (Read 1970).

Iron Oxide

Iron was occasionally found as a rusty/ dun coloured coating on fracture surfaces. All fractures where iron oxide was observed are believed to have been active water conduits.

Withamite

Withamite, a red variety of epidote, also amorphous was observed filling some fractures.

2.3 DESCRIPTION OF FRACTURE ORIENTATIONS

2.3.1 Method

Core orientation was determined using a Roctest core orientating device. This tool was run inside the core barrel, to the bottom of the borehole, prior to each core run. The construction of the orientation device is shown in Figure 2.2. Force, applied to the drill string, compresses the device, via its pressure rod which protrudes ahead of the bit face. In the final stages of compression of the device an 'impression' of the exposed stub of the core/ base of the borehole is recorded on movable steel pins located at the perimeter of the device. At the same time the down direction of the borehole is recorded by the impression left in a fixed (relative to the pins) aluminum washer (the mark ring), by a free floating steel ball bearing (the mark ball). Both the mark ball and the mark ring are contained in a telescopic ball chamber which closes on application of force down the drill pipe, leaving the impression of the mark ball (and hence the down direction) on the mark ring. Once the impression is taken the orientation device is recovered, and the core cut. At the end of the core run associated with the particular core imprint (as recorded by the pins) the imprint is matched to the face of the core. Alignment of the core and the orientation device, was assured by the use of a jig; the jig aligned the core section with the orientation device. The down direction, determined from the impression on the (replaceable) washer was then transferred to the reconstructed core, as a line representing the down direction. Although the method worked well for the triple tube core, the jig device did not accurately fit the double tube core recovered, introducing further inaccuracy to the results from double tube coring.

Figure 2.2 Core Orientation Device

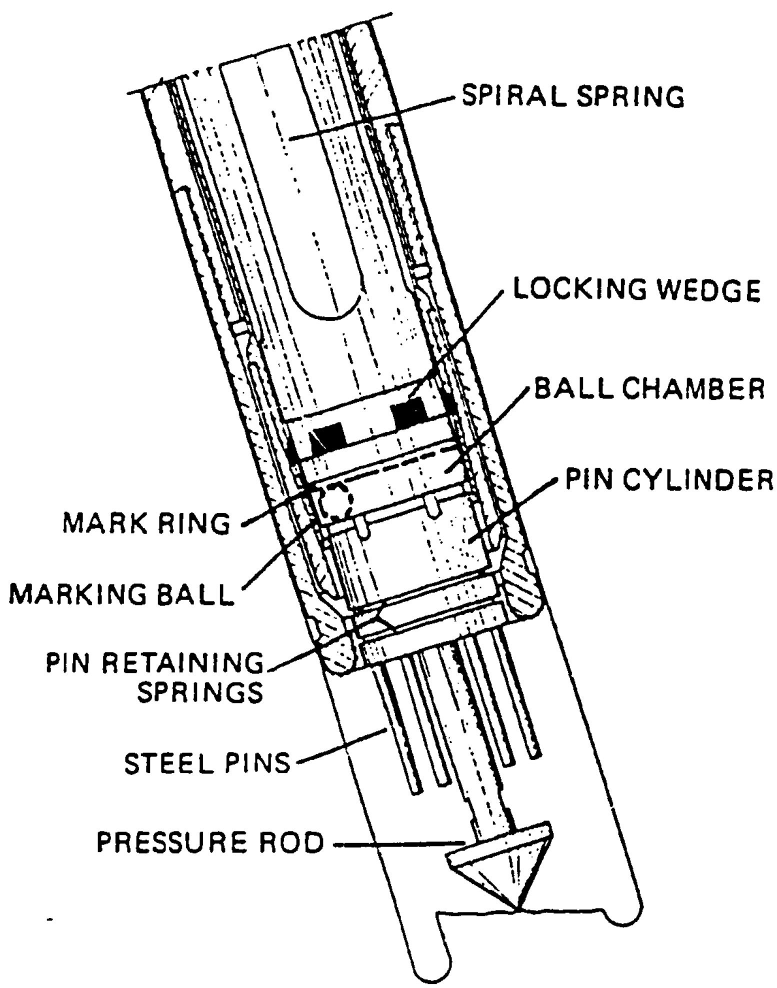

Diagram courtesy ROCTEST LTEE, MONTREAL

Measurements, used to calculate fracture orientations, were made in the field using the method described by Goodman (1976). Knowing the orientation of the borehole (and hence the core) two angles are needed to determine the orientation of a fracture;

i) the angle between the axis of the core and the fracture face (α) and,

ii) the angle between the reference line and the lowest point of the longest axis of the ellipse (β), formed by the intersection of the planar fracture surface with the circular core. The angle β was measured in a clockwise direction, looking down the direction of drilling, from the reference line to the long axis low point.

Figure 2.3 depicts the relationship of these angles with the core and a hypothetical planar feature in the core (after Goodman 1976)

Over 800 fracture orientations were measured. Once fracture orientation measurements had been made, fractures were described by recording type of fracture filling or coating material, nature of fracture surface, whether the fracture was natural or induced, its character (planar, curved, irregular) type of weathering and roughness. The rock type in which the fracture occurred was also recorded. An estimate of whether the fracture was opened or closed was made and this included

Figure 2.3 Angles measured to orientate planar features (after Goodman 1976)

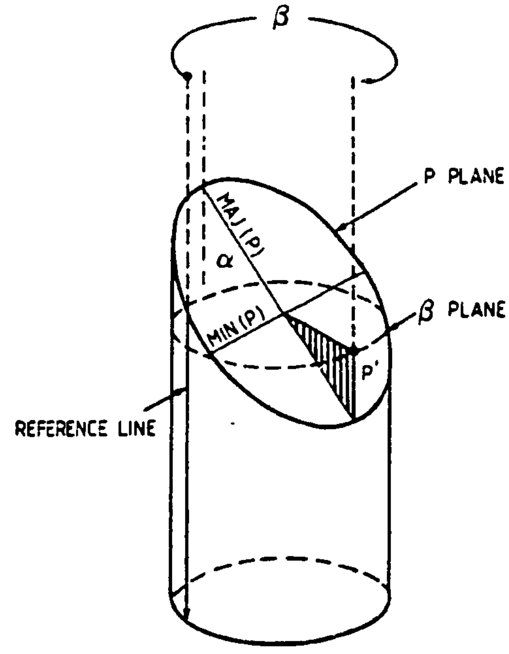

Method of measurement (Gale and Strahle 1988)

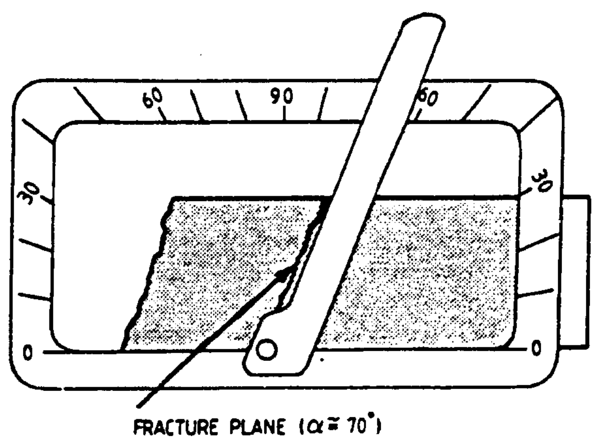

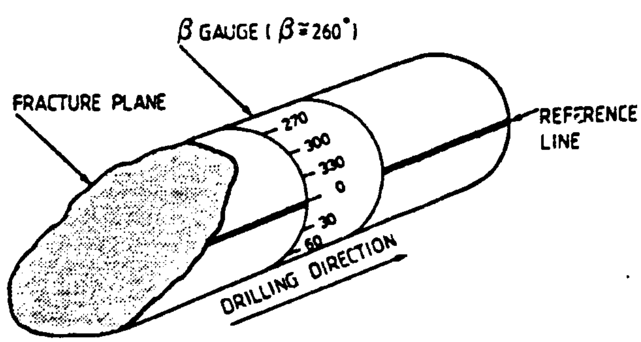

a qualitative estimate of how open the fracture was. Note that all subsequent comments regarding fractures refer only to rock discontinuities, open or closed, believed to be natural. Drilling breaks are no longer considered. The complete fracture data set for the core is provided in Appendix B.

2.3.2 Method of Interpretation of Fracture Data

The main intention, regarding the systematic calculation and recording of fracture orientation data was to decide:

a) if any consistent fracture sets could be identified in the NSCRV borehole,

b) if borehole intervals of high groundwater flux (as will be described in chapter 3) had any consistent fracture orientation(s),

c) if b) was found to be true, were these fractures associated with a particular mineral, or minerals, as recorded in the field.

All fracture data in the subsequent sections is presented on equal area Schmidt nets as projections of poles to planes. The method is described in many texts (e.g. Hobbs et al. 1976). The data were plotted and contoured using the program QUICKPLOT (van Everdingen et al. 1992). Eigen vectors of the principle data point clusters and their statistical significance are also calculated by

QUICKPLOT and are presented on the figures. Table 2.1 provides a synopsis of all fracture data.

A borehole which penetrates fractured material, and which is used to count numbers of fractures, will be biased towards planar features or fractures normal to the borehole (hereafter referred to as the borehole normal fractures). The borehole, in fact, represents a pole to these normal fractures. Conversely fractures parallel to the borehole, which can be visualized as having the same orientations as any planes which are tangential to a cylinder whose central longitudinal axis is represented by the borehole, will be under-sampled. Poles to these borehole parallel fractures will lie on the **great circle** representing the borehole normal plane A range of sampling biases occur between these two extremes (Terzaghi, 1965). No formal correction will be applied to the data; however, the orientation of the NSCRV borehole and a blind zone (for poles to planes) represented by an area lying within the great circles of planes 10° either side of the borehole normal plane are shown on Figure 2.4. The poles plotted within this blind zone would represent borehole parallel, and sub-parallel, fractures. The blind zone is a band striking northeast-southwest and dipping at 68° to the northwest. It should be noted that the blind zone must be considered as truly blind and that without information from orthogonal boreholes, or other sampling orientations, no inferences can be drawn regarding the

Table 2.1 SYNOPSIS OF FRACTURE ORIENTATION DATA

Interval		Data Set Num.	First Eigen Vector Poles to planes Dip dir. (°)	Dip (°)	Planes Strike (°)	Dip (°)	Dip. dir. (°)	95% Conf. Radius (°)	K
DATA DIVIDED BY DEPTH									
(m)	(m)								
9.86	25.00	64	19.9	14.2	109.9	75.8	199.9		1.8
25.00	50.00	99	182.2	11.1	272.2	78.9	2.2	15.9	1.8
50.00	75.00	109	200.2	10.8	290.2	79.2	20.2	14.7	1.8
75.00	100.00	49	183.7	7.9	273.7	82.1	3.7	24.9	1.7
100.00	125.00	57	252.6	33.3	342.6	56.7	72.6	18.6	2.0
125.00	154.46	132	184.6	23.0	274.6	67.0	4.6	11.0	2.2
DATA DIVIDED BY ROCK TYPE									
Green Granite		207	189.2	6.5	279.2	83.5	9.2	12.4	1.6
Pink Granite		109	294.1	49.8	384.1	40.2	114.1	12.8	2.1
Andesite		182	189.6	8.8	279.6	81.2	9.6		
Breccia		7			90.0	90.0	180.0		
ALL GROUNDWATER SAMPLE INTERVALS									
9.86	154.46	82	199.1	2.2	289.1	87.8	19.1	24.3	1.4
INDIVIDUAL GROUNDWATER SAMPLE INTERVALS									
SA1		8	14.9	14.8	104.9	75.2	194.9	65.1	1.7
SA2		17	208.5	1.8	298.5	88.2	28.5	53.0	1.4
SA3		7	213.2	22.8	303.2	67.2	33.2	24.9	6.8
SA4		11	21.4	5.2	111.4	84.8	201.4	53.5	1.7
SA5		9	196.7	3.8	286.7	86.2	16.7	n/a	n/a
SA6		8	18.7	13.2	108.7	76.8	198.7	38.4	3.0
SA7		3	354.5	8.4	444.5	81.6	174.5	n/a	n/a
SA8		10	192.2	12.9	282.2	77.1	12.2	39.9	2.4
SA9		9	196.0	9.1	286.0	80.9	16.0	59.2	1.7
				Avg.	247.3	79.8			

Figure 2.4 NSCRV BOREHOLE ORIENTATION AND BLIND ZONE (ARBITRARY 10° CONE AROUND THE DRILLHOLE)

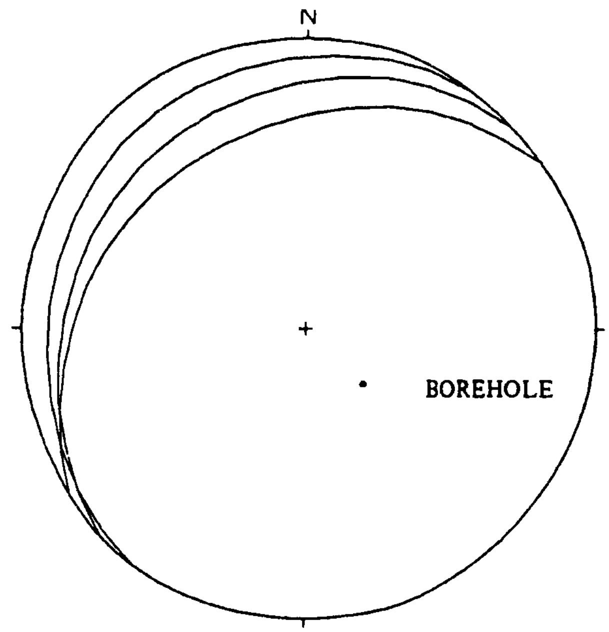

blind zone (i.e., a lack of sampled fractures could mean either there are none or that there are many but they have been under sampled).

The distribution of fractures is described in a non-rigorous statistical manner in later sections. However, of primary importance in this study are the fractures which conduct water. Fractures believed to be open (from inspection of the fractures surfaces and the degree of match between mirror surfaces) were logged as such and given an arbitrary weighting, completely open (weighting of 1) or a fraction thereof (usually half or quarter open) or closed with a weighting of zero. Figure 2.5 is a representation of this information and shows the estimated number of open fractures per metre, calculated as a smoothed average. The average was calculated by summing the weightings of the four fractures above and below the data point and dividing by the interval, in metres, that it spanned. This information is presented with the estimated groundwater flux from the interval and the estimated hydraulic conductivity in Chapter 3. There is a reasonable correlation between the fractures logged as open (or being significant water conductors) and the measured hydraulic conductivity.

Figure 2.5 NUMBER OF OPEN FRACTURES PER METRE VERSUS DEPTH

Open Fractures/metre

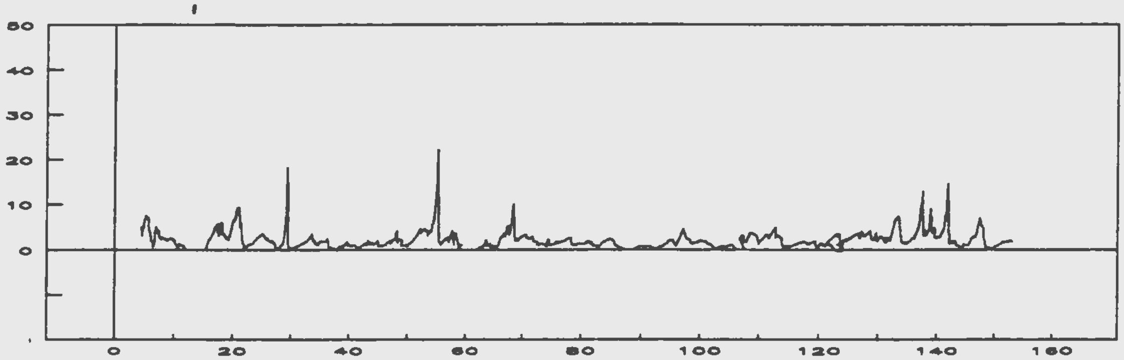

Depth in Borehole (m)

2.4 FRACTURE DATA PRESENTATION

2.4.1 Fractures Differentiated by Depth Intervals

Because of the large number of fractures measured, the fracture orientation data for the drilled interval 9.86 m to TD is arbitrarily divided into six intervals each of approximately 25 m length (Figure 2.6). It is apparent that the dominant sampled fracture set, throughout the borehole section, is approximately east-west and vertical. These vertical fractures are not contained in the blind zone for the borehole. In the surface interval a set of fractures dipping at approximately 30° to the southwest is also present. In addition the fracture sets in this surface interval (sampling andesite) are somewhat less well defined than in the deeper intervals. The blind zone described above seems to be under-represented.

The intervals from 25 to 100 m display a very strong east west striking (or more accurately approximately 280°-100°) set of fractures, dipping at ~80-85° to the north. An apparently conjugate fracture set is also sampled in the interval 50-75 m with one pair of the conjugate set striking northeast, dipping at ~12° to the southeast, and the second striking northwest, dipping at ~12° to the northeast.

The dominant fracture set over the interval 100-125 m is associated with the pink granite and strikes approximately north-northwest, dipping at ~57° to the east. A second conjugate set strikes north-northeast, dipping at ~55° to the

Figure 2.6 POLE PLOTS OF FRACTURE ORIENTATIONS, DIFFERENTIATED BY DEPTH

9.86 to 25 m

Max. value counted:
5.05 times uniform
at 217/79

Eigen values:
.483 .302 .2138
Eigen vectors:
Dip-Dir Dip
19.89 14.24
276.5 42.19
124.2 44.33

Confidence Radius
95% Signif.: 19.5 deg.
K = 1.81

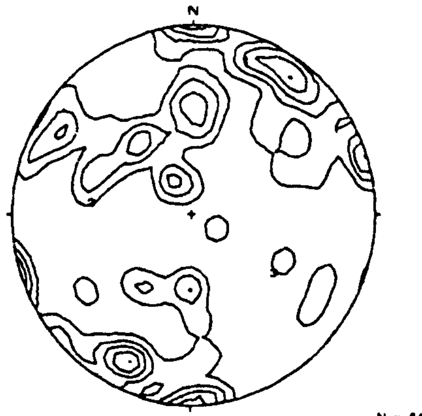

Contours:
1 2 3 4 5

25 to 50 m

Max. value counted:
7.90 times uniform
at 0/55

Eigen values:
.637 .230 .1321
Eigen vectors:
Dip-Dir Dip
182.2 11.10
337.6 77.82
91.26 4.940

Confidence Radius
95% Signif.: 15.9 deg.
K = 1.79

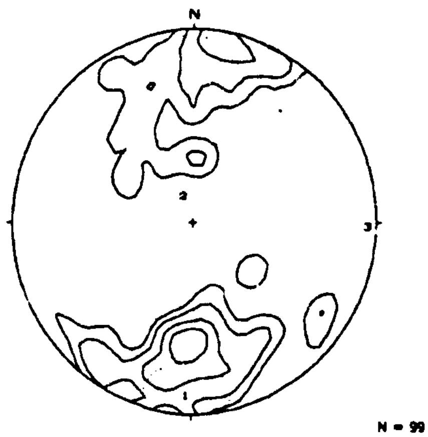

Contours:
1 2 4 6

50 to 75 m

Max. value counted:
8.57 times uniform
at 204/90

Eigen values:
.530 .310 .1595
Eigen vectors:
Dip-Dir Dip
200.2 10.82
319.5 68.69
106.6 18.12

Confidence Radius
95% Signif.: 14.7 deg.
K = 1.83

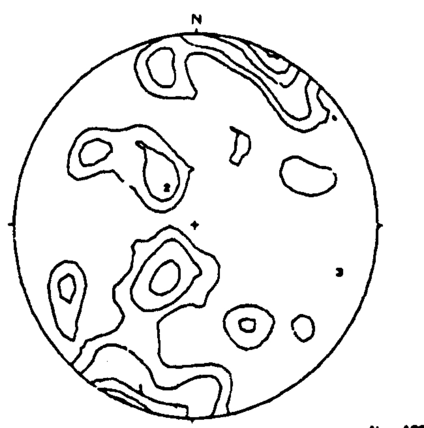

Contours:
1 2 4 6 8

Max Value counted	area of maximum data point concentration
K	Calculated by method of Fisher where 0 would indicate poles' uniform distribution across net, and infinity all poles pointed in same direction
Eigen Vectors	First Eigen Vector (1) is direction of the mean of the data (2) & (3) are orthogonal
Confidence Radius	Angular diameter in which the mean of the data set is contained at the 95% confidence level (i.e. it will be centred around (1)
Contours	shown as multiples of uniform distribution

Figure 2.6/ continued

75 to 100 m

Max. value counted:
10.3 times uniform
at 4/64

Eigen values:
.780 .138 0.080
Eigen vectors:
Dip-Dir Dip
183.7 7.851
90.68 21.26
292.9 67.19

Confidence Radius
95% Signif.: 24.9 deg.
K = 1.65

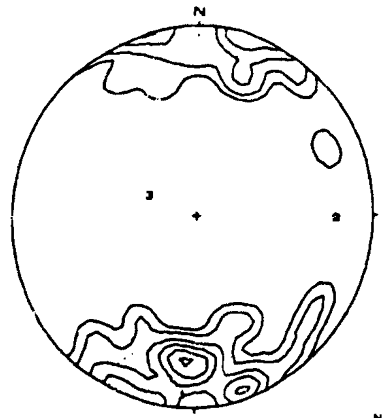

N = 49

Contours:
1 2 4 6 8 10

100 to 125 m

Max. value counted:
5.75 times uniform
at 120/59

Eigen values:
.497 .351 .1509
Eigen vectors:
Dip-Dir Dip
252.6 33.34
355.5 18.69
109.7 50.48

Confidence Radius
95% Signif.: 18.6 deg.
K = 2.01

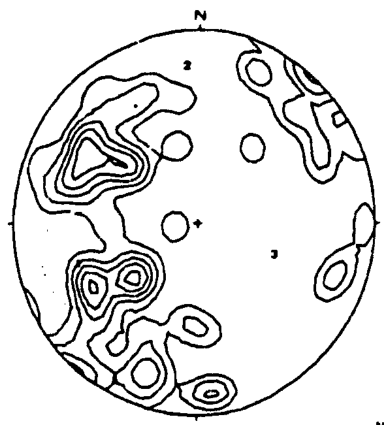

N = 57

Contours:
1 2 3 4 5

125 to 150 m

Max. value counted:
4.71 times uniform
at 340/79

Eigen values:
.456 .339 .2043
Eigen vectors:
Dip-Dir Dip
184.6 23.04
357.0 66.77
93.48 2.747

Confidence Radius
95% Signif.: 11.0 deg.
K = 2.23

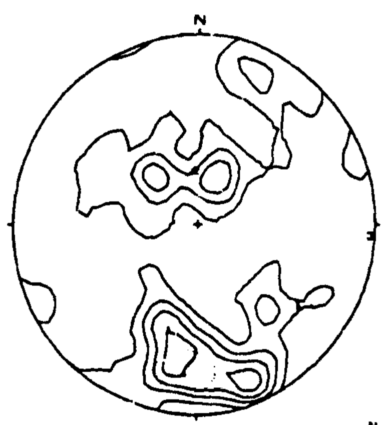

N = 132

Contours:
1 2 3 4

southwest. These conjugate fractures appear to have approximately the same orientation as those sampled in the interval 50-75 m.

The final depth differentiated interval is again dominated by an essentially east-west striking fracture set, dipping at ~77° to the north.

2.4.2 Fracture Differentiated by Fill Material

The seven fracture coatings/fillings logged in the field (calcite, chlorite, epidote, quartz, iron oxide, withamite and wolframite) are all confined to fracture sets with relatively well-defined orientations. Figure 2.7 shows pole plots of fractures coated/filled with the seven different fracture minerals. Table 2.2 is a tabular synopsis of this information. The depths at which the minerals were recorded were averaged, to provide the mean drilled depth at which minerals occurred, the standard deviation for the data was calculated and the range where these minerals are likely to occur is shown as the 95% confidence interval which is the mean±(2*the standard deviation).

Chlorite

Chlorite was the most prevalent fracture filling/coating logged (267) in the field. The dominant fracture orientation of chlorite filled fractures was two

Figure 2.7 POLE PLOTS OF FRACTURE ORIENTATIONS, MINERAL DIFFERENTIATED

CALCITE

Max. value counted:
7.39 times uniform
at 270/90

Eigen values:
.607 .257 .1349
Eigen vectors:
Dip-Dir Dip
3.400 .3688
273.3 10.07
95.48 79.91

Confidence Radius
95% Signif.: 20.2 deg.
K = 1.38

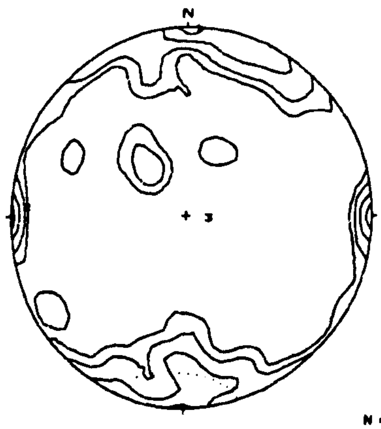

N = 124
Poles to Planes

Contours:
1 2 4 6

124 #
74.58 mean
45.90 SD
4.52 min
154.46 max
43.5 %OPEN

CHLORITE

Max. value counted:
4.84 times uniform
at 270/90

Eigen values:
.508 .270 .2216
Eigen vectors:
Dip-Dir Dip
181.1 7.537
274.3 23.03
74.17 65.62

Confidence Radius
95% Signif.: 10.2 deg.
K = 1.64

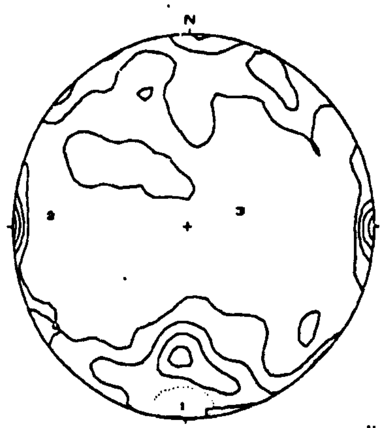

N = 293
Poles to Planes

Contours:
1 2 3 4

293 #
74.91 mean
47.48 SD
5.80 min
154.46 max
39.9 %OPEN

EPIDOTE

Max. value counted:
6.78 times uniform
at 30/24

Eigen values:
.510 .292 .1969
Eigen vectors:
Dip-Dir Dip
202.0 39.99
343.3 42.93
93.74 20.52

Confidence Radius
95% Signif.: 14.9 deg.
K = 2.16

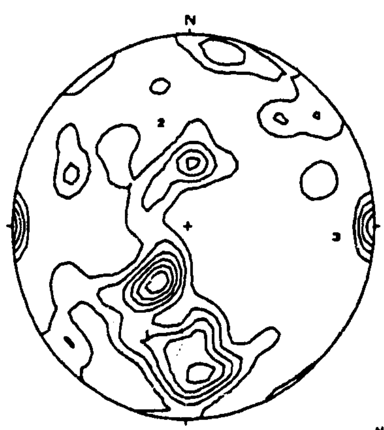

N = 76
Poles to Planes

Contours:
1 2 3 4 5 6

76 #
62.37 mean
31.85 SD
8.65 min
147.30 max
26.6 %OPEN

Figure 2.7/ continued

QUARTZ

Max. value counted:
9.05 times uniform
at 183/90

Eigen values:
.523 .352 .1236
Eigen vectors:
Dip-Dir Dip
353.8 4.049
84.11 3.311
213.2 84.76
Confidence Radius
95% Signif.: 31.2 deg.
K = 1.52

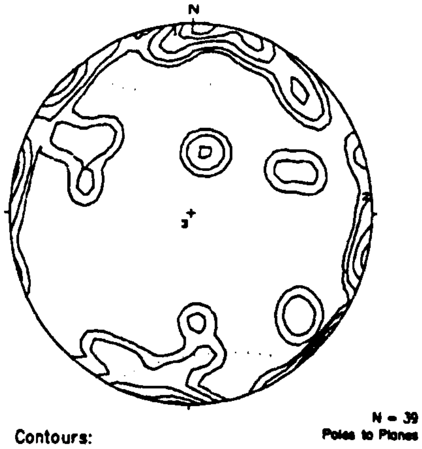

Contours:
1 2 4 6 8

39 #
33.48 mean
31.29 SD
8.84 min
137.41 max
42.3 %OPEN

FE

Max. value counted:
32.8 times uniform
at 270/90

Eigen values:
.516 .460 0.023
Eigen vectors:
Dip-Dir Dip
344.6 .6609
255.0 4.292
75.06 85.70
Confidence Radius
95% Signif.: 61.0 deg.
K = 1.36

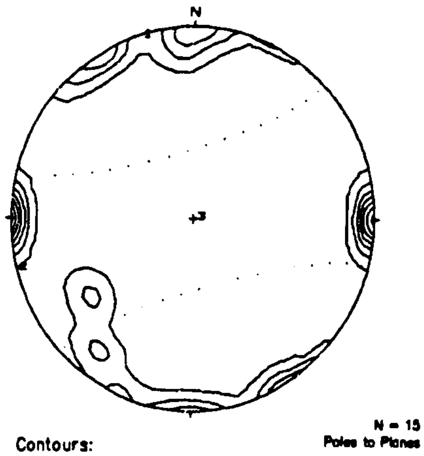

Contours:
1 5 10 15 20 25 30

15 #
27.13 mean
32.19 SD
4.66 min
113.40 max
56.7 %OPEN

WITHAMITE

Max. value counted:
15.6 times uniform
at 180/90

Eigen values:
.518 .313 .1675
Eigen vectors:
Dip-Dir Dip
325.3 5.773
55.42 1.033
155.5 84.13
Confidence Radius
95% Signif.: 42.0 deg.
K = 2.03

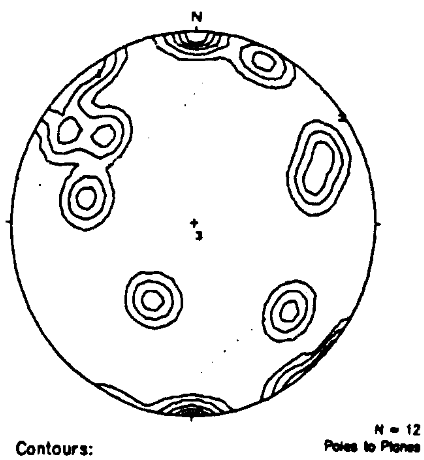

Contours:
1 3 6 9 12

12 #
33.65 mean
36.71 SD
8.50 min
148.31 max
37.5 %OPEN

Figure 2.7/ continued

WOLFRAMITE

Max. value counted:
14.4 times uniform
at 140/24

Eigen values:
.549 .279 .1709

Eigen vectors:
Dip-Dir Dip
303.0 57.98
141.6 30.64
46.66 8.385

Confidence Radius
95% Signif.: 25.1 deg.
K = 2.98

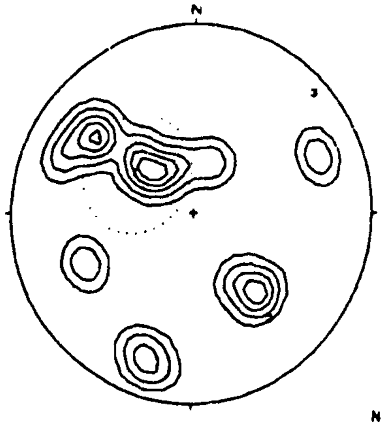

Contours:
1 3 6 9 12

17	#
129.41	mean
8.36	SD
112.68	min
139.71	max
77.9	%OPEN

Max Value counted	area of maximum data point concentration
K	Calculated by method of Fisher where 0 would indicate poles' uniform distribution across net, and infinity all poles pointed in same direction
Eigen Vectors	First Eigen Vector (1) is direction of the mean of the data (2) & (3) are orthogonal
Confidence Radius	Angular diameter in which the mean of the data set is contained at the 95% confidence level (i.e. it will be centred around (1)
Contours	shown as multiples of uniform distribution

Table 2.2 SYNOPSIS OF FRACTURE ORIENTATION, DIFFERENTIATED BY MINERAL TYPE

Interval			Data Set Num.	First Eigen Vector Poles to planes Dip. dir. (°)	Dip (°)	Planes Strike (°)	Dip (°)	Dip. dir. (°)	95% Conf. Radius (°)	K
DATA DIVIDED BY MINERAL TYPE	95% Confidence Interval (m)	(m)								
Calcite	0.00	166.37	124	3.4	0.3688	93.40	89.63	183.4	20.2	1.38
Chlorite	0.00	169.88	293	181.1	7.537	271.10	82.46	1.1	10.2	1.64
Epidote	0.00	126.08	76	202	39.99	292.00	50.01	22	14.9	2.16
Fe	0.00	91.51	15	344.6	0.6609	254.60	89.34	164.6	61	1.36
Quartz	0.00	96.05	39	353.8	4.049	263.80	85.95	173.8	31.2	1.52
Withamite	0.00	107.06	12	325.3	5.773	235.30	84.23	145.3	42	2.73
Wolframite	44.48	108.82	17	303	57.98	33.00	32.02	123	25.1	2.98

SYNOPSIS OF DEPTH INTERVALS (metres) OVER WHICH MINERALS WERE LOGGED

	Calcite	Chlorite	Epidote	Fe	Quartz	Withamite	Wolframite
#	124	293	76	15	39	12	17
mean depth	74.58	74.91	62.37	27.13	33.48	33.65	76.62
sd	45.90	47.48	31.85	32.19	31.29	36.71	16.06
95% min	0.00	0.00	0.00	0.00	0.00	0.00	44.50
95% max	166.37	169.88	126.08	91.51	96.05	107.06	108.75
min.depth	4.52	5.80	8.65	4.66	8.84	8.50	32.02
max.depth	154.46	154.46	147.30	113.40	137.41	148.31	89.63
mid.depth	79.5	80.1	78.0	59.0	73.1	78.4	60.8
%OPEN	43.5	39.9	26.6	56.7	42.3	37.5	0.0

NOTE
K is an estimate of the clustering of points where 0 is a uniform distribution and infinity is all vectors pointing in exactly the same direction

virtually vertical, orthogonal sets striking east-west and north-south. Chlorite filled/coated fractures are represented over the entire length of the NSCRV borehole.

Calcite

Calcite coated/filled fractures are typically sub or near vertical striking either north-south or east-west. Calcite was the second most prevalent mineral logged (124). Some minor calcite filled fracturing was also logged striking approximately northeast-southwest dipping at ~20° to the southeast. Calcite filled/coated fractures occur over the entire length of the NSCRV borehole.

Epidote

Epidote filled fractures do not display the dominant east-west sub or near vertical fracture orientation. However, the north-south vertical set is seen in conjunction with an approximately orthogonal set striking west-northwest and dipping at ~50° to the north. Epidote filled fractures occur throughout the length of the NSCRV borehole.

Quartz

Quartz filled/coated fractures, though they make up the fourth largest (mineralogically defined) group of fractures (39), are relatively rare when compared with the number of calcite or chlorite filled/coated fractures. Most of the quartz fractures logged were essentially vertical but displayed less preference for a particular orientation, than chlorite or calcite. Quartz fractures are most common in the upper 75% of the NSCRV borehole.

Wolframite

Wolframite-filled fractures strike approximately northeast-southwest and dip ~20° to the southeast. They occur over a discrete band from 112-139 m.

Iron Oxide

Iron oxide-stained fractures are almost exclusively represented in sub or near vertical fracture sets with the set constrained to the smallest arc striking north-south. A second, approximately orthogonal east-west set is also represented, however fractures in this set span a wider arc than those in the north-south set. The iron oxide fractures occur predominantly in the upper half of NSCRV.

Withamite

Withamite filled/coated fractures occur in a well defined set of fractures striking east-west with sub or near vertical dip. Some other minor orientations are also found. They are represented throughout the borehole but are more prevalent in the upper 75%.

2.4.3 Fractures Differentiated by Rock Type

The dominant fracture orientations, measured in the principal rock-types (Pink and Green varieties of granite and andesite), are shown in Figure 2.8. These will be discussed below and the fracture orientations will be further sub-divided on the basis of their mineralogy.

Andesite

Fractures in the andesite are dominated by those orientated east-west and being sub or near vertical (Figure 2.8). Some other minor fracture orientations are also apparent.

Of the fractures in the andesite Figure 2.9 shows them differentiated on the basis of mineralogy. Chlorite, quartz, and calcite fractures are found in the east-west set with some other minor orientations. The epidote fractures have their highest concentrations in horizontal or sub-horizontal fractures. Fractures filled with granite are relatively rare and are found orientated in a variety of directions.

Green Granite

Fractures in the green granite are typically of the east-west striking sub or near vertical set and typically coated/filled with calcite, chlorite, epidote, quartz

Figure 2.8 POLE PLOTS OF FRACTURE ORIENTATIONS; ROCK TYPE DIFFERENTIATED

GREEN GRANITE

Max. value counted:
5.95 times uniform
at 205/84

Eigen values:
.619 .214 .1659
Eigen vectors:
Dip-Dir Dip
189.2 6.530
302.3 73.70
97.51 14.86

Confidence Radius
95% Signif.: 12.4 deg.
K = 1.61

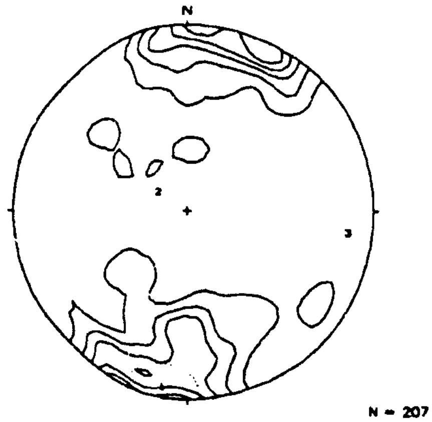

Contours:
1 2 3 4 5

PINK GRANITE

Max. value counted:
4.35 times uniform
at 125/55

Eigen values:
.414 .324 .2614
Eigen vectors:
Dip-Dir Dip
294.1 49.84
184.8 15.57
83.21 35.89

Confidence Radius
95% Signif.: 12.8 deg.
K = 2.10

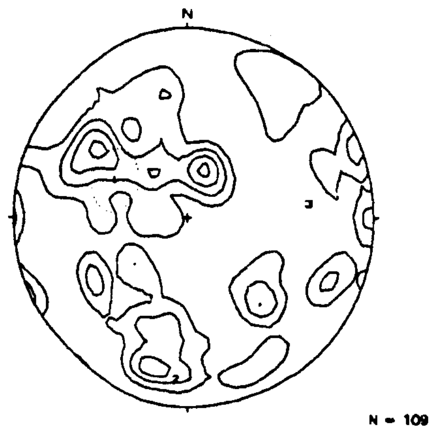

Contours:
1 2 3 4

ANDESITE

Max. value counted:
4.95 times uniform
at -8/64

Eigen values:
.526 .271 .2023
Eigen vectors:
Dip-Dir Dip
189.6 8.787
302.9 68.61
96.58 19.33

Confidence Radius
95% Signif.: 11.4 deg.
K = 1.82

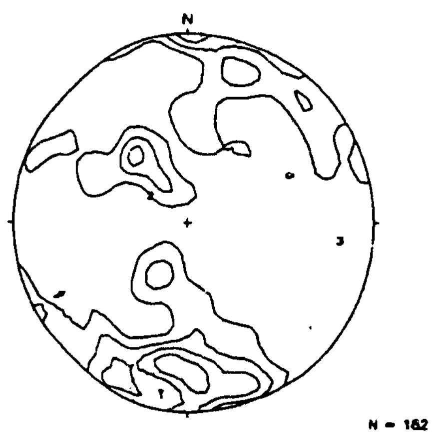

Contours:
1 2 3 4

Max Value counted	**area of maximum data point concentration**
K	**Calculated by method of Fisher where 0 would indicate poles' uniform distribution across net, and infinity all poles pointed in same direction**
Eigen Vectors	**First Eigen Vector (1) is direction of the mean of the data (2) & (3) are orthogonal**
Confidence Radius	**Angular diameter in which the mean of the data set is contained at the 95% confidence level (i.e. it will be centred around (1)**
Contours	**shown as multiples of uniform distribution**

Figure 2.8/ continued

BRECCIA

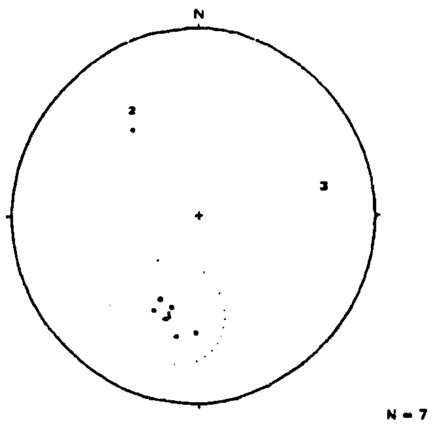

Eigen values:
.843 .153 0.002
Eigen vectors:
Dip–Dir Dip
197.1 44.34
328.3 33.95
77.97 26.51
Confidence Radius
95% Signif.: 24.3 deg.
K = 7.08

Figure 2.9 POLE PLOTS OF FRACTURE ORIENTATIONS IN ANDESITE, MINERAL DIFFERENTIATED

CALCITE

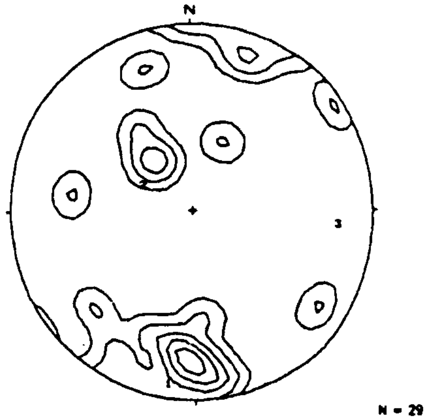

Max. value counted:
13.9 times uniform
at 4/69

Eigen values:
.663 .230 .1057
Eigen vectors:
Dip-Dir Dip
189.1 8.643
298.5 65.33
95.49 22.91
Confidence Radius
95% Signif.: 31.2 deg.
K = 1.71

Contours:
1 3 6 9 12

CHLORITE

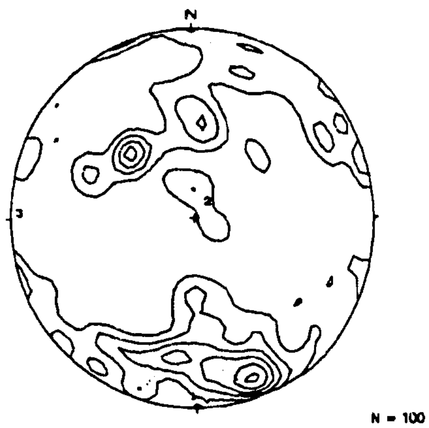

Max. value counted:
6.40 times uniform
at 340/79

Eigen values:
.516 .250 .2327
Eigen vectors:
Dip-Dir Dip
181.3 7.343
37.56 80.92
272.0 5.291
Confidence Radius
95% Signif.: 15.8 deg.
K = 1.79

Contours:
1 2 3 4 5 6

EPIDOTE

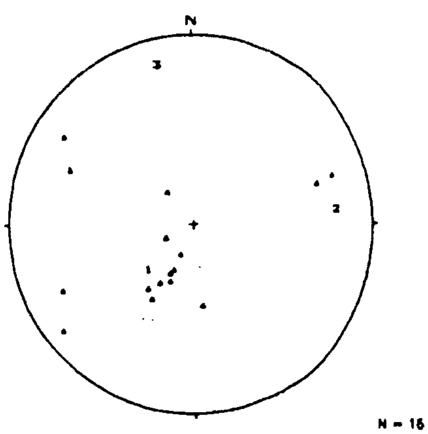

Eigen values:
.659 .234 .1064
Eigen vectors:
Dip-Dir Dip
227.3 62.45
84.02 22.69
347.6 14.77
Confidence Radius
95% Signif.: 22.3 deg.
K = 3.70

Max Value counted	area of maximum data point concentration
K	Calculated by method of Fisher where 0 would indicate poles' uniform distribution across net, and infinity all poles pointed in same direction
Eigen Vectors	First Eigen Vector (1) is direction of the mean of the data (2) & (3) are orthogonal
Confidence Radius	Angular diameter in which the mean of the data set is contained at the 95% confidence level (i.e. it will be centred around (1)
Contours	shown as multiples of uniform distribution

Figure 2.9 /continued

QUARTZ

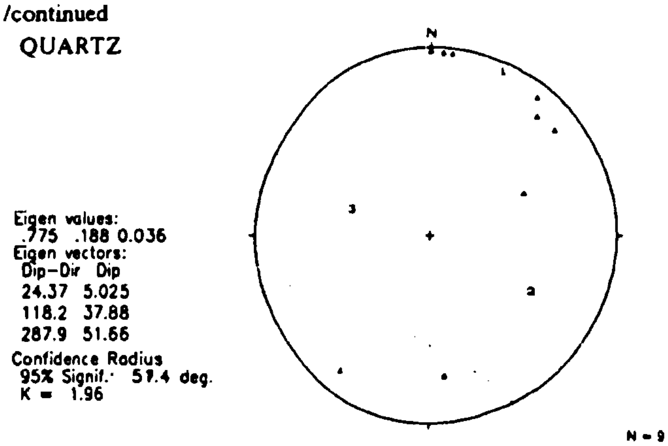

GRANITE

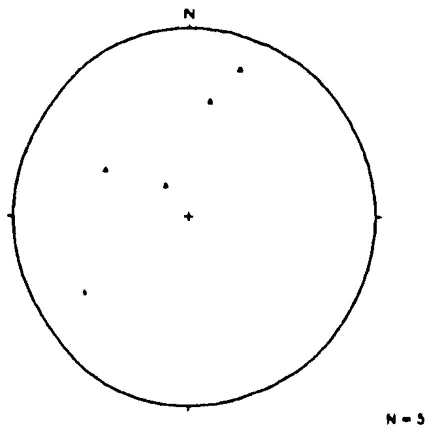

and iron oxide (Figure 2.10). Those coated or filled with calcite are most likely to be of the east-west vertical set. This is also true of chlorite, though there is more scatter. Quartz filled/coated fractures are predominantly east-west and sub or near vertical, though relatively rare and the same can be said of Fe coated fractures, which number only four. Epidote coats/ fills a set of fractures striking west-northwest and dipping at ~50° to the north.

Pink Granite

The fractures in the pink granite (Figure 2.11) have apparently less well defined fracture orientations; however it should be borne in mind that this interval was drilled with double tube core (resulting in larger fracture measurement errors). The dominant fracture set appears to strike north-northeast dipping at ~40° to the east-southeast, though there is much scatter.

Of the fracture minerals identified only three calcite fractures and 32 chlorite fractures were recorded in the pink granite. The principal chloritised fracture set has a similar orientation to the overall fracture orientation in the pink granite.

Figure 2.10 POLE PLOTS OF FRACTURE ORIENTATIONS IN GREEN GRANITE, MINERAL DIFFERENTIATED

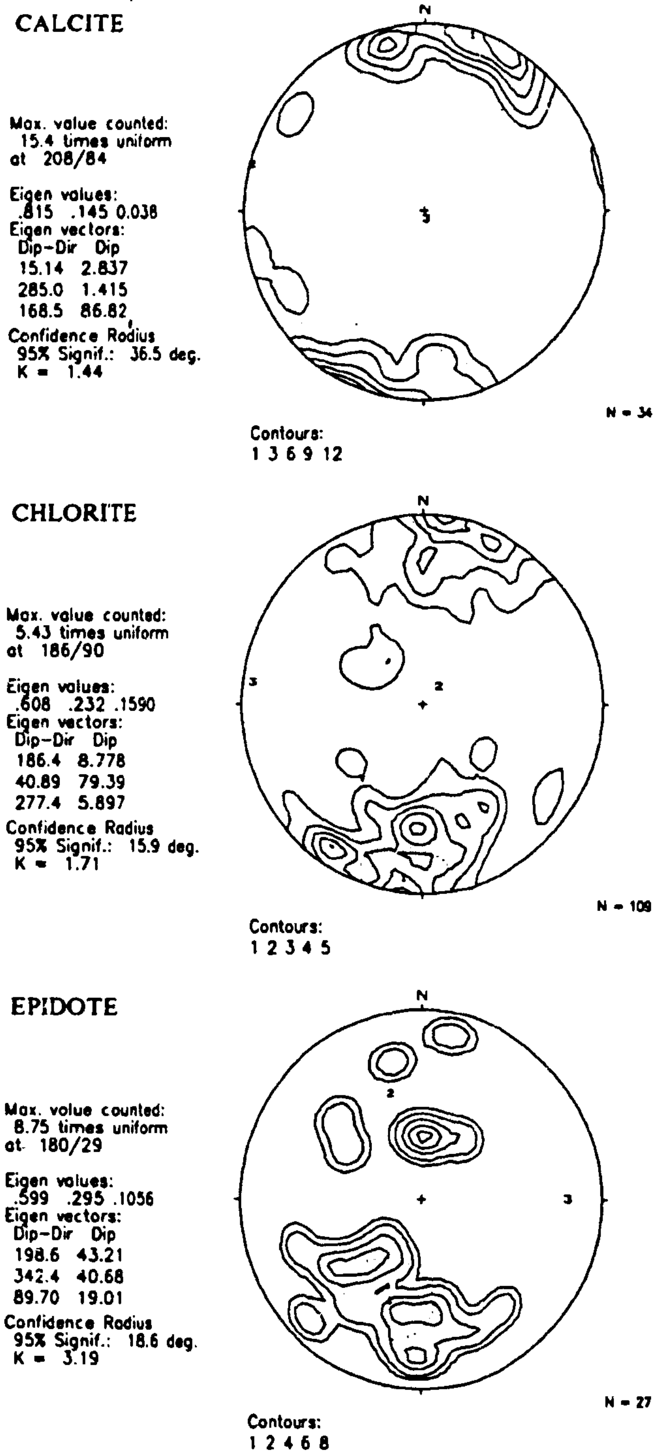

Max Value counted	**area of maximum data point concentration**
K	**Calculated by method of Fisher where 0 would indicate poles' uniform distribution across net, and infinity all poles pointed in same direction**
Eigen Vectors	**First Eigen Vector (1) is direction of the mean of the data (2) & (3) are orthogonal**
Confidence Radius	**Angular diameter in which the mean of the data set is contained at the 95% confidence level (i.e. it will be centred around (1)**
Contours	**shown as multiples of uniform distribution**

Figure 2.10/ continued

QUARTZ

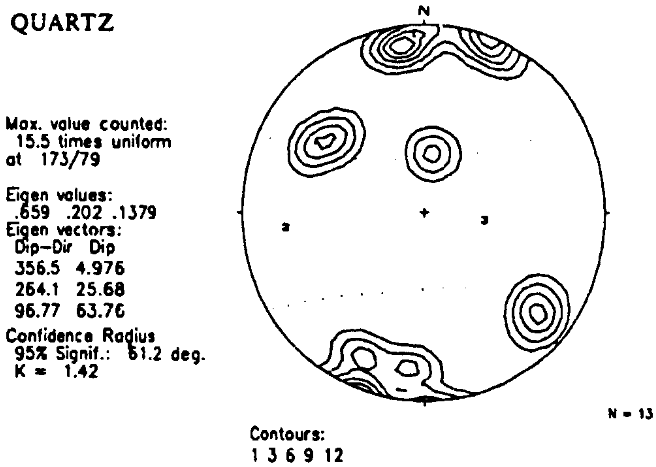

FE

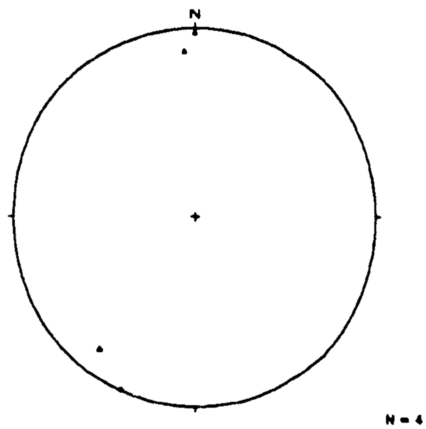

Figure 2.11 POLE PLOTS OF FRACTURE ORIENTATIONS IN PINK GRANITE, MINERAL DIFFERENTIATED

CALCITE

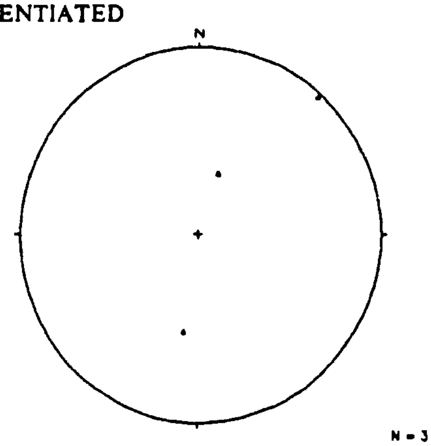

CHLORITE

Max. value counted:
8.03 times uniform
at 125/55

Eigen values:
.510 .325 .1640
Eigen vectors:
Dip-Dir Dip
301.7 43.81
195.5 16.18
90.57 41.72

Confidence Radius
95% Signif.: 21.0 deg.
K = 2.44

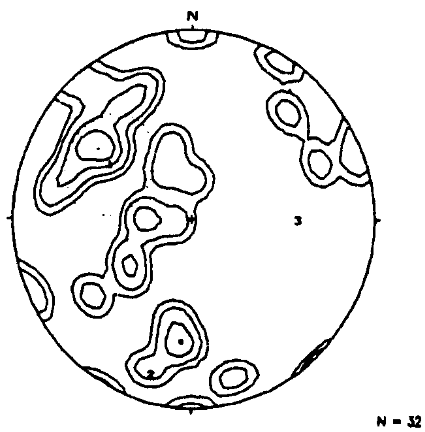

Contours:
1 2 4 6 8

WOLFRAMITE

Max. value counted:
16.0 times uniform
at 140/24

Eigen values:
.562 .296 .1409
Eigen vectors:
Dip-Dir Dip
292.5 60.37
148.5 24.71
51.28 15.29

Confidence Radius
95% Signif.: 25.1 deg.
K = 3.28

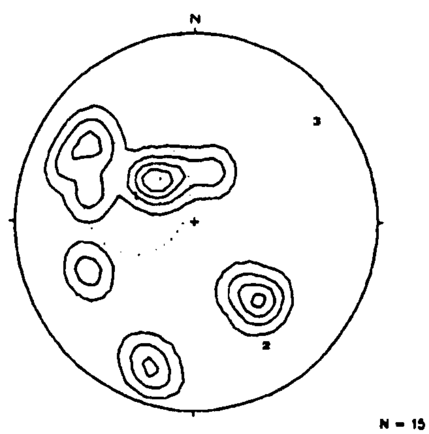

Contours:
1 4 8 12 16

Max Value counted	area of maximum data point concentration
K	Calculated by method of Fisher where 0 would indicate poles' uniform distribution across net, and infinity all poles pointed in same direction
Eigen Vectors	First Eigen Vector (1) is direction of the mean of the data (2) & (3) are orthogonal
Confidence Radius	Angular diameter in which the mean of the data set is contained at the 95% confidence level (i.e. it will be centred around (1)
Contours	shown as multiples of uniform distribution

2.4.4 Fracture Orientations in intervals sampled for groundwater

Groundwater samples were collected at NSCRV from nine intervals with relatively high hydraulic conductivities. The sampling methods are described in detail in chapter 3.

Of all the fracture minerals described calcite is believed (mainly on the basis of field observation) to be associated with the highest amount of water flow, all iron oxide coated fractures are also believed to be contemporary conductors of groundwater. Groundwater samples were collected predominantly from andesite (probably rafts in the granite) or the green granite, with no samples collected from the pink granite.

All of the sample intervals, from which groundwater samples were collected, were typified by fractures whose strikes lay in the east to southeast quadrant with a tendency to strike east or east-southeast, as shown on Figure 2.12. Figure 2.13 depicts the fracture orientations for individual intervals. The fractures were close to vertical with dip directions scattered north and south, approximately 10° either side of the vertical. Some minor north-south striking near vertical fractures were also logged.

Figure 2.12 COMPOSITE POLE PLOTS OF ALL FRACTURES, BELIEVED TO BE OPEN, IN THE NINE GROUNDWATER SAMPLE INTERVALS

Max. value counted:
10.6 times uniform
at 204/90

Eigen values:
.740 .146 .1126
Eigen vectors:
Dip–Dir Dip
199.1 2.194
292.2 54.61
107.5 35.29

Confidence Radius
95% Signif.: 24.3 deg.
K = 1.40

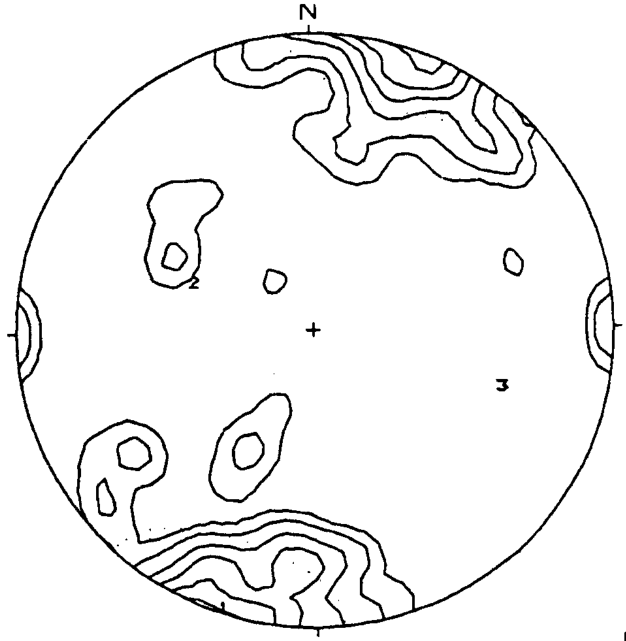

N = 82

Contours:
1 2 4 6 8 10

Max Value counted	**area of maximum data point concentration**
K	**Calculated by method of Fisher where 0 would indicate poles' uniform distribution across net, and infinity all poles pointed in same direction**
Eigen Vectors	**First Eigen Vector (1) is direction of the mean of the data (2) & (3) are orthogonal**
Confidence Radius	**Angular diameter in which the mean of the data set is contained at the 95% confidence level (i.e. it will be centred around (1)**
Contours	**shown as multiples of uniform distribution**

Figure 2.13

FIGURE SAMPLE INTERVAL FRACTURES

17.71 to 19.82 m

Sample (11)

Rock: Andesite

Mins: QZ,EP,CH,PY,GR

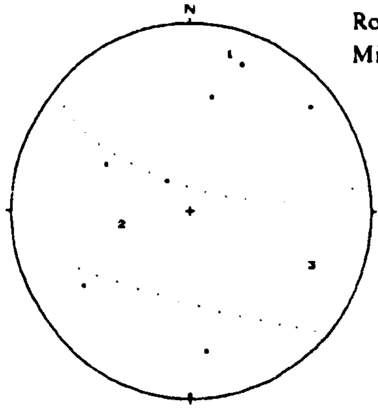

Eigen values:
.550 .332 .1173
Eigen vectors:
Dip–Dir Dip
14.86 14.82
260.0 57.72
112.9 27.95
Confidence Radius
95% Signif.: 65.1 deg.
K = 1.68

N = 8

18.61 to 21.77 m

Sample (1)

Rock: Andesite&Green Granite

Mins: GR,QZ,CH,WH,EP

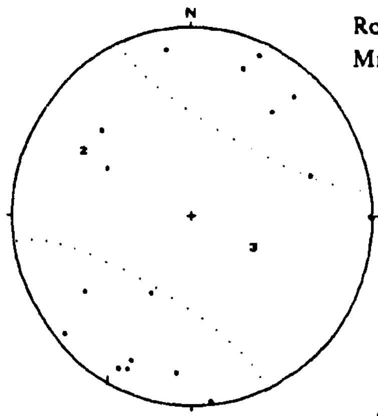

Eigen values:
.636 .229 .1335
Eigen vectors:
Dip–Dir Dip
208.5 1.800
299.6 30.91
115.5 59.02
Confidence Radius
95% Signif.: 53.0 deg.
K = 1.42

N = 17

55.75 to 57.86 m

Sample (7) & (10)

Rock: Andesite&Green Granite

Mins: CA/CL in granite
EP/CA in andesite

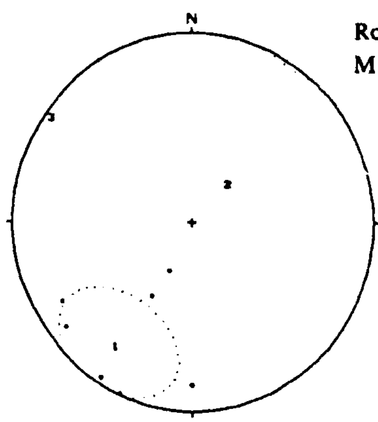

Eigen values:
.768 .146 0.084
Eigen vectors:
Dip–Dir Dip
213.2 22.83
43.74 66.81
304.8 3.785
Confidence Radius
95% Signif.: 24.9 deg.
K = 6.81

N = 7

Figure 2.13/ continued

68.58 to 70.69 m
Sample (6) & (8)

Rock: Green Granite
Mins: CA,CH,EP,AP

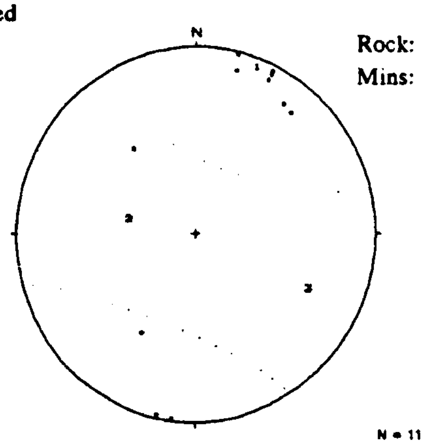

Eigen values:
.842 .111 0.045
Eigen vectors:
Dip-Dir Dip
21.37 5.171
282.9 58.38
114.5 31.09
Confidence Radius
95% Signif.: 53.5 deg.
K = 1.69

70.59 to 76.20 m
Sample (5)

Rock: Green Granite
Mins: AP,CA,CH,FE

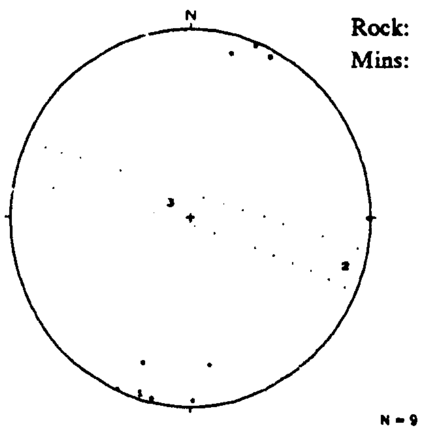

Eigen values:
.831 .140 0.027
Eigen vectors:
Dip-Dir Dip
196.7 3.759
106.0 10.85
305.5 78.49
Confidence Radius
95% Signif.: -83.4 deg.
K = 1.25

73.62 to 76.20 m
Sample (2)

Rock: Green Granite&Aplite
Mins: CH,CA,FE,QZ

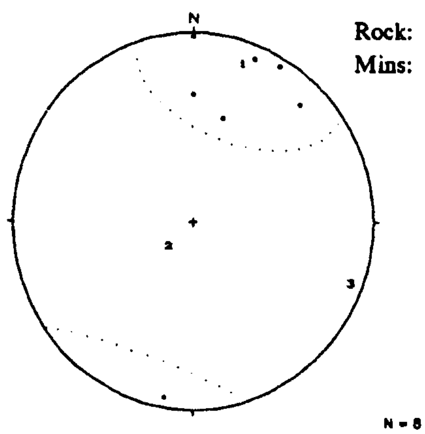

Eigen values:
.881 6.66 0.052
Eigen vectors:
Dip-Dir Dip
18.65 13.17
228.3 74.91
110.3 7.220
Confidence Radius
95% Signif.: 38.4 deg.
K = 3.02

Figure 2.13/ continued

76.35 to 78.46 m
Sample (9)

Rock: Green Granite
Mins: CA

Eigen values:
.882 .112 0.004
Eigen vectors:
Dip–Dir Dip
354.5 8.444
93.47 46.35
256.7 42.40

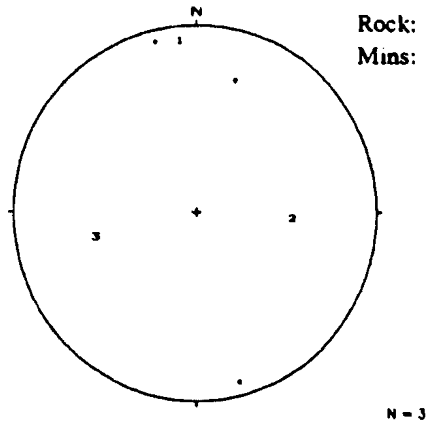

95.58 to 97.69 m
Sample (4)

Rock: Andesite
Mins: CH,CA,EP,G

Eigen values:
.919 .070 0.010
Eigen vectors:
Dip–Dir Dip
192.2 12.88
60.70 70.95
285.4 13.78
Confidence Radius
95% Signif.: 39.9 deg.
K = 2.42

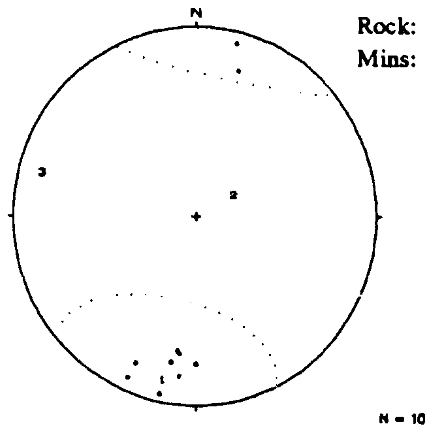

96.17 to 98.65 m
Sample (3)

Rock: Andesite
Mins: CA,CH

Eigen values:
.812 .130 .0573
Eigen vectors:
Dip–Dir Dip
196.0 9.059
102.4 21.32
307.6 66.65
Confidence Radius
95% Signif.: 59.2 deg.
K = 1.71

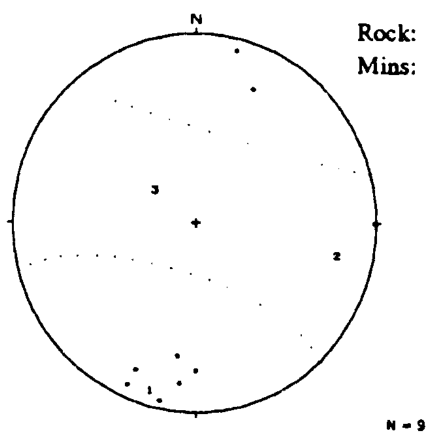

2.5 CONCLUSIONS AND INTERPRETATIONS

As noted above most of the fractures believed to be active water conduits have nearly vertical dips and strike approximately east-west. They are chiefly associated with calcite and iron oxide. The near vertical east-west open fractures are believed to be both reopened fractures (principally because they have the same orientation as the some of the older fracture sets) dating back to the emplacement of the granite and possibly modern (Wisconsinan) fractures. The open fractures are believed to be responding to a stress field in the granites which is controlled principally by the overburden pressure (Fertl, 1976) in which $\sigma_1 > \sigma_2 \geq \sigma_3$ and in this case where σ_1 is vertical and the two other orthogonal principal stresses are horizontal (Hubert and Willis, 1957). In this instance the apparent preference of the open fractures, for an east-west orientation, indicates that σ_3 is essentially north south, and is less than σ_2, with the σ_3 stress in the direction of the general slope of the area. This may be evidence that the stresses found in the shallow levels sampled at NSCRV are controlled by isostatic rebound resulting from geologically recent glacial melting. The possibility of faulting, induced by postglacial isostatic rebound has been mooted by many authors (see Grant 1989 for a review). Grant notes that large-scale slumping of mountain sides, observed in the mountains of the Northern

Peninsula, Newfoundland, may also be attributed to isostatic movements following ice cover melting.[1]

All fractures that are not essentially vertical (and even some that are) are believed to be Pre-Cambrian to Cambrian in age. They are thought to have resulted from the violent emplacement of the Holyrood Granite (Hughes 1971) at high pressures, and the associated final escape of fluids from the cooling magma body. It is believed that the horizonal σ_1 stress orientation occurred during (or shortly after) emplacement of the granite. After granite emplacement the stress field reverted to one controlled by the overburden gradient. The possibility of high pressures near surface may have resulted in σ_1 being horizontal inducing horizontal fractures to open (σ_3 vertical). If, as surmised, some of the fracture orientations observed are in fact conjugate, bifurcated by the horizontal plane, then these fractures may also be remnant indicators of this old stress field. Epidote fractures displayed a conjugate fracture set, bifurcated by the horizontal plane, with relatively rare vertical fractures. Fractures logged as wolframite filled/coated were also essentially horizontal. Withamite filled fractures are near vertical. However, in general most of the fracture orientations were near vertical and the majority of the

[1] Note: if fracture fill material in the principal water carrying fractures could be dated an idea of the age when the fractures became active (or were reactivated) could be obtained and thus their relationship to glacial retreat. Such information could provide an answer to the probability of post glacial slumping as a mechanism for inducing rock discontinuities and slumps.

chloritised fractures logged were vertical, with some minor near horizontal fracturing. These facts may indicate a stress field which changed from having σ_1 essentially horizontal to one in which it is essentially vertical.

CHAPTER 3: HYDRAULIC CONDUCTIVITY TESTING

3.1 INTRODUCTION

Between August 15th and November 1st 1989 a total of 83 intervals in the NSCRV borehole were isolated and tested for hydraulic conductivity and head, providing continuous hydraulic conductivity information along the entire hole. Groundwater samples were collected from those intervals isolated, having the highest hydraulic conductivities. The hydraulic conductivity tests were conducted either as falling or constant head tests, depending on the hydraulic nature of the interval being tested. All conductivity measuring methods were intended to determine the hydraulic conductivity of the bulk rock mass, rather than that of individual fractures.

3.2 METHODS OF HYDRAULIC CONDUCTIVITY AND HEAD TESTING

3.2.1 Description of the Straddle Packer Tool

Three different hydraulic conductivity testing methods were used at the NSCRV location. Several intervals were tested using different methods to determine if the results were comparable.

A straddle inflated packer system, following the design of Raven (1980) and Raven and Smedley (1982) (Figure 3.1a) was used to isolate the test intervals. Depth control was maintained by careful measurement of the length of schedule 80, ¾" steel tubing, below which the test tool was run. Hydro/pneumatic connection between the tool and the surface was maintained via a 150 m three core, neoprene sheathed, composite plastic tube bundle, each internal tube having a ¼" I.D. One tube was used as a nitrogen line for packer inflation with the other two tubes, open to the sample interval, used for head and flow measurement. The three core bundle was spooled on a drum and thus its length was constant for all tests. During each test the packers were inflated, at the depth of interest, to ~2.4 MPa above hydrostatic pressure. To ensure that the test interval was not pressurized by the inflation process all lines to the cavity were left open, on surface while packer inflation was in progress and a by-pass tube was used to equilibrate hydraulic heads in the interval below the bottom packer with the interval above the top packer. Great care was taken (by opening, closing and joining tubes under water) to ensure that, once the tubing was purged with water, no air was allowed to enter the bundle.

3.2.2 Hydrostatic Head measurements

Once the test tool was properly seated, and prior to hydraulic conductivity testing in each cavity, the cavity was shut-in (isolated) using surface valves. The pressure in the cavity was then allowed to equilibrate (or quasi

Figure 3.1 Hydraulic Conductivity testing Configuration

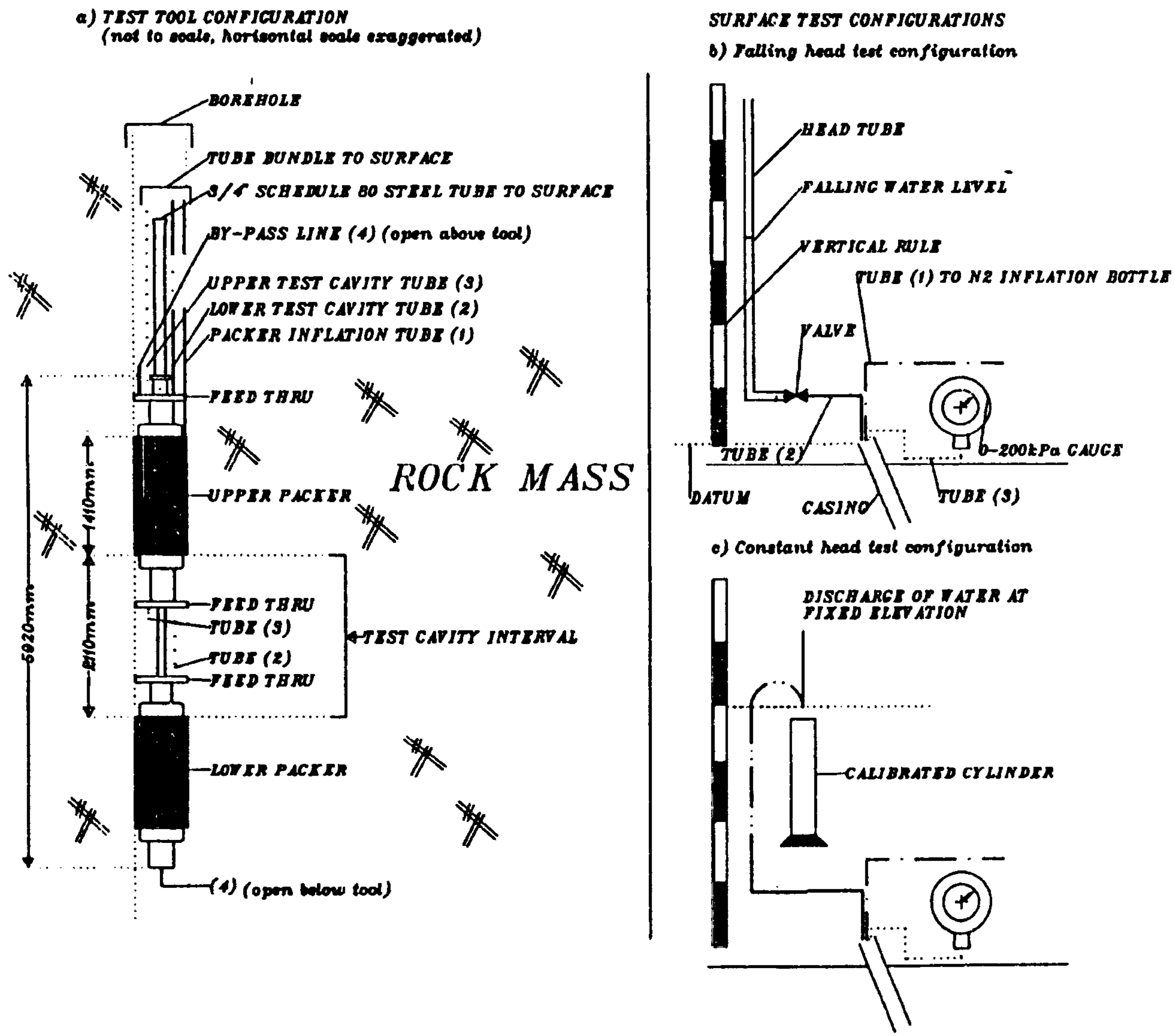

equilibrate) with the formation pressure. The cavity pressure was measured using a 0-200 kPa gauge at surface. All pressure measurements were corrected for the position of the gauge relative to the datum (the casing collar). This part of the test was the most time consuming often exceeding two to three hours. It can be argued that even this length of time was insufficient for true pressure equilibrium to be achieved but it is believed that the shape of the formation pressure build-up curves, that the final measured interval head pressure gives a good indication of the actual formation pressure. Examples of formation pressure build-up curves are provided in Figure 3.2. The data set is presented on Table 3.1. It should be noted that the shapes of these curves are also a function of hydraulic conductivity and that in general terms the steeper the initial pressure build-up, the higher the hydraulic conductivity. The head measurements indicate that the hydraulic conditions throughout virtually the entire length of the borehole were artesian. The artesian conditions allowed the use of constant head tests (with water flowing from the test interval) and rising head tests, for the measurement of hydraulic conductivity in almost all the intervals. Artesian conditions also permitted relatively simple positive pressure sampling for groundwater.

3.2.3 Falling (or rising) head test

Where the hydraulic conductivity of the test interval was determined to be insufficient to conduct a constant head test a falling (or in some cases rising)

Figure 3.2 Shut-in curves for selected formation tests. All shut-in pressures were subsequently checked by calculation using constant head test information

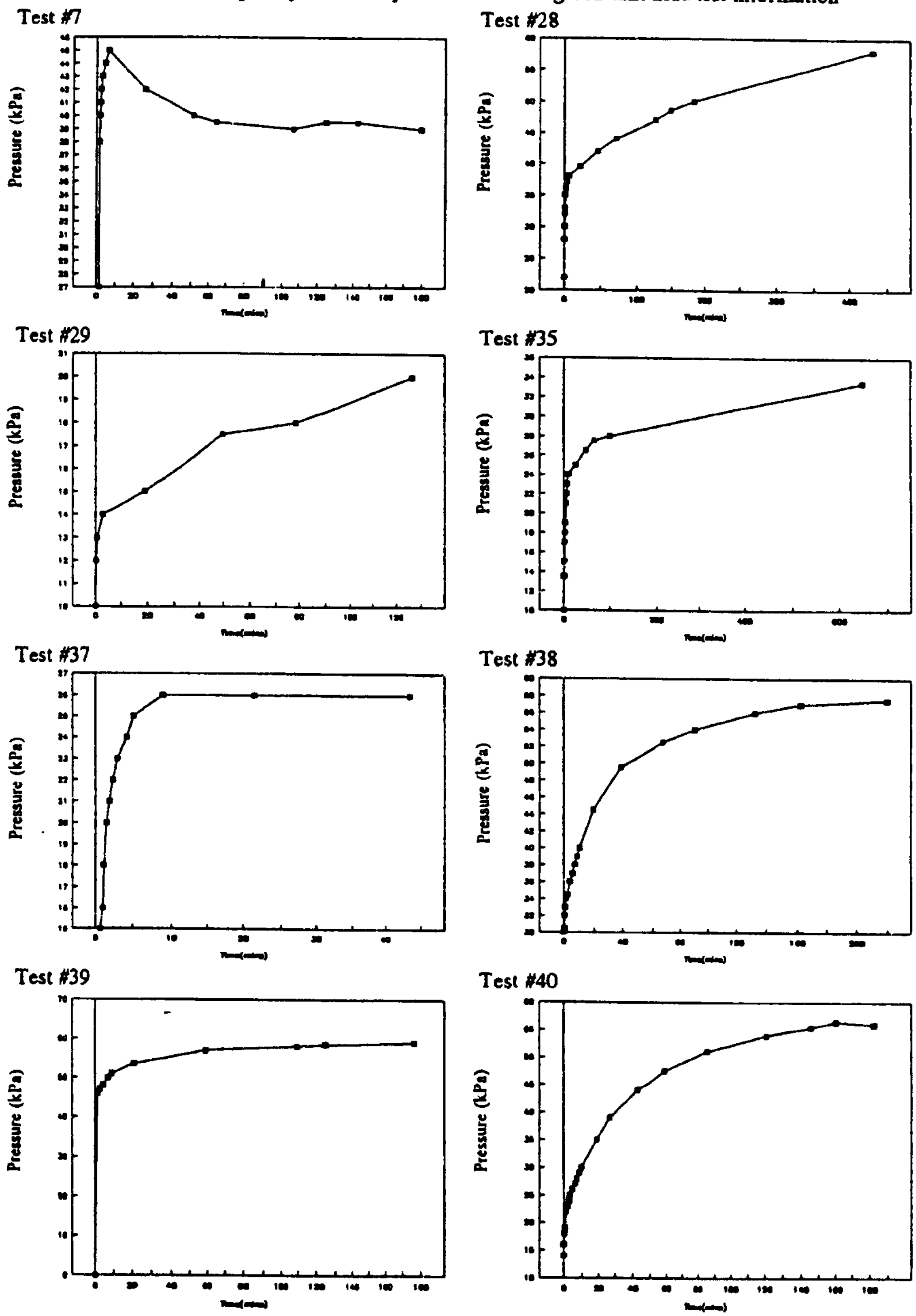

Figure 3.2 continued

Test #41

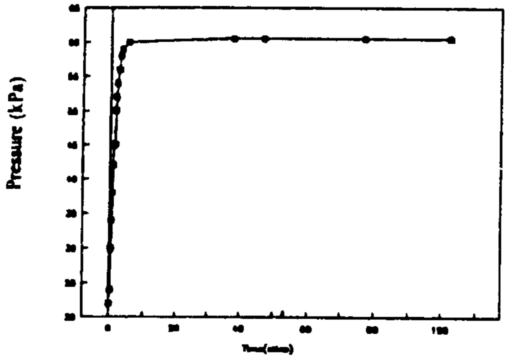

Test #42

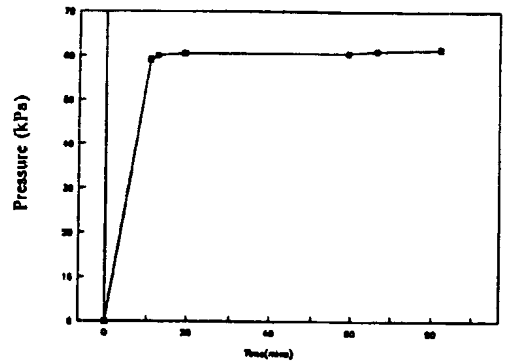

Test #46

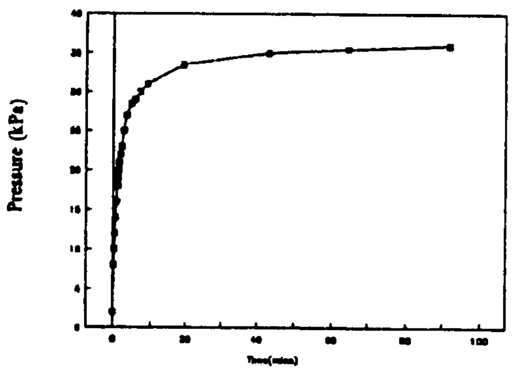

Test #52

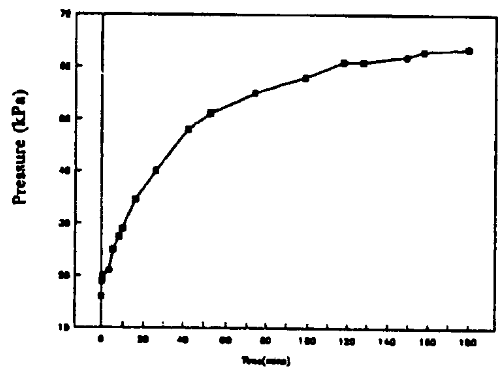

Test #76

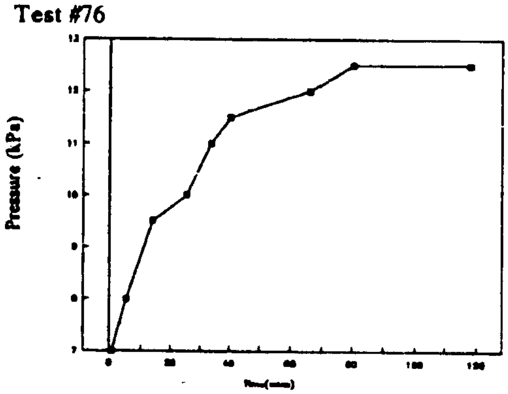

Table 3.1 COMPOSITE PHYSICAL HYDROGEOLOGICAL DATA, NSCRV.

Kch: Hydraulic conductivity from constant head test.
Kfh: Hydraulic conductivity from falling head test.
@K: Hydraulic conductivity from falling head test but using Thiem equation, P2 measured from cavity and and treating each time interval as constant head test.

Flux: refers to calculated flow from 2m interval with Borehole pressure at 0m.
Head Refers to formation pressure relative to the estimated datum at 12m above sea level.

Test#	Cavity depths(m):			K's (m/s)			HEAD		Test#	Cavity depths(m):			K's (m/s)			HEAD	
	Top (m)	Btm (m)	mid (m)	Kch (m/s)	Kfh (m/s)	@K (m/s)	(AD) (m)	flux (cm³/min)		Top (m)	Btm (m)	mid (m)	Kch (m/s)	Kfh (m/s)	@K (m/s)	(AD) (m)	flux (cm³/min)
83	3.58	5.69	4.64	6.67E-06			0.22	226.56	38	78.50	80.61	79.56	1.10E-07			6.24	106.82
82	5.61	7.72	6.67	7.23E-06			0.26	295.45	37	80.56	82.67	81.62	1.82E-08			3.25	9.18
81	7.60	9.71	8.66	8.18E-08			0.54	6.85	35	81.52	83.63	82.58	3.01E-09			8.24	3.86
80	9.63	11.74	10.69	2.34E-06			0.86	313.70	34	83.52	85.63	84.58		3.49E-11		1.37	0.01
79	11.69	13.80	12.75	1.69E-06			0.62	162.41	33	85.51	87.62	86.57		1.39E-09		5.90	1.28
78	13.68	15.79	14.74		1.09E-08	4.55E-08	0.01	0.01	32	87.52	89.53	88.53		1.63E-11		2.34	0.01
77	15.69	17.80	16.75	1.07E-06			1.22	203.30	31	89.58	91.69	90.64		8.90E-12		-0.16	0.00
76	17.73	19.84	18.79	3.78E-07			1.24	72.78	30	91.59	93.70	92.65		2.18E-10		2.59	0.09
75	19.76	21.87	20.82		1.92E-08	1.87E-07	0.16	0.47	29	93.57	95.68	94.63	3.23E-09			3.18	1.59
74	21.73	23.84	22.79		1.68E-08		0.01	0.02	28	95.85	97.69	96.77	1.05E-07			6.44	104.92
73	23.75	25.86	24.81		9.57E-12	2.19E-12	1.16	0.09	27	97.56	99.67	98.62		1.22E-11		4.63	0.01
72	25.77	27.88	26.83		1.55E-08	1.22E-07	0.11	0.26	26	99.55	101.66	100.61		6.19E-11		2.28	0.02
71	27.73	29.84	28.79		1.76E-08	3.35E-08	0.06	0.15	25	101.58	103.69	102.64		3.09E-11		4.53	0.02
70	29.75	31.86	30.81		1.58E-08	8.17E-08	0.11	0.27	24	103.60	105.71	104.66		0.00E+00		0.00	0.00
69	31.68	33.79	32.74		1.26E-11	2.44E-12	5.57	0.01	23	105.62	107.73	106.68		1.41E-10		4.63	0.10
68	33.70	35.81	34.76		2.51E-11	5.54E-12	5.33	0.02	22	107.69	109.80	108.75		2.53E-11		2.08	0.01
67	35.74	37.85	36.80		1.54E-11	7.44E-12	1.38	0.00	21	109.71	111.82	110.77		1.16E-10		3.36	0.06
66	37.72	39.83	38.78		3.03E-09		0.67	0.31	20	111.77	113.88	112.83		2.47E-11		2.28	0.01
65	39.76	41.87	40.82		9.01E-09		0.55	0.77	19	113.74	115.85	114.80		3.68E-11		3.69	0.02
60	45.17	47.28	46.23		1.26E-11		0.64	0.00	18	115.49	117.60	116.55		2.67E-11		2.28	0.01
57	46.07	48.18	47.13		9.70E-09		0.64	0.96	17	117.55	119.66	118.61		1.71E-10		5.00	0.13
56	48.09	50.20	49.15		4.75E-11		2.67	0.02	16	119.59	121.70	120.65		2.78E-11		3.61	0.02
54	49.71	51.82	50.77		1.73E-11		1.42	0.00	15	121.60	123.71	122.66		1.43E-10		3.30	0.07
53	51.72	53.83	52.78		2.55E-11		5.47	0.02	14	123.57	125.68	124.63		3.23E-11		5.24	0.03
52	53.74	55.85	54.80	3.79E-07			6.92	407.42	13	125.55	127.66	126.61		4.56E-11		1.93	0.01
51	55.75	57.86	56.81	3.78E-06			7.08	4156.60	12	127.53	129.64	128.59	8.06E-10	9.42E-10		2.95	0.40
50	57.71	59.82	58.77		3.99E-11		5.30	0.03	11	129.54	131.65	130.60		4.51E-11		2.51	0.02
49	59.70	61.81	60.76		1.48E-12		1.67	0.00	10	131.54	133.65	132.60		4.03E-10		2.90	0.18
48	61.70	63.81	62.76		3.90E-10		1.57	0.10	9	133.55	135.66	134.61		1.02E-11		1.47	0.00
46	62.59	64.70	63.65	2.91E-09			4.55	2.06	8	135.54	137.65	136.60		9.81E-11		1.98	0.03
45	64.58	66.69	65.64		2.30E-11		2.69	0.01	7	137.54	139.65	138.60	4.68E-09			4.15	3.02
44	66.59	68.70	67.65	5.76E-09			3.10	2.77	6	139.59	141.70	140.65	1.04E-10	1.13E-10		3.92	0.07
43	68.58	70.69	69.64	1.79E-06			6.87	1913.87	5	141.60	143.71	142.66		7.09E-11		2.78	0.03
42	70.59	72.70	71.65	3.60E-07			6.72	375.70	4	143.60	145.71	144.66		1.22E-11		3.76	0.01
41	72.56	74.67	73.62	9.33E-09			6.62	9.60	3	145.58	147.69	146.64	2.21E-09			3.45	1.19
40	74.55	76.66	75.61	9.84E-09			6.25	9.56	2	147.59	149.70	148.65	7.00E-09			4.31	4.70
39	76.56	78.67	77.62	1.69E-07			6.37	167.66	1	149.59	151.70	150.65	9.97E-10			1.51	0.23

TOTAL CALCULATED FLOW FROM WELL: 7506.64 cm³/min head test was conducted. The configuration for the falling head test is shown in Figure 3.1b. This method of hydraulic conductivity testing was developed by Hvorslev (1951) for the purposes of testing granular porous media; however, it is also frequently used in the testing of fractured media. The relatively good agreement between the falling head and the constant head tests, described below, is an indication that the method is valid for fractured media which approximates porous media.

The test was conducted using a straight vertical translucent ¼" I.D. polyethylene tube on surface, attached to a vertical scale, referenced to the datum. As far as possible the head tube was filled (or emptied), prior to starting a test, so that the head in the tube was in excess of 2 m different from that measured in the cavity. The head tube was then connected to one of the tubes to the test cavity, with the other tube blanked-off on surface. The test was started by opening a valve between the head tube and the tubing to the cavity. Recordings of head level variations, with respect to time, were made as the test proceeded. The results of the test were interpreted using the Hvorslev (1951) method, after a line of best fit had been applied to the data points. A programmable calculator was used in the field, to check results. Once a line had been fitted to the data the hydraulic conductivity was calculated using equation 3.1:

$$K_h = \frac{d^2 Ln(\frac{2mL}{D})}{8L(t_2 - t_1)} Ln(\frac{H_1}{H_2}) \qquad \textbf{(Equation 3.1)}$$

Where,

K_h - Horizontal conductivity [L]/[T]

d - Diameter of falling head tube [L]

D - Diameter of test cavity [L]

t_1 - Time at start of test [T]

t_2 - Time at end of test [T]

H_1 - Head level in falling head tube at start of test [L]

H_2 - Head level in falling head tube at end of test [L]

L - Length of test interval [L]

m - Geometric factor, taken as 1

m is typically calculated using equation 3.1a:

$$m = \sqrt{\frac{k_h}{k_v}} \qquad \textbf{(Equation 3.1a)}$$

where

k_v vertical hydraulic conductivity

k_h horizontal hydraulic conductivity

The use of $m = 1$ implies that $k_v = k_h$ this assumption is worthy of further study and is probably not the case in Holyrood Granite. As is shown later a nearly vertical fracture set is the dominant water conduit in the Holyrood Granite which implies $kv >> k_{h.}$

This method (using the equipment configuration shown in Figure 3.1b) can be used to quantify hydraulic conductivity up to approximately 1×10^{-8} m/s (established by experimentation in the field). This upper limit is a result of pressure losses in the small diameter tubing, used to connect the head tube with the test cavity. Pressure losses in tubing are proportional to the length of the tubing and thus the method would work if the connecting tube length were reduced. The problem of an upper limit of measurement is discussed in the method comparison section.

3.2.4 Constant head tests

Where possible, constant head tests were also conducted to determine the hydraulic conductivity of the test intervals. Once the pressure head in an interval had been determined a constant head test was conducted by allowing outflow from the test cavity to exit (consecutively) at two different, but fixed, levels below the maximum established head level in the test cavity. The two outflow levels were selected to give a relatively large difference in elevation between each other. At each fixed head level the water from the cavity was allowed to flow until the flow rate was essentially constant. At this time the flow rate, height of the exit tube above datum, and cavity pressure were recorded (a pressure gauge having been attached to the second tube in the test cavity to get a true pressure reading in the test cavity). The measurement of pressure in the test cavity avoided problems of head measurement inaccuracy, resulting from head loss in the small diameter tubing, and also provided additional data on the magnitude of head losses associated with the measurement lines. The results of the constant head test were interpreted using the Thiem equation (Equation 3.2), which is valid for steady state groundwater flow conditions:

$$K = \frac{Q}{2\pi \Delta H L} Ln\left(\frac{r_e}{r_w}\right) \qquad \textbf{(Equation 3.2)}$$

Where

K - equivalent rock mass hydraulic conductivity

r_e - The effective radius [L]

r_w - The wellbore radius [L]

Q - Flow rate at constant head [L^3]/[T]

L - Length of test interval [L]

ΔH - Head difference between true formation head and head in the test cavity [L]

In all cases r_e was assumed to be 5 m. By rearranging equation 3.2, and assuming that the effective radius remains constant for differing cavity test pressures (e.g. 5 m), then hydraulic conductivity can be calculated from the two constant head tests at different cavity pressures, without knowing the true formation pressure (at distance r_e from the well bore) using equation 3.3:

$$K = \frac{Ln\left[\frac{r_e}{r_w}\right](Q_h - Q_l)}{2\pi L(h_l - h_h)} \qquad \textbf{(Equation 3.3)}$$

Where

h_h - head in the cavity with discharge tube at high level [L]

h_l - head in the cavity with discharge tube at low level [L]

Q_h - discharge rate from the cavity with discharge tube at high level $[L^3]/[T]$

Q_l - discharge rate from the cavity with discharge tube at low level $[L^3]/[T]$

Equation 3.2 can then be re-arranged and the true formation pressure, at the depth of interest, calculated. Figure 3.3 shows a comparison of the results of calculating formation pressure from constant head tests and from shut-in pressures. The graph showing these results and a line of best fit for the data is shown. In general there is excellent agreement between the two methods, with the method of calculating

Figure 3.3 Comparison of formation pressure heads calculated from shut-in pressures and calculated from constant head test data.

Tabulated Results

Test #	Shut-in (m)	Calculated (m)	Best fit (m)
7	4.43	4.15	4.56
29	6.36	6.44	6.29
35	2.49	3.18	2.82
37	3.86	8.24	4.05
38	6.31	3.25	6.25
39	6.46	6.24	6.38
40	6.16	6.37	6.11
41	6.62	6.25	6.53
42	6.72	6.44	6.62
46	4.12	4.55	4.29
52	6.92	7.56	6.80
76	0.97	1.24	1.46
77	1.03	1.22	1.51
80	0.88	0.86	1.38
81	0.36	0.54	0.91
83	0.21	0.22	0.78

Regression Output:	
Constant	0.590
Std Err of Y Est	1.428
R Squared	0.742
No. of Observations	16
Degrees of Freedom	14
X Coefficient(s)	0.897
Std Err of Coef.	0.141

RESULTS PRESENTED GRAPHICALLY

From Constant Head Test (m above datum)

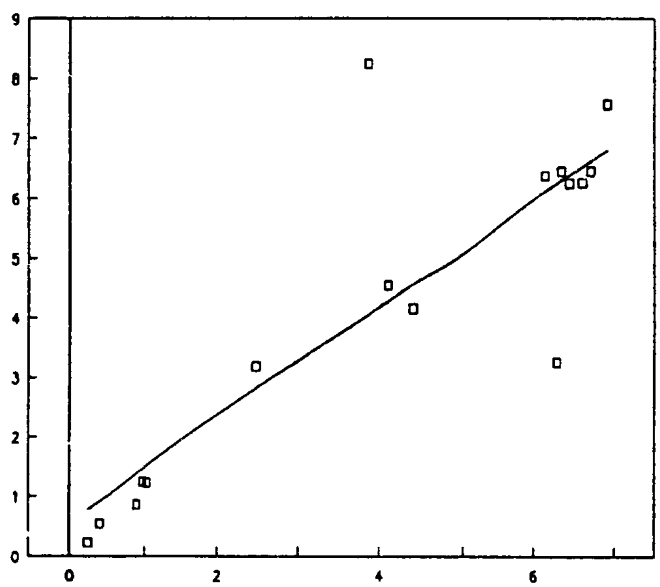

Formation head derived from shut-in pressure (m above datum) formation pressure from constant head tests providing marginally higher estimates of formation pressure.

3.2.5 Falling head test while measuring the test cavity pressure

Falling head tests were conducted with the cavity pressure being measured directly with a pressure gauge blanking-off the spare cavity tube. Using the Thiem equation each time interval of the test was interpreted, with the assumption that flow had reached steady state for the small intervals of the test. This then gave an "instantaneous hydraulic conductivity". All instantaneous hydraulic conductivities for each test were then averaged to provide a value of hydraulic conductivity. When compared with the Hvorslev method of interpretation the results differed by almost an order of magnitude (see Figure 3.4). The method of calculating instantaneous hydraulic conductivities is not considered to be particularly valid; however, it was used for those intervals which could not be tested using the constant head method and, furthermore, had hydraulic conductivities of approximately 1×10^{-8} m/s. Intervals with hydraulic conductivities of approximately 1 x 10-8 m/s, tested in this manner, account for less than 0.015% of the total estimated groundwater flux to the wellbore at NSCRV.

3.2.6 Comparison of Hydraulic Conductivity Testing methods

Figure 3.4 is a graph/table showing intervals whose hydraulic conductivities were measured using at least two of the three methods detailed above. There is a very good agreement in results between the constant head and falling head methods, where both methods were used. Unfortunately there is no comparison dataat hydraulic conductivities of $\geq 1 \times 10^{-8}$ m/s. Data from the third method is provided in Table 3.1. As noted above results from this method are believed to be the least reliable.

3.3 OVERVIEW OF HYDRAULIC CONDUCTIVITY AND HEAD MEASUREMENT RESULTS

A synopsis of the results of hydraulic conductivity and head measurements is provided in Table 3.1. The range of values measured is:

a) for hydraulic conductivity; from 1.48×10^{-12} to 7.23×10^{-6} m/s and,

b) for formation head; from -0.16 to 8.24 m (approximately 11.84 to 20.24 m above sea level) from datum, with only one interval having a negative head.

Using the hydraulic conductivity and the formation pressure data the flux for each interval was calculated using the Thiem equation (equation 3.2), with

Figure 3.4 COMPARISON OF PERMEABILITY MEASUREMENT METHODS USED AT NSCRV

Kch: Hydraulic conductivity from constant head test.
Kfh: Hydraulic conductivity from falling head test.
@K: Hydraulic conductivity from falling head test but using Thiem equation, P2 measured from cavity and and treating each time interval as const head test.
AD: Above specified datum

Test#	Cavity depths(m): Bottom (m)	top (m)	mid (m)	K's (m/s) Kch (m/s)	Kfh (m/s)	@K (m/s)	Head(AD) (m)	flux (cm³/min)
78	13.68	15.79	14.74		1.09E-08	4.55E-08	0.01	0.01
75	19.76	21.87	20.82		1.92E-08	1.87E-07	0.16	0.47
73	23.75	25.86	24.81		9.57E-12	2.19E-12	1.16	0.00
72	25.77	27.88	26.83		1.55E-08	1.22E-07	0.11	0.26
71	27.73	29.84	28.79		1.76E-08	3.35E-08	0.06	0.15
70	29.75	31.86	30.81		1.58E-08	8.17E-08	0.11	0.27
69	31.68	33.79	32.74		1.26E-11	2.44E-12	5.57	0.01
68	33.70	35.81	34.76		2.51E-11	5.54E-12	5.33	0.02
67	35.74	37.85	36.80		1.54E-11	7.44E-12	1.38	0.00
12	127.53	129.64	128.59	8.06E-10	9.42E-10		2.95	0.37
6	139.59	141.70	140.65	1.04E-10	1.13E-10		3.92	0.07

Log K vs Depth for three different permeability measurement methods

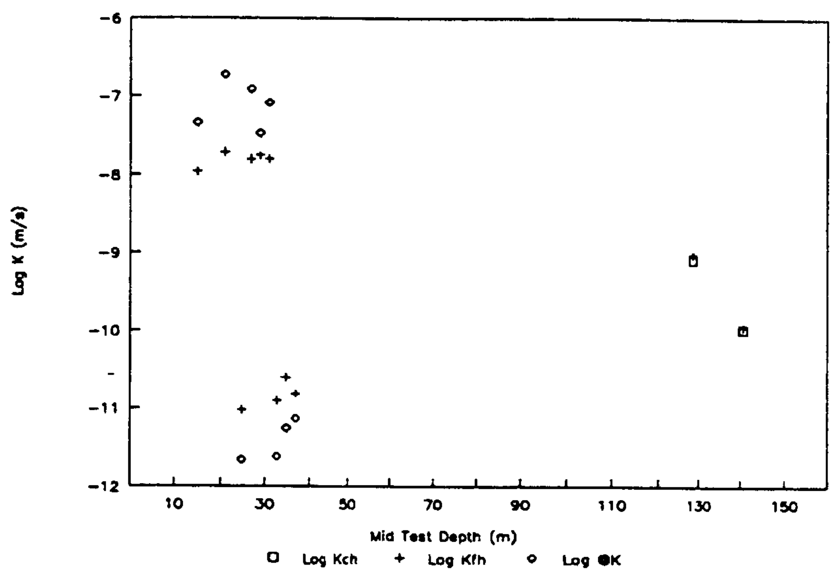

an r_e of 5 m, and an average hydraulic conductivity, for each interval calculated **only** from the average of the falling head and constant head interpretations. In the figure indicating the sum of the interval fluxes (given in non consistent units of cm3/min) no attempt has been made to correct the total estimated hole flux for the error associated with overlapping test sections. The integrated flow rate from the borehole of ~8 l/min approximates the value measured in the field of 10-15 l/min.

An 'average' hydraulic conductivity, for the entire hole section, was calculated using equation 3.4, given by Gutjahr et al. (1978) for porous media, and more recently used by Cacas et al. (1990) for interpretation of data from fractured media:

$$K_m = K_{geom}\left(1 + \frac{(\sigma_{\Sigma LnK}^2)}{6}\right) \qquad \textbf{(Equation 3.4)}$$

Where

Km - Estimated mean hydraulic conductivity [L]/[T]

Kgeom - Geometric mean of the all the punctual (small interval) hydraulic conductivity measurements

$\sigma_{\Sigma LnK}^2$ - Variance of the natural log of all the punctual hydraulic conductivity measurements.

The average hydraulic conductivity, calculated using equation 3.4 is 4.74 x 10−9 m/s. This figure will be used, as the value for hydraulic conductivity, for all subsequent hydraulic calculations. Figure 3.5 summarizes the hydraulic data (over the interval tested). It appears to show that the hydraulic conductivity is at a maximum over the shallowest 25 m of depth and again between 55 to 60 m and 70 to 80 m, below which it decreases again to a value of approximately 10−10 to 10−12 m/s. A smoothed value of hydraulic conductivity is also shown, calculated from the average of the two hydraulic conductivity measurements above and below the mid hydraulic conductivity measurement (a total of five measurements). Overall there is a slight trend of decreasing hydraulic conductivity with depth (Figure 3.6). A regression analysis applied to Log hydraulic conductivity versus depth gives a line of best fit with a formula:

$$Log\ K = 0.1925[Depth(m)] - 7.45796 \qquad \textbf{(Equation 3.5)}$$

The calculated correlation coefficient r, for this line is 0.468. The correlation is significant at the 95% level, using a two tailed test (Mendenhall and Sincich 1988). Figure 3.6 shows the hydraulic conductivity data, plotted against depth,

Figure 3.5 COMPARISON OF INTERVAL FLUX, FORMATION HEAD AND HYDRAULIC CONDUCTIVITY

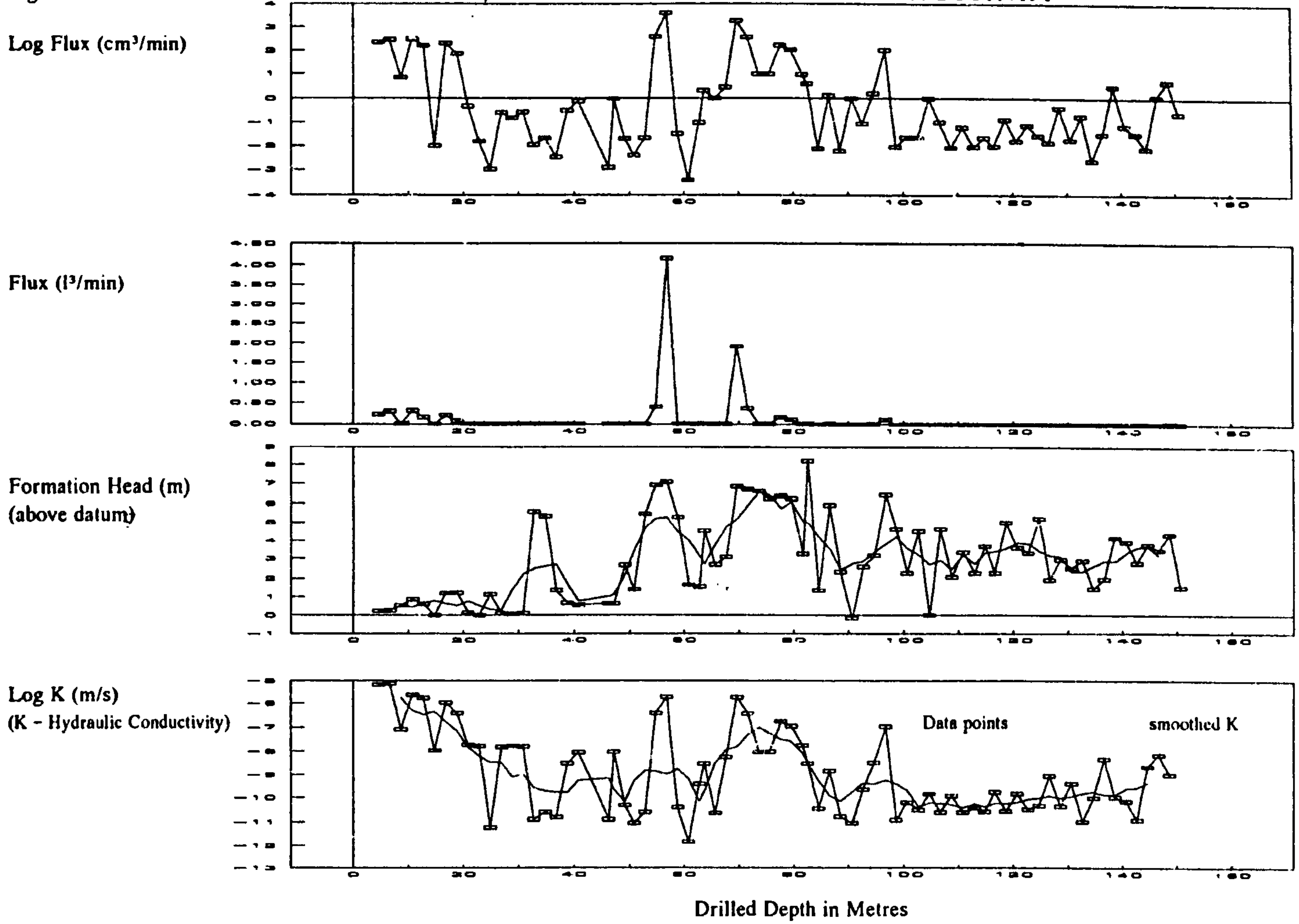

Figure 3.6 GRAPHS SHOWING PUNCTUAL HYDRAULIC CONDUCTIVITY AND LINE OF BEST FIT FOR CONDUCTIVITY MEASUREMENTS

Punctual Hydraulic Conductivities and Line of Best Fit

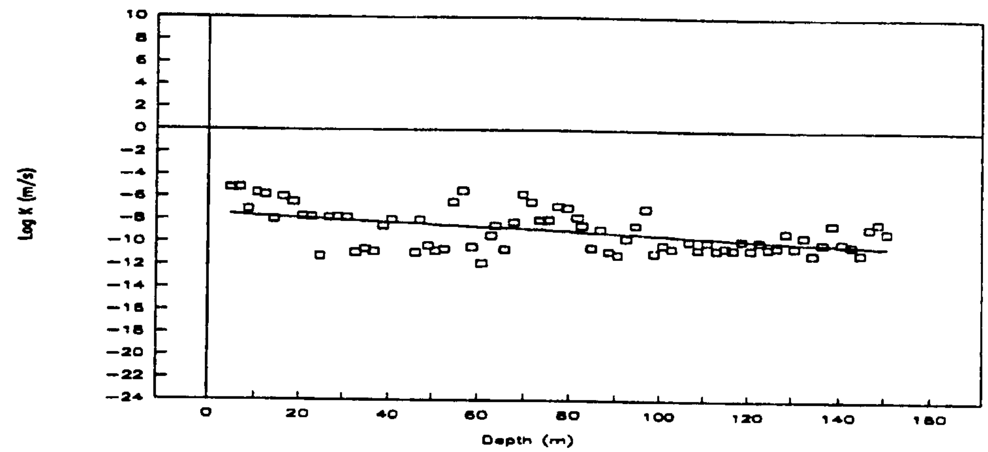

with the line of best fit. There is a recognisable trend of decreasing conductivity with depth.

As shown in Figure 3.5 the formation head appears to reach a maximum at the 55-65 m and 70-80 m at approximately 7 m above datum. The apparent decrease below this depth may possibly be real or it may be a result of insufficient time allowed for the pressure in the test cavity to equilibrate with the formation pressure. A smoothed head value, calculated in the same manner as for hydraulic conductivity is also shown.

The flux graphs, show that the significant flow from NSCRV is confined to approximately 5 zones, a top 20 m interval and then zones at 57, 70, 77 and 97 m. Of these zones the most significant, in terms of flux contribution to the borehole is the one at ~57 m. Figure 3.7 shows flux in conjunction with those fractures logged as open.

3.4 CONCLUSIONS

The results of hydraulic conductivity testing indicate that the major flow at NSCRV borehole (by volume) is from a few discrete fracture zones. However,the frequency of occurrence of high flow zones cannot be estimated from the data collected. The formation head varies from −0.16 to 8.24 m and the NSCRV borehole

Figure 3.7 Plots showing the open fractures/ metre logged and the hydraulic conductivities measured at NSCRV

Open fractures/ metre logged in the NSCRV core

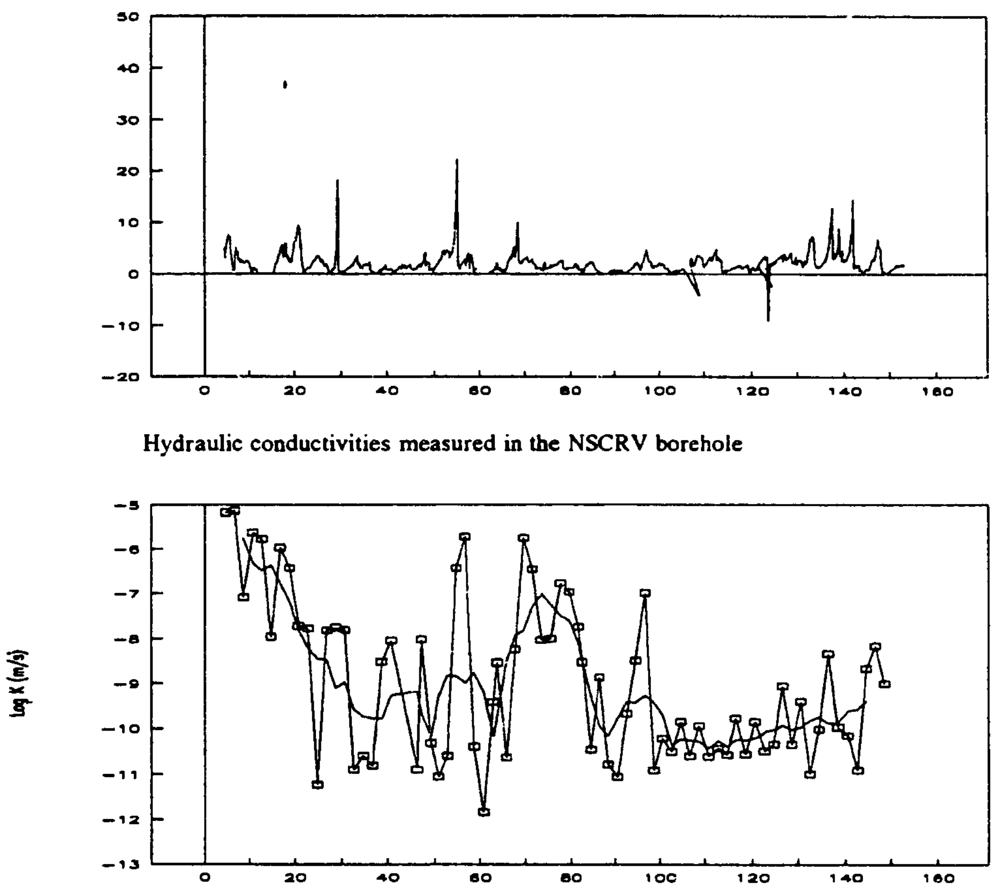

is artesian along virtually its entire length. The average hydraulic conductivity at NSCRV is 4.74 x 10^{-9} m/s calculated from hydraulic conductivity readings ranging from 1.48 x 10^{-12} to 7.23 x 10^{-6} m/s. This value is close to the hydraulic conductivity value (1 x 10^{-9} m/s) used by Nordstrom et al. (1985) as an average for preliminary modelling of flow in the Stripa Granite. The hydraulic conductivity shows a reduction with depth which can be estimated using equation 3.5.

CHAPTER 4: GEOCHEMICAL METHODS AND DATA QUALITY

4.1 DATA COLLECTED

4.1.1 Sampling methods

To ensure the collection of representative samples, and to avoid sampling-induced changes in water chemistry, a strict protocol was followed for groundwater sampling at the NSCRV location. The general nature of the sample suite collected at the NSCRV location and methods used for collection will be discussed in this chapter.

Any zones identified, during hydraulic conductivity testing as having significant hydraulic conductivity, were sampled prior to deflating the straddle packer system. Zones observed to have significant flow during drilling were also sampled (prior to hydraulic conductivity testing), either using the test tool run on the drilling rig wire line or run on 1" schedule 80 steel tubing. The interval tested, for samples collected while drilling, varied between 2.48 and 3.16 m. The depth control of the inflated tool, run on a wireline, was not believed to have been as accurate as for the tool run on the tubing string. It is estimated that the accuracy of placement of the tool run on a wireline was as poor as ±3 m, while placements of the tool made using the tubing string were probably in the order of ±5 mm per 3 m length of pipe run, leading to a range of accuracy of ±0.25 m at TD. All samples shown as having tool configuration 3/211R in Appendix C, were collected during hydraulic conductivity testing, and are believed to have the best depth control.

As all sampled intervals were artesian no pumping was required for sampling; therefore, all samples were collected under positive pressure and are free from degassing-induced chemical effects. The initial time series of samples from the interval 18.61 to 21.77 m was collected using 1/4" polyethylene tubing. All subsequent samples were collected through 3/16" polyethylene. The 3/16" sample tubing was contained in a 3–core bundle with a central wire strain member and an external sheath. The 3/16" bundle was held on a reel for ease of use and its entire length was used regardless of sampling depth: Thus regardless of depth, all samples were collected using the same tube having an invariant length. The sampling configuration used to collect each sample is listed in column five of Appendix C.

Any intervals with high flow rates were also sampled immediately after hydraulic conductivity testing. The test cavity length for this phase of sampling was 2.11 m and sampling was through two tubes, of the 3/16" three core bundle, joined together at surface to provide higher flow rates. For this phase of testing and sampling the tool was only carried on the end of rods.

Once sampling was started water flowing from the test cavity was carefully monitored to ensure the cavity was completely flushed. Approximately eight sample interval volumes (SIVs) were usually flushed before a final sample was collected from an interval. During sampling pH was measured using a Fisher Accumet pH/mV meter and pH electrode inserted in a plexiglass flow cell. The temperature compensating probe, of the pH meter, was inserted into a separate port in the flow cell. Temperature readings were apparently affected by sunlight and air temperature, especially in shallower intervals where much of the sample tubing length was above ground. As far as possible the on surface sample tubing was shielded from sunlight and kept cool.

As the time required to flush eight SIVs was sometimes in excess of 24 hours the pH meter was calibrated frequently. Stock pH solutions, brought to the temperature of the out-flowing water, were used for calibration. Conductivity was measured using a conductivity meter calibrated using 1000 μS calibration fluid. Wherever possible Eh readings were also taken using the pH meter with a platinum electrode and an Ag-AgCl reference electrode inserted into the flow cell, Eh readings were corrected to read Eh. A series of Eh readings were recorded after the last sample in a time series had been collected. Eh measurements were recorded until the Pt electrode potential had stabilised, sometimes requiring up to 2 hours.

At each sampling two 125 ml low density polyethylene bottles, previously leached with 30% HNO_3 and flushed three times with de-ionized, distilled water, were used for sample collection. Prior to collection the bottles were flushed a further three times, with the water to be sampled. Within 6 hours of the collection of a sample alkalinity measurements were made on unfiltered samples. A 20 ml aliquot of sample was added to a 50 ml beaker containing a pH probe. 0.0253N nitric acid was titrated into the sample and the pH versus titrant volume recorded. An end point was determined graphically from the first derivative of pH vs volume. Alkalinity was calculated using the formula:

(Equation 4.1)

$$\text{Total Alkalinity (as } HCO_3^-) \ (mg/L) = 61.\frac{\text{mls titrant x } [HNO_3]\,m}{\text{mls of acid used}}$$

All sample not used for alkalinity titration was filtered through a 0.45 μm cellulose nitrate filter. One filtered 125 ml aliquot was acidified with 1 ml of 16N ultrapure HNO_3 to be used for ICP-MS analysis. An unacidified sample was collected for analysis of SO_4^{2-}, Cl^- and F^- by HPLC. At the end of each time series a small (unfiltered) glass bottle was also collected for analysis of ^{18}O and ^{2}H.

4.1.2 Analytical Methods

A total of 27 major and trace elements, shown on the pull-out Appendix C, were analyzed on all samples by inductively coupled plasma mass spectrometry (ICP-MS). Li was analyzed, by ICP-MS, on six samples after the main ICP-MS analyses had been performed. Analyses for the elements Ca, Mg, Al, Fe, Si were carried out by flame atomic absorption (AA) and ICP-MS, while K and Na were analyzed only by AA. Analyses for the anions F^-, Cl^- and SO_4^{2-} were made using high performance liquid chromatography (HPLC) in conjunction with a variable wavelength UV detector operated in indirect photometric mode (Small and Miller, 1982). This provided analyses, for Cl^- and SO_4^{2-}, by two different methods (assuming all S detected by ICP-MS occurs as sulphate).

Oxygen-18 (^{18}O) analyses were made on a VG-Instruments PRISM isotope ratio, gas mass spectrometer. Sample preparation involved equilibrating 50 μL aliquots of sample with CO2 of known isotopic composition, in a sealed tube procedure described by Schillereff and Welhan (in prep). Deuterium (2H) analyses were made, at the University of Waterloo, on selected samples using the uranium reduction technique.

4.1.3 Quality of non isotope analyses

Data quality was checked initially by charge balancing four different combinations of data, derived from different analytical methods, using the formula

$$CBE=\frac{\Sigma zm_c-\Sigma zm_a}{\Sigma zm_c+\Sigma zm_a}\ x\ 100\% \qquad \text{(Equation 4.2)}$$

Where

z - is the number of charges on a particular ion

m_a - number of moles of a particular anion

m_c - number of moles of a particular cation

CBE - charge balance error

The value resulting from Equation 4.2 is referred to as the charge balance error (CBE) (Freeze and Cherry, 1979). The four different data set combinations (see final columns Appendix C), based on various combinations of analytical methods are:

i) **ICP:** All ICP-MS analyses with Na and K from AA and HCO_3 from alkalinity titrations.

ii) **ICP+AA:** As for i) but replace the ICP-MS analyses of Ca, Mg, Al, Cl, Fe and Si with those made using AA.

iii) **AA+HPLC:** As for ii) but replace the analyses of SO_4^{2-} and Cl^- by ICP-MS with analyses made using HPLC.

iv) **ICP+HPLC:** As for i) but replace the analyses of SO_4^{2-} and Cl^- by made by ICP-MS with HPLC analyses.

As can be seen in Appendix C, the average CBE, for any data combination from the final values, is always less than 5%. The maximum individual CBE is 8.13%. The average CBE for the ICP-MS data set is slightly larger than any of the selected combinations (though still only -1.02%), however the standard deviation of the CBE derived from this data set is the lowest of any of the sets, resulting in the smallest range of values around zero charge balance. For this reason the ICP-MS data set is selected for all chemical modelling calculations, with the exception of Fe which will be discussed below, Na and K which were only analyzed by AA, and F which was only analyzed by HPLC. It is noticeable that there is a general decrease in the absolute values of charge balance with increased SIV flushing during a time series, and that the final samples (in any of the time series) have the lowest value of CBE. For these reasons all chemical modelling will use the ICP–MS analyses of the final samples collected from each interval (see Appendix C), as these are likely to be the most representative (Robin and Gilham 1987), having been taken after the greatest sample interval flushing. In some cases, where a particular value for the last sample may be spurious (e.g. SO_4 value for 71.65 m interval), the average of the previous values in the time series was used.

Except for I, K, La, Mo, Na, P, Rb, Ti and U, element specific, data quality checks were also performed on all element analyses. The element specific checks were conducted either by performing linear regressions on elements analyzed by two different methods, and/or by analysing known USGS standards by ICP–MS. The results of these data quality checks are discussed below.

The results of linear regressions performed on element concentrations determined by two different analytical techniques for each sample are shown in Figures 4.1 and 4.2. Figure 4.1 presents ICP-MS analyses plotted against AA analyses and Figure 4.2 shows ICP-MS analyses plotted against HPLC analyses. The ICP-MS analyses are arbitrarily selected as the dependant variable. Normally this selection implies that there is no error associated with the independent variable. This is not the case with these data sets, resulting in a data quality interpretation which is only semi-quantitative.

Figure 4.1

ICP-MS analyses (ppm) vs AA analyses (ppm)

Calcium analyses

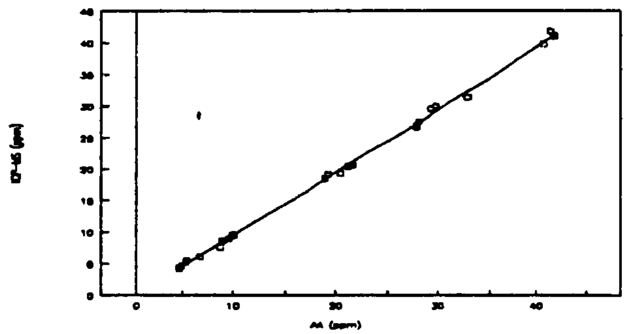

Calcium

Regression Output:	
Constant	-0.4204
Std Err of Y Est	0.4778
R Squared	0.9987
No. of Observations	27
Degrees of Freedom	25
X Coefficient(s)	0.9921
Std Err of Coef.	0.0071

Magnesium analyses

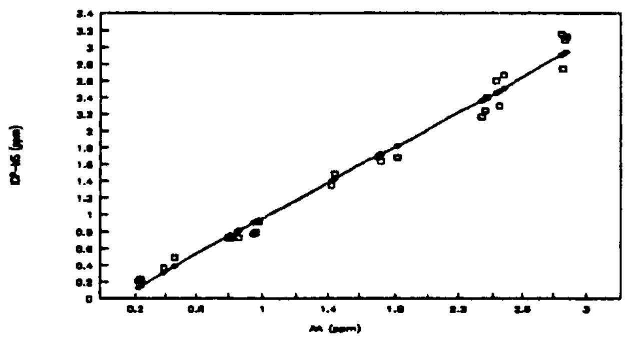

Magnesium

Regression Output:	
Constant	-0.1013
Std Err of Y Est	0.1254
R Squared	0.9852
No. of Observations	27
Degrees of Freedom	25
X Coefficient(s)	1.0573
Std Err of Coef.	0.0259

Silicon analyses

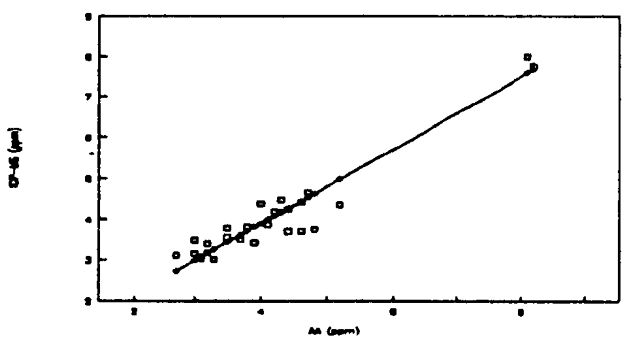

Silicon

Regression Output:	
Constant	0.2885
Std Err of Y Est	0.3724
R Squared	0.9330
No. of Observations	27
Degrees of Freedom	25
X Coefficient(s)	0.9026
Std Err of Coef.	0.0484

Figure 4.1 (continued)

Iron analyses

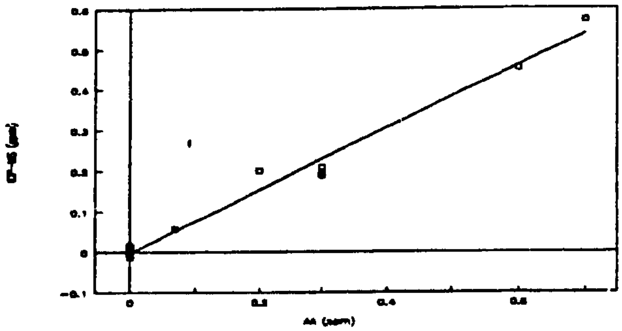

Iron

Regression Output:

Constant	-0.0012
Std Err of Y Est	0.0219
R Squared	0.9839
No. of Observations	19
Degrees of Freedom	17
X Coefficient(s)	0.7678
Std Err of Coef.	0.0238

Aluminum analyses

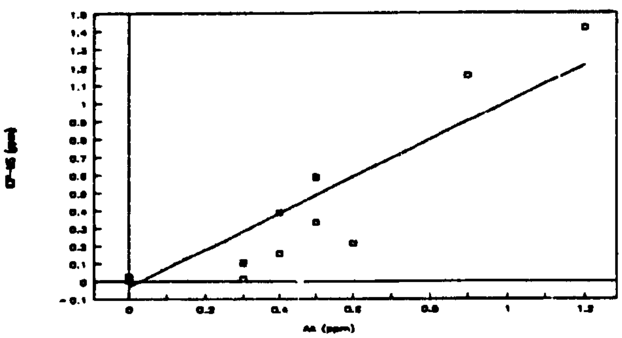

Aluminum

Regression Output:

Constant	-0.0293
Std Err of Y Est	0.1431
R Squared	0.8470
No. of Observations	27
Degrees of Freedom	25
X Coefficient(s)	1.0317
Std Err of Coef.	0.0877

Figure 4.2
ICP-MS analyses (ppm) vs HPLC analyses (ppm)

Sulphate

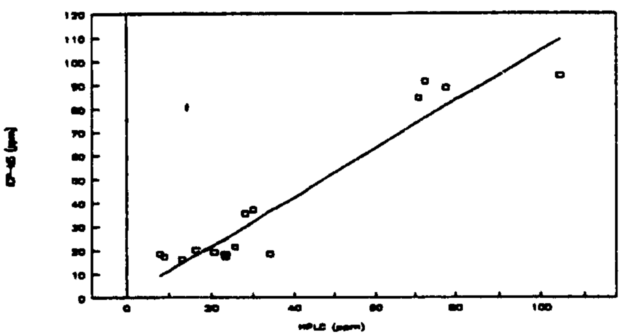

Sulphate

Regression Output:

Constant	1.0154
Std Err of Y Est	9.8233
R Squared	0.9074
No. of Observations	16
Degrees of Freedom	14
X Coefficient(s)	1.0348
Std Err of Coef.	0.0884

Chloride

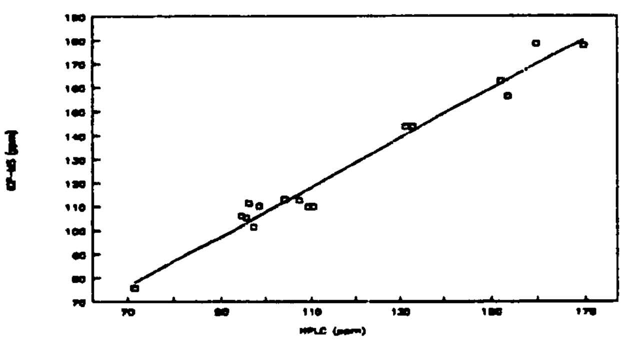

Chloride

Regression Output:

Constant	3.7671
Std Err of Y Est	5.3594
R Squared	0.9704
No. of Observations	16
Degrees of Freedom	14
X Coefficient(s)	1.0388
Std Err of Coef.	0.0485

If the analyses had been perfectly accurate the slope of the best fit line through the data sets would be +1, intercept 0 and coefficient of regression +1 (√Rsquared). The sum of the difference of the slope from 1 and the standard error of the coefficient, expressed in per cent is arbitrarily defined as:

(Equation 4.3)

Estimated Uncertainty =

± (Standard error of the X coefficient + Absolute value(1-x-coefficient) x100%

Based on the data in Figures 4.1 and 4.2 the likely ranges of uncertainties for the six elements [Ca, Mg, K, Si, Al, S (as SO_4^{2-}) and Cl], estimated using equation 4.3, ranges from 1.5-25.6%. A synopsis of error estimates, for the six elements listed above and derived using equation 4.2, is presented in Table 4.1. When one considers the large effect that SO_4^{2-} and Cl should have on the CBE (due to their high concentrations) then the low overall CBE's suggest that the errors associated individually with these two anions is smaller than that estimated by equation 4.3. No error value can be calculated for Na, but the analytical error is believed to be of the same order as Ca i.e.~1.5%.

The high correlation coefficient for the Fe analyses, in combination with the large deviation of the slope from +1, points to a systematic error in one of

Table 4.1 Relative analytical errors estimated by comparing different methods of analysis

Table 4.1 Relative analytical errors estimated by comparing two different methods of analysis.

Element	Slope of regression line	Relative %error (Calculated using Equation 4.3)	Coefficient of Correlation
Ca	0.992095	1.505	0.99935
Mg	1.057314	8.320	0.99259
Si	0.902595	14.577	0.96594
Fe	0.767820	25.600	0.99192
Al	1.031707	11.942	0.92030
SO4	1.034756	12.312	0.95256
Cl	1.033884	8.735	0.98508

the Fe analyses. The most significant source of error is believed to be in the ICP-MS analyses and is discussed below.

The analysis of USGS water standards gives further information about the quality of the NSCRV analyses. Table 4.2 is a compilation showing the average relative differences calculated using equation 4.4:

Table 4.2

COMPARISON OF GIVEN CONCENTRATIONS OF ELEMENTS IN USGS STANDARD WATERS WITH VALUES DETERMINED USING ICP-MS

All values in ppb except where noted

	Average relative differences										
Element	Full Range					Modified range				Lower limit of quantitation	
	# of analyses					#analyses					
		L.Limit (ppb)	U.Limit (ppb)	%	2d		L.Limit (ppb)	%	2d	ICP-MS	Mod.llq
Al	5	49.0	221.0	1.5	6.8					6.4	
As	5	3.7	77.0	24.1	60.7	1	77.0	-5.5	n/a	0.3	77.0
B	5	119.0	363.0	1.2	10.3					21.0	
Ba	5	7.9	191.0	-0.2	4.9					0.4	
Br	1	135.0	135.0	427.0	n/a		n/a			4.0	See text
Ca	5	11.5	70.0	-1.2	5.5					3332.8	11.5
Cd	5	1.9	14.3	0.8	11.7	4	2.9	-1.9	4.8	0.0	2.9
Cl(ppm)	6	46.0	508.0	-15.5	30.7	4	266.0	5.0	1.6	0.3	~70
Cu	5	17.0	76.2	-8.3	7.6	4	20.0	-6.6	4.0	0.4	20.0
Fe	5	7.0	159.0	-25.7	45.6	4	33.2	-14.4	7.4	47.8	?
Li	5	16.3	195.0	-0.3	4.5					ng	
Mg	5	2.1	60.4	-2.3	10.5					2.3	
Mn	5	7.2	68.0	-8.2	12.5	4	33.4	-5.2	4.8	0.2	33.4
Ni	5	6.0	54.0	-12.8	11.5					0.4	
Pb	5	8.6	34.6	3.4	9.4	4	10.9	1.3	4.9	0.2	11.0
Si	4	6877.0	24479.0	-0.5	4.5	3	145.5			145.5	
S ppm	6	25.0	182.0	-15.3	7.3					24.3	
Sr	5	61.0	1512.0	-1.9	4.6					0.0	
V	5	5.1	37.9	-2.5	9.4					0.2	
Zn	5	37.4	87.0	8.4	33.9	4	66.0	0.2	9.8	0.9	66.0

N.B. Lower and upper limits refer only to the range of standards analysed
2d is twice the standard deviation for the data set analysed
% represents % average difference of analysed values from known concentrations
See text for explanation of modified range
Si (as SiO_2)
S (as SO_4)

$$\%RD = \frac{\sum_{i=1}^{i=n} (usgs_i - ICP\text{-}MS_i)}{n} \qquad \textbf{(Equation 4.4)}$$

Where:

%RD	percent relative difference
$USGS_i$	published concentration of USGS sample n
$ICP\text{-}MS_i$	concentration of USGS sample n as measured by ICP-MS
n	number of samples tested

and the 95% confidence interval (2σ) for ICP-MS analysis of 20 different elements, at a variety of concentrations, in USGS water standards. The number of standards analyzed and the total range of their given concentrations is also shown, in the column titled 'Full Range'. Where it was obvious that the lower concentration standards analyzed were in error, those analyses were discarded and the lower limit of quantitation (llq) was raised to reflect the range of concentrations that were satisfactorily analyzed, as shown in the columns 'Modified Range', Table 4.2. The last two columns of table 4.2 show the llq:

a) as reported for ICP–MS analyses, as 10 x the standard deviation of the background for a particular element (Longerich et al. 1986).

b) from inspection of the analytical results of the USGS water standards (where applicable). Some of the llq's normally reported by ICP-MS appear to be too low as the machine is apparently not capable of accurate analysis at this llq (i.e., As, Cd, Cl, Cu, Fe, Mn, Zn), with the exception of the llq for Ca which is believed to be too high (pessimistic).

Of the 20 elements run as standards only 7 had absolute errors greater than 5%; however, all element data are considered to be usable. Analytical errors associated with specific elements are discussed below.

The ICP–MS Fe analyses demonstrate an extremely close linear correlation with the AA analyses (Fig 4.1), however with a slope significantly less than 1.0. Above a concentration of 33.1 ppb they show a relatively low standard deviation of analysis. In view of these facts and the -14.4% systematic error shown in the analyses of USGS standards (Table 4.2 modified range), the ICP–MS analyses will be used but will be corrected by a factor of 1.168 (calculated from 100/(100-14.4)) and used for all subsequent discussion.

The concentration given by the USGS for Br in their standard (Table 4.2) is considered to be dubious as the error range associated with the given concentration is essentially equal to the concentration given (135±130 ppb). The Br results measured using the ICP-MS are believed correct for the following reasons:

a) The most probable value listed for the USGS water standard is given as 135±130 ppb i.e. the concentration of Br in the standard is not accurately known,

b)all of the final sample values presented in Appendix C have Br/Cl ratios of 0.013, which is an unlikely coincidence if the error of analysis is as high as 427% (the average relative difference calculated for Br using equation 4.3)

c) a seawater sample collected from Conception Bay, diluted with distilled water and analyzed had a chloride concentration of 93.04 ppm and a Br concentration of 0.33 ppm, when analyzed by ICP−MS (Appendix C). The ratio of these values is within 0.12% of the Br/Cl mass ratio of seawater of 0.0036 (67ppm/18800ppm Krauskopf 1967). This indicates the probable accuracy and precision of the Br analyses, and further supports the contention that the given concentration of the USGS Br standard, is in error. No statement can really be made about the accuracy or precision of the Br analyses, though the llq can be set at 0.138 ppm as this is the lowest recorded Br concentration in the final sample data set.

The ICP-MS Cl analyses are considered to be good, especially at the concentrations found at NSCRV, with a maximum error of 5% and an uncertainty range of 1.6% at the 95% confidence interval.

As has been found in other studies (i.e. Nordstrom et al. 1985) the accuracy of the sulphate analyses are relatively poor, though they appear to be useable. Comparison of ICP-MS and HPLC analyses indicates a probable uncertainty of determination of 12.3%. Analysis of USGS sulphate standards indicated a systematic error of -15.3% for ICP–MS analyses. Using the latter value all ICP-MS values were corrected using the same method as for the Fe analyses.

Li was the only alkali element analyzed by ICP-MS. Li had very little error associated with its analysis (-0.3% average difference from the values given for the USGS standards). The alkaline earth elements (Mg, Ca, Sr, Ba) all had errors less than 2.3%, with a maximum 2σ deviation of 10.5% at the 95% confidence level.

The analytical error for Si is believed to be extremely low at -0.5% with an uncertainty of 4.5% at the 95% confidence level.

Though the iodine analyses were not checked by running standards it is believed (S.Jackson and H.Longerich, pers. comm., 1990) that the accuracy of the analyses is poor as a result of both instrument memory effects and the various oxidation states in which iodine may occur.

In conclusion the overall quality of the analyses for the NSCRV samples is believed to be high.

4.1.4 Quality of Isotope analyses

Isotope analyses were performed on 17 samples for $^{18}O/^{16}O$ and 7 samples for $^{2}H/^{1}H$. The results of all isotope analyses are shown in Appendix C. Table 4.3 shows, in detail, the results of all laboratory ^{18}O analyses on both samples and standards. From repeat analyses it was determined that the average standard deviation (σ) of the differences between all repeats was 0.08 ‰. From this value the ^{18}O analytical error (2σ), comprised of both machine and sample preparation errors, was estimated to be ±0.16 ‰. Only one repeat was conducted for the ^{2}H analyses, with a difference of 1.68 ‰. The value assigned to the analytical error for all the ^{2}H analyses was ± 1.68 ‰, which is comparable to the 2σ uncertainty reported by the lab that performed the analyses (University of Waterloo).

Table 4.3 COMPOSITION OF ALL 18O ANALYSES. ALL SAMPLES PREPARED, EXTRACTED AND ANALYZED TOGETHER

>>>NOTE: All standard deviations are unbiased estimates

			AVERAGES			
Sample	Prep#	dO	Batch	Sample	Prep#	dO
NSCRV4B	NS1	-8.598	<NS1>	TW	NS6	-5.713
NSCRV10A	NS2	-8.311		TW	rpt*NS6	-5.679
NSCRV3A	NS3	-8.306		TW	NS7	-5.501
NSCRV5C	NS4	-8.036		TW	rpt*NS7	-5.501
NSCRV5B	NS5	-8.361		TW	NS8	-5.605
TW	NS6	-5.713			average:	-5.600
TW	rpt*NS6	-5.679			std.dev:	0.1057
TW	NS7	-5.501				
TW	rpt*NS7	-5.501				
TW	NS8	-5.605				
NSCRV3D	NS9	-8.498	<NS2>	TW	NS15	-5.622
NSCRV1C	NS10	-8.269		TW	NS24	-5.578
NSCRV4C	NS11	-8.481			average:	-5.600
NSCRV7B	NS12	-8.271			std.dev:	0.0324
NSCRV4A	NS14	-8.424				
NSCRV6A	NS17	-8.213				
NSCRV3B	NS18	-8.366				
NSCRV3C	NS19	-8.407				
NSCRV8A	NS20	-8.337				
NSCRV7A	NS21	-8.454				
NSCRV11A	NS22	-8.215				
TW	NS15	-5.622				
TW	NS24	-5.578				
NSCRV5A	NS25	-8.209	<NS3>	TW	NS29	3.522
NSCRV2D	NS26	-8.330				
NSCRV3D	NS27	-8.572				
NSCRV4C	NS28	-8.481				
TW	NS29	-5.600				

DATA QUALITY CHECKS

BETWEEN RUN REPEATS

NSCRV3D	NS9	-8.498
NSCRV3D	NS27	-8.572
	average:	-8.535
	std.dev:	0.0735
NSCRV4C	NS11	-8.481
NSCRV4C	NS28	-8.481
	average:	-8.481
	std.dev:	0.0007

*rpt: refers to the repeat of an individual preparation on the prism

RESULTS OF UNCORRECTED TW'S

<NS1>	TW	NS6	3.394
	TW	rpt*NS6	3.427
	TW	NS7	3.601
	TW	rpt*NS7	3.601
	TW	NS8	3.499
		average:	3.5044
		std.dev:	0.1073
<NS2>	TW	NS15	3.430
	TW	NS24	3.472
		average:	3.451
		std.dev:	0.042
<NS3>	TW	NS29	3.522
Total averages:			3.493
Total SD's:			0.0823

4.1.5 Quality of pH and Eh measurements

Great care was taken in the calibration of the pH meter and in field pH measurement. The pH buffer solution temperatures were always allowed to equilibrate with out-flowing sample prior to calibration of the pH meter. All bubbles were removed from the flow cell and a great deal of effort was expended ensuring that the sample tubing was gas free. The relatively high specific conductance of the samples (usually >500 μS) taken at NSCRV indicates that ionic strength is high enough to expect that pH readings stabilise quickly.

Despite the efforts made to ensure accurate pH readings, inspection of the variability of pH readings, over a time series (Figure 4.3), reveal that the pH readings vary by ±0.15 pH units. This is more than an order-of-magnitude higher than the expected accuracy of pH readings of ±0.01 pH units, under static conditions. Whether the variations in pH readings reflect true variations in groundwater pH, or whether they are a function of instrument errors, or fluctuations in field environmental conditions is not known. However, this variation in pH is comparable to those reported by Bottomley et al. (1984) during the sampling of groundwater in fractured granite rocks. The effect of errors in pH on calculated mineral saturation indices is discussed in Chapter 8.

Figure 4.3 VARIATION OF pH MEASUREMENTS, VERSUS AMOUNT OF SAMPLE INTERVAL FLUSHING FOR SELECTED SAMPLE INTERVALS: DEGREE OF INTERVAL FLUSHING IS MEASURED IN NUMBER OF VOLUMES DISPLACED (SIV's)

Mid Sample Point 56.81 m

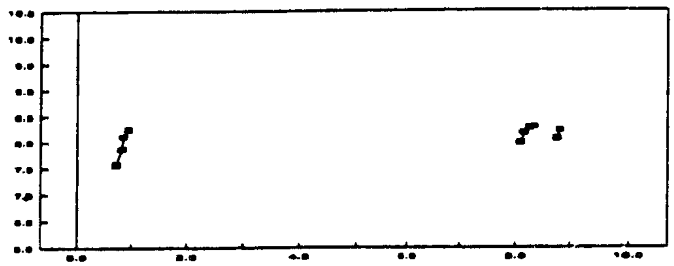

Mid Sample Point 74.91 m

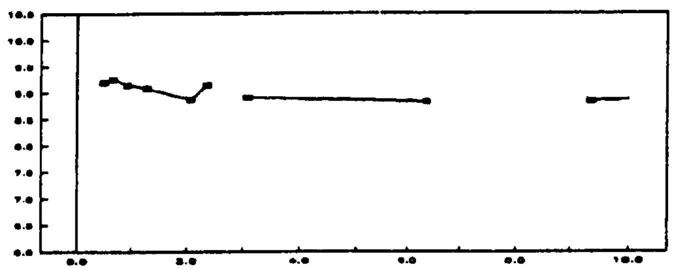

Mid Sample Point 77.41 m

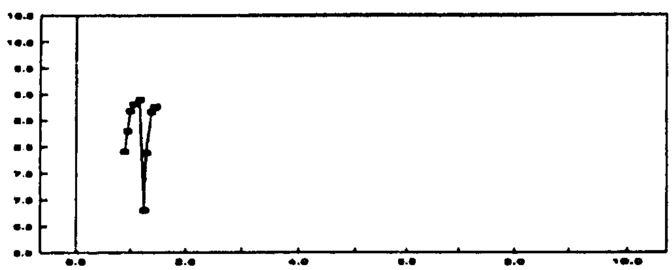

Mid Sample Point 97.41 m

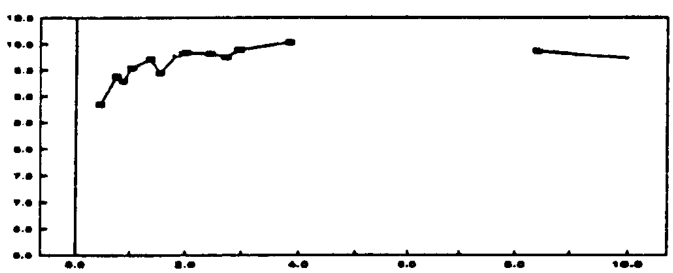

No statement regarding the accuracy of Eh measurements can really be made since no standardization or calibration checks (other than shorting the instrument to zero the voltmeter output) were performed. The reported Eh values should be used with caution.

The accuracy of alkalinity titration was ±0.1 ml of standard acid. This translates to an accuracy of alkalinity determination ranging from ±5 to ±10% for the highest to the lowest alkalinity samples at NSCRV. The effects on calculated mineral saturations on inaccuracies in alkalinity measurements will be discussed in Chapter 8.

4.1.6 Efficacy of sample interval flushing

Of the 9 intervals sampled, 6 had more than 2 samples collected over a time series. Some major parameters from the six intervals have been plotted against the number of SIV's flushed prior to collection of a sample, and are presented on Figure 4.4. The presentation of the data in this manner is intended to:

a) justify the general use of the final sample, in any time series, for subsequent chemical modelling,

Figure 4.4 GRAPHS SHOWING EFFECT OF FLUSHING SAMPLING CAVITY ON SPECIFIC ELEMENTS: CONCENTRATION VS SIV FLUSHED (CONCENTRATION IS THE CONCENTRATION AT THE INITIAL SAMPLING DIVIDED BY CONCENTRATION AT SUBSEQUENT SAMPLINGS)

20.19 m

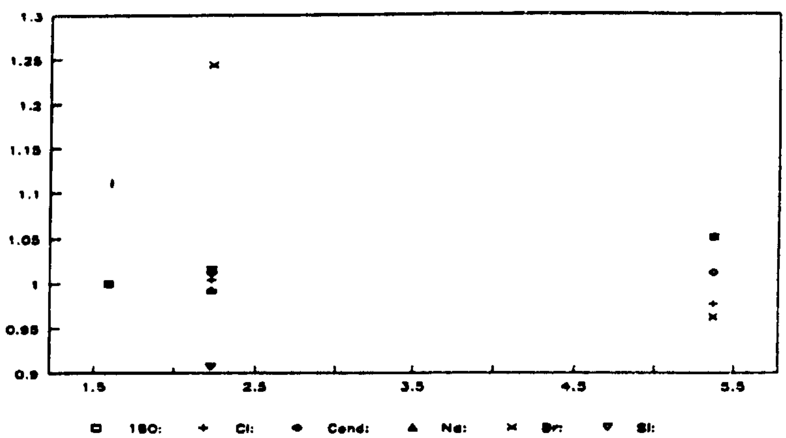

56.81 m

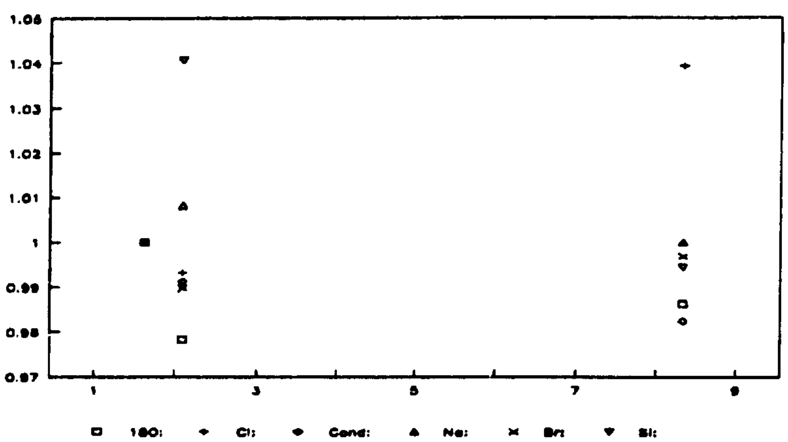

71.65 m

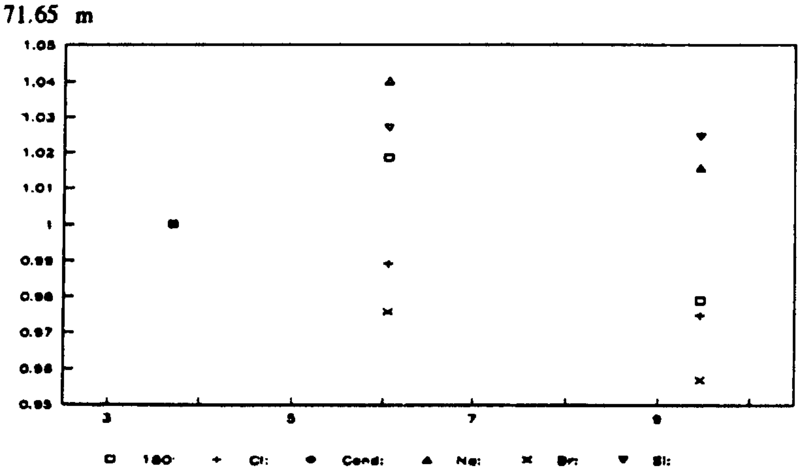

Figure 4.4 (continued)

74.91 m

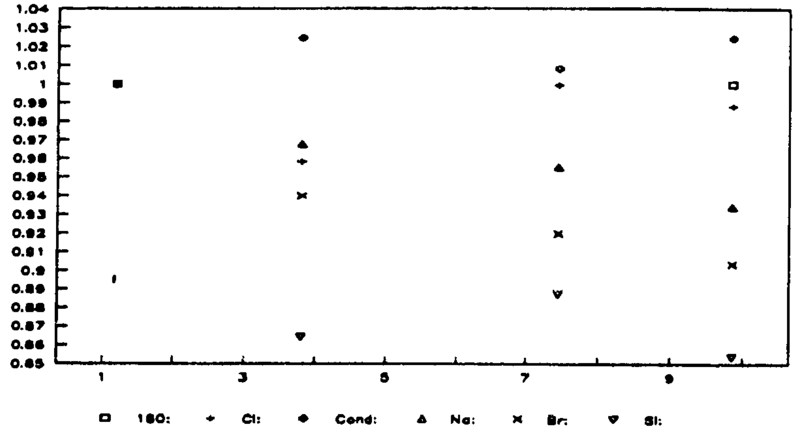

96.64 m

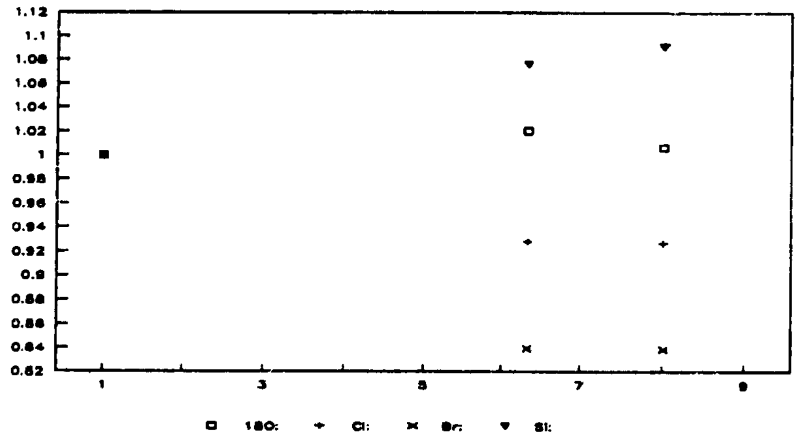

97.41 m

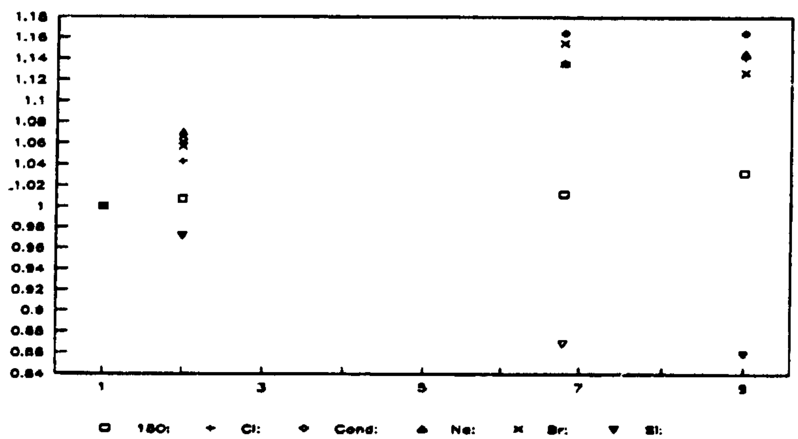

b) show that all members in a time series (of any particular element) are relevant and,

c) that they can be used to identify spurious analyses (in a time series) resulting either from sampling or analytical errors.

The parameters plotted against SIV are Cl^-, Br^-, Na^+, Si, ^{18}O and conductivity. Of the selected parameters Cl^-, Br^- and ^{18}O are the most conservative and are believed to be the best indicators of the effect of flushing on the sample interval. Chloride has the lowest uncertainty and is considered to be the most reliable indicator of sample flushing. Conductivity should also be a good indicator of sample interval flushing. Na^+ and Si will be relatively poor indicators of the success of sample interval flushing as they will be affected by chemical reactions (such as precipitation or solution of aluminosilicates).

In general, time variations in Cl^- and Br^- concentrations follow each other. ^{18}O values show relatively little variation over a time series; for this reason the value of ^{18}O for the last sample in the 71.65 m time series is considered spurious and is not used in discussion of variations in ^{18}O values. As the ^{18}O values selected as being representative, are not necessarily the last ones in a time series (whereas all other parameters are) the ^{18}O selected for discussion are summarized below in Table 4.4.

Table 4.4. $\delta^{18}O$ values selected as being representative of virgin formation water at NSCRV

Depth (m)	Sample I.D.	SIV's flushed	$\delta^{18}O$
18.77	11(17)	1.70	-8.215
56.81	10(2)	8.50	-8.311
69.64	8(5)	8.32	-8.337
71.65	5b(14)	6.05	-8.361
74.91	2d	9.85	-8.330
96.64	4c(3)	8.01	-8.481
97.41	3d(16)	9.00	-8.572

Si frequently displays a trend in concentration, with increased flushing, which is opposite to the concentration trends for the two halogens. The relatively monotonic variations in the parameters Cl^-, Br^-, Na^+, Si, ^{18}O are taken as further evidence that the quality of analyses from NSCRV is good. It should be noted that Br shows relatively more change, through a time series, in the deeper sample intervals.

4.2 CONCLUSIONS

The NSCRV geochemical data set is of good quality; however, analyzed values of SO_4 and Fe will be corrected before use for chemical modelling. The analysis of samples during flushing of sample intervals, prior to collection of a final sample, further supports the reliability of the analytical data and final sample values will be used for all subsequent geochemical modelling. The corrected final ^{18}O values presented in Table 4.4 will be used for all subsequent discussion of ^{18}O.

CHAPTER 5: GEOCHEMICAL TRENDS AT NSCRV

5.1 OVERVIEW OF WATERS AT NSCRV

In this chapter variations of groundwater chemistry that occur with depth in the NSCRV borehole are described using three different approaches:

a) variations of single chemical parameters versus depth and permeability,

b) variations of bulk groundwater chemistry versus depth described using Piper diagrams,

c) variations of groundwater chemistry with depth described using mineral stability diagrams.

5.1.1 Variations of single chemical parameters with depth and permeability.

Many of the chemical parameters analyzed show a distinct linear correlation with either depth or hydraulic conductivity and, in some cases, with both parameters. This is not surprising as the hydraulic conductivity is itself correlated with depth.

Five geochemical parameters have been selected to illustrate the correlation with depth and hydraulic conductivity (K): Si, Cl^-, ^{18}O, Na^+ and Li^+. Graphs of these parameters versus hydraulic conductivity and depth are shown on Figure 5.1 together with the results of linear regression analyses. A line of best fit, calculated from the results of the regression analyses, is plotted on each graph. To test whether either hydraulic conductivity and/or depth are correlated with the chemical parameter of interest, a statistical test using the test statistic r (correlation coefficient) as an estimator of **rho** (the population correlation coefficient) was conducted (see Mendenhall and Sincich 1988). Table 5.1 shows the results of this exercise. Where the test indicates that hydraulic conductivity and/or depth contribute some information about the value of a particular chemical parameter, that table entry is shaded.

Table 5.1 Results of statistical test to determine the statistical significance of the correlation of hydraulic conductivity or depth with concentration of an element

# samples	Parameter	x - K (r)	x - Depth (r)	significant for r > t (t)
8	Si	0.9381	0.5831	0.707
8	Cl	0.8367	0.7348	0.707
7	$\delta^{18}O$	0.7416	0.9008	0.754
8	Na	0.8775	0.8307	0.707
5	Li	0.9231	0.9887	0.878

Table 5.1 suggests that information about the likely concentration of Si can only be gained from hydraulic conductivity, and about the likely value of ^{18}O only

Figure 5.1 GRAPHS SHOWING CORRELATION OF ELEMENT CONCENTRATION WITH BOTH LOG HYDRAULIC CONDUCTIVITY (K) AND DEPTH.

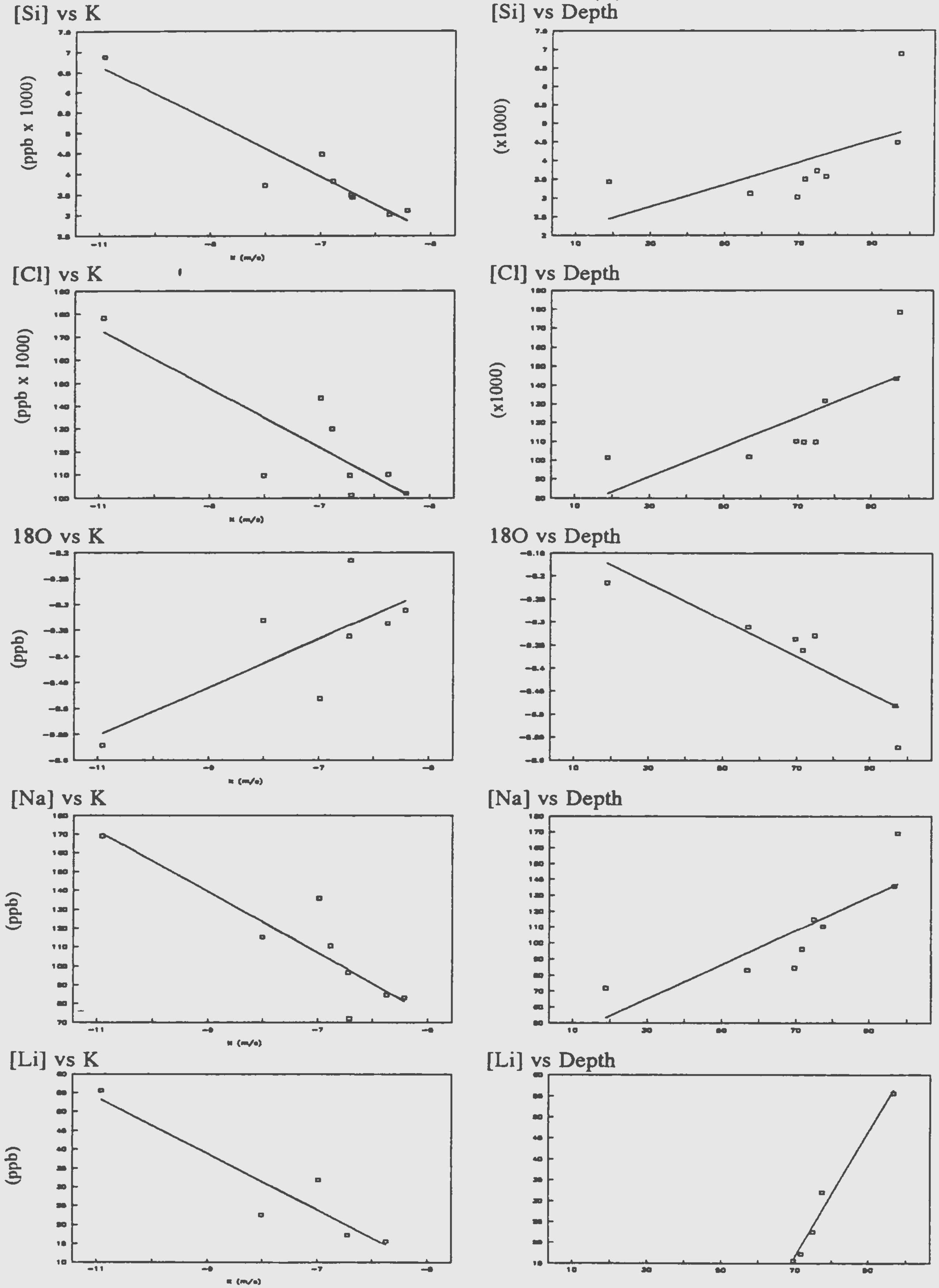

from depth. The implications of this will be discussed more fully in subsequent chapters. Briefly, it is suggested that the correlation of ^{18}O with depth is a reflection of the nature of flow through the Holyrood Granite. That is, above a certain scale length or representative elemental volume (REV), flow is relatively ordered, and flow in the aquifer can be approximated using a simple porous media model. The only statement that can be made about the size of the REV in the Holyrood Granite is that it is less than the scale length of the borehole (100 m) and possibly as large as 20 m (borehole length divided by the number of sample intervals showing monotonic chemical and isotopic variations). The correlation of increasing concentration of Si with decreasing hydraulic conductivity, alone, suggests that higher degrees of rock water interaction and silicate dissolution in stagnant low permeability zones determine Si concentrations, rather than mixing or flow between REVs within the aquifer/fracture system.

5.1.2 Description of variations of bulk groundwater chemistry with depth: Piper diagrams

The inorganic geochemical data from NSCRV can also be described using Piper diagrams. This simple method of description gives an indication of the bulk changes in groundwater chemistry with depth and points towards a mechanism by which the NSCRV waters may have evolved to their present chemistry.

Relative abundances (as milliequivalents) of the major ions (Ca, Mg, Na+K, Cl, HCO_3+CO_3, SO4) are shown on the Piper diagram (Figure 5.2). The data points representing the relative ion concentrations of the deepest and shallowest waters at NSCRV are identified on Figure 5.2 as **D** and **S** respectively. The point labelled **SW** represents seawater composition. The Piper diagram reveals that the shallow waters at NSCRV evolve from being Ca-Na-bicarbonate (with minor chloride) to being an Na-Cl type water with some bicarbonate. The trends of the data points in the cation and anion trilinear fields seem to suggest that bulk groundwater chemistry either evolves (with depth) towards a seawater-like composition, or possibly a modified seawater composition depleted in SO_4 and Mg. Alternatively it may define a mixing relationship between two end members. However, the non-linear composition trend shown in the central diamond field indicates that simple mixing, alone, cannot explain the major ion trends.

The progressive change in water chemistry shown in Figure 5.2 is believed to be evidence that the shallow waters may have evolved, in part, by mixing with seawater and in-part by rock-water interaction. As is apparent in the Piper diagram even the shallow waters have a large fraction of Na and Cl, which may be evidence of a significant seawater component. The hypothesis of saltwater mixing, coupled with rock water interaction, will be pursued in Chapter 8.

Figure 5.2 PIPER DIAGRAM FOR NSCRV SAMPLE ANALYSES AND SEAWATER

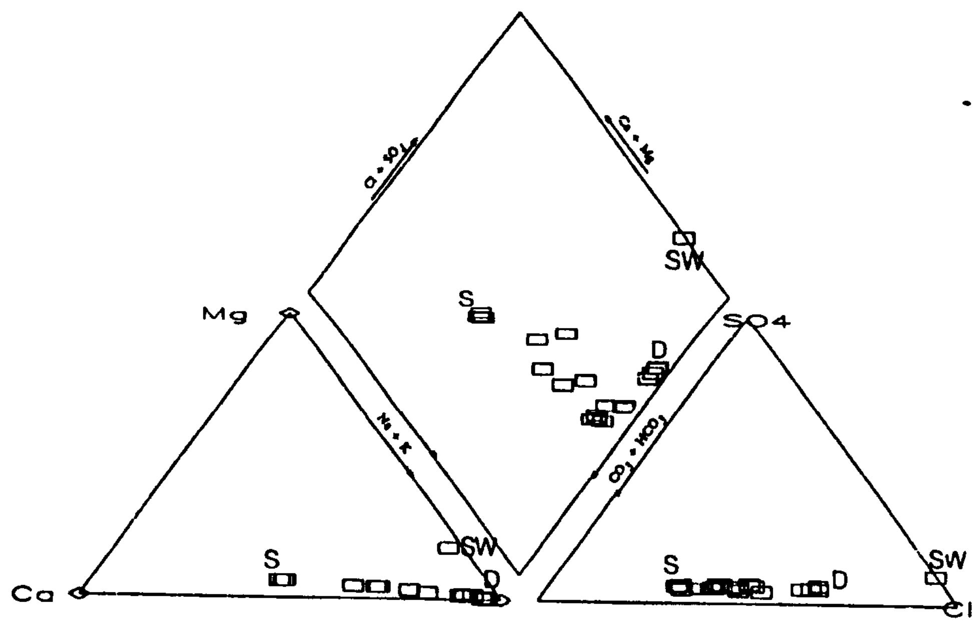

SYMBOLS INDICATE:

D Deepest sample interval
S Shallowest sample interval
SW Seawater

5.1.3 Description of variations of groundwater chemistry with depth: Mineral stability diagrams.

The construction of mineral stability diagrams is outlined in Garrels and Christ (1965). Before describing the NSCRV waters in the context of mineral stability diagrams an important factor should be considered:

The positions of the phase boundaries on the diagrams are dependant on the thermodynamic data used to construct the phase diagrams. The differences between the values of thermodynamic properties of identical minerals (for the enthalpy and equilibrium constant, or free energy, of the mineral dissociation reaction), published by different researchers, is usually small; however, even small differences in thermodynamic data values may result in large differences in the estimated positions of calculated mineral stability boundaries. To illustrate this point the mineral stability diagram in Figure 5.3 shows mineral stability boundaries in Log [K]/[H] vs Log[H_4SiO_4] space, constructed with the thermodynamic data of a variety of workers. The thermodynamic data was derived from Helgeson et al. (1978), Hemingway et al. (1982) and data supplied in a modified data base (See Appendix D for explanations of modification of pyrophyllite data) by Lindberg, R.D 1986 et al. (unpublished). Data which is internally inconsistent confounds Gibb's Phase Rule and appears

Figure 5.3 MINERAL STABILITY DIAGRAMS CONSTRUCTED FOR COMPARISON OF THERMODYNAMIC DATA

NOTE: Lines not meeting at triple points highlight inconsistent thermodynamic data

Data of Helgeson et al (1978)

Log [K]/[H] vs Log[H4SiO4]

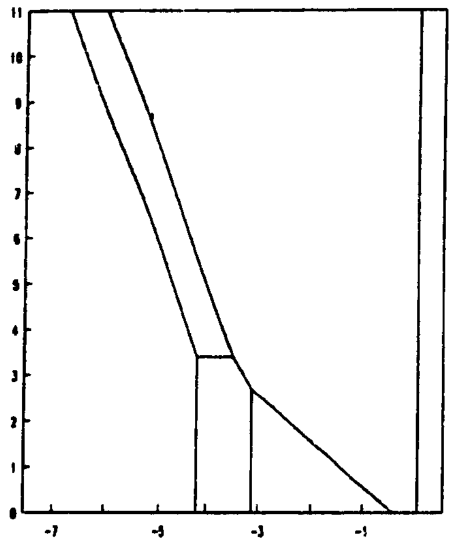

Data of Hemingway et al (1982)
(1982) with that of Robie et al (1978)

Log [K]/[H] vs Log[H4SiO4]

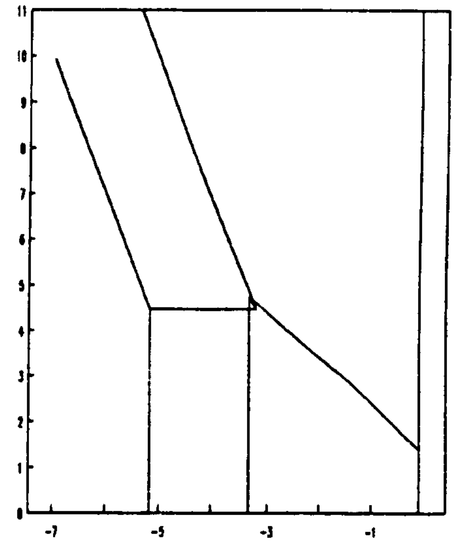

Data from PHRTHERM

Log [K]/[H] vs Log[H4SiO4]

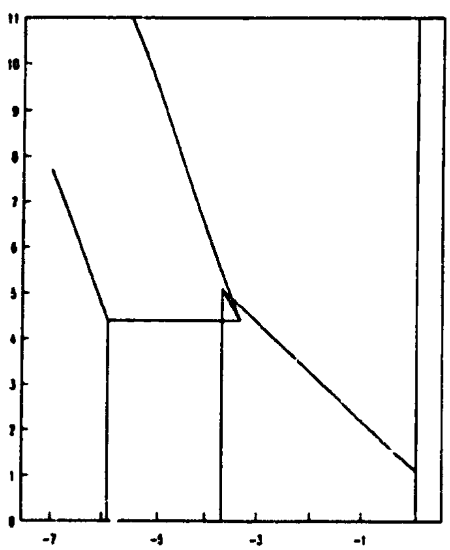

Data from PHRTHERM:Sign of LogK pyrophyllite changed from original PHRTHERM

Log [K]/[H] vs Log[H4SiO4]

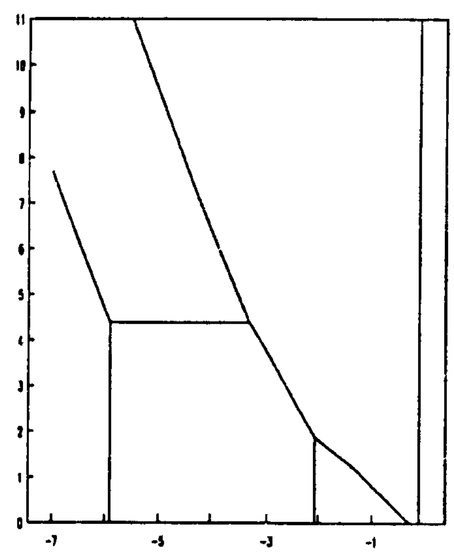

as non-meeting "triple points" on Figure 5.3. The evaluation of the stability of minerals with which waters may be in equilibrium may be in error due to inconsistencies in the thermodynamic data used to calculate stability boundaries. Appendix D describes in detail the comparison of various data bases and concludes, (partly on the basis of consistency and partly on the basis of usage by various authors) that the Helgeson thermodynamic data base is the most reliable, this is reflected in its internal consistency, at least for the low ionic strength silicate system. This is the data base used for subsequent discussions and the modelling of the common minerals with PHREEQE (using the HELGTHEM data base, see Appendix D and E). Additional discussion of the data base is provided in Chapter 8.

In some instances it may be difficult to rationalize the saturation states of aluminosilicate minerals, as derived using mineral stability diagrams and geochemical modelling with programs such as PHREEQE. This is illustrated in the following example:

Figure 5.4 shows the locations of data points which represent the compositions of the NSCRV waters sampled, average seawater (Nordstrom et al. 1979), and average seawater equilibrated with anorthite, using PHREEQE/HELGTHEM, for the four spaces Log{Na}/{H}, Log{K}/{H},

Figure 5.4 MINERAL ACTIVITY STABILITY DIAGRAMS CALCULATED FROM THE DATA OF HELGESON ET AL (1978)

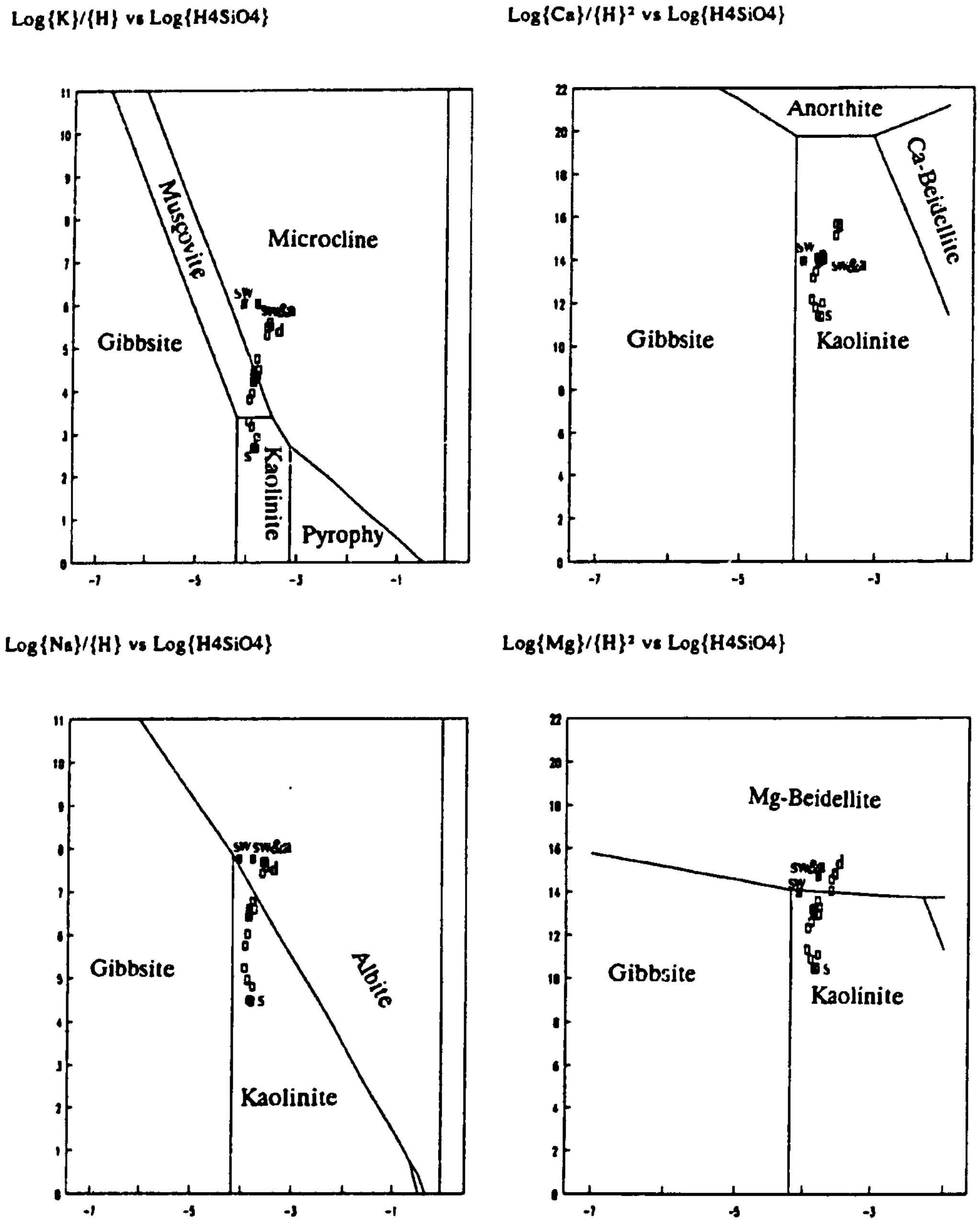

S-shallowest D-deepest SW-seawater SW+A seawater equilibrated with anorthite

$Log\{Mg\}/\{H\}^2$ and $Log\{Ca\}/\{H\}^2$ vs $Log\{H_4SiO_4\}$. Of particular interest is the location of the point representing seawater, equilibrated with anorthite, in $Log\{Ca\}/\{H\}^2$ vs $Log\{H_4SiO_4\}$ space. The point is well outside the anorthite stability field, in the kaolinite stability field, and reflects the paucity of Ca in seawater relative to the activities of other elements.

Points in Figure 5.4 representing shallowest (S), and deepest (D) waters are identified as are points which represent average seawater composition (SW), and average seawater composition equilibrated with anorthite (SW+A). The diagrams show the stability fields of common aluminosilicates in terms of ions. Activities of elements were calculated using PHREEQE with the HELGTHEM data base.

For all the diagrams shown, with the exception of $Log\{Ca\}/\{H\}^2$ vs $Log\{H_4SiO_4\}$, the NSCRV waters show a trend, with increasing TDS, towards a composition which approximates seawater (in terms only of the elements presented on the diagrams), but with a higher concentration of H_4SiO_4. The higher concentration of H_4SiO_4 may be a result of rock water interaction. Hydraulic conductivity has previously been shown to display a strong inverse correlation with concentration of H_4SiO_4: The decrease in H_4SiO_4 activity shown by the mid samples is believed to reflect the permeability variations in the sample intervals (highest permeability in the mid intervals and hence decreased rock-water interaction).

The transgression across mineral stability boundaries by the observed trend of chemical evolution is difficult to rationalize. By thermodynamic laws, the evolution of a water, once it has reached a mineral stability boundary should, in general, proceed along that boundary until one phase disappears during incongruent dissolution. The Log{Na}/{H} vs Log{H_4SiO_4} trend might possibly be consistent with such evolution, as might be the {Mg} data. However, for Log{K}/{H} and Log{Ca}/$\{H\}^2$ vs Log{H_4SiO_4} it is difficult to explain the nature of the trends in terms of thermodynamic equilibrium alone, even allowing for an error in thermodynamic data. This point again indicates the probable significance of mixing, but may also be attributable to impure mineral phases (compared with the ideal phases of the diagrams), or may reflect the kinetics of the system.

5.2 CONCLUSIONS

Strong correlations exist between the activity of H_4SiO_4 and permeability and ^{18}O and depth. Cl, Na and Li are strongly correlated with both depth and permeability.

The NSCRV groundwaters appear to display an evolutionary trend towards seawater composition which is manifest on both Piper and mineral stability diagrams. The trend is apparently a result of a combination of mixing and rock-water interaction. Hydrogeochemical trends are also seen, apparently a function of depth and permeability.

The well preserved hydrogeochemical trends (regardless of the validity of any assumptions about what the trend may represent) are believed to be reflections of the relatively ordered nature of flow within the Holyrood Granite. These trends may further support the assumption that groundwater flow in the Holyrood Granite may be modelled using an equivalent porous medium approach and an appropriate scale length (possibly on the order of tens of metres).

CHAPTER 6: INTERPRETATION OF AQUEOUS ISOTOPE DATA

6.1 DISCUSSION

As a result of isotopic fractionation caused by varying temperatures, values of $\delta^{18}O$ and $\delta^{2}H$ in precipitation from different latitudes have been found to plot on a straight line. This line is referred to as the Meteoric Water Line (MWL) and has the general form (Craig, 1961):

$$\delta^{2}H = 8 . \delta^{18}O + 10 \qquad \textbf{(Equation 6.1)}$$

Although the slope of 8 is nearly constant globally, the intercept can vary considerably, reflecting local meteorological, topographic and seasonal conditions (Gat, 1981).

The isotope data from NSCRV plots on or near the MWL (Figure 6.1). There is no evidence for evaporation having taken place (which will tend to alter the isotopic signature of the waters, moving the points off the MWL to the upper right).

Figure 6.1 ISOTOPE DATA FOR NSCRV PLOTTED AGAINST THE METEORIC WATER LINE

Data plotted showing limited range of possibl: values for lower latitudes

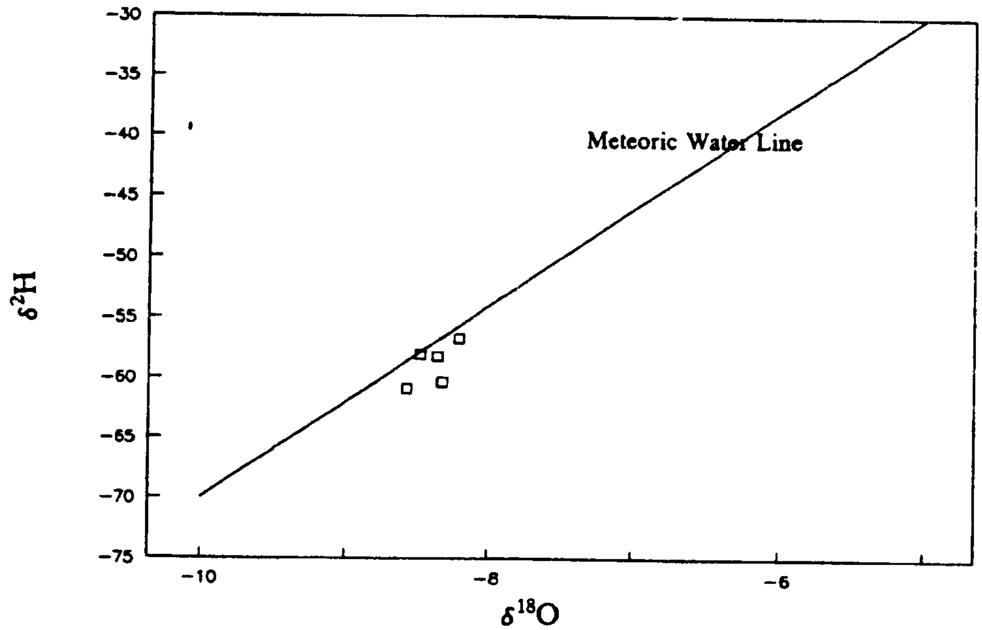

Note: Data used were only those samples which had both oxygen and hydrogen isotope data at the same depth and the same time of collection. See Appendix C final sample values.

The location of the group of points on the meteoric water line is consistent with the latitude of NSCRV. A linear relationship between $\delta^{18}O$ values of average annual precipitation and the average annual air temperature is by given by equation 6.2 (Dansgaard, 1964):

$$\delta^{18}O_{m} = 0.695T - 13.6 \qquad \textbf{(Equation 6.2)}$$

In Equation 6.2 $\delta^{18}O_{m}$ is the mean annual $\delta^{18}O$ value of precipitation and T is the mean annual surface air temperature in degrees centigrade. No estimate of error is provided for values calculated using equation 6.2. Yurtsever (1975) confirmed, for four stations in Greenland and Europe, that average monthly $\delta^{18}O$ values ($\delta^{18}O_{mo}$) are linearly related to average monthly surface temperatures in degrees centigrade (T) by the equation:

$$\delta^{18}O_{mo} = (0.521 \pm 0.014)T - 14.96 \pm 0.21 \qquad \textbf{(Equation 6.3)}$$

Where $\delta^{18}O_{mo}$ is the mean monthly $\delta^{18}O$ value.

Assuming that groundwater isotopic compositions reflect the local weighted mean annual isotopic compositions of precipitation (Gat, 1981), the use of Equation 6.2, and the average of the final ^{18}O values presented in Table 4.4, results in an estimate of the mean annual air temperature (MAT) at the time of recharge of 7.5°C. Using Equation 6.3 the MAT is 12.5°C. However, the position of the NSCRV borehole, at the discharge end of a regional flow system makes it highly unlikely that the isotopic values measured in the individual fractures represent monthly mean precipitation that has preserved its isotopic identity since the time of recharge. Therefore, the MAT estimated using Equation 6.2 is considered more plausible than the latter value. The MAT for a meteorological station operated by The Atmospheric and Environmental Service of Environment Canada approximately 100 m from the NSCRV location is given as 6.1 °C. A synopsis of the weather data at the Seal Cove weather station is provided in Table 6.1.

The use of the MAT for aquifer calculations implies an assumption that water recharging the aquifer represents precipitation falling throughout the year. This assumption is incorrect as the aquifer is preferentially recharged at certain times of the year: For instance, a smaller portion of summer rain is expected to recharge the aquifer and a large part of the snowfall which melts to form runoff may be excluded from the aquifer as it runs over frozen ground. The water balance diagram Figure 6.2 (Nolan, Davis and Associates Ltd, 1989), constructed using the Seal Cove AES data reveals that most recharge is expected to occur in the periods March- April and October- November. The mean monthly temperatures for these periods are (averages for the two sets of consecutive months) 1.05 °C and 6.25 °C respectively.

Table 6.1 Synopsis of Weather data at NSCRV

SEAL COVE
47° 27′N 53° 4′W 15 m

Daily Maximum Temperature	0.8	0.6	2.7	6.7	11.6	17.3	21.9	21.0	17.2	12.1	7.9	3.0	10.2
Daily Minimum Temperature	-6.5	-6.9	-4.3	-1.0	2.2	6.7	11.2	11.9	8.1	4.1	0.9	-3.9	1.9
Daily Temperature	-2.9	-3.1	-0.8	2.9	6.9	12.1	16.6	16.5	12.7	8.1	4.4	-0.5	6.1
Standard Deviation, Daily Temperature	1.9	2.2	1.7	1.2	1.4	1.6	1.4	1.7	1.0	0.8	1.5	2.1	0.7
Extreme Maximum Temperature	15.0	14.4	16.7	18.3	26.1	30.0	31.7	31.0	26.7	27.8	21.1	15.6	31.7
Years of Record	18	18	18	18	18	17	18	18	19	19	19	19	
Extreme Minimum Temperature	-20.6	-26.7	-18.3	-16.0	-7.8	-4.4	0.0	0.0	-1.1	-5.6	-16.0	-18.9	-26.7
Years of Record	18	18	18	18	18	18	18	18	18	18	19	19	
Rainfall	87.8	75.5	81.5	78.9	74.5	73.6	65.7	100.1	93.2	128.1	114.7	99.3	1072.9
Snowfall	51.2	46.5	35.9	9.9	1.6	0.2	0.0	0.0	0.0	0.7	6.6	33.3	185.9
Total Precipitation	137.3	124.6	121.2	95.4	75.9	73.6	65.7	100.1	93.2	128.8	121.2	135.9	1272.9
Standard Deviation, Total Precipitation	45.7	63.3	39.5	38.4	24.4	30.9	33.4	76.0	41.0	49.3	45.5	54.0	166.7
Greatest Rainfall in 24 hours	90.7	61.7	53.3	62.2	31.0	55.4	53.8	71.4	68.1	52.8	66.8	79.2	90.7
Years of Record	19	18	18	18	18	18	19	18	19	18	20	19	
Greatest Snowfall in 24 hours	38.1	43.2	38.1	38.1	10.2	5.1	0.0	0.0	0.0	10.2	27.9	29.5	43.2
Years of Record	18	16	18	17	17	19	20	19	20	20	20	19	
Greatest Precipitation in 24 hours	90.7	61.7	53.3	62.2	31.0	55.4	53.8	71.4	68.1	52.8	69.9	79.2	90.7
Years of Record	19	17	18	18	18	18	19	18	19	18	20	19	
Days with Rain	7	5	7	9	10	8	8	10	10	14	11	9	108
Days with Snow	6	5	4	2	0	0	0	0	0	0	1	4	22
Days with Precipitation	12	11	12	11	11	9	8	10	10	14	12	13	133

From Environment Canada Canadian Climate Normals 1951-1980, Temperature and Precipitation.

Figure 6.2 Evapotranspiration diagram for Seal Cove

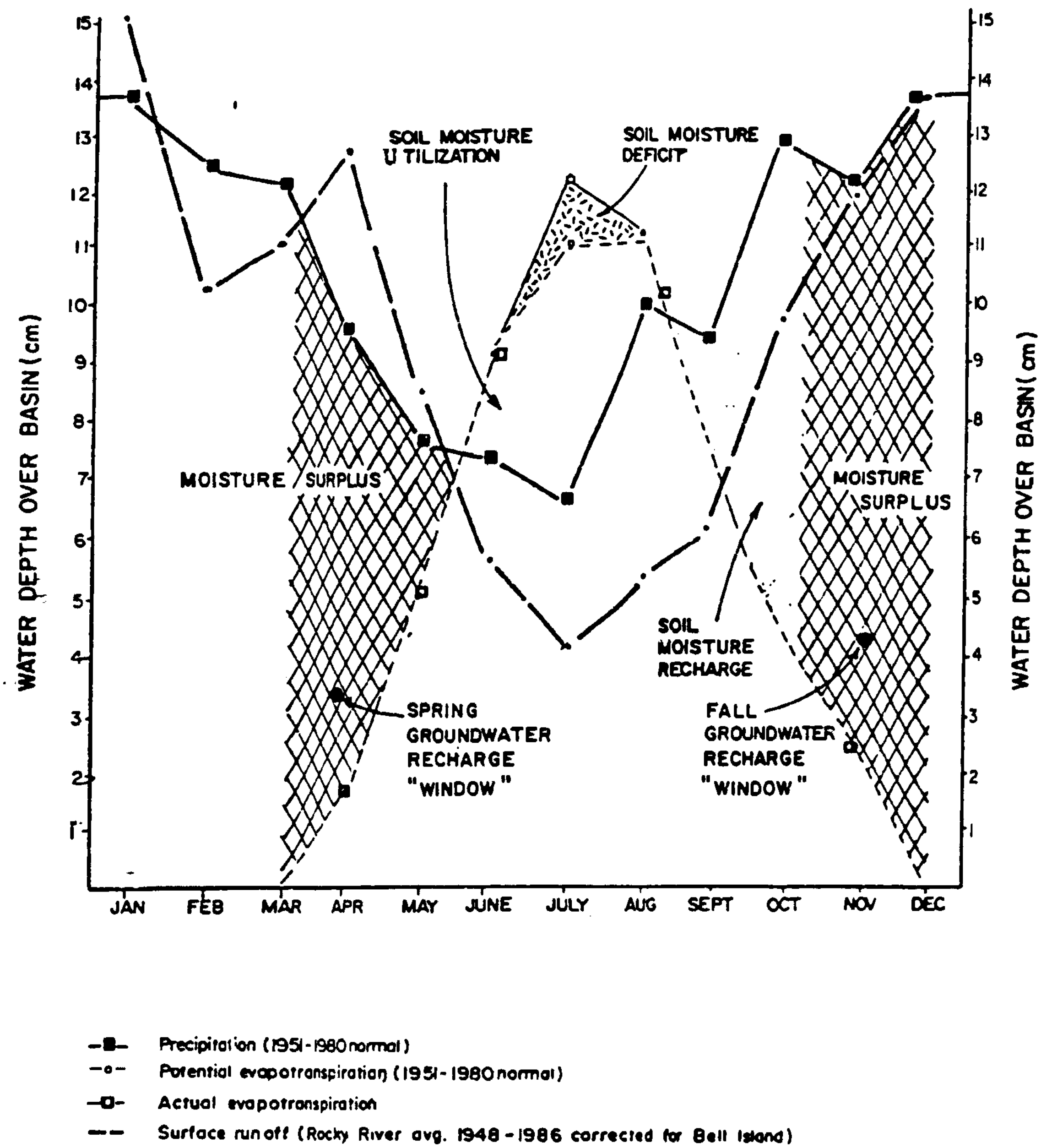

If one assumes that recharge occurs only during these periods, then an estimation of the average temperature of the most significant part of the total recharge is 3.9°C. The disparity between this estimate and that derived from $\delta^{18}O$ data may be the result of:

a) periods of recharge occurring only during the warmer periods of the recharge seasons (the mean monthly temperature for April is 2.9 °C and for October 8.1 °C.),

b) underestimation of the significance of recharge during the summer and overestimation of the importance of spring recharge (the latter possibly being reduced due to frozen ground),

c) aquifer recharge occurring during a previous (warmer) climatic period, (the estimated water residence time for the deepest water sample collected is in the range 1560 to 15 600 yrs, based on preliminary flow modelling)

d) MAT estimated from the sea level AES station may be an overestimate relative to the MAT of the location of actual system recharge.

Isotope fractionation as a result of variations in temperature arises not only from variations in latitude but also due to variations of altitude at a given location. The latter phenomenon is referred to as the altitude effect. The variation of $\delta^{18}O$ with altitude is typically in the range 0.15 - 0.5‰ $\delta^{18}O$/100m of vertical elevation (Gat 1981).

If the flow net for NSCRV (Figure 1.3) is to be believed then the deepest NSCRV samples could have been recharged at altitudes of ~170 m above borehole elevation and represent groundwater carried along regional flow paths. The shallowest NSCRV samples were likely recharged at a much lower altitude (~60 m) by local flow systems. If an average altitude effect of 0.325‰ $\delta^{18}O$/100 m is assumed then the 0.32‰ range of observed final $\delta^{18}O$ values is quite reasonable: The calculated difference in $\delta^{18}O$ between water recharged at 60 m and 170 m would be 0.36‰. A linear regression analysis of the final values of the $\delta^{18}O$ vs. depth in metres shows that the slope of the best fit line is -0.397 ‰ $\delta^{18}O$/100 m <u>of drilled depth</u>; however, as a result of the saltwater wedge, the flowlines at NSCRV are believed to be compressed: 100 m of depth is estimated to represent ~147 m of altitude (samples from ~20 m and 95 m, recharged at altitudes of ~60 and ~170 m respectively) and the gradient of the best fit line represents an altitude effect of 0.27 ‰/100 m <u>of altitude</u>. This value is close to the assumed average altitude isotopic gradient of 0.325‰/100 m.

6.2 CONCLUSIONS

The stable isotope data appear to indicate that an altitude effect is preserved in the groundwater samples analyzed at NSCRV, this may be further evidence for the well ordered nature of the flow in the Holyrood Aquifer; therefore, the ^{18}O data could be consistent with a local recharge derivation, at or near current mean annual temperatures of recharge.

CHAPTER 7: ANALYSIS OF FRACTURE MINERALOGY

7.1 ANALYSIS OF FRACTURE MINERALOGY

Hydrogeochemical modelling of the groundwaters of the Holyrood Granite is discussed in Chapter 8. However, prior to the modelling it is useful to identify the minerals, which by precipitating or dissolving within the fracture flow system, control the evolution of groundwater chemistry. The minerals and gases which seem likely to control the groundwater chemistry of a hydrogeochemical system are referred to as plausible phases (Plummer et al. 1983). The selection of a set of plausible phases may, in part, be made by conducting thermodynamic speciation calculations, using chemical analyses of the groundwaters of interest. The speciation calculations help to identify potential or actual phases which are likely to be close to saturation, as well as those minerals present in the rock-mass which are likely to be dissolving. The list of minerals calculated to be at, or close to, saturation in the NSCRV groundwaters is extensive (partly a result of the high number of element analyses): If all the minerals were included in geochemical model the number of variables in the model would make a solution almost impossible. The analysis of fracture minerals helps to limit the number of plausible phases for modelling which, in turn, places constraints on reaction paths for the NSCRV groundwaters.

In order to identify which minerals may be influencing the groundwater chemistry in the Holyrood Granite analyses of fracture surfaces were conducted using X-ray diffraction (XRD) and scanning electron microscopy (SEM) techniques, coupled with energy dispersive electron microprobe analysis (EDM).

7.2 SAMPLE COLLECTION AND ANALYSIS

Samples were collected from fractures which had been logged as likely to be open, or partially open, and hence potentially conducting groundwater.

7.2.1 Analysis of Fracture flakes by SEM

For SEM analysis, flakes picked from fracture surfaces were glued to a glass plate (orientated with the original fracture surface upwards) and coated with a thin film of carbon in an evaporative container.

A total of 18 fracture flakes were photographed by SEM and analyzed using EDM. A photograph of as much of the chip as possible was taken (x20 magnification) and then a portion of the chip analyzed (approximately 1/4 to 1/3 of the area photographed). Once the initial coarse analysis had been made individual crystals (or areas on crystals) were selected, photographed and analyzed, at magnifications of approximately x1000, but in some cases at magnifications of greater than x3000. Individual crystals were selected for analysis either on the basis of being representative of the entire mass or as appearing anomalous. Output from the SEM was in the form of photographs, and output from the EDM was in the form of an energy spectrum, with results of calculations of the relative percentages of selected oxides in the area analyzed.

7.2.2 Analysis of Fracture Minerals by XRD.

Sample collection for XRD analysis was achieved by lightly scraping across fracture surfaces with a knife, the material from this process being collected in individual bottles. The scrapings were subsequently ground with a pestle and mortar in acetone and then spread on a glass plate for XRD analysis. Unfortunately, in many cases, the amount of sample (both available and removed) was insufficient for satisfactory analysis using the equipment available at the time of analysis. A total of 18 powder plates were analyzed using a RIGAKU XRD instrument. As noted above there was frequently a problem with insufficient sample.

7.3 METHODS OF DATA INTERPRETATION

7.3.1 Interpretation of SEM/EDM data.

The microprobe analyses of mineral aggregates and individual crystals are semi quantitative. The semi-quantitative nature of the analyses is in part a result of the lack of any measure of either the water content or the CO_2 content, which may constitute more than 20%, by weight, of some minerals. The lack of OH and CO_2 analyses precludes the direct calculation of a meaningful chemical formula from the EDM analyses, in the manner outlined by Deer et al. (1966). Instead, a scheme was devised in which all the analyses were successively checked for a variety of minerals. For this purpose, an assumption was made that each analysis represented a particular mineral, with a weight percentage of water, and a number representing the number of oxygen atoms in the unit cell (both representative of the mineral being compared) arbitrarily assigned to each chemical analysis. The analyses were then corrected to the arbitrarily assigned water content and their stoichiometry recalculated using the method outlined in Deer et al. (1966). In this manner the entire set of analyses was scanned for formulae matching those of chlorite, kaolinite/halloysite, pyrophyllite, feldspars, mica and zeolites. Calcite, quartz and iron precipitates were also identified by inspecting the EDM results. The formula used for correcting analyses for water content was verified by using selected analyses from Deer et al. (1966), removing the water content, normalising the remaining oxide values to 100% and then adding water back to the analyses using the method outlined below.

7.3.1.2 Recalculation Scheme for Mineral Analyses

For a mineral composed of n oxides, h to j, where oxide h is the assigned weight percentage of water ($wt\%_{H2O}$) then the weight percentage of each oxide (prior to the introduction of water) must be "corrected" to accommodate the introduction of water so that:

$$\sum_{n=h}^{j} \%_n = 100\% \qquad \text{(Equation 7.1)}$$

A factor K is calculated, from the assigned percentage of water, where:

$$K = 1 + \frac{f_w}{1-f_w} \qquad \text{(Equation 7.2)}$$

where f_w is given by $wt\%_{H2O}/100$. Modifying the scheme outlined in Deer et al. (1966) T_{mod} (as opposed to T) is derived by:

$$T_{mod} = \sum_{n=1}^{j} \frac{\%_n . O_n}{MW_n} + \frac{\%_{water}}{2 . MW_{water}} \qquad \text{(Equation 7.3)}$$

where:

$\%_n$ - percentage of oxide n prior to correction for water

MW_n - molecular weight of oxide n

O_n - number of oxygen atoms in the oxide n

MW_{water} - Molecular weight of water

The number of cations of each element (C_n) in the formula is derived from each oxide by:

$$C_n = \frac{1}{K} \cdot \frac{O_{tot}}{T_{mod}} \cdot \frac{\%_n \cdot O_n}{MW_n} \cdot R_n \qquad \textbf{(Equation 7.4)}$$

where:

O_{tot} - total number of oxygen atoms in a crystal unit cell (of the assumed mineral)

R_n - ratio of cations:number of oxygen atoms in the oxide n

7.3.2 Method of Interpreting XRD data

Most of the XRD data was interpreted using peak matching software available on the RIGAKU. Minerals thought to be clays were glycolated and re-analyzed. Peak shifts noted after glycolation indicated the presence of hydratable clays.

7.4 RESULTS

Due to the large amount of data generated by XRD and SEM/EDM, only selected examples of the results are presented in the following section in conjunction with Table 7.1 which identifies possibilities for mineral matches from the SEM/EDM data and mineral matches obtained from the XRD data. The ranges of atomic properties used to match the SEM data with a variety of minerals is given in Table 7.2. Mineral groups identified are discussed individually. The data set was scanned for zeolites and amphiboles, without success.

Calcite

Calcite was identified on numerous fracture planes at drilled depths from 8.50 m to 137.62 m. The identification of calcite was made using with XRD and SEM/EDM. A typical EDM spectrum for calcite, from a fracture plane at 53.97 m is shown in Figure 7.1a; an XRD spectrum from a calcite fracture coating at 72.48 m is presented on Figure 7.1b.

Chlorite

Chlorite was only detected using the SEM and identifications of some certainty were only found at 55.36 m or greater depths. An EDM spectrum for chlorite, made from fracture material at 147.31 m, is shown on Figure 7.2. The results of calculating chemical formulae from the EDM data for selected analyses, using the paramcters indicated are shown in Table 7.3. The results indicate that the chlorite composition varies with both Mg and Fe rich varieties occurring.

Table 7.1 Table showing minerals identified by microprobe and XRD

		CALCITE			AMPHIBOLES	CHLORITE					CLAYS							TALC/PYROPHYLLITE		FELDSPAR	
			QUARTZ			%water content															
SAMPLE	DEPTH			IRON		1	10	11	12	13	ka	ha	il	mt	nt	bd	sp	ta	py	ab	olig
NSCRV 6A	6.43											s									
NSCRV 6B	6.43											s									
NSCRV 11A	8.50																				
NSCRV 11B	8.50																				
NSCRV 11lge	8.50					X			X	X											
NSCRV 10A	53.97	X																			
NSCRV 10B	53.97	s													-						
NSCRV 10lge	53.97	s																			
NSCRV 4A	55.36																				
NSCRV 4lg	55.36	s																			
NSCRV 5A	55.36																				
NSCRV 5Alge	55.36																				
NSCRV 5B	55.36					s		s	s	s											
XRD	67.60	X																			
NS 1g	68.64											s									
NS1	68.64											s							s		s
NS1B	68.64											s									s
NSCRV 2A	68.64					s			s	s											
NSCRV 2B	68.64																				
NSCRV 2D	68.64									s											
NSCRV 3A	68.64					s			s	s											
NSCRV 3B	68.64		s																		
NSCRV 3lg	68.64											s									s
r.NSCRV 2A	68.64					s		s	s	s											
r.NSCRV 2B	68.64																				
r.NSCRV 2C	68.64																				
NSCRV 14A	71.80				s							s									
NSCRV 14B	71.80												s								
NSCRV 14C	71.80		s																		
NSCRV 14D	71.80		s																		
NSCRV 14lge	71.80		s										s								
NSCRV 15A	72.48	X – s																			
NSCRV 15B	72.48	s																			
NSCRV 15C	72.48	s																			
NSCRV 15D	72.48	s																			
NSCRV 15lge	72.48	s																			

TABLE 7.1/continued

SAMPLE	DEPTH	CALCITE	QUARTZ	IRON	AMPHIBOLES	CHLORITE %water content 1	10	11	12	13	CLAYS ka	ha	il	mt	nt	bd	sp	TALC/PYROPHYLLITE ta	py	FELDSPAR ab	olig
NSCRV 17A	72.51																				
NSCRV 17B	72.51																				
NSCRV 17lge	72.51																				
NSCRV 18A	78.30	X																			
NSCRV 18B	78.30																				
NSCRV 18lge	78.30																				
NSCRV 12A	95.42	s													-						
NSCRV 12B	95.42																				
NSCRV 12lge	95.42																				
NSCRV 16A	136.53	s	s									s									
NSCRV 16D	136.53			s																	
NSCRV 16E	136.53						s	s	s												
NSCRV 16E	136.53																				
NSCRV 16F	136.53			s																	
NSCRV 16lge	136.53																				
XRD	137.62	X																			
NSCRV 8A	139.69																				
NSCRV 8B	139.69																				
NSCRV 8C	139.69																				
NSCRV 8lg	139.69	s																			
NSCRV 9A	139.69																				
NSCRV 9B	139.69	s	X																		
NSCRV 9C	139.69			s																	
NSCRV 9lg	139.69			s																	
NSCRV 7A	147.31																				
NSCRV 7B	147.31																				
NSCRV 7lg	147.31						s	s	s												
XRD	148.31													X	X						
NSCRV 13A	151.81	s																			
NSCRV 13B	151.81							s													
NSCRV 13lge	151.81	s	s																		

LEGEND:

Analytical method
- X analysis by XRD at depth shown
- s analysis by electron microprobe at depth shown and positions indicated on photographs

Mineral Abbreviations
- ka kaolinite
- ha halloysite
- il illite
- mt montmorillonite
- nt nontronite
- bd beidellite
- sp saponite
- ta talc
- py pyrophyllite
- ab albite
- olig oligoclase

Table 7.2 SELECTION CRITERIA FOR MINERALS ANALYZED BY ELECTRON MICROPROBE

CHLORITE										
water %		1	10	11	12	13				
O total		28	36	36	36	36				
IDEAL	Al+Si	8–12	8–12	8–12	8–12	8–12				
	remainder	12	12	12	12	12				
CRITERIA	Al+Si	7.8–13	7.8–13	7.8–13	7.8–13	7.8–13				
	remainder	11.5–12.5	11.5–12.5	11.5–12.5	11.5–12.5	11.5–12.5				
CLAYS										
water %		14.09	17.43		8.84	22.8	22.64	22.9		
O total		18	18		24	24	24	24		
		kao	hal		ill	mont	beid	sapon		
IDEAL	Si	4.0	4.0	Si+Al	8–12	8–12	8–12	8–12		
	remainder	4.0	4.0	remainder	4	4	4	6		
CRITERIA	Si	3.5–4.5	3.5–4.5	Si+Al	7–13	7–13	7–13	7–13		
	remainder	3.5–4.5	3.5–4.5	remainder	3–5	3–5	3–5	3–5		
TALC & PYROPHYLLITE					**FELDSPARS**					
water %		4		0	water %		0			
O total		24		24	O total		32			
		talc		pyroph	All feldspars					
IDEAL	Si	8	Si	8	IDEAL	Si+Al	15.5–16.5			
	Mg	6	Al	4		Na+K+Ca	3–4			
CRITERIA	Si	7–9	Si	7–9	CRITERIA	Si+Al	14.5–17.5			
	Mg	5–7	Al	3–5		Na+K+Ca	2.5–4.5			
ZEOLITES										
water %		9.47	13.35	13.91	11.94	15.42	17.76	22.04	14.41	16.58
O total		80	80	80	30	72	72	72	48	32
		natro	thom	scol	mes	heul	stilb	chabz	laum	phill
IDEAL	Si+Al	~40	~40	~40	~15	~36	~36	~36	~24	~24
	Na+K+Ca	~15	12	8	3.75	~6	~6.5	~4	~4	~4
CRITERIA	Si+Al	35–45	35–45	35–45	13–17	31–41	31–41	31–41	21–27	21–27
	Na+K+Ca	12–17	10–14	6–10	3–4.5	4–8	3.5–6	4.5–8.5	2.5–5.5	2.5–5.5
MICAS							**AMPHIBOLES**			
water %		2	3	4.5	7	12	water %	2		
Ototal		24	24	24	24	24	O total	24		
IDEAL	remainder	11.81–14.17	11.81–14.17	11.81–14.17	11.81–14.17	11.81–14.17	IDEAL	remainder	~13	
	Na+K+Ca	5.85–8.19	5.85–8.19	5.85–8.19	5.85–8.19	5.85–8.19		Na+K+Ca	2–3	
CRITERIA	remainder	11.3–4.7	11.3–4.7	11.3–4.7	11.3–4.7	11.3–4.7	CRITERIA	remainder		
	Na+K+Ca	5.5–8.5	5.5–8.5	5.5–8.5	5.5–8.5	5.5–8.5		Na+K+Ca		

Figure 7.1a ED spectrum for calcite from 53.97 m

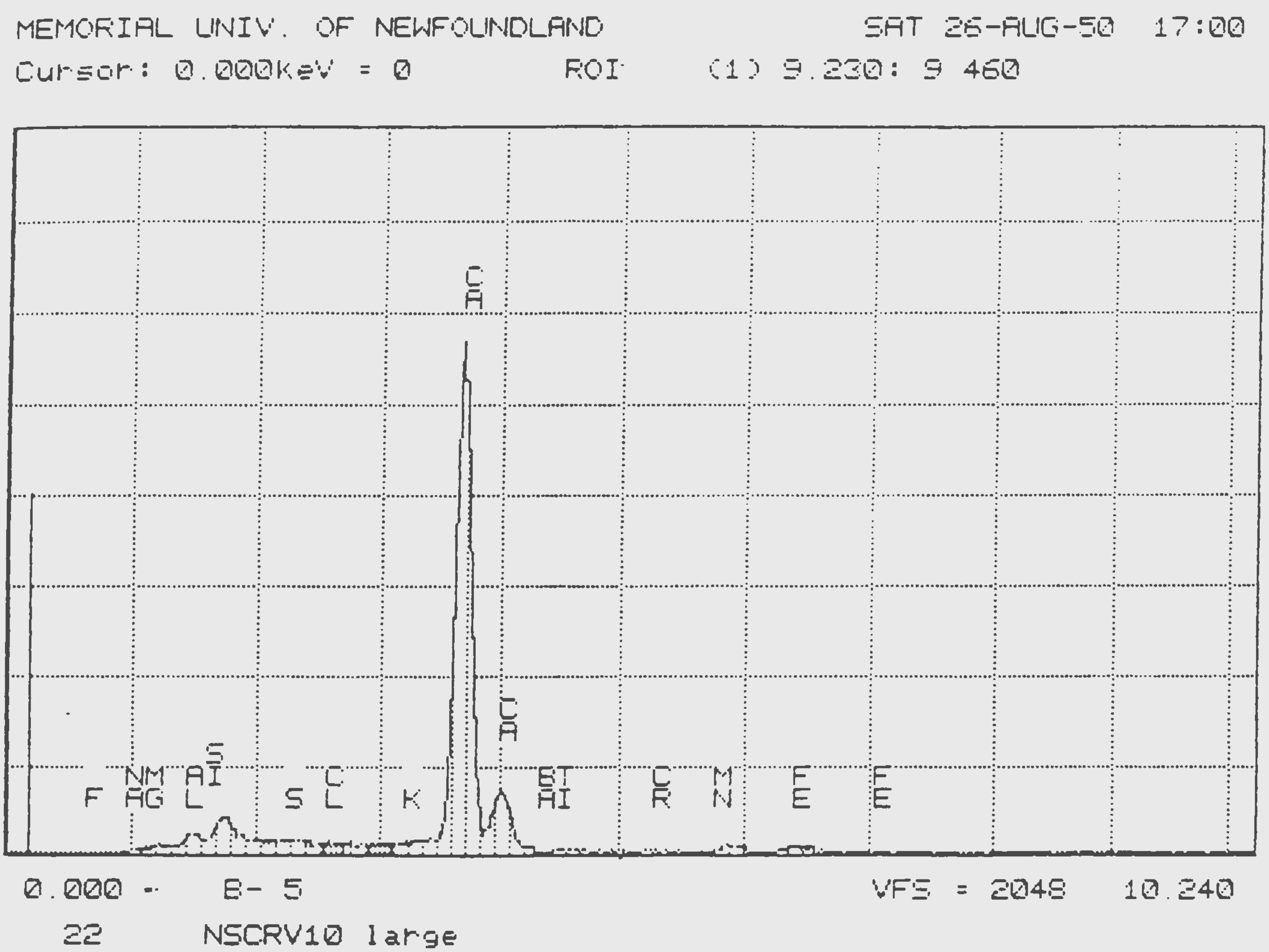

Figure 7.1b XRD spectrum of calcite from 72.48 m

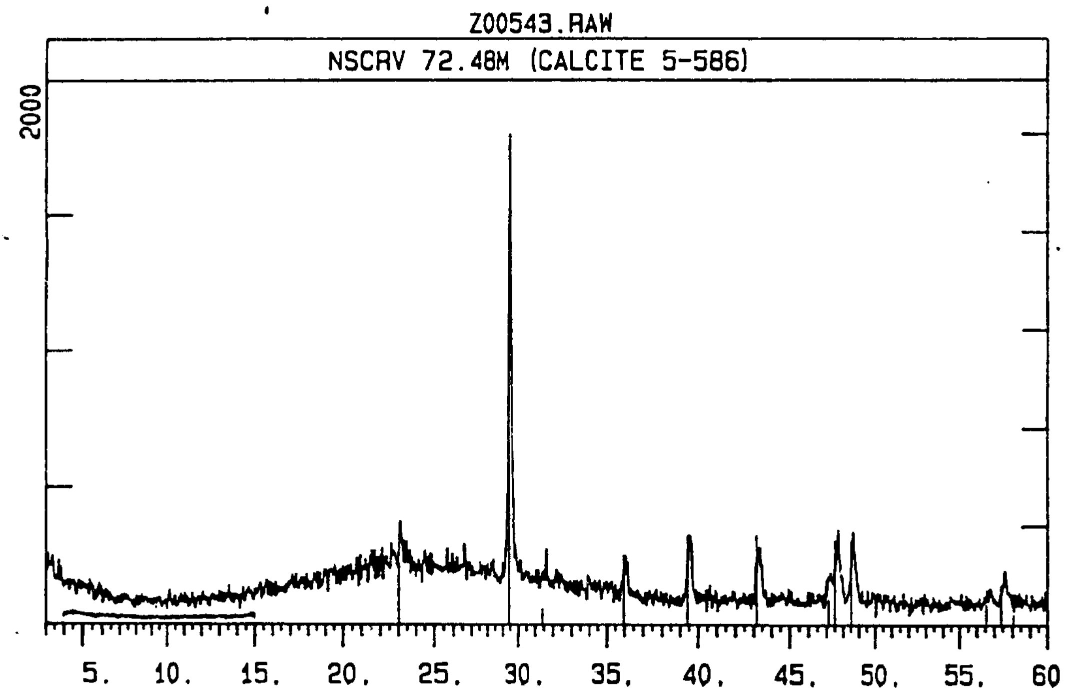

Figure 7.2 SEM photograph of Chlorite from 147.31 m

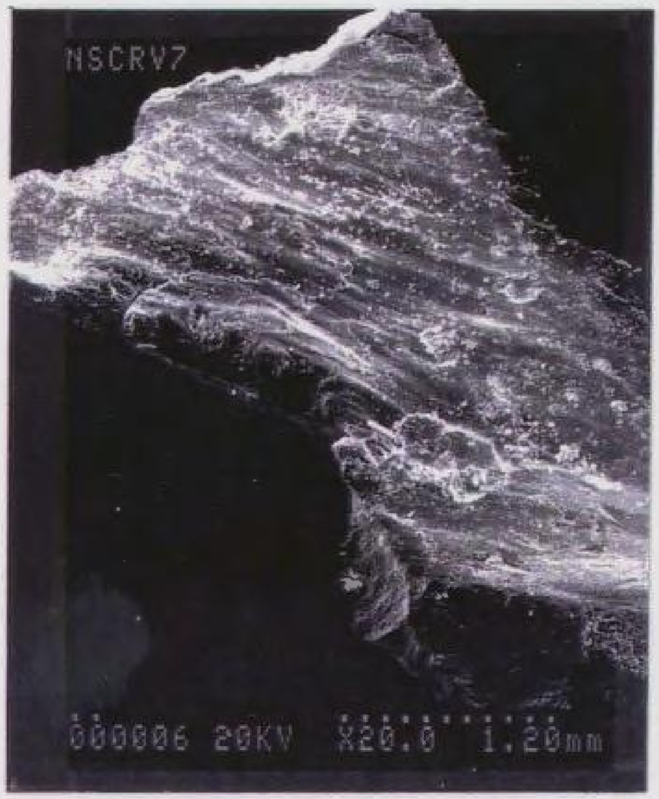

Table 7.3 Selected Chlorite Compositions, calculated from ED microprobe data.

CHLORITE														
%water>	11.00										%water>	13.00		
Tot #Ox>	36.00										Tot #Ox>	36.00		
Sample	NSCRV 5B		r.NSCRV 2A		NSCRV 16E		NSCRV7 lgc		NSCRV 13B		NSCRV 5B		r.NSCRV 2A	
Depth	55.36		68.64		136.53		147.31		151.81		55.36		68.64	
Si	7.28	8.00	5.23	8.00	6.98	8.00	7.55	8.00	7.25	8.00	6.97	8.00	4.97	8.00
Al	0.72		2.77		1.02		0.45		0.75		1.03		3.03	
Al	1.76		1.41		3.13		2.65		2.18		1.34		0.95	
Ti	0.00		0.00		0.00		0.00		0.00		0.00		0.00	
Fe2+	6.90		3.34		2.18		1.72		4.41		6.61		3.17	
Fe3+	0.00		0.00		0.00		0.00		0.00		0.00		0.00	
Mn	0.15	10.93	0.02	11.86	0.00	11.91	0.00	12.01	0.18	11.73	0.15	10.12	0.02	10.88
Mg	1.48		6.34		5.61		6.47		4.10		1.41		6.02	
Ca	0.39		0.01		0.10		0.55		0.47		0.37		0.01	
Na	0.25		0.75		0.90		0.61		0.38		0.24		0.71	
K	1.31		0.00		0.17		0.00		0.03		1.25		0.00	
Ba	0.03		0.00		0.00		0.00		0.04		0.03		0.00	
Ni	0.00		0.00		0.00		0.00		0.02		0.00		0.00	
Cu	0.05		0.00		0.00		0.00		0.02		0.04		0.00	
Zn	0.01		0.00		0.00		0.00		0.00		0.01		0.00	
S	0.00		0.23		0.00		0.02		0.00		0.00		0.22	
Cr	0.02		0.00		0.00		0.00		0.01		0.02		0.00	
Cl	0.00		0.00		0.05		0.00		0.00		0.00		0.00	

A range of representative formulae derived from the calculated chemical formulae is:

$Mg_{1.48}Fe_{6.90}Al_{1.76}(Si_{7.28}Al_{0.72})O_{20}(OH)_{16}$ to

$Mg_{6.47}Fe_{1.72}Al_{3.10}(Si_{7.55}Al_{0.45})O_{20}(OH)_{16}$

Assuming all iron in the formula is Fe^{3+}, charge balance in the two examples is $53.66^{+}:56^{-}$ and $58.95^{+}:56^{-}$.

Halloysite

The presence of halloysite was only detected using the SEM/EDM. It should be noted that in the initial coarse search of EDM data, to identify kaolinite and halloysite, using the parameters identified in Table 7.2, no matches with kaolinite were found. Matches were obtained only at the higher water content of halloysite and then only at depths of 68.64 m or higher. Table 7.4 shows hypothetical halloysite composition calculated using the appropriate water content and molecular structure.

Both halloysite and kaolinite are members of the kandite family of clays, of which only halloysite is capable of swelling. Kandites are noted for their inability to accept inter layer cations and for their inflexibility in composition. These points may cast some doubt on the calculated compositions. Any cation exchange ability that they do have is accommodated on the ends of the clay layers. Figure 7.3

Table 7.4 Selected Halloysite Compositions, calculated from ED microprobe data.

HALLOYSITE
water%> 17.43
Tot #Ox> 18.00

		NSCRV 6A 6.43		NSCRV 6B 6.43		NS lge 68.64		NS1 68.64		NS1B 68.64		NSCRV 3lge 68.64		NSCRV 14A 71.80		NSCRV 16A 136.53		NSCRV 8C 139.69	
A	Si	3.56	3.56	3.94	3.94	3.90	3.90	4.23	4.23	4.36	4.36	4.27	4.27	3.79	3.79	4.09	4.09	3.91	3.91
	Al	1.48		1.73		1.51		2.04		1.78		1.13		1.38		0.43		0.91	
	Ti	0.00		0.00		0.00		0.00		0.00		0.00		0.00		0.00		0.00	
	Fe2+	1.29		0.68		1.03		0.15		0.42		0.68		0.36		0.60		0.82	
B	Fe3+	0.00	3.33	0.00	3.01	0.00	3.23	0.00	2.42	0.00	2.67	0.00	2.23	0.00	2.02	0.00	1.53	0.00	2.78
	Mn	0.10		0.02		0.05		0.00		0.01		0.03		0.00		0.01		0.03	
	Mg	0.46		0.57		0.64		0.23		0.46		0.39		0.27		0.49		1.02	
	Ca	0.57		0.42		0.44		0.42		0.02		1.13		0.30		0.78		1.39	
C	Na	0.43	1.21	0.64	1.21	0.48	0.92	0.92	1.33	0.84	0.87	0.27	1.40	0.58	0.88	1.48	2.25	0.18	1.58
	K	0.21		0.16		0.00		0.00		0.00		0.00		0.00		0.00		0.01	
B+C			4.54		4.22		4.15		3.75		3.54		3.63		2.90		3.78		4.36
	Ba	0.06		0.01		0.00		0.00		0.00		0.00		0.01		0.00		0.00	
	Ni	0.04		0.01		0.05		0.00		0.00		0.01		0.00		0.00		0.00	
	Cu	0.06		0.01		0.03		0.00		0.00		0.01		0.00		0.00		0.00	
	Zn	0.03		0.01		0.03		0.00		0.02		0.00		0.00		0.00		0.01	
	S	0.00		0.00		0.00		0.00		0.00		0.00		0.66		0.00		0.00	
	Cr	0.08		0.01		0.00		0.00		0.00		0.00		0.00		0.00		0.00	
	Cl	0.00		0.00		0.00		0.00		0.00		0.00		0.00		0.00		0.00	
	S	0.00		0.00		0.00		0.00		0.00		0.00		0.00		0.00		0.00	
A+B+C			8.10		8.16		8.05		7.99		7.90		7.90		6.68		7.87		8.27

Figure 7.3 SEM photograph of Dickite from 136.53 m (A,B,C are analysis points, indicated on tables)

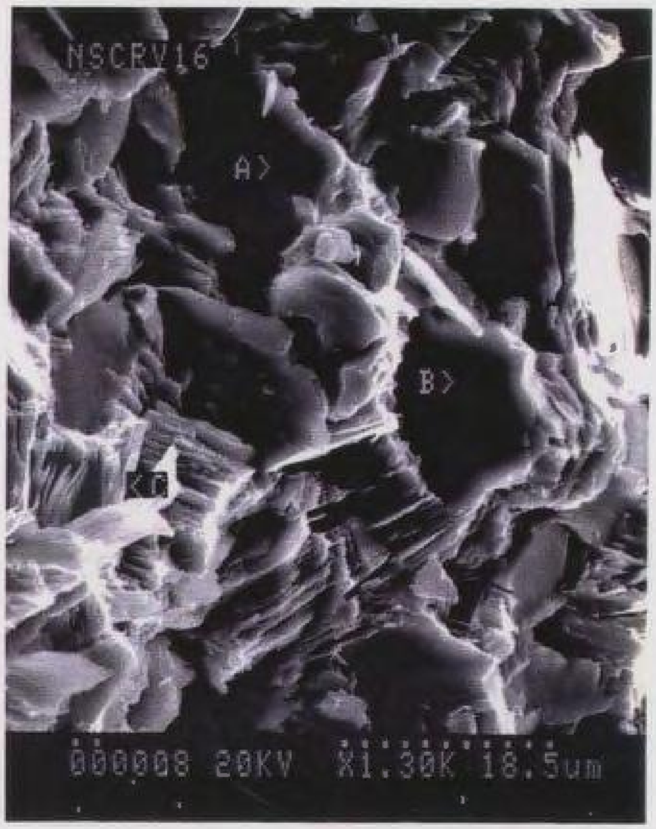

is an SEM photograph of a sample from 136.54 m, thought to be books of a kandite form, dickite (note that the book form is more common in dickite, another kandite variety). An example formula from the calculated chemical compositions is:

$$Al_{1.73}Fe_{0.66}Mg_{0.57}Na_{0.64}K_{0.16}(Si_{3.94}Al_{0.06}O_{10})(OH)_8.$$

Illite

Illite was only inferred from EDM on a sample from 71.80 m. The calculated compositions of the two analyses on a fracture flake from this depth are given in Table 7.5. The analyses presented are somewhat deficient in Al; however, it should be noted that the illite composition presented in Deer et al. (1966,p251#3) also has considerably less than ideal fractions of Al.

Smectites

Montmorillonite and saponite are believed to have been identified on a fracture surface from 148.31 m, using XRD. The minerals were glycolated to confirm their presence. The XRD traces from these analyses are shown on Figure 7.4.

Pyrophyllite

A possible pyrophyllite match was obtained on samples from 68.64 m although the match with halloysite, which was also obtained, is believed to be more

Table 7.5 Selected Illite Compositions, calculated from ED microprobe data.

ILLITE

,water>	8.84
Tot #Ox>	24.00

	Sample	NSCRV 14B		NSCRV 14lge	
	Depth	71.80		71.80	
A	Si	7.71	8.00	7.31	8.00
	Al	0.29		0.69	
B	Al	1.81	2.54	1.49	2.54
	Ti	0.00		0.00	
	Fe2+	0.16		0.67	
	Fe3+	0.00		0.00	
	Mn	0.08		0.00	
	Mg	0.00		0.22	
	Ca	0.48		0.17	
C	Na	0.10	0.65	0.62	1.50
	K	0.56		0.88	
	Ba	0.04		0.01	
	Ni	0.00		0.00	
	Cu	0.06		0.01	
	Zn	0.00		0.00	
	S	0.00		0.02	
	Cr	0.07		0.01	
	Cl	0.00		0.00	

Figure 7.4 XRD spectrum for montmorillonite from 148.31 m

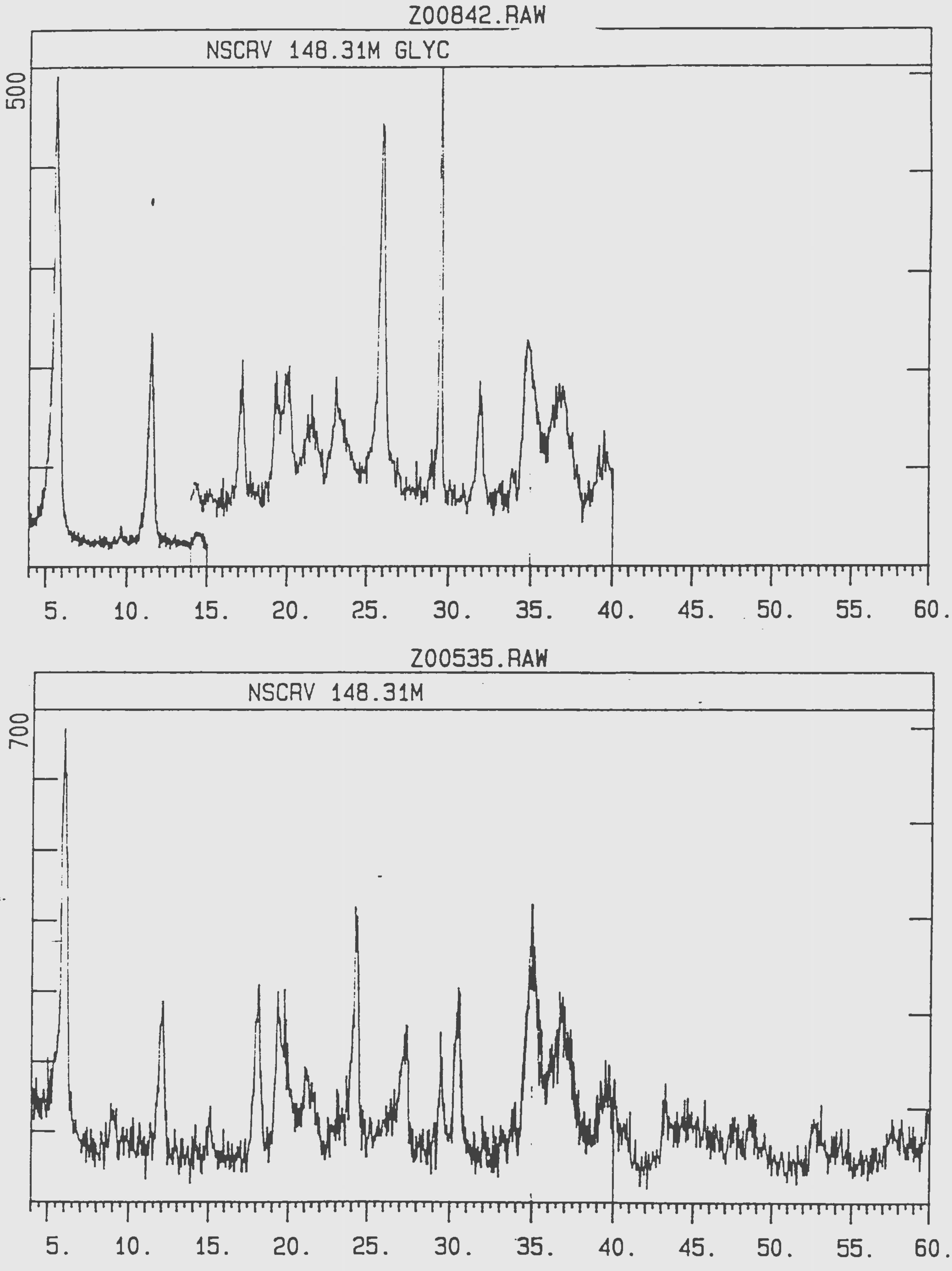

probable. Nevertheless, pyrophyllite will be considered as a plausible phase as it is apparently at saturation in the groundwaters of the Holyrood Granite. An active pyrophyllite mine is situated on the east edge of the study area.

Quartz

Quartz was identified on many fracture surfaces below 68.64 m, both by SEM and XRD. Example traces for quartz from both SEM and XRD are provided on Figure 7.5 a and b.

7.5 ELEMENTS IDENTIFIED.

Using the EDM some elements of interest were also detected on fracture surfaces. Unfortunately in most instances it was not possible to associate these elements with a mineral. Elements of note are as follows:

Barium

Barium was detected at 68.64 m in conjunction with high chlorine and iron on a mineral base believed to be chlorite. No sulphur was detected at the same location and thus the barium is not believed to have been associated with barite.

Figure 7.5a) ED spectrum of quartz from 71.80 m (NSCRV 14lge)

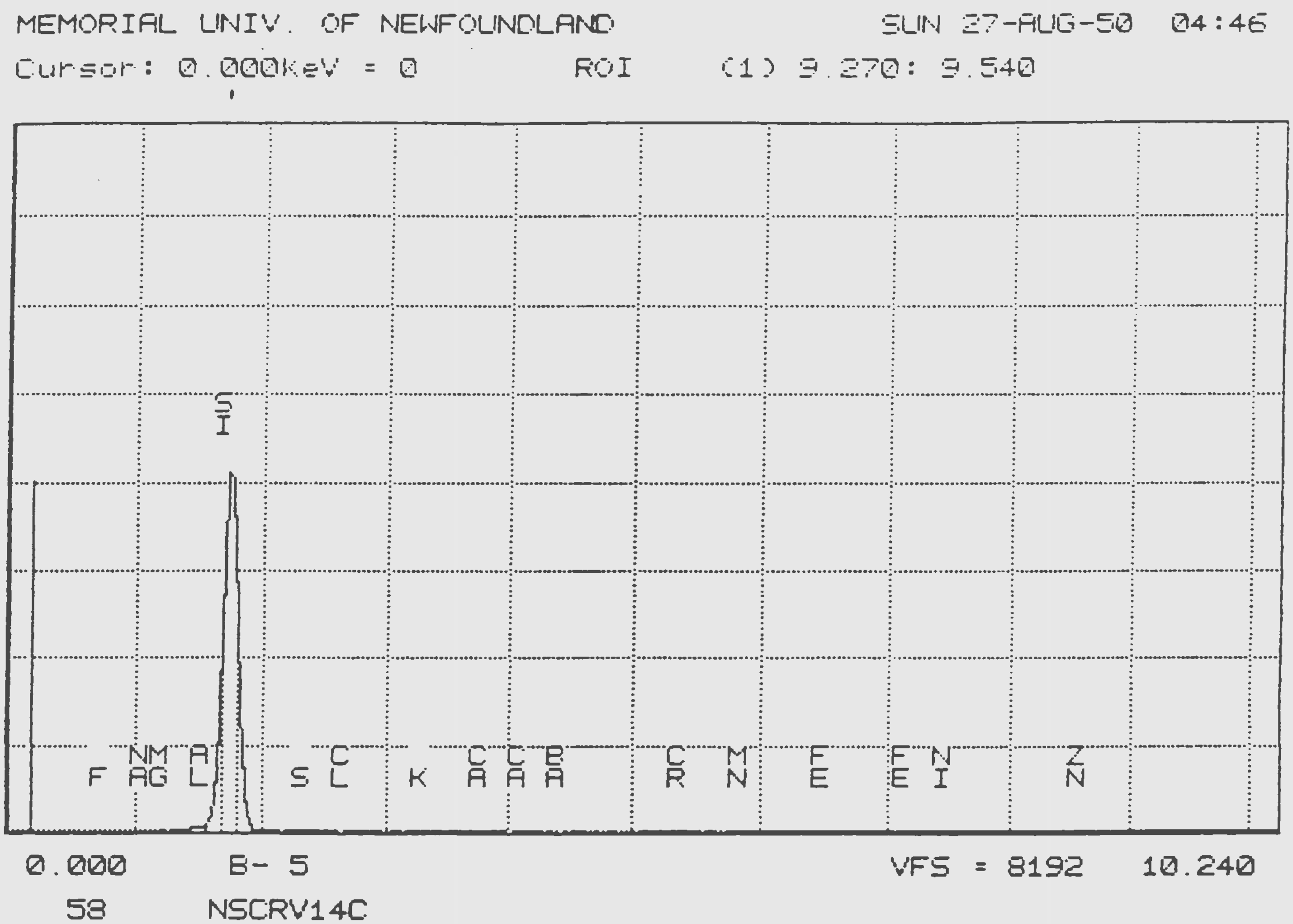

Figure 7.5b XRD spectrum, of quartz from 139.69 m

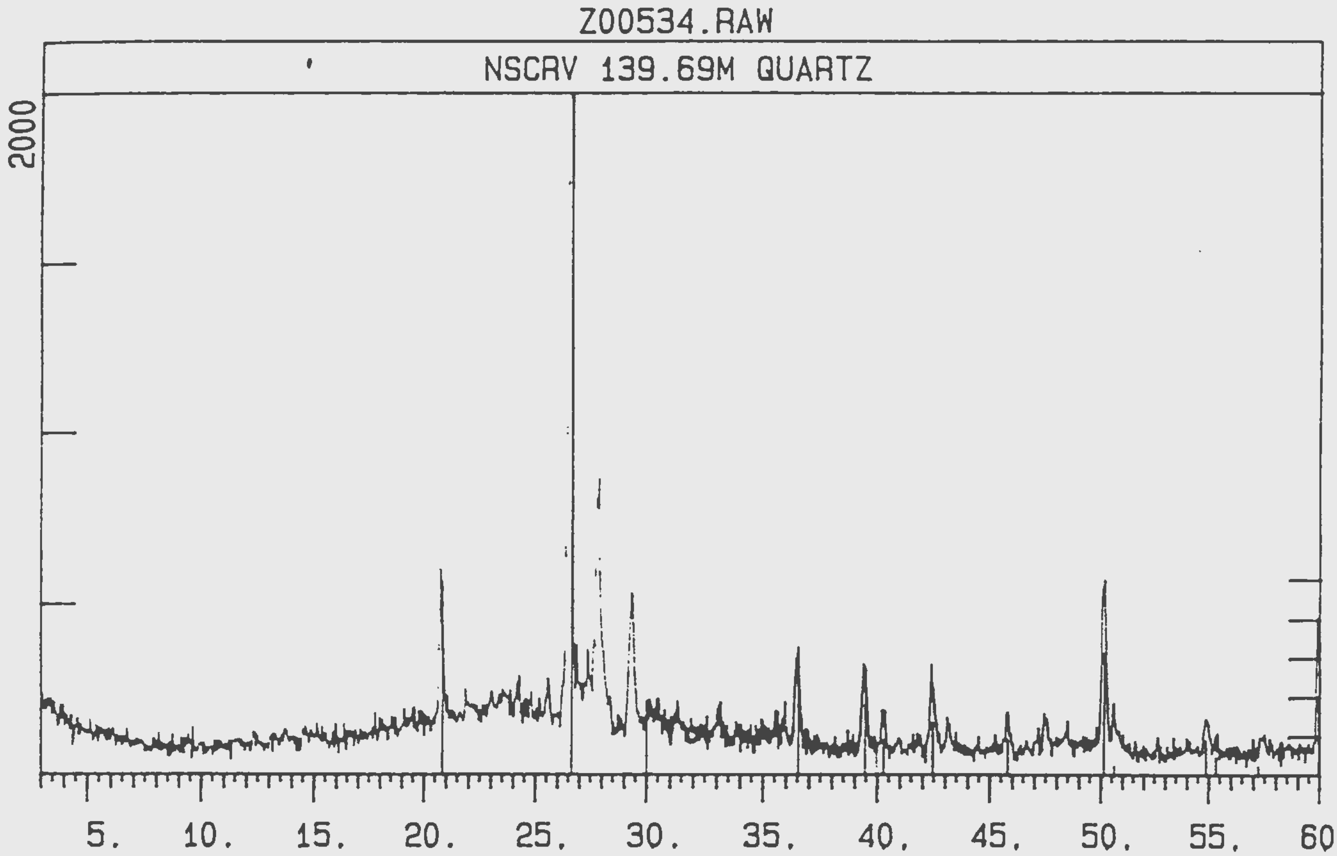

Chlorine

Chlorine, in association with both iron, barium and traces of sulphur, was detected at several locations on the sample from 68.64 m. It was also detected on a generally calcitic fracture surface at 72.48 m.

Iron

Iron is common, especially in analyses that matched chlorite. It was also detected virtually alone at one point at 136.53 m, at a depth where a chlorite match was made, and in conjunction with silica and some aluminum at 29.48 m. The latter analysis was from a distinctive crystal of octahedral shape shown in Figure 7.6. The form of the mineral precludes it being the sheet silicate greenalite (septachlorite group).

Sulphur

Traces of sulphur were detected at 68.64 m.

Titanium

Titanium was detected on the sample from 72.51 m in conjunction with an unmatched analysis which was possibly chlorite and at 139.69 m in conjunction with chlorite. The latter mineral had been logged as the titanium bearing mineral wolframite in the field.

Figure 7.6 SEM photograph of octahedral crystal, high in iron, from 29.48 m (A,B,C are analysis points, indicated on tables)

7.6 CONCLUSIONS

For the purposes of this study the methods used to detect minerals appear to have some value, however it should be noted that this approach is not infallible and it has been used only as an indicator of plausible phases.

Several minerals were identified using XRD and SEM/EDM. The presence of calcite and quartz is confirmed and calcite appears to have been precipitated over the entire NSCRV interval, whereas quartz was only detected on fracture surfaces at 68.64 m or deeper.

Other minerals identified with less certainty, are Fe− and Mg−rich chlorite, found throughout the drilled section; halloysite and illite, found at 68.64 m or deeper, and montmorillonite and saponite only detected on an isolated fracture surface at 148.31 m. Plagioclase feldspar, possibly oligoclase may also be present. Other indirect evidence supports the possibility of the presence of these minerals:

i) the formation of montmorillonite and saponite is favoured under alkaline, low potassium conditions (such as are found in the modern Holyrood Granite groundwaters),

ii) the Holyrood Granite has been noted as being strongly chloritised by McCartney et al. (1966), Papezik (1970) and Strong and Minatidis (1975),

iii) the composition of many of the NSCRV waters plot in the stability fields of plagioclase feldspars.

All of these minerals will be assumed to be plausible phases for the purposes of geochemical modelling, in addition some of the component minerals of granite will be added to the set of plausible phases.

CHAPTER 8: HYDROGEOCHEMICAL MODELLING

8.1 INTRODUCTION

Groundwater flow models can provide information regarding flow paths in aquifers. Geochemical models provide information regarding the probable evolutionary pathways of groundwater in the subsurface. These pathways may be controlled by mixing of groundwater of differing origins and by chemical reactions occurring in the aquifer. The chemical reactions may themselves be controlled by the mineralogy of the aquifer. The information gained from the two models (flow and geochemical) can be used to corroborate results of the other. The uncalibrated flow model used in this study only provides a very general concept of flow patterns in the Holyrood Aquifer. The use of geochemical modelling to define probable end-members in the mixing and evolutionary sequence of the groundwater lends credibility to the flow model and results in a tenable model for flow and groundwater evolution in the aquifer. The geochemical modelling presented in this section is used to define plausible end-members involved along a reaction path, and define plausible phases involved in the groundwater evolution.

A variety of input parameters are required to successfully model the evolution of an aqueous solution from an initial composition to another intermediate or "end-member" composition. The evolution of the aqueous solution can be driven by (amongst other things): variations of P_{co2} (whether the system is open or closed to CO_2), mineral solution or precipitation, temperature and pressure variations, by mixing of aqueous solutions of differing composition, and by reversible exchange of mass between aqueous and solid phases.

All geochemical modelling of the NSCRV waters was conducted with a view to solving the inverse problem defined by Plummer (1984) as "..[an attempt] to find a set of net mass transfer reactions that are thermodynamically feasible and satisfy the mass balance criteria using the available hydrochemical data." To this end geochemical modelling was conducted in two phases as described by Plummer et al. (1983):

a) **speciation calculations** were performed to determine the saturation states of a variety of minerals, expressed as mineral saturation indices (SIs)[2]. These calculations were intended to identify those minerals likely to be involved in the evolution of the groundwater at NSCRV as a result of their intimate thermodynamic relationship with possible and actual solid phases. Assuming equilibrium SIs are positive if the solution is oversaturated with respect to a mineral (which should be precipitating) and negative if the solution is undersaturated with respect to a mineral (which should be

[2]SI is defined as Log (IAP/K) and IAP and K are respectively the ion activity product and equilibrium constant

dissolving). The speciation calculations were performed using the computer program PHREEQE (Parkhurst et al. 1980).

b) **mass balance calculations**, were conducted to define possible evolutionary pathways for the NSCRV waters from a hypothetical starting composition (recharge waters) to the observed composition. A series of calculations were made using a variety of combinations of the plausible phases described in Chapter 7 (with the addition of NaCl). The mixing of two end-member waters of differing compositions was also incorporated into the calculations. Two additional constraints also applied to the mass-balance equations a) redox constraints to determine if oxidation and reduction could be significant processes in the evolution of groundwater, b) mixing constraints (primarily as indicated by chloride concentrations) in an attempt to determine feasible end members for mixing. With the limited isotopic data isotope constraints were not applied as very small variances in isotopic composition would lead to large changes in model results which were not necessarily justifiable in terms of the analytical uncertainties associated with the isotope data.

The mass balance calculations can indicate whether a plausible species has;

i) been lost from the solution (by precipitation if it is a mineral or off-gassing for volatile components) or,

ii) been added to the solution; by dissolution of a mineral, or gaseous, phase.

The theory behind chemical mass balance calculations has been described by Parkhurst et al. (1982) and implemented in the mass balance calculation program BALANCE (Parkhurst et al. 1982) and NETPATH (Plummer et al. 1991). In this study the calculations were performed using the matrix inversion and multiplication techniques used in BALANCE and executed on Lotus 1-2-3 spreadsheet software. A summary of this spreadsheet approach is provided in Appendix G.

The results of the mass balance calculations were compared with the saturation states determined from the speciation calculations; plausible reaction combinations were selected from over 50 possible mass transfer models tested.

Ideally the plausible mass balance models would be tested for thermodynamic feasibility by reaction path modelling. In this study a comparison of mass balance models with the results of speciation calculations was used to identify models which are likely to be thermodynamically feasible.

8.2 DATA AND THERMODYNAMIC DATABASE QUALITY

Geochemical modelling requires two broad groups of input parameters before any modelling can be performed;

a) chemical analyses of the aqueous solutions of interest (in this case groundwater and an assumed starting end-member) and,

b) thermodynamic data for both the aqueous species in solution (or believed to be in solution) and the minerals which are believed to be dissolving or precipitating.

The combination of accuracy of the chemical analyses and the consistency and reliability of the thermodynamic data will in a large part dictate how successfully an aqueous reaction may be modelled.

8.2.1 Groundwater Data Quality

As discussed in Chapter 4 the water samples collected from the NSCRV borehole are believed to be representative. Furthermore the concentration of an element in the virgin groundwater, at a particular depth, is considered to be best represented by the last sample collected (in a sequential time series of samples) from any given interval. The last recorded field values (in a time series) of pH, Eh and alkalinity were also used for modelling purposes. Wherever possible only ICP-MS analyses were used for geochemical modelling. Where values of Eh were not available, the value of Eh from an adjacent sample interval was assumed. Results of Eh measurements were used indirectly in some of the mass balance models, all of these were discarded as plausible models as they did not reflect the results of speciation calculations.

For almost all of the common minerals the hydrogeochemical analyses from NSCRV are both complete and saturation sufficient (as defined by Plummer et al. 1983), i.e., there are sufficient chemical data to calculate the saturation indices of the mineral phases considered. However, it is possible that the aluminum analyses in fact represent contamination from dust in the laboratory (H.Longerich pers. comm) rather than true concentrations of Al in native formation waters. The problem of hydrogeochemical data being saturation insufficient with respect to aluminum is a common one and has been discussed by Plummer et al. (1983). If aluminum is omitted from the NSCRV chemical analyses then the data are rendered saturation insufficient for all Al bearing minerals.

For this alumino-silicate dominated system the SI's of the alumino-silicates are of particular interest and omission of aluminum from the data set means that concentration of aluminum must be estimated by some other means. If this is not done the saturation states of the aluminum bearing minerals cannot be determined, and the results of subsequent modelling (which will be used to interpret plausible evolutionary paths for the NSCRV groundwater) may be difficult to verify. Furthermore it may be difficult to solve a set of mass balance equations, using several aluminum bearing minerals when aluminum is omitted (though this is suggested by Plummer et al.), as many minerals are indistinguishable if their aluminum stoichiometry is omitted (i.e., the omission of Al makes some mass balance equations the same, resulting in an uninvertible matrix). Fortunately, there is evidence that the Al analyses are in fact reasonable (as discussed in Chapter 4) and the analyzed Al concentrations were used for all calculations.

8.2.2 Thermodynamic Data

As noted in Chapter 5, extensive checking was performed on the mineral thermodynamic data base, supplied with PHREEQE. The outcome of this evaluation was a decision to replace the thermodynamic data for Gibbsite, Kaolinite, Low-Albite, Muscovite, Anorthite, Pyrophyllite, Microcline, Chlorite and Na-, K-, Ca-, Mg-Beidellite (provided in the data base supplied with PHREEQE), with the data of Helgeson (1969) and Helgeson et al. (1978). In addition the following substitutions were made:

a) Chlorite-M and Chlorite-K were removed from the data base and replaced only by Chlorite,

b) Halloysite was removed and replaced by Kaolinite,

c) the original Nontronites (Na, K, Mg, Ca) were replaced by Na, K, Mg, Ca Beidellites.

The thermodynamic data review is presented in Appendix D. A listing of the thermodynamic data base used for hydrogeochemical modelling is supplied in Appendix E. The re-compiled and checked data base is referred to as HELGTHEM. The following convention is used to differentiate results that may be affected by the data base:

a) upper case names (e.g. CALCITE) indicate minerals for which the original data base information was used,

b) lower case names with the first letter capitalised (e.g. Calcite) designate minerals relying on the Helgeson data.

Thermodynamic data derived by different workers should generally not be mixed as it will be inconsistent (see for instance Nordstrom and Munoz 1985); however the Helgeson data are extensive enough that all of the major minerals are represented, and should be consistent for the phases of interest. The remaining original data supplies extensive information about minor or rare mineral phases. The problem of mixing data bases is further discussed in Appendix D.

A further check of the modified thermodynamic data base and program was made by comparing SIs derived for various minerals using PHREEQE with the results of other program/data base combinations for the same aqueous solution. Nordstrom et al. (1979) compared the SI's calculated for nineteen (19) different minerals, using 11 different hydrogeochemical modelling programs and data bases, for two analyses of typical seawater and river water. Using typical seawater (as defined by Nordstrom et al. 1979) speciation calculations were made using PHREEQE with both the original data base and the HELGTHEM data base. The results of these calculations are compared with the results from the 11 other hydrogeochemical modelling programs presented by Nordstrom et al. (1979) and presented in Table 8.1.

In Table 8.1 only the minerals Gibbsite and Kaolinite have been modelled using both original thermodynamic data and HELGTHEM. All other minerals were modelled with the original thermodynamic data. The ranges of calculated SIs for each mineral, originally published by Nordstrom et al. (1979), are also provided. It can be seen that of the 19 minerals modelled using PHREEQE/HELGTHEM, only 3 (hydroxyapatite, ferric-hydrate, and hematite) fall

Table 8.1 THERMODYNAMIC DATA TEST USING THE SEAWATER TEST CASE OF NORDSTROM ET AL (1979) AND RUNNING PHREEQUE USING THE DATA BASES PHRTHERM.DAT AND HELGTHEM.DAT

Mineral	Current Data Bases phrtherm	Helgthm	Published SI ranges avg	max	min	Comparison Data bases/Programs EQUIL	EQ3	GEOCHEM	MIRE	SEAWAT	SOLMNEQ	WATEQF	WATEQ2	WATSPEC
Calcite	0.8312	0.8312	0.685	0.806	0.597	0.60	0.806	0.67	0.621	0.631	0.597	0.742	0.774	0.72
Dolomite	2.4810	2.4810	2.373	3.439	1.790	2.30	3.439	1.79	2.277	2.305	2.219	2.330	2.394	2.30
Siderite	-7.5970	-7.5970	-7.922	-2.650	-12.420	-2.65	-10.726	-12.42	-4.077		-6.691	-9.006	-8.973	-8.83
Rhodochrosite	-3.8481	-3.8481	-3.440	-0.487	-4.450	-3.57	-4.444	-4.45	-0.487		-3.709	-3.727	-3.695	
Gypsum	-0.3409	-0.3409	-0.537	-0.348	-0.840	-0.47	-0.399	-0.76		-0.840	-0.441	-0.439	-0.348	-0.60
Celestite	-0.6713	-0.6713	-0.731	-0.130	-1.320			-0.13			-0.988	-0.610	-0.609	-1.32
Barite	0.0346	0.0346	1.428	7.642	-0.340			1.12	7.642		-0.0501	0.097	0.097	-0.34
Hydroxyapatite	-0.2119	-0.2119	3.221	7.140	0.605	4.16		3.53			7.14	0.605	0.670	
Fluorite	-0.7490	-0.7490	-1.352	-0.742	-2.610	-1.61		-2.61			-1.048	-0.742	-0.751	
Ferric Hydrate	2.1078	2.1078	-0.504	0.712	-2.930			-2.93				0.712	0.706	
Goethite	6.5063	6.5063	5.774	7.809	2.580	5.64		2.58				7.809	7.803	5.04
Hematite	18.0212	18.0212	12.396	16.518	5.650	8.21	16.518	5.65				15.228	15.229	13.54
Gibbsite	-1.2387	-0.4087	-1.733	0.216	-4.954	-0.63	0.216	-0.57			-4.954	-1.685	-1.817	-2.69
Birnessite	-3.0029	-3.0029	-2.332	-1.010	-2.993			-1.01				-2.993	-2.993	
Manganite	-1.3448	-1.3448	-1.567	-1.335	-2.030			-2.03				-1.335	-1.336	
Chalcedony	-0.5497	-0.5497	-0.660	-0.415	-1.410		-0.415	-1.41			-0.522	-0.537	-0.537	-0.54
Quartz	-0.0597	-0.0597	-0.083	-0.040	-0.143	-0.14	-0.143	-0.04			-0.092	-0.055	-0.054	-0.06
Kaolinite	1.2019	-0.5781	-1.334	0.645	-2.384	-0.47	0.645	-0.67			-2.108	-2.108	-2.384	-2.24
Sepiolite	-1.7296	-1.7296	0.456	1.090	-1.960	-1.96		1.09			1.059	1.059	1.034	

☐ Minerals with SI's calculated using PHRTHERM c: HELGTHEM, that fall outside the range of SI's given by Nordstrom et al (1979) far outside the SI ranges calculated by other speciation programs and these minerals have such a wide published range of SIs that it cannot be stated whether the PHREEQE/HELGTHEM calculated SI is satisfactory or unsatisfactory.

Based on the thermodynamic data base checks, discussed in Chapter 4 and reviewed above, it is believed that the PHREEQE/HELGTHEM combination provides geochemical modelling results which are consistent with the other commonly used program/database combinations. All subsequent references to PHREEQE will imply the use of the HELGTHEM data base.

8.3 HYDROGEOCHEMICAL MODELLING

8.3.1 Speciation Calculations

Before attempting to solve the forward hydrogeochemical problems at NSCRV, speciation calculations for each NSCRV analysis were made. The NSCRV data are theoretically saturation sufficient (at most sample depths) with respect to 321 phases, contained in the data base. Those phases which approach or exceed saturation, at any of the sampled depths, are presented in Table 8.2. It should be noted that blanks on Table 8.2 indicate that during analysis certain elements present in the indicated mineral's composition, at the depth shown, were not detected (i.e., the analyses are naturally saturation insufficient). The criterion for incorporating a mineral phase into Table 8.2 was that its SI, at any of the sampled depths, should exceed -0.2. If this

Table 8.2 MINERALS FOUND TO HAVE SATURATION INDICIES >-0.2, FROM INITIAL SPECIATION CALCULATIONS

DEPTH>>	18.77	56.81	69.64	71.65	74.91	77.41	96.64	97.41
General								
pH	7.50	8.22	7.70	8.43	8.80	8.76	9.05	9.61
CO2(GAS)	-2.6708	-3.3104	-2.9789	-3.5482	-3.9283	-3.9170	-4.2227	-5.0064
Hydrated Sheet Silicates								
Na-beid	-1.8073	-0.4358	-1.9167	-0.2616	1.4115	-0.6871	0.3506	3.4817
K-beid	-2.1905	-0.8665	-2.3423	-0.7349	0.9128	-1.2003	-0.2594	2.9645
Ca-beid	-1.4126	-0.0715	-1.5544	0.0594	1.6505	-0.3917	0.5445	3.6247
Mg-beid	-1.5857	-0.2321	-1.7160	-0.1051	1.4806	-0.5601	0.3455	3.4344
ILLITE	-2.6547	-0.8073	-2.6685	-0.5772	1.2373	-0.8145	0.1690	3.3445
MONTMORI	-2.0458	-0.7021	-2.1897	-0.5702	1.0201	-1.0187	-0.0701	3.0091
Kaolinit	1.1258	2.1279	1.0239	2.1446	3.4265	1.6640	2.3275	4.6733
TALC	-8.3611	-4.1767	-7.3254	-3.1928	-2.0024	-1.3851	-1.2287	2.4695
Pyrophyl	-0.0241	0.8914	-0.2115	1.0027	2.3279	0.5311	1.2617	3.8821
PREHNITE	-7.8711	-4.1569	-7.4272	-3.5159	-1.4133	-2.7525	-1.3604	3.0953
Sheet Silicates								
Muscovit	1.2550	3.3977	1.2180	3.5695	5.8627	3.1165	4.3067	8.7508
ANNITE	-13.4635				8.3178	4.5116	-2.9095	3.4360
GREENALI	-15.6126				3.8616	1.0392	-7.5554	-3.2603
Carbonate Minerals								
ARAGONIT	-0.9598	-0.2217	-0.9020	-0.1710	-0.1516	0.0800	-0.1603	0.0631
CALCITE	-0.7195	0.0186	-0.6535	0.0693	0.0887	0.3202	0.0493	0.2747
OTAVITE	-1.0696	-0.7079	-1.0804	-0.5404	-0.3785	-0.4904	-0.3133	-0.1503
Silica								
CHALCEDO	-0.1099	-0.1532	-0.1481	-0.1059	-0.0843	-0.1015	-0.0863	0.0524
QUARTZ	0.4787	0.4354	0.4467	0.4827	0.5044	0.4872	0.4782	0.6187
CRISTOBA	0.0146	-0.0287	-0.0202	0.0186	0.0403	0.0231	0.0249	0.1646
Feldspars								
Low albi	-1.7364	-0.5398	-1.6258	-0.1623	0.9691	-0.0058	0.8631	2.9585
ANALBITE	-2.1236	-0.9270	-2.0196	-0.5495	0.5819	-0.3930	0.5022	2.5956
Microcli	-0.0686	0.9855	-0.0730	1.2350	2.2898	1.2716	1.8012	4.1789
H SANIDI	-1.1022	-0.0481	-1.1167	0.2014	1.2562	0.2380	0.8077	3.1824
Hydroxides								
BOEHMITE	-0.9149	-0.3706	-0.9451	-0.4095	0.2098	-0.6542	-0.2684	0.7607
Gibbsite	0.0522	0.5965	0.0421	0.5576	1.1769	0.3128	0.6185	1.6535
GOETHITE	6.8208				7.1351	6.1658	5.8921	6.9275
LEPIDOCR	6.8380				7.1523	6.1830	5.6919	6.7435
DIASPORE	1.0096	1.5539	0.9925	1.5150	2.1342	1.2702	1.6035	2.6365
Manganese Minerals								
PYROLUSI	0.1119	1.8687	-0.6849	-5.5647	-10.8115	-10.9846	-5.3895	-4.8500
BIRNESSI	-0.3303	1.4265	-1.0170	-6.0069	-11.2537	-11.4268	-6.2697	-5.6977
NSUTITE	0.2597	2.0165	-0.4270	-5.4169	-10.6637	-10.8368	-5.6797	-5.1077
BIXBYITE	0.1858	2.2594	-1.6452	-4.7274	-9.3411	-9.6072	-3.6243	-1.9372
HAUSMANN	-1.9458	0.4445	-4.8170	-6.0957	-10.0762	-10.4354	-4.0412	-1.2082
MANGANIT	0.4897	1.5265	-0.3970	-1.9669	-4.2737	-4.4068	-1.5297	-0.6777
Phosphates								
FCO3APAT		13.6281	9.4743	16.9078		17.8001	15.6147	17.4967
MNHPO4(C		-0.6567	-1.1079	0.0504	-50.3319	-0.1909	-0.2495	-0.3147
FLUORAPA		5.3146	3.1601	7.3519		7.7494	7.2232	8.1438
Zeolites								
LEONHARD	8.0353	12.6218	8.3258	13.4213	16.8708	13.7175	15.5686	22.8045
LAUMONTI	-2.6734	-0.3802	-2.5575	0.0195	1.7443	0.1677	1.2098	4.8191
PHILLIPS	-0.2287	0.8966	-0.1194	1.2101	2.3032	1.3067	1.7820	4.0352

Table 8.2/ continued

Zinc Species								
ZN(OH)2	-2.5702	-1.8672	-2.3676	-0.8691	-0.8861	-1.1067	-0.6545	-0.1865
ZNO(ACTI	-2.3801	-1.6771	-2.1775	-0.6790	-0.6961	-0.9166	-0.4644	0.0037
ZNSIO3	0.9681	1.6278	1.0463	2.6732	2.6779	2.4401	3.2509	3.8322
WILLEMIT	-3.4272	-2.0645	-3.2033	-0.0210	-0.0333	-0.4916	0.9979	2.0305
Iron Species								
FE(OH)3S	5.5379				5.8522	4.8829	4.3918	5.4434
FERRIHYD	3.3179				3.6322	2.6629	2.1718	3.2234
FE3(OH)8	0.5265				7.6294	4.7614	0.8582	4.3039
FEOH)2.7	8.2241				8.1588	7.2245	6.6574	7.5689
HEMATITE	18.5259				19.1545	17.2159	16.6968	18.7656
MAGHEMIT	10.0261				10.6547	8.7160	7.7339	9.8371
MAGNETIT	13.9252				21.0281	18.1601	15.0143	18.4040
MAG-FERR	6.3943				9.1082	7.3983	7.1809	10.2775
HERCYNIT	-8.8430				-0.1194	-2.7767	-4.5944	-1.2182
Framework Silicates								
Analcime(Na), Wairakite(Ca), Leucite(K)								
LEUCITE	-3.0295	-1.9322	-3.0180	-1.7299	-0.6968	-1.6978	-1.0949	1.1375
WAIRAKIT	-7.8614	-5.5682	-7.7934	-5.1684	-3.4436	-5.0203	-3.7875	-0.1923
ANALCIME	-1.5933	-0.3554	-1.4465	-0.0252	1.0845	0.1268	0.9802	2.9370
Others								
BARITE	0.4324	0.1149	0.2468	0.0950	-0.6456	0.1750	-0.1165	-0.5398
CHRYSOTI	-10.7374	-6.4664	-9.6566	-5.5771	-4.4301	-3.7783	-3.5283	-0.1167
DIOPSIDE	-7.1112	-4.3676	-6.5042	-3.7196	-2.9088	-2.4943	-2.0563	0.2530
FLUORITE	-0.0012	0.1467	-0.1538	0.0615	-0.3280	-0.0327	-0.1668	-0.0269
TREMOLIT	-16.1122	-6.4404	-13.8513	-4.1606	-1.3487	0.0977	1.0856	9.4057
CUPROUSF	8.7300				15.0585	13.9729	11.5940	13.0159
CUPRICFE	14.8915				15.3743	13.2793	13.1882	15.3448

criterion was met at any depth then the SI for the mineral at all other depths was included in the table. The selection of an SI of -0.2 is somewhat arbitrary though it has been noted by Plummer (1984) that the SI of simple minerals probably cannot be calculated to better than ±0.1 units of SI and the error of the estimate of SI for more stoichiometrically complex solids may be as much as ±2.0. These errors are large when it is considered that SI is a logarithmic number.

The results presented in Table 8.2 indicate that the NSCRV waters are super-saturated with respect to quartz at all depths and very close to being saturated with respect to the amorphous silica chalcedony at all depths; however, quartz was only identified in fractures below 68.64 m. The NSCRV waters become saturated below 70 m with respect to the carbonates calcite and aragonite, but never reach saturation with respect to dolomite, probably as a result of the low concentration of Mg, which decreases with depth. Only calcite was identified on fracture planes but it was identified over virtually the entire range of the borehole.

The common aluminosilicates ; the feldspars low albite and analbite appear to approach saturation with depth which agrees with the mineral activity diagrams shown in Chapter 5. Microcline is near or exceeds saturation at all depths. The NSCRV waters are undersaturated with respect to anorthite at all depths though they move towards anorthite saturation with increasing depth. No feldspars were positively identified on fracture plane minerals.

Within the group of clay minerals (hydrated sheet silicates) all the NSCRV waters are super-saturated with respect to kaolinite. They apparently also reach saturation with respect to illite and montmorillonite and the beidellites at depths greater than ~70 m. The mineral halloysite was possibly identified below 68.64 m. Illite and montmorillonite were possibly identified on fracture planes at 71.80 m.

With depth, the waters become over saturated with respect to pyrophyllite, possibly as a result of the two orders of magnitude increase in Al concentration, and a large increase in pH and silica concentration (see Figure 5.4 for the space $\text{Log}\{K\}/\{H\}$ vs $\text{Log}\{H_4SiO_4\}$). No positive matches were made with pyrophyllite in fracture plane surfaces.

The aluminum hydroxide, gibbsite, is apparently at (or slightly above) saturation throughout the NSCRV waters. No positive matches were made with gibbsite in fracture plane surfaces.

The NSCRV waters are saturated with respect to barite at shallow depths but become undersaturated with depth, probably a result of the decrease of dissolved barium concentration with depth, rather than variations in SO_4 with depth. Both barite and sulphate were identified on fracture plane surfaces; however, no positive (or even tentative) matches with barite were made.

The NSCRV waters do not achieve saturation with respect to chlorite (or at least the chlorite included in HELGTHEM) and hence chlorite is not shown in Table 8.2. This result may be reasonable as the chloritisation of the granite probably occurred at much higher temperatures than seen in the present waters.

The manganese minerals, such as pyrolusite, are oversaturated in the surface NSCRV waters but become undersaturated with depth. There was no evidence to reflect this in the fracture plane analyses.

Many other minerals appear to be at or to reach saturation in the NSCRV waters including the framework silicates, zeolites, simple hydroxides and many of the common iron minerals. With respect to the latter, however, Plummer (1984) notes that SI calculations of iron hydroxides may be particularly inaccurate if the ferric/ferrous iron concentration has not been determined in the field.

Despite the large number of minerals apparently at, or above, saturation only a limited number of those shown in Table 8.2 were detected in the fracture planes; furthermore, and as noted above (and with the caveat than nearly all mineral identifications are tentative) these minerals displayed only an approximate correlation with the calculated SI's. These inconsistencies are probably a function of a variety of factors such as: the system being at partial equilibrium, or the system not reaching equilibrium because of short-circuiting along fractures, inherent errors in the thermodynamic data or aluminum concentration data noted above, and the method of analysing for fracture plane minerals

8.3.2 Mass Balance calculations

Mass balance calculations were made using the NSCRV water analyses and a set of plausible phases selected primarily on the basis of results of fracture mineral analyses. Sodium chloride was added to the list of plausible phases (in addition to the chloride from the seawater mixing noted below) as a surrogate for other Cl^- containing phases, such as inclusion fluids and amphiboles. Mixing equations were added to the mass balance; the end members for mixing were considered to be seawater and meteoric water. The selection of these end members was based on the proximity of the ocean, the geological and the glacial history of the area, and the probable mixing scenarios deduced from isotope data.

As discussed previously the isotopic data were not considered to be useful for the purposes of resolving mixing scenarios, though they were used to reject scenarios. This aspect is further discussed in section 8.4.

Over fifty mineral/element combinations were tested; of these combinations many resulted in uninvertible matrices, or mixtures of seawater/ freshwater that had no physical meaning (e.g., apparent mixing of negative amounts of seawater with greater than 100% volumes of meteoric water). From the original combinations a total of 47 were successfully run (i.e., produced invertible matrices). Of the 47, four models were selected as being of possible interest. The selection process was based on similarity between the mass balance results, and the results of speciation calculations (i.e., that similar combinations of minerals were precipitating or dissolving in both calculations).

The results of the four selected mass balance calculations are presented in Table 8.3 at each of the sample depths. All mathematically possible mass balance models are included in Appendix F. An abbreviated synopsis of the phases and elements used in the calculations is provided on the first two lines of each combination in Table 8.3. The two assumed mixing solutions appear as phases which requires another equation in terms of the mixing proportions. Mix 1 is meteoric water, with a P_{co2} of $10^{-2.67}$ as found in the shallowest water from NSCRV. Mix 2 is

Table 8.3 MASS BALANCE CALCULATION RUNS SELECTED FOR PHREEQE MODELLING

MASS BALANCE MODEL T_A

Plausible Phases										
Anorth	Alb	CO2	Calc	NaCl	Micr	S-min	Na-Beid	Mix1	Mix2	
Elements										
Ca	TC	Si	Na	Al	Mg	RS	SO4	Cl	Mix	

DEPTH (m)	18.77	56.81	69.64	71.65	74.91	77.41	96.64	97.41
	mmoles of plausible phase added(+) or lost(-) from the groundwater system							
Anorth	0.7699	0.6689	0.6127	0.4931	-0.4762	-0.2416	0.1260	-1.4470
Alb	0.7283	1.1613	0.9900	1.4090	1.7698	1.0994	1.9397	1.7791
CO2	2.0566	2.2995	1.4994	2.1476	1.4024	1.2776	1.6756	-0.4151
Calc	-0.0057	-0.0004	0.1121	0.0023	0.7049	0.7048	0.0087	1.5534
NaCl	1.8863	1.8622	1.9777	2.3850	2.7938	3.0861	3.9483	4.9376
Micr	-0.0214	-0.5445	-0.4203	-0.9247	-2.0655	-1.2060	-1.7273	-2.7997
S-min	0.1499	0.1630	0.1880	0.1755	0.1967	0.2378	0.4511	1.1216
Na-Beid	-0.9642	-0.8385	-0.7703	-0.6308	0.5373	0.2533	-0.1990	1.6895
Mix1	0.9983	0.9982	0.9980	0.9987	0.9995	0.9989	0.9998	0.9998
Mix2	0.0017	0.0018	0.0020	0.0013	0.0005	0.0011	0.0002	0.0002

DEPTH (m)	18.77	56.81	69.64	71.65	74.91	77.41	96.64	97.41
	mmoles of elements added(+) or lost(-) from the groundwater system							
Ca	0.7825	0.6876	0.7461	0.5088	0.2344	0.4750	0.1366	0.1081
TC	2.0547	2.3031	1.6159	2.1527	2.1086	1.9850	1.6849	1.1388
Si	0.1222	0.1111	0.1076	0.1243	0.1323	0.1269	0.1592	0.2445
Na	3.1274	3.6146	3.6799	4.1931	5.0022	4.8064	5.9069	7.3554
Al	0.0003	0.0009	0.0003	0.0008	0.0037	0.0005	0.0009	0.0219
Mg	0.0946	0.0988	0.1099	0.0691	0.0295	0.0609	0.0097	0.0086
RS	9.4429	10.5070	7.4934	9.8748	6.8891	6.7416	9.4423	5.0986
SO4	0.2002	0.2155	0.2463	0.2122	0.2124	0.2701	0.4563	1.1262
Cl	2.8581	2.8765	3.1067	3.0949	3.0964	3.7114	4.0475	5.0263

MASS BALANCE MODEL T_C

Plausible Phases											
Anorth	Alb	CO2	Calc	NaCl	Micr	S-min	Qtz	Na-Beid	Mix1	Mix2	
Elements											
Ca	TC	Si	Na	Al	Mg	K	RS	SO4	Cl	Mix	

DEPTH (m)	18.77	56.81	69.64	71.65	74.91	77.41	96.64	97.41
	mmoles of plausible phase added(+) or lost(-) from the groundwater system							
Anorth	0.7699	0.6689	0.6127	0.4931	-0.4762	-0.2416	0.1260	-1.4470
Alb	0.7376	1.2562	1.0639	1.5673	2.1195	1.3040	2.2313	2.2546
CO2	2.0566	2.2995	1.4994	2.1476	1.4024	1.2776	1.6756	-0.4151
Calc	-0.0057	-0.0004	0.1121	0.0023	0.7049	0.7048	0.0087	1.5534
NaCl	1.8863	1.8622	1.9777	2.3850	2.7938	3.0861	3.9483	4.9376
Micr	0.0337	0.0243	0.0231	0.0241	0.0317	0.0208	0.0212	0.0523
S-min	0.1499	0.1630	0.1880	0.1755	0.1967	0.2378	0.4511	1.1216
Qtz	-0.0917	-0.9455	-0.7372	-1.5773	-3.4865	-2.0396	-2.9067	-4.7414
Na-Beid	-0.9918	-1.1233	-0.9923	-1.1059	-0.5129	-0.3610	-1.0745	0.2613
Mix1	0.9983	0.9982	0.9980	0.9987	0.9995	0.9989	0.9998	0.9998
Mix2	0.0017	0.0018	0.0020	0.0013	0.0005	0.0011	0.0002	0.0002

DEPTH (m)	18.77	56.81	69.64	71.65	74.91	77.41	96.64	97.41
	mmoles of elements added(+) or lost(-) from the groundwater system							
Ca	0.7825	0.6876	0.7461	0.5088	0.2344	0.4750	0.1366	0.1081
TC	2.0547	2.3031	1.6159	2.1527	2.1086	1.9850	1.6849	1.1388
Si	0.1222	0.1111	0.1076	0.1243	0.1323	0.1269	0.1592	0.2445
Na	3.1274	3.6146	3.6799	4.1931	5.0022	4.8064	5.9069	7.3554
Al	0.0003	0.0009	0.0003	0.0008	0.0037	0.0005	0.0009	0.0219
Mg	0.0946	0.0988	0.1099	0.0691	0.0295	0.0609	0.0097	0.0086
K	0.0519	0.0432	0.0442	0.0373	0.0373	0.0325	0.0230	0.0540
RS	9.4429	10.5070	7.4934	9.8748	6.8891	6.7416	9.4423	5.0986
SO4	0.2002	0.2155	0.2463	0.2122	0.2124	0.2701	0.4563	1.1262
Cl	2.8581	2.8765	3.1067	3.0949	3.0964	3.7114	4.0475	5.0263

Table 8.3/ continued

MASS BALANCE MODEL S_H

Plausible Phases: Anorth, Alb, CO2, Calc, NaCl, Illite, Mix1, Mix2

Elements: Ca, TC, Si, Na, Al, Mg, Cl, Mix

mmoles of plausible phase added(+) or lost(−) from the groundwater system

DEPTH (m)	18.77	56.81	69.64	71.65	74.91	77.41	96.64	97.41
Anorth	1.2209	2.9607	2.4294	4.0781	6.7773	4.0171	6.4429	8.0125
Alb	0.9438	2.1632	1.7866	2.9607	4.8678	2.9198	4.6530	5.7966
CO2	2.5646	4.7274	3.4281	5.9198	8.9662	5.7203	8.2879	9.4114
Calc	−0.5280	−2.4622	−1.8445	−3.8165	−6.9362	−3.7843	−6.6772	−8.3646
NaCl	−1.8931	−7.1622	−5.4408	−10.025	−17.768	−9.1420	−15.630	−19.399
Illite	−1.4719	−3.5146	−2.8892	−4.8331	−8.0082	−4.7624	−7.6252	−9.4781
Mix1	0.9916	0.9823	0.9849	0.9768	0.9631	0.9773	0.9652	0.9568
Mix2	0.0084	0.0177	0.0151	0.0232	0.0369	0.0227	0.0348	0.0432

mmoles of elements added(+) or lost(−) from the groundwater system

DEPTH (m)	18.77	56.81	69.64	71.65	74.91	77.41	96.64	97.41
Ca	0.7825	0.6876	0.7461	0.5088	0.2344	0.4750	0.1366	0.1081
TC	2.0547	2.3031	1.6159	2.1527	2.1086	1.9850	1.6849	1.1388
Si	0.1222	0.1111	0.1076	0.1243	0.1323	0.1269	0.1592	0.2445
Na	3.1274	3.6146	3.6799	4.1931	5.0022	4.8064	5.9069	7.3554
Al	0.0003	0.0009	0.0003	0.0008	0.0037	0.0005	0.0009	0.0219
Mg	0 0946	0.0988	0.1099	0.0691	0.0295	0.0609	0.0097	0.0086
Cl	2.8581	2.8765	3.1067	3.0949	3.0964	3.7114	4.0475	5.0263

MASS BALANCE MODEL S_K

Plausible Phases: Anorth, Alb, CO2, Calc, NaCl, Micr, Na−Beid, Mix1, Mix2

Elements: Ca, TC, Si, Na, Al, Mg, K, Cl, Mix

mmoles of plausible phase added(+) or lost(−) from the groundwater system

DEPTH	18.77	56.81	69.64	71.65	74.91	77.41	96.64	97.41
Anorth	0.9059	2.0696	1.7048	2.8299	4.6889	2.7799	4.4322	5.5772
Alb	0.7829	1.7233	1.4281	2.3466	3.8421	2.3117	3.6674	4.5972
CO2	2.1925	3.7002	2.5915	4.4843	6.5676	4.2992	5.9819	6.6090
Calc	−0.1417	−1.4011	−0.9800	−2.3345	−4.4603	−2.3167	−4.2975	−5.4707
NaCl	1.8863	1.8622	1.9777	2.3850	2.7938	3.0861	3.9483	4.9376
Micr	0.0337	0.0243	0.0231	0.0241	0.0317	0.0208	0.0212	0.0523
Na−Beid	−1.1279	−2.5261	−2.0861	−3.4462	−5.6858	−3.3870	−5.3872	−6.7734
Mix1	0.9983	0.9982	0.9980	0.9987	0.9995	0.9989	0.9998	0.9998
Mix2	0.0017	0.0018	0.0020	0.0013	0.0005	0.0011	0.0002	0.0002

mmoles of elements added(+) or lost(−) from the groundwater system

DEPTH (m)	18.77	56.81	69.64	71.65	74.91	77.41	96.64	97.41
Ca	0.7825	0.6876	0.7461	0 5088	0.2344	0.4750	0.1366	0.1081
TC	2.0547	2.3031	1.6159	2.1527	2.1086	1.9850	1.6849	1.1388
Si	0.1222	0.1111	0.1076	0.1243	0.1323	0.1269	0.1592	0.2445
Na	3.1274	3.6146	3.6799	4.1931	5.0022	4.8064	5.9069	7.3554
Al	0.0003	0.0009	0.0003	0.0008	0.0037	0.0005	0.0009	0.0219
Mg	0.0946	0.0988	0.1099	0.0691	0.0295	0.0609	0.0097	0.0086
K	0.0519	0.0432	0.0442	0.0373	0.0373	0.0325	0.0230	0.0540
Cl	2.8581	2.8765	3.1067	3.0949	3.0964	3.7114	4.0475	5.0263

seawater of the Nordstrom et al. (1979) composition. TC is total carbon as calculated using PHREEQE during the speciation calculations. RS is redox state also calculated by PHREEQE and expressed as THOR in PHREEQE. S-min is an undefined sulphate bearing mineral (i.e. no differentiation between for instance, barite or anhydrite) with sulphate at an operational valence (Parkhurst et al. 1980) of 6^{+}. The table shows both the number of millimoles of a mineral precipitated (negative) from the system or dissolved (positive) into the system, and the fraction of the end-member solutions mixed.

The four mass transfer models chosen fall into two series;

i) the T_A and T_C combinations (10 and 11 plausible phases, respectively, requiring the same number of variables), both of which have an unspecified sulphate mineral added and a redox constraint. As noted above the redox value was determined during the PHREEQE speciation calculations,
ii) the S_H and S_K combinations (9 and 10 plausible phases) which have no sulphate variable and no redox state constraint.

Close scrutiny of the four mineral combinations presented in Table 8.3 reveals that only one mineral combination has any validity: The phase combination of model T_A can be rejected as a feasible reaction path since the mass balance requires that anorthite be precipitated. The phase combination T_C also requires precipitation of anorthite and solution of calcite in the deeper sample intervals. The phase combination S_H requires that halite is precipitated which is obviously incorrect at the salt concentrations seen at NSCRV. The only feasible phase combination found is that of model S_K; however, even this combination requires addition of a carbon source (CO_2) to the deeper sample intervals. Whether there is a mechanism in the Holyrood Aquifer which does this is not known. Carbon isotope data would add a further useful and relevant constraint to the mass balance calculations. Unfortunately no carbon isotope data are currently available for NSCRV.

The results of the balance calculations indicate that:

1) for a successful mass balance result (i.e one that is consistent with calculated saturation states) NaCl must always be included as a mineral phase (where NaCl is a surrogate for fluid inclusion or amphibole derived chloride),
2) if NaCl is included, as a mineral phase, then the mixing proportion of seawater **decreases** with depth,
3) a carbon source is required for a feasible mass balance result. Carbon addition is known to occur in regional groundwater flow (Plummer, 1977) and deep groundwater in granitic rocks can contain large concentrations of

hydrocarbon gases that were apparently generated in-situ (Frape and Fritz, 1987). Carbon isotope data would help to further constrain the mass balance equations,

4) no satisfactory model was found in which seawater was the sole source of Cl.

8.4 TEST OF MASS BALANCE MIXING HYPOTHESIS USING OXYGEN AND HYDROGEN ISOTOPE DATA

The calculated mixing proportions of end member waters implied in mass balance model S_K, may be tested using the analyzed isotope data and assumed isotope compositions for the mixing components (the end-members). In this manner it may be possible to corroborate the results of mass balance modelling. Unfortunately the proportion of seawater mixed is so small that it must have an isotopic composition which is extreme (negative or positive) compared with the isotopic composition of the meteoric component to have any significant effect.

Two different mixing scenarios were tested using two different compositions for the minor mixing fraction (Mix 2 the seawater component in the balance calculations) and using a constant composition for the major mixing fraction (Mix 1, shallow groundwater in the balance calculations). Initially, no allowance was made for the altitude effect described in Chapter 6. The assumed compositions for the end-members are:

i) Major mixing fraction (meteoric water) with isotopic composition: $\delta^{18}O$ of -8.079, $\delta^{2}H$ of -55.39. The isotopic composition of ^{18}O at 0 m depth was calculated from the equation for the line of best fit for the ^{18}O analyses, the value for ^{2}H was then back calculated using the equation for the meteoric water line (Equation 6.1),

ii) The minor mixing fraction assumed to be either:

a) glacial meltwater of approximate composition $\delta^{18}O$ of -41 (Faure 1986) and a $\delta^{2}H$ value of -318 (calculated from the equation for the meteoric water line and the $\delta^{18}O$ value of -41.00)

b) seawater of composition $\delta^{18}O$ of 0.5, $\delta^{2}H$ of 5.00 (Faure 1986).

Using the two possible mixing combinations (i.e., shallow NSCRV groundwater mixed with glacial meltwater and shallow NSCRV water mixed with seawater), the following two scenarios were considered:

SCENARIO 1: In contradiction to the selected plausible mass balance models, there is no contribution of NaCl from the rock mass and all chloride is derived from the minor mixing fraction. See for instance mass balance model N_A, Appendix F.

SCENARIO 2: There is some contribution of NaCl from the rock mass and the mixing fraction of seawater decreases with depth, as seen in balance model S_K.

Table 8.4 presents a synopsis of the results of these computations. The four possible mixing scenarios are numbered 1A, 1B, 2A and 2B. The isotope compositions were calculated using equation 8.1:

$$\delta Tot = X_{mix1} \cdot \delta_{mix1} + X_{mix2} \cdot \delta_{mix2} \qquad \textbf{(Equation 8.1)}$$

$\delta\ Tot$	isotopic composition of observed groundwater
$X_{mix\ n}$	fraction of component n (where n is 1 or 2)
$\delta_{mix\ n}$	isotopic composition of component n

A line of best fit was applied to all results (both actual and calculated) and it is the change in the isotope composition, from 0 m to 97.41 m which is reviewed. The observed change in isotopic composition at NSCRV is −0.335 for $\delta^{18}O$ and −2.94 for $\delta^{2}H$ (based on a least-squares linear fit to data shown in Figure 5.1, where the deep waters are depleted in the heavy isotope relative to shallow groundwater.

Note that all of the calculated mixing effects in Table 8.4 will have superimposed on them an altitude effect which will result in a further decrease in the $\delta^{18}O$ values of about 0.33‰ and for $\delta^{2}H$ of about 2.94‰, respectively, between the shallow waters and the deep waters. Thus, for the four mixing models tested,

Table 8.4 Hypothetical mixing of end members of differing isotopic compositions

	Modelled change in $\delta^{18}O$	Modelled change in $\delta^{2}H$	Observed change $\delta^{18}O/\delta^{2}H$
HYPOTHESIS 1:	MIXING WITHOUT ADDITION OF NaCl (Seawater source only)		
1A) Mix 2 Glacial	-0.292	-2.33	-0.335/-2.94
1B) Mix 2 Seawater	0.076	0.54	
HYPOTHESIS 2:	MIXING WITH ADDITION OF NaCl		
2A) Mix 2 Glacial	-0.005	n/a	
2B) Mix 2 Seawater	-0.013	-0.09	

model 1A would result in a net change in $\delta^{18}O$ of approximately −0.61‰ between the shallow and the deep intervals; Model 1B would result in a change in $\delta^{18}O$ value of approximately −0.24‰; model 2A would result in a change of $\delta^{18}O$ value of −0.32‰; and model 2B would result in a change of −0.33‰. Thus model 1A may certainly be rejected, and model 1B should probably be rejected, indicating that Hypothesis 1 is incorrect. This is consistent with the mass balance evidence.

Both of models 2A and 2B appear to produce plausible results; however, model 2A (mixing of meteoric water with glacial meltwater) is completely inconsistent with the indicator originally used to determine the mixing proportions; that is chloride concentration. The only consistent model is one in which seawater mixes with meteoric water to provide part of the chloride concentration with the balance of the chloride derived from an undetermined source in the rock mass.

8.5 TEST OF GEOCHEMICAL MODELLING RESULTS USING CHLORIDE DATA

Nordstrom et al. (1985) proposed that the gradual leaching of fluid inclusions from the rock mass of the Stripa Granite could account for the entire salinity of the Stripa groundwaters (assuming that the Stripa groundwater is under static hydrologic conditions). The inclusion fluid at Stripa is believed to be relatively enriched in halides (especially Cl) and represents an estimated 17 L of inclusion fluid per m^3 of rock mass. It averages approximately 3% (by weight) of NaCl, equivalent to a concentration of 278 ppm of chloride in the bulk rock (Nordstrom et al. 1985).

The salt content of the inclusion fluids, expressed in terms of NaCl, is higher in unfractured than fractured parts of the Stripa rock mass (Fontes et al. 1989), being 40‰ and 17‰ in the unfractured and fractured parts of the rock respectively. This is equivalent to 210 and 130 ppm Cl in the fractured and unfractured rock respectively (note that the 278 ppm figure is from Nordstrom et al. (1985) while the 210 & 130 ppm values are from Fontes et al. 1989, hence the apparently incorrect average value)

Assuming a 1% porosity in the granite, Nordstrom et al. (1985) showed that a concentration of Cl of ~28 g/L could develop, in the groundwater, if all the fluid inclusions were leached. To test this theory Nordstrom went on to compare the Br/Cl ratios (both elements assumed to be conservative tracers) in fluid inclusions with those in the groundwater. An average Br/Cl ratio for samples leached from fluid inclusions in Stripa Granite was 0.0101 ± 0.0015; Stripa groundwater averaged 0.0107 ± 0.001 (in comparison the average Br/Cl ratio for all of the NSCRV waters is an extremely consistent 0.0013 and in seawater is 0.00356). Based on this reasoning Nordstrom et al. (1985) concluded that leaching of fluid inclusions could be invoked as a mechanism for adding salinity to the Stripa groundwaters. Nordstrom et al. (1985) also studied the I/Cl ration of the inclusion fluid and groundwater but I is not considered to be conservative, being susceptible to reaction with organic matter in a variety of valence states (Fontes et al. 1989).

Fontes et al. (1989) reviewed the hypothesis that fluid inclusions could account for groundwater salinity in the Stripa granite and concluded that it was incompatible with the available facts because:

a) there were possible flaws in the leaching experiments reviewed by Nordstrom et al. (1985),

b) incompatibility of the inclusion data with known groundwater SO_4 concentrations,

c) a lack of a satisfactory mechanism to account for the transfer of inclusion fluid to the groundwater and no evidence for any flushed voids in any of the Stripa rocks analyzed, and

d) no evidence to suggest that the groundwater at the Stripa site is in any way stagnant, as required by a fluid inclusion mass calculation.

The possibility that the salinity in the Stripa Granite is derived from dissolution of halide-containing micas was also discounted by Fontes et al. Their argument was based on a probable lack of mass balance between the known amount of alteration of biotite to chlorite (with release of chloride) in combination with probable over-estimation of the chloride content of the biotites. However Edmunds et al. (1985) considered the breakdown of biotite as a plausible means of developing salinity in the Carnmellis Granite, U.K.

Despite the objections of Fontes et al. (1989) to fluid inclusion salinity accounting for the groundwater salinity in the Stripa Granite, fluid inclusions offer a possible source of Cl in the Holyrood Granite. An alternative source might be grain boundary salts, or ejection of chloride from biotites during chloritisation. Therefore recognising that 'NaCl' is a surrogate for a rock-derived Cl source, the phases selected for mass balance modelling in section 8.3.2 all appear to be plausible and justifiable. Furthermore, the hypothesis of seawater addition in small amounts is not inconsistent with the observed shifts in isotope values. The proposed Cl sources are examined in the following section, in light of the expected Cl/Br ratio variation expected during mixing.

Figure 8.1 shows the correlation of the fraction of seawater (calculated using mass balance) mixed with NSCRV waters, and the inverse correlation of mmoles of modelled NaCl added to the NSCRV waters, both with respect to Log hydraulic conductivity. Both correlations are significant at the 95% level. Table 8.5 shows these results in terms of calculated additions of Cl to the NSCRV waters from seawater and from the rock-mass. All rock-mass halide contributions (here assumed to be from fluid inclusions, FI) are designated by a superscript-°. The values were calculated as follows:

Figure 8.1 CORRELATION BETWEEN MODELLED NaCl AND SEAWATER ADDITIONS TO GROUNDWATER IN THE HOLYROOD GRANITE, AND HYDRAULIC CONDUCTIVITY

Log mmoles NaCl added vs Log K

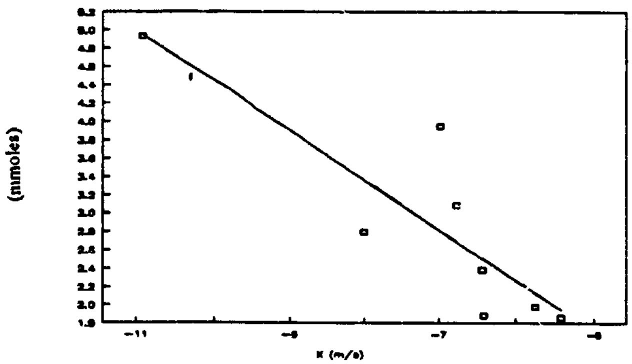

Regression Output:
For y=Mx + C

C	-1.017
Err of C	0.608
R^2	0.739
No. Obs.	8.000
°Freedom	6.000
M	-0.547
Std Err of M	0.133

Log Fraction of Seawater Mixing vs Log K

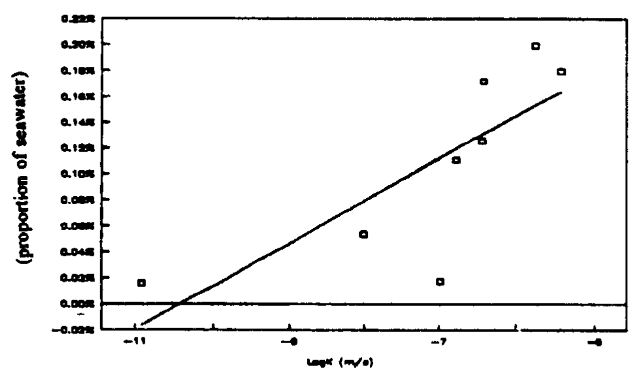

C	0.003
Err of C	0.000
R^2	0.603
No. Obs.	8.000
°Freedom	6.000
M	0.000
Std Err of M	0.000

Table 8.5 Calculated contributions of halides from seawater and a rock source

Sample Depth (m)	LogK (m/s)	Seawater fraction calculated from mass balance	observed halide concentrations Cl (ppb)	Br (ppb)	Br/Cl	Calculated halide contributions from seawater Cl (ppb)	Br (ppb)	Calculated rock derived halide contribution Cl° (ppb)	Br° (ppb)	Br°/Cl°
18.79	-6.42	0.0017	101321	138.7	0.001369	34020	114.9	66875	23.8	0.000356
56.81	-5.42	0.0018	101973	138.5	0.001358	35509	119.9	66020	18.6	0.000281
69.64	-5.75	0.0020	110132	145.4	0.001320	39520	133.4	70117	12.0	0.000171
71.65	-6.44	0.0013	109715	146.1	0.001332	24852	83.9	84555	62.2	0.000735
75.61	-8.01	0.0005	109769	145.9	0.001329	10594	35.8	99049	110.2	0.001112
77.62	-6.77	0.0011	131570	172.5	0.001311	21891	73.9	109410	98.6	0.000901
96.64	-6.98	0.0002	143485	189.7	0.001322	3472	11.7	139980	177.9	0.001271
98.62	-10.91	0.0002	178183	239.4	0.001344	3107	10.5	175051	228.9	0.001308
			19805000	66872.00	0.003377					

See text for explanation for derivation of results

i) contribution of Cl° from the rock mass (equation 8.2):

$$Cl^{\circ}\ \mu g/L = NaCl\,(\mu M/L) * MW_{Cl}\,(g/M) \qquad \textbf{(Equation 8.2)}$$

Where:

NaCl - moles chloride contributed to the groundwater from the rock mass as calculated using mass balance model S_K

MW_{Cl} - Molecular weight of chlorine

ii) contributions of Cl and Br, to the groundwater, from seawater (using equation 8.3):

(Equation 8.3)

$$H\ (ppm) = [X_{sea} * [H_{sea}]\,M/kg * MW_{H}(g/M)] * 1000$$

Where:

H - calculated halide concentration in ppm

H_{sea} - halide concentration in seawater in Moles/kg

X_{sea} - fraction of seawater contributing to mixture, as calculated using mass balance model S_K

MW_H - molecular weight of halide in g/mole

Rock derived Br (Br°) was calculated by subtracting the calculated Br concentration contributed from seawater, from the analyzed Br concentration. This value is shown as the calculated remainder on Table 8.5.

The results shown on Table 8.5 indicate that modelled Cl contribution from seawater decreases from approximately 34%, in the higher permeability zones, to less than 2% in the lower permeability zones, while modelled contributions of rock derived chloride (Cl°) rise from approximately 66% to 98%. The general increase in Cl° is interpreted as a manifestation of increased rock-water interaction, also reflected in the inverse correlation of silica concentration with Log hydraulic conductivity (Figure 5.1).

8.5.1 Discussion

If the interpretations of an isotope altitude effect and the probable ordered nature of flow in the Holyrood Aquifer are coupled with halide contribution inferred from assumed seawater and the rock-mass sources then a possible mechanism for the addition of seawater to the aquifer may be hypothesised.

It is proposed that seawater, in the amounts calculated from the mass balance model S_K, may be (or may have been) provided to the aquifer in precipitation enriched in Cl and other compounds by seawater aerosols. This mechanism could provide saltwater to the recharging aquifer in amounts which would be an inverse function of the distance of the recharge point from the coast line (and an inverse function of the altitude of recharge). The calculations in Table 8.5 indicate that the modelled seawater (or aerosols) contribute approximately 34 ppm chloride in shallow groundwaters at the NSCRV site, decreasing to approximately 3 ppm Cl in the deepest groundwater, derived from higher elevations inland. Schillereff (1992) analyzed samples from shallow depths in wells at altitudes between 100 and 120 m, in the Seal Cove River Valley (approximately 2.5 km inland and up the Seal Cove River of the NSCRV location). The samples had Cl concentrations in the range 5.2 to 8.1 ppm, which compare favourably with the calculated seawater chloride addition in deep NSCRV samples of 3.1 to 3.4 ppm in the 90 m sample intervals (which are assumed to have been recharged at an altitude of approximately 170 m), shown on Table 8.5.

McCullough (1984) has published information regarding chloride concentration in precipitation at St.John's airport, with a maximum concentration, for the period of recorded, in December of 0.14 ppm. Samples analyzed during August had no detectable Cl in them. The St.John's site is only 1-2 km from the coast. Cicerone (1984) has noted that marine precipitation may have chloride concentrations of up to 10 ppm, which is comparable to the calculated figures (in Table 8.5) for non rock-mass chloride contribution at NSCRV.

In Chapter 6 it was noted that recharge to the Holyrood aquifer occurred primarily during March-April and October-November. These are periods when strong northerly winds, which might be expected to have significant fetch over the ocean, carry precipitation to the Newfoundland east coast. These winds are more likely to carry high aerosol salt concentrations than the westerly and southwesterly winds that prevail in summer when aquifer recharge is likely to be minimal. Thus, a significant range of Cl concentrations is likely in precipitation over the study area, and the possibility exists that precipitation during periods of principal aquifer recharge in NSCRV may also be coupled with high levels of chloride in the precipitation.

Unfortunately no precise information is available regarding concentration of chloride in near coastal precipitation at NSCRV. If aerosol salt concentrations are high the isotope data corroborate the mass balance model of seawater salt addition. The calculated contributions of aerosol/seawater derived chloride are also consistent with chloride concentrations observed in shallow groundwaters (Schillereff,1992) that are recharged 2.5 km inland from NSCRV. However, it must also be noted that an additional, non-seawater, source of salts has to be invoked in order to explain the observed flow system, and groundwater chemical and stable isotope characteristics.

8.6 CONCLUSIONS

The hydrogeochemical modelling conducted on the NSCRV groundwaters indicates that the chemical evolution of groundwater at NSCRV is consistent with the presence of mineral phases in NSCRV core and with the addition of a seawater like component. However, to achieve consistency with isotope analyses and with data from other parts of the aquifer, an additional rock-mass source of chloride is required in the mass balance models.

At this time there is no direct observational evidence of a chloride source in the rock-mass of the Holyrood Aquifer, or of seawater providing significant amounts of salt to the shallow groundwater near the coast. However, a model in which rock-mass derived NaCl is added to the groundwater in increasing proportions with depth and in which a seawater component is present in decreasing proportions with depth, is the only interpretation consistent with; i) isotopic data; ii) inferred recharge elevations and flow paths in the aquifer; iii) the correlations between ionic concentrations, depth and hydraulic conductivity, and; iv) geochemical data from inland wells at higher elevations.

CHAPTER 9: CONCLUSIONS & INTERPRETATIONS

9.1 SUMMARY OF RESULTS

The study location lies on the northern perimeter of the Holyrood Granite. The NSCRV borehole is located in the discharge area of the aquifer with artesian conditions along virtually its entire length. The groundwater flow through the Holyrood Granite, as interpreted from results in the NSCRV borehole, appears to be controlled by nearly-vertical east-west fractures. The near-vertical fractures may be a result of post glacial isostatic movements resulting either in reopening of pre-existing fractures, or creation of new fractures.

Groundwater flow boundaries in the study area are the surface/groundwater divide south of the study area, the saltwater freshwater interface and the assumed no flow boundary resulting from essential loss of permeability at depth. Stable isotopic data, ^{18}O and ^{2}H indicate that the NSCRV waters are meteoric and that they may reflect their original altitude of recharge under climatic temperatures similar to the present day. The retention of an altitude dependant isotopic signature appears to indicate that the flow through the Holyrood Granite is well ordered and follows approximately the flow paths derived from a simple flow model.

Based on this simple model the approximate residence time in the aquifer (from recharge to point of sampling in NSCRV borehole) is believed to be in the range 1560 to 15 600 y. This range of residence times assumes an aquifer bulk hydraulic conductivity of approximately 4.74×10^{-9} m/s, estimated from the results of hydraulic conductivity testing results at NSCRV, a flow porosity in the range 2 to 20‰ and an average hydraulic gradient of 0.03.

As a result of rock-water interaction in the granite, minerals precipitated in fractures are calcite, quartz, and with a lesser degree of certainty, Fe and Mg chlorite, halloysite and illite, the smectite clays, montmorillonite and saponite, and iron oxides (These minerals were presumably formed under contemporary hydrogeochemical conditions). Feldspar minerals are inferred to play a role in groundwater evolution in the granite, probably with anorthite, albite and potassium feldspar dissolving.

Examination of groundwater chemical compositions indicate that NSCRV groundwaters lie in or close to the stability fields for kaolinite, K-Feldspar/Muscovite, and chlorite. The waters evolved from surface waters of Na-bicarbonate composition towards an NaCl dominated composition. The changes in groundwater chemistry can be modelled geochemically using a set of seven minerals (including NaCl) comprised of some of those detected on fracture planes, and mixing a seawater like end member and a hypothetical dilute groundwater with a P_{co2} of $10^{-2.67}$. Feldspars (principally anorthite, plagioclase and microcline) are a necessary requirement in the group of plausible phases used to derive a thermodynamically feasible result from mass balance calculations. A hypothetical NaCl phase is also a necessary member of the group of plausible phases. There is no direct evidence that NaCl (or a rock-mass chloride source) is available in the Holyrood Aquifer, although indirect evidence for its existence is found in studies of other granitic terrains.

CO_2 cannot justifiably be omitted from any group of plausible phases; however, its inclusion leads to a result which requires a deep source of carbon. This might possibly be in the form of organic acids, though there is no evidence in this study to suggest this. Quartz is noticeably absent from the group of plausible phases used in the successful mass balance calculation. The absence of quartz as a required phase suggests that crystalline quartz is not being deposited from present day groundwaters and that quartz saturation is controlled by amorphous silica varieties.

The integration of a variety of information presented in this thesis provides evidence that the results of mass balance modelling are plausible and that the inclusion of an NaCl phase (assumed to be equivalent to a rock-mass chloride source) and seawater as an aqueous end-member is plausible and necessary. Furthermore, the integration of results does not reveal any inconsistencies between the physical, hydrogeochemical and isotopic data sets and the models proposed for them.

A positive inverse correlation has been established between concentrations of such species as Si, Cl and the hydraulic conductivity. The presence of an altitude effect in these groundwaters lends support to the generalized flow model proposed for the aquifer. Examination of various mixing scenarios using plausible isotopic end-members does not discredit the notion of an altitude affect being manifest in the isotope compositions. The modelled mixing fractions of the two aqueous end-members and the modelled addition of a chloride phase were used to estimate the chloride contributions from seawater and from the rock mass. The contribution from a seawater source was found to be inversely proportional to distance from the coastline. On the other hand the calculated addition of a chloride-containing phase was inversely correlated with hydraulic conductivity.

The inverse correlation of hydraulic conductivity with concentration of Si and Cl, the presence of a possible altitude effect, and the range of chloride concentration in shallow boreholes at higher altitudes in the aquifer indicate that both a rock-mass source of chloride (and probably bromide) and a saltwater component were introduced to the aqueous phase during its evolution.

Circumstantial evidence suggests that the addition of a seawater component from precipitation which has entrained marine aerosols. No other scenario can explain the addition of a saltwater component to the aquifer in decreasing amounts away from the coastline. Recent marine inundations may have been partly responsible but appear to have affected only coastal areas below an altitude of 6 to 8 m (relative to present day).

9.2 FUTURE WORK

This research has raised many interesting questions. Regarding addition of a saltwater like component to the aquifer. Can coastal precipitation in the NSCRV area contain concentrations of Cl as high as 34 ppm (in the near coastal environment) or is the chloride source in fact anthropogenic (i.e road salt)?

With regard to the possibility of a rock mass source of chloride it would seem worthwhile to investigate possible sources, within, or associated with, the primary mineral phases of the Holyrood Granite. Furthermore it may be possible to differentiate two potential chloride sources using ^{36}Cl as a tracer. Other indicators (though unfortunately not conservative) might be SO_4 and associated sulphur and oxygen isotope data; sulphate is often a large component of marine aerosols (Cicerone 1984).

Further work on the significance of Br, and the accuracy of its analysis is also necessary as this anion may be an extremely useful tracer. This study has demonstrated that Cl/Br ratios are apparently significantly different from seawater, but that they appear to show a remarkable degree of consistency. Further work on Br/Cl ratios in primary mineral phases in the Holyrood Granite should be conducted to determine the significance and veracity of these findings.

REFERENCES

BOTTOMLEY, D.J., ROSS, J.D. and B.W. GRAHAM. 1984. A Borehole Methodology for Hydrogeochemical Investigations in Fractured Rocks. Wat. Res. Rsch. **v20** no.9 pp 1277-1300.

BRUCKNER, W.D. 1979. Geomorphology of the Avalon Peninsula of Newfoundland. Government of Newfoundland and Labrador, Department of Mines and Energy. Report 79-4, 42 p.

BUSENBERG, E. and CLEMENCY, C.V. 1976. The Dissolution Kinetics of Feldspars at 25deg. C and 1 atm CO2 partial pressure. Geochim.cosmochim.Acta **v40** pp41-49

BUTTON, J.R. 1991. Groundwater evolution in the Seal Cove River Valley. unpublished Honours dissertation, Memorial University of Newfoundland.

CACAS, M.C., LEDOUX, E., DE MARSILY, G., TILLIE, BARBREAU, A. DURAND, E. FEUGA, B. and PEAUDECERF, P. 1990. Modelling Fracture Flow With a Stochastic Discrete Fracture Network: Calibration and Validation 1. The Flow Model. Wat. Res. Rsch. **v26** no.3 pp479-489.

CHEENEY, R.F. 1983. Statistical Methods in Geology. George Allen and Unwin 169 p.

CICERONE, R. 1984. Halogens **in** Global Trophosperic Chemistry. A Plan for action. Global Trophosperic Chemistry Panel, Board of Atmospheric Sciences and Climate Committee on Physical Sciences Mathematics and resources. National Resources Council. National Academic Press. Washington D.C.

CRAIG, H. 1961. Isotopic variations in meteoric water. Science, 133, pp1702-1703.

DANSGAARD, W. 1964. Stable isotopes in precipitation. Tellus, 16, No.4, 436-468.

DEER, W.A., HOWIE, R.A. and ZUSSMAN, J. 1966. An Introduction to the Rock Forming Minerals. Longmans , London. 528p

EDMUNDS, W.M., ANDREWS, J.N., BURGESS, W.G., KAY, R.L.F. and LEE, D.J. 1984. The evolution of saline and thermal groundwaters in the Carnmellis granite. Min.Mag.**48** pp407-424

EDMUNDS, W.M., KAY, R.I.F. and McCARTNEY, R.A. 1985. Origin of Saline waters in the Carnmellis Granite (Cornwall, England): Natural processes and reaction during hot dry rock reservoir circulation. Chem.Geol.**v49** pp287-301

FAURE, G., 1986. Principles of Isotope Geology. John Wiley and Sons Inc. 589 p

FERTL, W.H. 1976. Abnormal Formation Pressures. Elsevier Scientific Publishing Company, Developments in Petroleum Science 3. 382 p.

FONTES, J.C. LOUVAT, D. and MICHELOT, J.L. 1989. **Some constraints on geochemistry and environmental isotopes for the study of fracture flow in crystalline rocks.** The Stripa case. **in** IAEA . 1989. Isotope techniques in the study of the hydrology of fractured and fissured rocks. IAEA-AG-329. STI/PUB/790.

FRAPE, S.K, FRITZ, P. and McNUTT, R.H. 1984. Water-Rock interaction and chemistry of groundwaters from the Canadian shield. Geochim.cosmochim.Acta **v48** pp1617-1627.

FRAPE, S.K. and FRITZ, P. 1987. Geochemical trends for groundwaters from the Canadian Shield: **in** Saline waters and gases in crystalline rocks, **Eds.** Fritz, P. and Frape,S.K.; Geol.Soc. Can. Spec. Pap. **33** pp19-38.

FREEZE, R.A and CHERRY, J.A. 1979. Groundwater. Prentice-Hall. Englewood Cliffs, N.J. 604pp

FRITH, R.A. and POOLE, W.H. 1972. Late Pre-Cambrian rocks of eastern Avalon Peninsula, Newfoundland. A volcanic Island arc complex. Can.J.Earth Sci. v9 p72.

GARRELS, R.M. and CHRIST, C.L. 1965. Solutions, Minerals and Equilibria. Harper and Row, New York.

GALE, J.E. and STRAHLE, A. 1988. Site Characterization and Validation-Drift and Borehole Fracture Data. Stage I. Stripa Project IR88-10 Internal Report.

GARRELS, R.M. and MacKENZIE, F.T. 1967. Origin of the chemical composition of some springs and lakes. Adv. Chem. Series **67** pp222-242.

GASCOYNE, M., DAVISON,C.C., ROSS,J.D. and PEARSON,R. 1987. Saline Groundwaters and Brines in Plutons in the Canadian Shield; **in** Saline waters and gases in crystalline rocks, Editors Fritz P., and Frape S.K.; Geol.Ass. Can Special Paper,1987 pp 53–68.

GAT, J.R. 1981. The isotopes of hydrogen and oxygen in precipitation **in** P.Fritz and J.Ch.Fontes, eds., Handbook of Environmental Isotope Geochemistry, vol 1A, pp21-47. Elsevier, Amsterdam, p45 p.

GOODMAN, R.E. 1976. Methods of Geological Engineering in Discontinuous Rocks. West Publishing Co 472 p.

GRANT, D.R. 1989. Quaternary Geology of the Atlantic Appalachian region of Canada; Chapter 5 **in** Quaternary Geology of Canada and Greenland, R.J.Fulton (ed.); Geol.Surv.Can No.1.

GUTJAHR, A.L., GELHAR, W., BAKR, A.A and McMILLAN, J.R. 1978. Stochastic analysis of spatial variability in subsurface flow, 2, Evaluation and application. Wat. Res. Rsch. v**14** no.5 pp953-960

HELGESON, H.C., DELANY, J.M. NESBITT, H.W. and BIRD, D.K. 1978. Summary and critique of the thermodynamic properties of rock forming minerals. Am.J.Sci. **v278a**

HELGESON, H.C. 1968. Evaluation of irreversible reactions in geochemical processes involving minerals and aqueous solutions-I. Thermodynamic relations. Geochim.Cosmochim.Acta.**v32** pp853-877

HELGESON, H.C. 1969. Thermodynamics of hydrothermal systems at elevated temperatures and pressures. Am.J.Sci. **v267** pp729-804.

HEMINGWAY, B.S, HAAS, J.L. and ROBINSON, G.R. 1982. Thermodynamic properties of selected minerals in the system Al_2O_3-CaO-SiO_2-H_2O at 298.15 K and 1 bar (10^5 Pascals) pressure and at higher temperatures. USGS Bull. No1544 70pp

HENDERSON, E.P. 1972. Surficial Geology of Avalon Peninsula, Newfoundland, GSC, Memoir 368, 121 p.

HOBBS, B.E., MEANS, D.M. and WILLIAMS, P.F. 1976. An outline of Structural Geology. John Wiley and Sons, New-York. 571 p.

HOLDREN,G.R. and BERNER.R.A. 1979. Mechanism of Feldspar weathering-I. Experimental studies. Geochim.Cosmochim.Acta.**v43** pp1161-1171

HUBBERT, M.K and WILLIS, D.G. 1957. Mechanics of Hydraulic Fracturing. Trans, AIME, 210: pp 153-168.

HUGHES, C.J. 1971. Anatomy of a granophyre intrusion. Lithos 4, 1971, pp 403-415.

HUGHES, C.J. and BRUCKNER, W.D. 1971. Late Pre-Cambrian Rocks of Eastern Avalon Peninsula, Newfoundland- a Volcanic Island Complex. Cand.J.Ea.Sci. Vol 8 pp 899-915

HUNT, B. 1983. Mathematical Analysis of Groundwater Resources. Butterworths. pp271

HUTCHINSON, R.D. 1953. Geology of the Harbour Main Map-Area, Newfoundland. Memoir 275, Geological Survey of Canada, 43 p.

HVORSLEV, M.J. 1951. Time Lag and Soil Permeability in groundwater observations. U.S. Army Corps Engrs. Waterways Exp.Sta.Bull.36, Vicksburg, Miss.

KAMINENI, D.C. 1987. Halogen-bearing minerals in plutonic rocks: a possible source of chlorine in saline groundwater in the Canadian Shield.**in** Saline waters and gases in crystalline rocks, Editors Fritz P., and Frape S.K.; Geol.Ass. Can Special Paper,1987 pp69-79.

KING, A.F. 1990. Geology of the St.John's Area. Report 90-2. Geol.Surv. Branch Dept. Min.Energy. Govt.Nfld. and Lab. 88 p.

KNAPP,R.B. 1975. An analysis of the porosities of fractured crystalline rocks: M.S.thesis, University of Arizona, 90 p.

KRAUSKOPF, K.B. 1979. Introduction to geochemistry. 2nd. Edition. McGraw-Hill international series in the planetary sciences. 617pp.

KROGH, T.E., STRONG, D.F. and PAPEZIK, V.S. 1983. Precise U-Pb ages of zircons from volcanic and plutonic units in the Avalon Peninsula **in** Abstracts with Programs 1983, 18th Annual Meeting Northeastern Section ,Geol.Soc.Am Volume 15 page 135.

LAWSON, A.C. 1890. Note on the Pre-Palaeozoic surface of the Archean terranes of Canada; Geol.Soc.Am.Bull v.1, pp 163-174.

LONGERICH, H.P., STRONG, D.F. and KANTIPULY, C.J. 1986. Progress in evaluation of instrumental and other parameters affecting chemical and isotopic analysis by Inductively coupled plasma mass spectrometry (ICP-MS). Can. J. Spectroscopy v31, No.5 pp 111-121

MacPHERSON. 1982. Postglacial vegetational history of the eastern Avalon, Newfoundland, and Holocene climatic change along the eastern Canadian seaboard; Geographie physique et Quaternaire, v. 36, pp 175-196.

McCARTNEY, W.D. 1967. Geology of the Whitbourne Map-Area, Newfoundland. Geological Survey of Canada. Memoir 341. 135 p.

McCARTNEY, W.D. 1969. Geology of Avalon Peninsula, southeast Newfoundland. pp 115-129 in North Atlantic Geology and continental drift a symposium (M.Kay Editor) Mem 12, Amer.Assoc.Petrol.Geol., Tulsa, Oklahoma. 1082p.

McCARTNEY W.D., POOLE W,H., WANLESS R.K. and WILLIAMS H. 1966. Rb/Sr age and geological setting of the Holyrood granite, southeast Newfoundland. Can.J.Earth Sci.v3 p947-957.

McCULLOUGH, P.M. 1984. The Spatial and Temporal Variations of Acidic Precipitation in Newfoundland: from Source to Receptor. MSc Thesis, Memorial University of Newfoundland, Department of Geography.

MENDENHALL, W. and SINCICH, T. 1988. Statistics for the engineering and computer sciences. Collier Macmillan Canada Inc. pp1036.

MORGAN, C.O., and WINNER, M.D. 1962. Hydrochemical facies in the 400 ft and 600 ft sands of the Baton Rouge area, Louisiana. U.S. Geol. Surv. Prof. Paper 450-B, B120-121

MOSER,H., WOLF, M., FRITZ, P., FONTES, J-CH, FLOROWSKI, T. and PAYNE, B.R. 1989. Deuterium, oxygen-18, and Tritium in Stripa Groundwaters.Geochim.cosmochim.Acta v53 pp 1757-1763.

NERETNIEKS, I. 1980. The influence of microfissures in crystalline rock on radionuclide migration. in Predictive Geology with emphasis on nuclear waste disposal **Eds** Marsily,G. and Merriam, D.F. Computers and Geology **v4**. Pergamon. pp137-152

NESBITT, H.W and YOUNG, G.M. 1984. Prediction of some weathering trends of plutonic and volcanic rocks based on thermodynamic and kinetic considerations. Geochim.cosmochim.Acta **v48** pp1523-1534.

NOLAN, DAVIS AND ASSOCIATES LTD. 1989. Hydrogeology and Groundwater Resources Management Bell Island, Conception Bay, Newfoundland. Government of Newfoundland and Labrador. Water resources Report 3-1, Groundwater Series.

NORDSTROM, D.K, ANDREWS J.N., CARLSSON L., FONTES J-C., FRITZ P., MOSER H., and OLSSON T. 1985. Hydrogeological and Hydrogeochemical investigations in boreholes. Final report of the phase I geochemical investigations of the Stripa granite. OECD pub. **85-06**

NORDSTROM, D.K. and MUNOZ, J.L. 1985. Geochemical Thermodynamics. Benjamin/Cumming. pp477

NORDSTROM,D.K.,PLUMMER,L.N.,WIGLEY,M.L.,WOLERY,T.J.,BALL,J.W., JENNE,E.A., BASSETT,R.L., CRERAR,D.A., FLORENCE,T.M., FRITZ,B., HOFFMANN,M., HOLDREN,G.R., LAFON,G.M., MATTIGOD,S.V., McDUFF,R.E., MOREL,F., REDDY,M.M., SPOSITO,G., and THRAILKILL,J. 1979. A Comparison of Computerized Chemical Models for Equilibrium Calculations in Aqueous Systems **in** Chemical Modelling in Aqueous Systems Editor E.V.Jenne. Am.Chem.Soc Symposium Series 93

NORDSTROM,D.K., OLSON, T. CARLSSON, L. and FRITZ, P. 1989. Introduction to the hydrogeochemical investigations within the International Stripa Project. Groundwaters.Geochim.cosmochim.Acta **v53** pp 1717-1726.

NORTON, D. and KNAPP, R. 1977. Transport phenomena in hydrothermal systems: The nature of porosity. Am.J.Sci. **v277** pp913-936

PACES, T. 1972. Chemical characteristics and equilibration in natural water-felsic rock-CO_2 system. Geochim.cosmochim.Acta **v36** pp217-240.

PACES, T. 1973. Steady-state kinetics and equilibrium between groundwater and granitic rock. Geochim.cosmochim.Acta **v37** pp2641-2663.

PAPEZIK, V.S. 1970. Petrochemistry of volcanic rocks, Avalon peninsula, Newfoundland. Can.J.Ea.Sci v7 pp1485-1498.

PARKHURST, D.I., PLUMMER, L.N. and THORSTENSON, D.C. 1982. BALANCE - A computer program for calculation of chemical mass balance. U.S. Geol. Surv. Water Res. Invest. **82-14**, 33pp. NTIS Tech. Rpt. PB82-255902, Springfield. VA 22161.

PARKHURST,D.L.,THORSTENSON.D.C. and PLUMMER, N.L. 1980. PHREEQE - A computer program for geochemical calculations. U.S. Geol. Surv. Water Res. Invest. **80-96** 210pp. NTIS Tech. Rpt. PB81-167801, Springfield. VA 22161.

PLUMMER, N.L. 1977. Defining Reactions and Mass Transfer in Part of the Floridan Aquifer. Wat. Res. Rsch. **v13** no.5 pp801-812.

PLUMMER, N.L. 1984. Geochemical Modelling: A comparison of forward and inverse methods.**in** Hitchcon, B and Wallick, E.I., eds, First Canadian/American Conference on Hydrogeology, Practical Applications of Ground Water Geochemistry: Worthington Ohio, National Water Well Association p.149-177.

PLUMMER, N.L., PARKHURST, D.I. and THORSTENSON, D.C. 1983. Development of reaction models for ground-water systems. Geochim.cosmochim.Acta **v47** pp665-686

PLUMMER, N.L., PRESTEMON, E.C and PARKHURST, D.L. 1991. An interactive code (NETPATH) for modeling net geochemical reactions along a flow path. U.S.G.S. Water-Resources Investigations report 91-4078, Reston, Virginia. 227 p

RAVEN, K.G. 1980. Studies in Fracture Hydrology at Chalk River Nuclear Laboratories: 1977/78/79. At. Energy Can. Ltd. Technical Record, TR-113

RAVEN, K.G. and SMEDLEY, J.A. 1982. CRNL ground water flow study-summary of FY 1981 research activities, unpublished National Hydrology Research Institute report submitted to Atomic Energy of Canada Ltd for publication AECL Technica, Record.

READ, H.H. 1970. Rutley's Elements of Mineralogy, 26th Edition. George, Allen & Unwin 560 p.

REYNOLDS, D. 1950. Gas Fluidisation as a Geological Process. Am.J.Sci. 250

ROBIE, R.A. and HEMINGWAY, B.S. and FISHER, J.R. 1978. Thermodynamic properties of minerals and related substances at 298.15 K and 1 bar (10^5 Pascals) pressure and at higher temperatures. USGS Bull. No1452 456pp.

ROBIN, M.J. and GILHAM, R.W. 1987. Field Evaluation of Well Purging Procedures. Groundwater Monitoring Review, Fall 1987.

SCHILEREFF, H.S. 1992. A Physical Hydrogeological and Hydrogeochemical Study of Groundwater/ Surface Water Interaction in a Granitic Terrain in Eastern Newfoundland. PhD Thesis, Memorial University of Newfoundland 377 p.

SEDERHOLM, J.J. 1967. Selected Works. Granites and Migmatites. Oliver and Boyd, Edinburgh and London.

SMALL, H and MILLER Jr., T.E. 1982. Indirect Photometric Chromatography. Anal.Chem v54 No.3 March 1982. pp 462-469.

STRONG, D.F., O'BRIEN, S.J., TAYLOR, S.W., STRONG, P.G. and WILTON, D.H. 1978. Aborted Rifting in Eastern Newfoundland. Can.J.Ea.Sci v15 pp117-131.

STRONG, D.F and MINATIDIS, D.G. 1975. Geochemistry and Tectonic setting of the late PreCambrian Holyrood plutonic series of eastern Newfoundland. Lithos 8 pp283-295.

TAYLOR, S.W., O'BRIEN, S.J. and SWINDEN, H.S. 1979. Geology and Mineral Potential of the Avalon Zone and Granitoid Rocks of Eastern Newfoundland. Report 79-3. Mineral Development Division, Department of Mines and Energy, Government of Newfoundland and Labrador.

TERZAGHI, R.D. 1965. Sources of Error in Joint Surveys. Geotechnique, v. 15, pp 287-304.

VAN EVERDINGEN, D.A., VAN GOOL, J.A.M and VISSERS, R.L.M. 1992. Quickplot: A microcomputer based program for processing of orientation data. Computers and Geoscience. Vol 18, No 2/3, pp 183-287.

WILLIAMS, H. KENNEDY, M.J. and NEALE, E.R.W. 1974. The northeastward termination of the Appalachian orogen in The Ocean Basins and Margins **Edited** by A.E.M. Nairn and F.G.Stehli. New York, Plenum Pub. Corp, Vole 2 p 70-123.

YURTSEVER, Y. 1975. Worldwide survey of stable isotopes in precipitation. Rept. Section Isotope Hydrology, International Atomic Energy Agency, Vienna, November, 1975, 40p.

APPENDICES

APPENDIX A Core Log

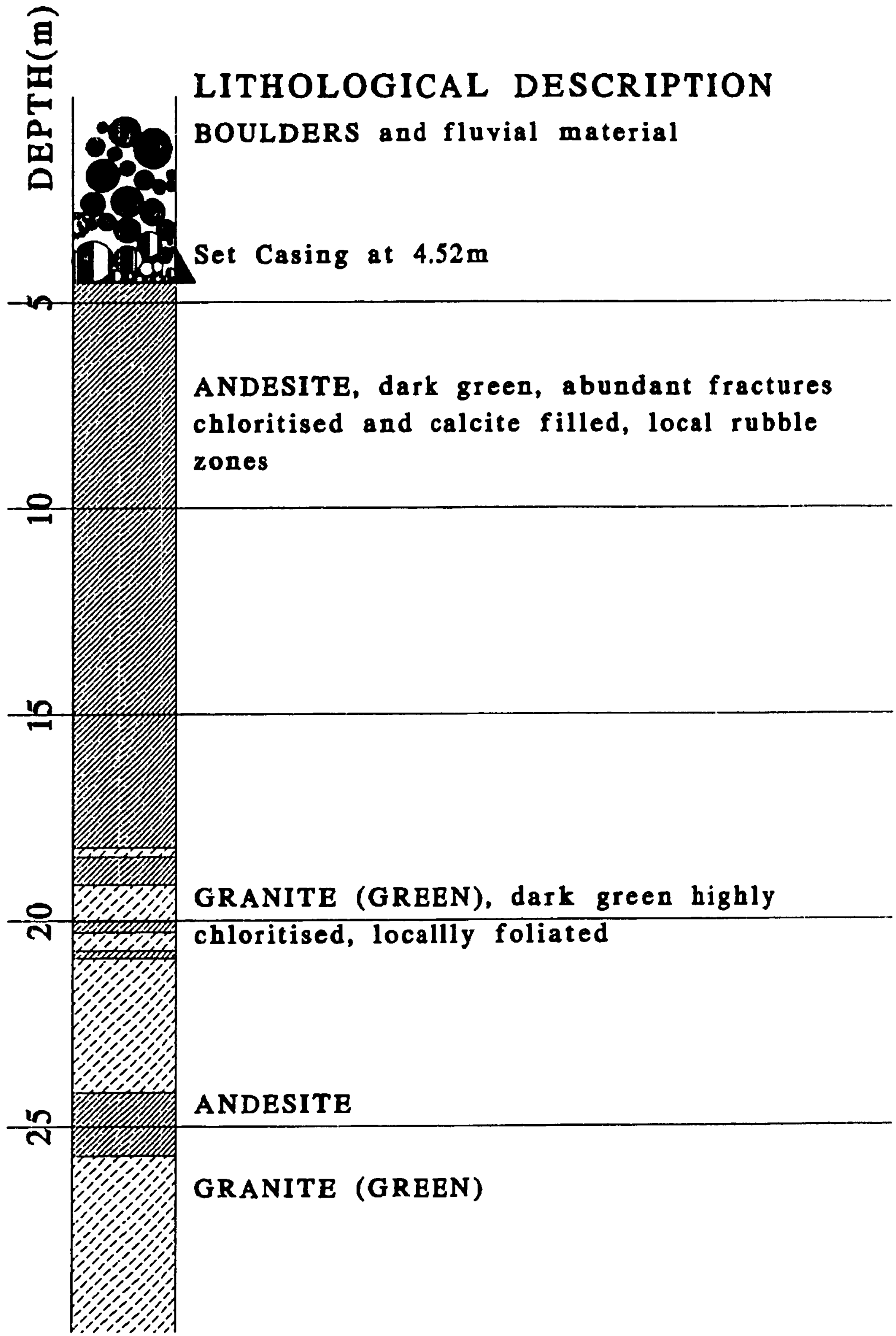

DEPTH(m)
LITHOLOGICAL DESCRIPTION
BOULDERS and fluvial material
Set Casing at 4.52m
5
ANDESITE, dark green, abundant fractures chloritised and calcite filled, local rubble zones
10
15
GRANITE (GREEN), dark green highly chloritised, locallly foliated
20
ANDESITE
25
GRANITE (GREEN)

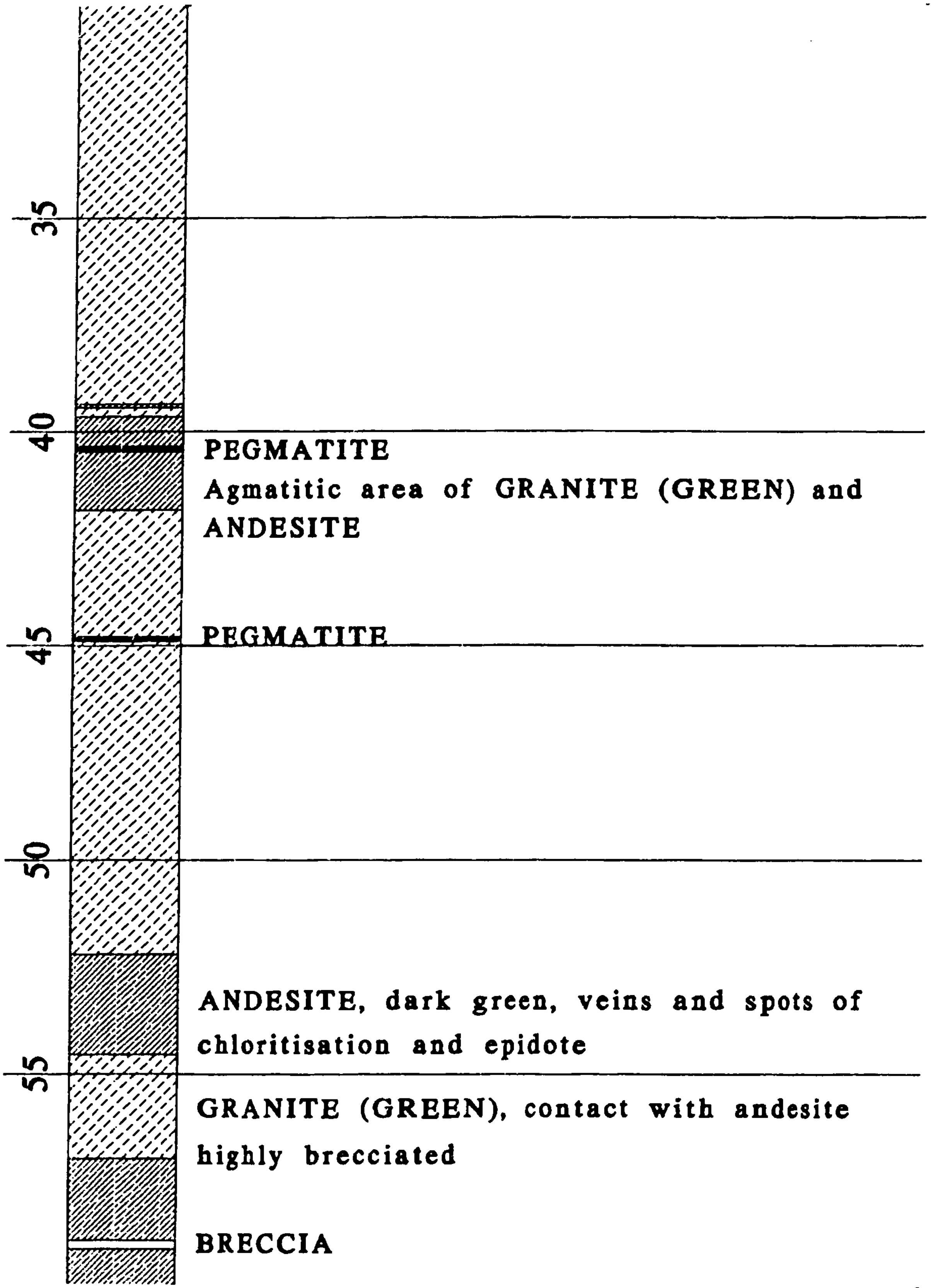
35
40
PEGMATITE
Agmatitic area of GRANITE (GREEN) and ANDESITE
PEGMATITE
45
50
ANDESITE, dark green, veins and spots of chloritisation and epidote
55
GRANITE (GREEN), contact with andesite highly brecciated
BRECCIA

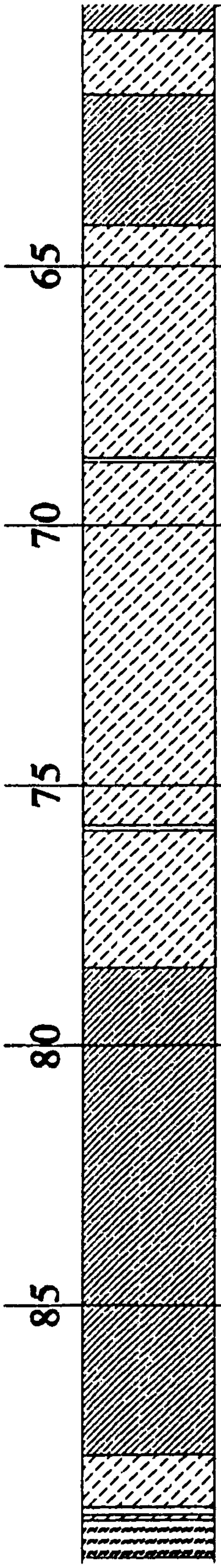

GRANITE (GREEN), local nebulous xenoliths

GRANITE (GREEN), highly chloritised/ epidotised, abundant skeins of chlorite/epidote in lower part, increasingly pink

BRECCIA, of GRANITE (GREEN)

GRANITE (GREEN), rare xenoliths, 1-2cm, andesite and basalt

APLITE, vein, white locally pink, sugary texture, abundant epidote veins and skeins local pink granite patches

ANDESITE, dark green

GRANITE (GREEN), overall green hue on coarse white granite, abundant skeins chlorite and epidote, rare pink granite patches, local aplite veins containing xenoliths of granite

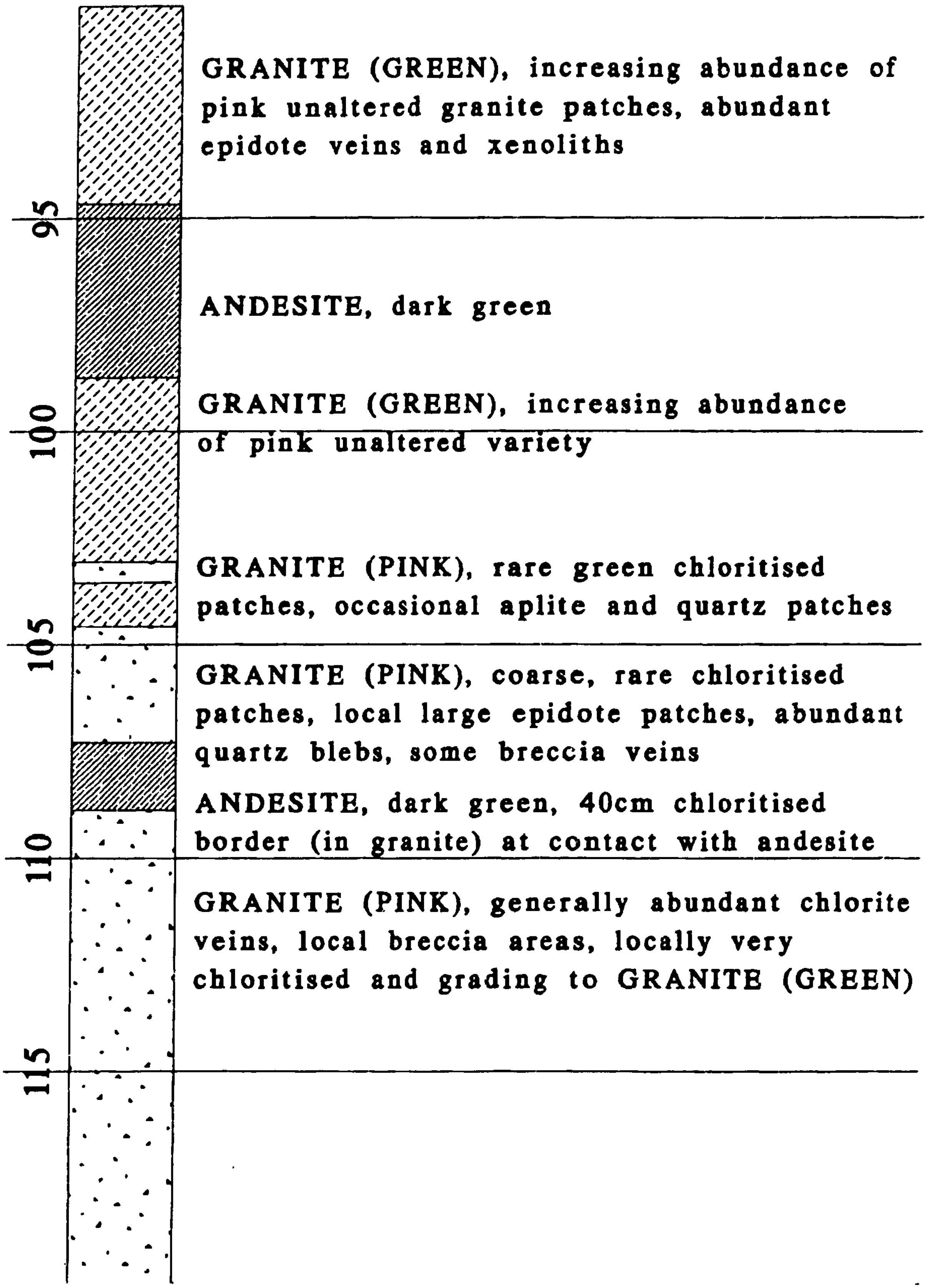
GRANITE (GREEN), increasing abundance of pink unaltered granite patches, abundant epidote veins and xenoliths
95
ANDESITE, dark green
GRANITE (GREEN), increasing abundance of pink unaltered variety
100
GRANITE (PINK), rare green chloritised patches, occasional aplite and quartz patches
105
GRANITE (PINK), coarse, rare chloritised patches, local large epidote patches, abundant quartz blebs, some breccia veins
ANDESITE, dark green, 40cm chloritised border (in granite) at contact with andesite
110
GRANITE (PINK), generally abundant chlorite veins, local breccia areas, locally very chloritised and grading to GRANITE (GREEN)
115

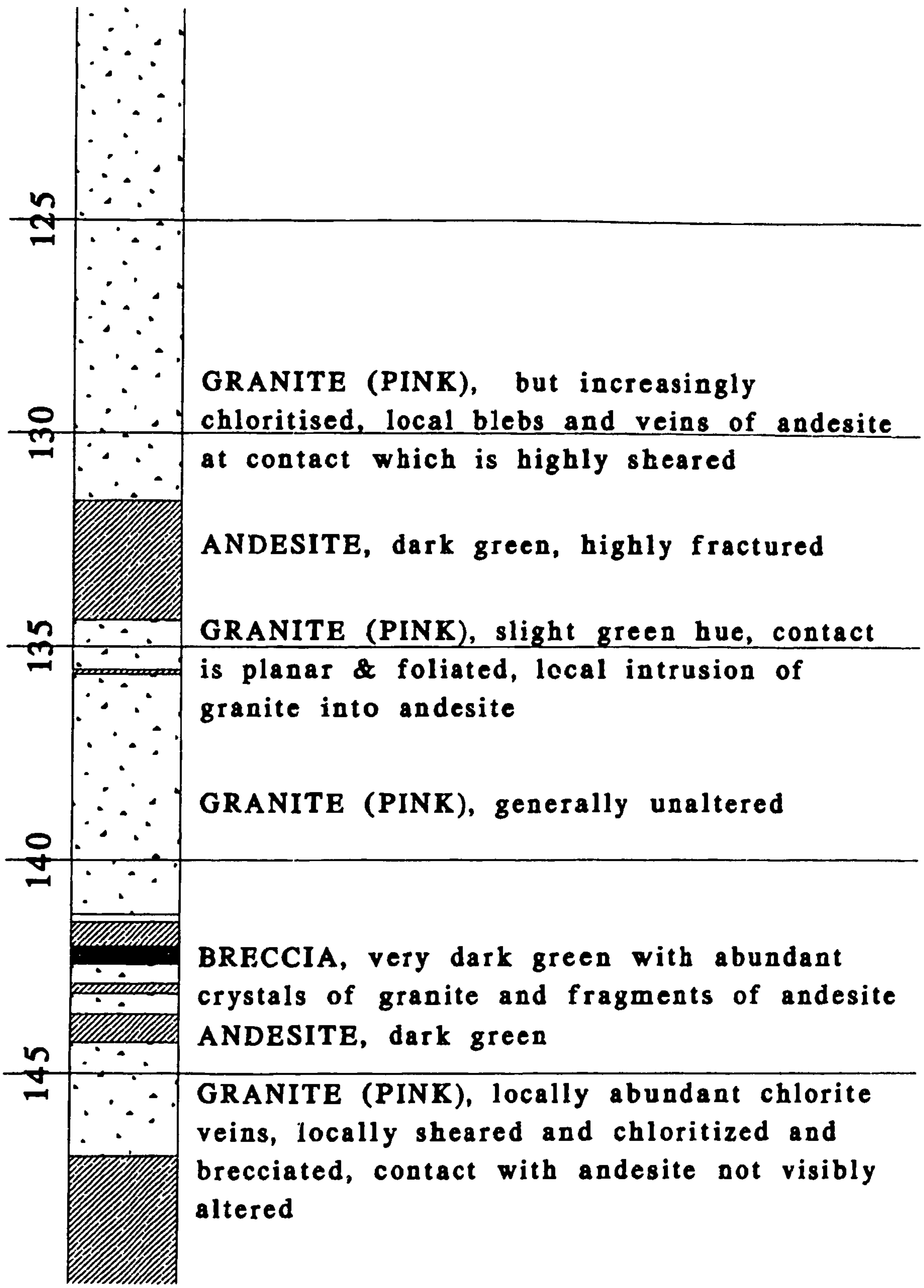
125
130
135
140
145
GRANITE (PINK), but increasingly chloritised, local blebs and veins of andesite at contact which is highly sheared
ANDESITE, dark green, highly fractured
GRANITE (PINK), slight green hue, contact is planar & foliated, local intrusion of granite into andesite
GRANITE (PINK), generally unaltered
BRECCIA, very dark green with abundant crystals of granite and fragments of andesite
ANDESITE, dark green
GRANITE (PINK), locally abundant chlorite veins, locally sheared and chloritized and brecciated, contact with andesite not visibly altered

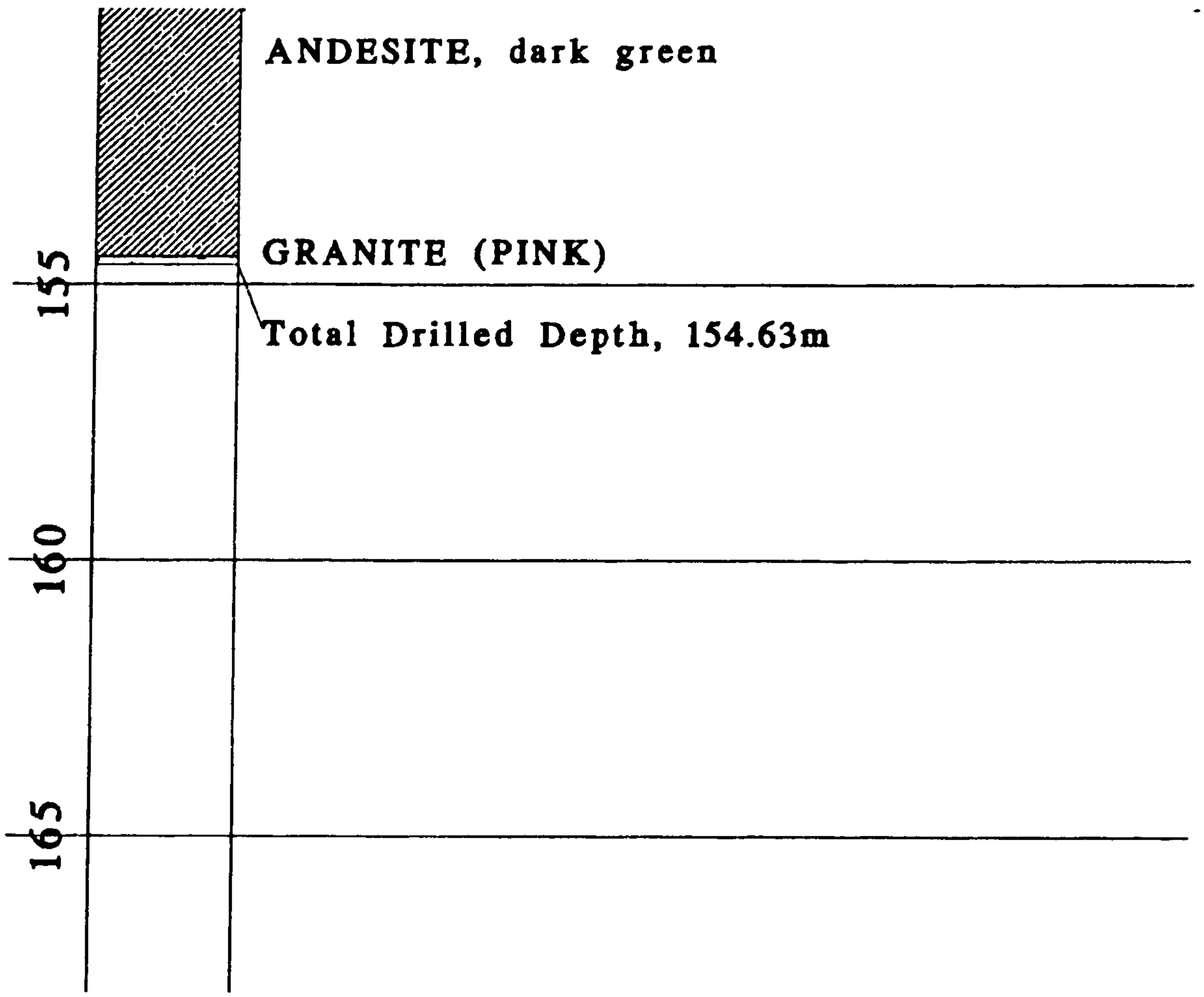
ANDESITE, dark green
GRANITE (PINK)
155
Total Drilled Depth, 154.63m
160
165

APPENDIX B Fracture Data

Fracture data from NSCRV
Scribe mark at bottom of core.
Hole azimuth: 135 deg.
Hole plunge : 68 deg.

COLUMN DESCRIPTIONS	
Column	Descriptor
A	crushed zone begins(B), or stops (S)
B	fracture (Y) or blank
C	new rock type (Y) or blank
D	fracture type sealed (S), coated(C), fresh(F)
E	number of fractures
SMT	Fracture surface description
F	Orientated (blank) or orientation lost (N)
G	Alpha angle
H	Beta angle
RCK	Rocktype
AZ.	Dip Azimuth
DIP	Dip angle
Open?	field estimate of how open fracture believed to be, where 1 is maximum aperture, blank indicates closed

ABBREVIATIONS		
Rock Types		
AND	Andesite	
APL	Aplite	
BRC	Breccia	
GRG	Green Granite	
GRP	Pink Granite	
PEG	Pegmatite	
Fracture Fill/Coat		
CA	Calcite	
CL	Chlorite	
EP	Epidote	
FE	Iron Oxide	
PY	Pyrite	
QZ	Quartz	
WH	Whithamite	
WF	Wolframite	
Fracture surface description		
P	Planar	FIRST LETTER
C	Curved	
S	Stepped	
I	Irregular	
R	Rough	MODIFIERS
S	Smooth	
K	Slickensides	

DEPTH	A	B	C	D	E	MINERA	SMT	F	G	H	RCK	AZ.	DIP	OPEN?	Open fRACS (/m)	Total Fractures (/m)
4.52				S	1	CA	P/R	N	84		AND			1		
4.59				S	1	CA	S/S	N	90		AND			1		
4.59				S	1	CA	P/S	N	28		AND					
4.66	B					FE	W	N			AND					
4.77	S					FE	W	N			AND				5.00	5.00
4.84				S		CA	S/S	N	48		AND				3.76	4.30
5.04				S	1	CA	C/S	N	90		AND				2.97	3.96
5.21	B			C			W	N			AND			1	3.70	3.70
5.32	S			C			W	N			AND			1	4.85	4.85
5.52		Y		C	1	CA	P/S	N	65		AND			0.5	5.24	5.71
5.60		Y		C	1		P/R	N	62		AND			0.5	6.37	6.86
5.74		Y		C	1	FE	P/R	N	50		AND			1	7.14	7.69
5.80		Y		C	1	CL	P/S	N	62		AND			1	7.56	9.30
5.89		Y		C	1		P/S	N	58		AND			0.5	7.14	10.99

6.06		Y	C	1	CL	P/S	N	40		AND			1	7.14	11.90
6.12			S	1		P/S	N	56		AND				6.88	12.50
6.18		Y	C	1	FE	P/R	N	60		AND			1	4.95	10.99
6.43		Y	C	2	FE	R/R	N	60		AND			1	3.89	11.11
6.44			S	1	CA	P/S	N	30		AND				3.80	12.66
6.54			S	1	CA	S/S	N	60		AND				2.06	10.31
6.71			F	1		P/R	N	55		AND				2.13	10.64
6.79			F	1		P/R	N	70		AND				1.32	13.16
6.85			S	1	CA	S/S	N	56		AND				0.63	11.25
7.09		Y	C	1	FE	R/R	N	85		AND				0.68	12.16
7.12			S	1	CA	R/R	N	10		AND				0.85	15.25
7.19			S	1	CA	R/	N	90		AND				2.27	13.64
7.24		Y		1		P/R	N	60		AND			0.5	3.57	12.86
7.28			S	1	CA	R/R	N	90		AND				5.10	18.37
7.30			S	1		C/R	N	50		AND				3.79	12.12
7.45		Y	C	1	CL	P/R	N	68		AND			1	3.68	10.29
7.55			S	1	CA	P/S	N	0		AND			1	4.32	8.64
7.58		Y	C	1	CA	P/R	N	68		AND				4.40	7.69
7.78	B		C		FE		N			AND				3.75	5.83
7.87	S		C		FE		N			AND				4.09	6.36
8.05		Y	C	1	CAFE	P/R	N			AND			1	4.09	6.36
8.19		Y	C	1	CACL	P/K	N	54		AND			1	2.78	5.56
8.50		Y	C	1	CAWH	P/R	N	55		AND			0.5	2.59	4.02
8.55			S	1	CAWH	P/R	N	41		AND				2.28	4.06
8.65		Y	C	1	CLEP	P/R	N	60		AND			1	2.76	4.97
8.84			S	1	QZCL	C/R	N	10		AND				2.39	4.79
9.52		Y	C	1	CLQZ	P/R	N	62		AND			1	2.41	5.42
9.84			S	1	QZEP		N			AND				2.49	4.97
9.86		Y	C	1	CL	P/R		40	355	AND	130	85	0.500	2.32	4.64
10.07		Y	C	1	CL	P/S		50	280	AND	171	49	0.500	2.00	5.14
10.16		Y	C	1	CL	P/S		63	270	AND	180	61	0.500	2.59	6.67
10.36		Y	C	1	CL	P/S		35	282	AND	162	35	1.000	2.27	8.18
10.59			S	1	CL	P/S		23	22	AND	295	69		2.03	7.32
10.59			S	1	QZ	P/S		18	225	AND	246	46		1.96	8.82
10.87		Y	C	1	CL	P/S		14	270	AND	176	12		1.47	8.82
10.94		Y	C	1	CL	P/S		52	270	AND	179	50		1.00	9.00
11.09		Y	C	1	CA	P/S		65	205	AND	203	78		0.00	9.41
11.09		Y	C	1	CA	P/S		35	22	AND	308	72		0.48	6.67
11.18		Y	C	1	CA	P/S		36	297	AND	147	43		1.20	8.43
11.36		Y	C	1	CLCA	P/S	N	15		AND				1.25	8.75
11.44	B						N			AND				1.12	7.87
11.64	S						N			AND			0.500	0.93	6.48
11.70		Y	C	1	CLQZ	P/S	N	40		AND			0.500	0.94	6.60
11.74		Y	C	1	CLQZ	P/S	N	47		AND				0.84	5.88
11.98		Y	C	1	QZ	P/R	N	15		AND				0.85	5.93
12.17		Y	C	1	CL	P/R	N	43		AND				0.87	6.96
12.24		Y	S	1	QZ	S/S	N	15		AND				0.40	7.26
12.55		Y	C	1	CLQZ	P/S	N	38		AND				0.00	5.77
12.62		Y	C	1	CL	P/S	N	80		AND				0.00	6.43
12.79		Y	C	1	CLQZ	P/S	N	48		AND				0.00	5.52
12.94		Y	C	1	CLQZ	P/S		46	85	AND	356	47		0.00	5.70
13.30			S	1	CLQZ	S/S		18	180	AND	252	88		0.00	6.30
13.38		Y	C	1	QZCL	P/S		90		AND	180	88		0.00	4.76
13.80		Y	C	1	CL	P/S		31	90	AND	2	32		0.00	5.11
13.82		Y	C	1		P/S		25	350	AND	115	81		0.00	5.74
13.82	B						N							0.00	7.37
14.09	S						N							0.00	6.42
14.16		Y	C	1	CL	P/S		15	180	AND	255	88		0.00	9.72

14.16		Y		C	1	CL	P/S		28	300	AND	135	39		0.00	9.72
14.25		Y		C	1	CL	P/S		18	45	AND	296	47		0.00	9.09
14.47		Y		C	1	CLQZ	P/S		28	340	AND	119	72		0.00	14.29
14.52		Y		C	1	CL	P/S		19	320	AND	113	52		0.00	18.37
14.54		Y		C	1	CL	P/S		30	300	AND	138	41		0.00	18.00
14.59		Y		C	1	CL	P/S		59	180	AND	211	88		0.00	19.57
14.65		Y		C	1	CL	P/S		41	180	AND	229	88		0.00	23.68
14.65		Y		C	1	CL	P/S		31	300	AND	139	41		0.00	22.50
14.66		Y		C	1	CL	P/S		20	180	AND	250	88		0.00	18.00
14.71		Y		C	1	CL	P/S		38	265	AND	186	36		0.00	12.68
14.85		Y		C	1	CL	P/S		18	280	AND	148	19		0.00	12.00
14.92		Y		C	1	CL	P/S		5	77	AND	298	13		0.00	9.09
15.04		Y		C	1	CLEP	P/S		44	265	AND	185	42		0.00	8.57
15.30		Y		C	1	CL	P/S		54	202	AND	214	75		0.00	7.96
15.40		Y		C	1	CL	P/S		30	90	AND	2	31		0.00	8.65
15.64		Y		C	1	CL	P/S		57	135	AND	25	68		0.00	9.18
15.71				S	1	QZ	S/S		86	195	AND	184	87		0.00	5.36
15.84				S	1	QZ	S/S		83	185	AND	187	87		0.00	4.82
15.89				S	1	QZ	S/S		53	155	AND	35	76		0.52	4.12
15.90				S	1	EPCLWH	P/R		33	340	AND	124	73		1.16	4.65
16.72				S	1	CL	P/R		17	355	AND	107	85		1.69	4.52
16.96		Y					P/R		35	230	AND	223	49		2.17	3.80
17.34		Y		C	1	QZ	P/R		52	190	AND	218	82	1.000	2.06	3.61
17.36		Y		C	1		C/R		28	120	AND	43	41	1.000	2.06	3 61
17.48		Y		C	1		P/R		98	145	AND	354	84	1.000	4.10	5.74
17.68		Y					P		53	188	AND	217	83	1.000	4.90	5.88
17.83				S	1	QZEP	P/S		39	195	AND	230	76		5.62	6.74
17.84				S	1	QZCL	S/S		62	75	AND	353	64		4.60	5.75
17.94		Y		C	1	PY	S/S		87	78	AND	0	88	1	3.09	4.12
17.98	B							N							3.75	5.00
18.23	S							N							4.17	6.94
18.23			Y					N			GRG				5.06	6.33
18.45								N			GRG				5.62	5.62
18.48		Y	Y	C	1	GR	P/S		15	280	AND	142	17	1	5.95	5.95
18.55		Y		C	1	GR	P/R		52	255	AND	191	52	1	5.56	5.56
18.63		Y		C	1	GR	P/R		65	220	AND	200	72	1	3.36	3.36
18.83		Y		C	1	GR	P/R		29	145	AND	56	61	1	3.50	3.82
18.82		Y		C	1	GR	P/R		20	310	AND	118	44	1	3.43	4.00
19.13			Y					N			GRG				2.89	3.47
19.72								N			GRG				2.69	3.59
20.02		Y		C	1	QZCL	P/S		46	200	AND	222	74	0.5	2.85	3.80
20.23		Y		C	1	CL	P/S		41	170	AND	49	84	0.5	2.49	3.31
20.28			Y					N			GRG				2.19	3.12
20.30		Y		C	1	WH	C/		35	320	GRG	132	57	0.5	4.33	5.77
20.41		Y		C	1		P/R		83	20	GRG	354	88	1	6.18	6.74
20.63		Y		C	1	QZWH	P/R		65	195	GRG	204	82	1	6.67	6.67
20.73			Y					N			AND				7.14	6.59
20.76		Y		C	1		P/R		63	148	AND	24	77	1	6.50	7.00
20.91			Y					N			GRG			1	7.45	7.45
21.13		Y		C	1	CLEP	P/C		44	220	GRG	219	60	1	8.33	8.33
21.19		Y		C	1	CL	P/F		61	155	GRG	27	79	1	9.21	9.21
21.30				S	1	WH	C/R		32	110	GRG	29	38		9.30	9.30
21.35		Y		C	1	QZ	P/S		70	105	GRG	6	72	1	8.70	8.70
21.47		Y		C	1	QZ	P/S		76	310	GRG	171	78	1	9.21	11.84
21.49		Y		C	1	QZ	P/S		60	140	GRG	24	72	1	5.77	7.69
21.62		Y		C	1	WHQZ	P/R		16	210	GRG	252	59	1	4.95	6.93
21.83		Y		C	1		P/R		10	320	GRG	102	51	1	6.00	6.00
21.89				S	1	WH	P/R		26	200	GRG	243	70		5.26	5.26

22.23								N			GRG				3.51	3.51
22.31								N			GRG				1.75	1.75
22.35								N			GRG			1	1.21	1.21
22.42								N			GRG				0.44	0.44
22.63								N			GRG				0.38	0.00
23.33								N			GRG				0.36	0.00
23.48								N			GRG				0.68	0.34
24.17			Y					N			AND				0.69	0.69
24.88	B							N			AND				1.05	1.39
25.09	C							N			AND				1.26	1.68
25.27		Y		C	1		P/K		44	140	AND	39	64	1	1.63	2.03
25.33		Y		C	1		P/K		46	310	AND	147	57	1	2.55	3.06
25.50		Y		C	2		P/K		50	65	AND	342	55	1	3.23	4.52
25.71			Y					N			GRG	270	89		3.45	4.60
25.94		Y		C	1	CL	P/S		12	0	GRG	282	89	1	3.23	4.84
26.13		Y		C	1	CLEP	P/S		41	75	GRG	345	44	1	3.19	4.79
26.43				S	1	CL	P/R		14	300	GRG	114	33		2.73	4.92
26.83		Y		C	1	CL	P/S		76	110	GRG	5	78	1	2.33	4.65
27.13				S	1	WH	P/R		10	320	GRG	102	51		2.65	5.96
27.21		Y		C	1		P/R		62	130	GRG	19	70	1	2.04	6.12
27.33		Y		C	1	CL	P/R		58	95	GRG	4	59		1.61	7.26
27.43		Y		C	1	CL	P/R		69	122	GRG	12	73		1.96	8.82
27.45		Y		C	1	CL	P/R		58	105	GRG	10	60		1.28	11.54
27.60		Y		C	1	CL	P/R		73	35	GRG	346	81		1.35	10.81
27.67		Y		C	1	CL	P/R		60	88	GRG	0	61		0.00	12.31
27.85				S	1	CA			60	185	GRG	210	85		0.00	11.43
27.91				S	1	EP	P/S		50	85	GRG	357	51		0.00	9.64
27.95				S					50	85	GRG	357	51		0.00	8.25
27.98		Y		C	1	CL	P/R		66	50	GRG	345	72		0.00	6.78
28.13		Y		C	1	CL	P/R		51	95	GRG	5	52		0.43	6.90
28.28				S	1	EP	P/R		55	52	GRG	338	64		0.45	7.21
28.57		Y		C	1	CL	P/R		42	51	GRG	326	55		0.39	6.30
28.65		Y		C	1	CL	P/S		83	175	GRG	187	89		0.38	6.92
29.01		Y		C	1	CL	P/S		60	350	GRG	150	84	0.5	0.39	7.09
29.02		Y		C	1	CL	P/R		61	200	GRG	208	78		0.95	8.57
29.22		Y		C	1	CL	P/R		73	200	GRG	196	82		1.12	10.11
29.28		Y		C	1	CL	P/R		85	230	GRG	183	84		3.17	14.29
29.40		Y		C	1	CL	P/S		57	85	GRG	358	58		5.00	18.00
29.33		Y		C	1		P/S		60	190	GRG	210	83	0.5	4.63	16.67
29.46		Y		C	1	CL	C/R		64	135	GRG	19	73		8.11	24.32
29.48		Y		C	1	FE	PRD		50	155	GRG	37	75	1	11.29	29.03
29.51		Y		C	1	FECL	P/R		78	290	GRG	176	77	0.5	18.18	40.91
29.56		Y		C	1	CL	P/R		52	80	GRG	353	53	0.5	11.84	23.68
29.59		Y		C	1	CL	P/R		57	70	GRG	348	60	0.5	14.81	33.33
29.59		Y		C	1	CL	P/R		63	275	GRG	177	61	0.5	14.81	33.33
29.62		Y		C	1	CLFE	PRK		83	170	GRG	187	89	0.5	10.34	31.03
29.71		Y		C	1	CL	PSK		37	85	GRG	355	38	0.5	6.25	22.50
29.73		Y		C	1	CL	SSK		50	85	GRG	357	51		2.13	9.57
29.75		Y		C	1	CL	PRK		67	70	GRG	352	69		0.94	5.66
29.80		Y		C	1	CL	P/K		78	150	GRG	11	85		0.62	5.59
29.96				S	1	EP	P/S		43	40	GRG	322	62		0.19	3.38
30.53				S	1	EP	P/S		43	80	GRG	351	45		0.17	3.14
31.18		Y		C	1	WH	P/K		90		GRG	180	88		0.17	3.14
31.23		Y		C	1		P		13	120	GRG	64	33		0.17	2.76
32.37				F	1			N			GRG				0.18	2.54
32.60		Y		C	1	CACL	P	N			GRG			0.5	0.43	2.98
32.62				S	1	EP	P/C		62	110	GRG	11	65		0.67	3.11
32.70				F				N			GRG				0.85	2.98

32.72			F				N			GRG				1.52	5.30
32.88	Y		C	1	CL	P/K		28	78	GRG	341	31	0.5	1.74	6.09
33.43	Y		C	1	CL	P/K		59	45	GRG	338	69	0.5	1.64	5.74
33.58	Y		C	1	CL	P/K		46	90	GRG	1	47	0.5	1.80	5.04
33.69			F	1			N			GRG				1.75	5.59
33.75	Y		C	1	CL	P/R		33	165	GRG	56	78		2.11	6.34
33.84	Y		C	1	CL	P/K		70	130	GRG	14	76	0.5	3.06	9.18
34.09	Y		C	1	CL	P/K		55	335	GRG	147	75	0.5	3.53	10.59
34.15			S	1	EP	S/S		27	135	GRG	54	52		2.87	10.34
34.30	Y		C	1	CL	P/S		54	160	GRG	35	80	0.5	1.94	6.20
34.41	Y		C	1	CL	P/S		56	160	GRG	33	80	0.5	2.14	5.71
34.43	Y		C	1	CL	P/S		56	160	GRG	33	80	0.5	1.97	5.51
34.56			S	1	EP	P/R		44	160	GRG	44	77		1.39	4.17
35.04			F				N			GRG				1.70	4.08
35.24	Y		C	1	CL	P/R		64	95	GRG	3	65	0.5	1.12	3.35
35.36			F				N			GRG				1.09	3.28
35.59			F				N			GRG				1.09	3.26
35.77	Y		C	1	CL	P/K		72	260	GRG	183	70	0.5	1.80	4.32
36.20			S	1	CL	P/K		38	245	GRG	208	42		1.95	4.69
36.26	Y		C	1	QZ	P/S		72	185	GRG	198	86	0.5	1.74	4.17
36.40	Y		C	1	QZEP	P/S		90		GRG	180	88	0.5	1.80	5.04
36.43	Y		C	1	QZEPCL	P/R		28	265	GRG	188	26	0.5	1.84	5.88
36.52			F				N			GRG				1.90	7.62
36.80	Y		C	1	CL	P/R		42	10	GRG	313	82	0.5	2.40	7.69
36.98	Y		C	1	CL	P/S		50	45	GRG	330	63		1.32	4.64
37.13	Y		C	1	CL	S/R		46	215	GRG	219	64		0.77	3.08
37.25			S	1	EP	P/R		48	100	GRG	10	50		0.52	2.58
37.30	Y		C	1	CL	P/S		48	100	GRG	10	50	0.5	0.50	2.51
37.91					CL			61	310	GRG	160	67		0.27	2.16
38.38			F				N			GRG				0.23	1.35
38.46			F				N			GRG				0.23	0.91
38.79			F				N			GRG				0.22	0.43
38.83	Y				CA		N			GRG				0.00	0.00
39.35		Y					N			AND				0.74	0.00
39.44		Y					N			GRG				0.77	0.00
39.60			F				N			GRG				0.65	0.00
39.65		Y					N			AND				0.61	0.00
39.73	Y		C			P/S		62	122	AND	16	68	1	1.29	0.65
39.76					F		N							1.13	0.56
40.34		Y						85	180	PEG	185	88		1.76	1.18
40.48		Y					N			AND				1.62	1.08
40.90	Y		C	1	CA	S/R		68	80	AND	357	69	1	1.49	1.00
41.21			F				N			AND				0.97	0.97
41.30	Y		C	1	CA	S/R		76	60	AND	353	79	1	0.79	1.19
41.50			F				N			AND				0.83	1.66
41.74			F				N			AND				1.00	2.49
41.83		Y					N			GRG				0.51	2.56
42.87			S	1	CL	P/S		67	275	GRG	178	65		0.53	3.17
42.89			S	1	CL	P/S		60	236	GRG	198	63		0.29	3.51
42.91			S	1	CL	P/S		69	240	GRG	191	70		0.62	4.35
43.16			S	1	EP	P/S		48	105	GRG	14	51		0.59	4.73
43.19			S	1	EP	P/S	N			GRG				1.42	8.49
43.21	Y		C	1	CL	P/R		74	330	GRG	166	80	0.5	1.24	6.61
43.35	Y		C	1	CL	P/S		56	245	GRG	196	58	0.5	1.06	4.26
43.52			S	1	CLPY	P/S		54	270	GRG	180	52		1.23	4.29
43.93	Y		C	1	CL	P/R		52	102	GRG	10	54	0.5	1.32	4.09
44.10			F				N			GRG				1.89	4.07
44.79	Y		C	1	CLEP	P/R		63	58	GRG	346	68	0.5	1.74	4.43

44.79	Y						N			BRC				1.24	3.47
44.90	Y	Y	C	1	CA	P/S		35	345	GRG	126	77	0.25	1.66	4.22
44.93	Y		C	1	CA	P/S		68	210	GRG	199	77	1	1.08	3.35
44.93	Y		C	1	CA	P/S		90		GRG	180	88		1.94	5.63
45.54	Y		C	1	EP	P/S		73	100	GRG	3	74	0.25	1.76	5.63
45.59	Y		C	1	CLCA	P/S		20	60	GRG	309	35	0.25	1.50	4.50
46.19			S	1	EP	S/S		75	228	GRG	190	77		1.30	3.79
46.21	Y		C	1	CL	P/S		49	270	GRG	179	47	0.5	0.72	3.31
46.21	Y		C	1	CL	R/R		0	220	GRG	271	49	0.25	0.79	3.17
46.90	Y		C	1	CLPY	P/S		80	235	GRG	186	80	0.5	0.89	3.11
47.04			F				N			GRG				1.00	3.43
47.35			S	1	CLEP	P/R		23	285	GRG	146	26		1.18	3.14
47.75			F				N			GRG				1.16	3.09
47.84	Y		C	1	CL	P/R		68	210	GRG	199	77	0.5	1.92	4.62
47.94			F				N			GRG				1.35	3.38
48.12	Y		C	1	CLCA	P/S		58	305	GRG	160	63	0.5	2.07	4.96
48.15	Y		C	1	CLPY	P/S		30	18	GRG	302	74	0.5	2.48	4.96
48.20	Y		C	1	CLPY	P/S		32	20	GRG	304	73	0.5	2.65	6.19
48.52			F				N			GRG				3.40	8.64
48.56	Y		C	1	CLCA	P/S		34	295	GRG	146	40	0.5	4.17	12.12
48.96	Y		C	1	CLEP	P/S		80	195	GRG	190	85	0.5	1.77	5.51
48.97			S	1	EP	P/S		30	265	GRG	188	28		1.48	4.61
48.75	Y		C	1	EP	P/S		22	305	GRG	123	40	0.25	2.25	5.74
48.78			S	1	CL	P/S		17	60	GRG	304	34		2.29	6.67
49.42			F				N			GRG				2.12	6.60
49.72	Y		C	1	EP	P/S		34	315	GRG	133	53	0.5	1.77	6.19
49.74	Y		C	1	CL	P/S		47	300	GRG	154	52	1	0.94	2.82
49.76	Y		C	1	EP	P/S		30	275	GRG	170	29		0.79	2.26
50.02			F				N			GRG				0.87	1.98
50.10	Y		C	1	EP	P/S		18	148	GRG	69	61	0.25	0.81	2.31
50.88			F				N			GRG				0.94	2.09
50.99			F				N			GRG				0.51	2.06
51.44			F				N			GRG				0.92	2.05
51.88			S	1	CL	C/R		5	120	GRG	78	31		1.18	2.17
52.13	Y		C	1	CA	C/R		75	330	GRG	167	81	1	1.89	2.83
52.19		Y	S	1	EP	P/R		18	200	AND	251	69		2.33	3.26
52.46		Y	C	1		S/R		37	240	AND	214	44	1	2.86	4.17
52.86	Y		C	1	CA	P/S		64	310	AND	162	69	1	4.00	6.00
53.00	Y		C	1	CA	P/S		24	285	AND	147	27	1	4.61	6.38
53.14	Y		C	1	EP	S/S		16	210	AND	252	59	1	3.65	5.06
53.36	Y		C	1	CA	S/S		22	285	AND	144	25	0.5	4.11	5.06
53.38	Y		C	1	CA	S/S		24	292	AND	138	31	0.5	4.55	6.61
53.54	Y		C	1		P/S		23	220	AND	242	52	0.5	4.42	7.08
53.97	Y		C	1	CA	C/R		78	60	AND	354	80	1	4.09	7.27
54.04			F				N			AND				4.12	8.25
54.07			S	1	CAEP	P/S		36	185	AND	234	84		3.02	6.03
54.13	Y		C	1		P/S		36	300	AND	144	44	0.5	3.51	6.14
54.24	Y		C	1		P/S		30	320	AND	126	56	0.5	4.37	6.80
54.33	Y		C	1		P/R		32	290	AND	150	36	0.5	4.04	7.07
54.54		Y					N			GRG				4.29	7.62
54.68	Y		C	1	EP	P/R		63	295	GRG	167	64	1	4.81	7.69
55.00	Y		C	1	CL	P/S		33	330	GRG	126	65	1	5.49	8.79
55.03	Y		C	1	CL	P/S		39	60	GRG	330	48	0.5	5.75	9.20
55.12	Y		C	1	CL	P/S		38	50	GRG	322	53	0.5	7.35	11.76
55.17	Y		C	1	CL	P/S		20	305	GRG	121	39	0.5	8.73	14.29
55.15	Y		C	1	QZCL	P/S		27	325	GRG	121	59	0.5	15.28	25.00
55.20	Y		C	1	QZCL	C/S		35	30	GRG	310	65	0.5	16.18	26.47
55.22	Y		C	1	QZCL	C/S		40	20	GRG	312	75	0.5	22.22	33.33

55.31	Y		C	1	QZCL	S/S		32	315	GRG	130	52	0.5	12.24	18.37
55.36	Y		C	1	CA	P/R		78	80	GRG	358	79	1	10.38	16.98
55.37	Y		C	1	CL	C/R		39	65	GRG	334	46	1	12.82	23.08
55.39	Y		C	1	CL	C/R		48	52	GRG	332	58	1	10.98	21.95
55.66	Y		C	1	CA	S/R		13	175	GRG	77	86	0.5	11.76	26.47
55.68			S	1	CL	S/R		20	220	GRG	245	51		8.97	20.51
55.59			S	1	CA	P/S		87	195	GRG	183	87		6.25	20.00
55.63			S	1	CA	P/S		76	325	GRG	168	80		1.71	5.48
55.65			S	1	CA	P/S		70	330	GRG	162	79		1.53	6.11
55.75			F				N			GRG				1.06	5.67
55.77			S	1	CA	S/S		66	175	GRG	24	89		0.97	5.16
56.85	Y		C	1	CACL	S/S		28	160	GRG	60	73	1	0.94	5.03
56.97	Y	Y	C	1	CA		N			AND			0.5	1.18	3.79
57.09			S	1	CA	P/R		74	88	AND	0	75		1.35	3.92
57.14			S	1	EP	S/S		20	100	AND	26	23		1.42	4.27
57.22			S	1	EP	S/S		31	110	AND	30	37		2.75	8.26
57.76			F	1				58	170	AND	32	86	1	2.02	9.09
57.79	Y		C	1	EPCA	P/S		37	165	AND	52	79	0.25	1.69	8.99
57.88	Y		C	1	EP	I/R		23	100	AND	23	26	0.25	1.61	8.60
57.94			S	1	EP	S/S		34	85	AND	354	35		2.91	9.30
57.96			S	1	EP	S/S		24	105	AND	31	29		4.10	13.11
57.98			F				N			AND				3.08	12.31
58.07			S	1	EP	S/S		12	95	AND	24	14		1.82	7.29
58.08	Y		C	1	EP	S/S		18	98	AND	24	21	1	1.58	6.32
58.37			S	1	EPCA	S/		22	330	AND	114	62		1.00	3.33
58.44	Y		C	1	CAWH	P/R		90		AND	180	88	0.5	2.63	6.58
58.84		Y					N			BRC				2.75	6.59
58.89		Y					N			GRG				3.61	7.23
59.46			F				N			GRG				3.70	11.11
58.74	Y		C	1	CL	P/S	N			GRG			0.5	3.08	7.69
58.98	Y		C	1	CL	S/S	N			GRG			0.5	0.93	2.48
58.91			S	1	CL	P/R		20	155	GRG	68	67	0.5	0.83	2.78
58.91	Y		C	1	CL	P/S		55	155	GRG	33	77		0.98	3.27
59.09		Y					N			AND				0.59	2.35
60.45		Y					N			GRG				0.43	2.59
60.69			S	1	CLEP	S/R		12	290	GRG	118	23		0.19	1.94
60.99			F				N			GRG				0.00	1.86
61.29			S	1	AP	S/S		69	65	GRG	351	72		0.00	1.53
61.30			S	1	EP	P/S		45	130	GRG	33	58		0.00	2.78
61.49			F				N			GRG				0.00	3.77
61.60			S	1	AP	S/S	N			GRG				0.00	2.14
61.70		Y					N			AND				0.00	2.80
62.25			S	1	CA	S/S		65	100	AND	5	66		0.00	2.75
62.28			S	1	EP	S/S		24	155	AND	64	68		0.00	2.91
63.33			F				N			AND	270	89		0.00	3.43
63.43			S	1	CA	S/S	N			AND	NOTE:CHANGE TO			0.00	3.52
63.48			S	1	AP	P/S		75	170	AND	15	88		0.00	4.67
63.55			S	1	EP	S/S		4	101	AND	66	13		0.33	4.67
63.64			S	1	EP	S/S		26	111	AND	36	34		0.89	12.50
63.69			S	1		S/S		16	111	AND	51	27		1.41	11.27
63.75	Y					P/K		20	83	AND	345	22		1.37	9.59
63.78	Y		C	1	CL	P/S		53	143	AND	31	70	0.5	1.90	8.86
63.89			S	1	EP	S/S		16	281	AND	142	18		2.11	9.86
64.14	Y		C	1	CL	P/S		48	147	AND	37	70	0.5	1.97	9.21
64.21		Y					N			GRG				2.05	9.59
64.34	Y		C	1	CA	P/S		63	157	GRG	25	81	0.5	1.33	7.08
64.35			S	1	CA	S/S		82	138	GRG	6	86		0.93	6.48
64.45			S	1	EP	P/S		28	267	GRG	184	26		1.11	7.78

64.48		S 1	EP	S/S		27	129	GRG	51	47		1.11	7 78
64.91		S 1	CL	P/R		75	124	GRG	9	79		1.27	10.13
64.97		F			N			GRG				0.65	10.39
65.04		S 1	EP	P/R		26	101	GRG	22	29		0.59	9.41
65.11	Y	C 1	CA	P/R		65	181	GRG	205	87	0.5	0.60	9.52
65.13		S 1	CA	S/I	N			GRG				0.82	11.48
65.12		S 1	EP	P/R		28	118	GRG	41	40		0.81	11.29
65.30		S 1	EP	P/R		24	115	GRG	43	35		0.66	10.53
65.32		S 1	EP	P/R		16	106	GRG	43	24		0.64	10.26
65.52		F			N			GRG				0.00	7.48
65.59		S 1	CLEP	S/S		50	120	GRG	23	57		0.45	7.27
65.80		S 1	CL	S/R		10	101	GRG	46	16		0.65	5.23
65.89		S 1	CL	S/R		16	83	GRG	341	18		0.62	4.32
66.20		S 1	EP	S/S		28	249	GRG	214	32		0.68	4.08
66.22	Y	C 1	CA	P/S		68	295	GRG	170	68	0.5	0.63	4.38
66.83	Y	C 1	CL	S/R		16	18	GRG	287	72	0.5	0.97	4.55
66.94		F			N			GRG				1.48	4.14
66.99		F			N			GRG				2.50	5.00
67.19	Y	C 1	AU		N			GRG				2.46	4.23
67.34	Y	C 1	CL	S/R		20	286	GRG	140	24	0.5	3.61	5.15
67.58	Y	C 1	CAEP	P/R		74	203	GRG	195	82	1	2.87	4.10
67.60	Y	C 1	CA	P/S		70	173	GRG	20	89	1	3.69	4.92
67.64	Y		CL		N			BRC				3.72	5.79
67.80	Y				N			GRG			0.5	5.00	6.36
68.16	Y	C 1		P/S		54	152	GRG	33	75	0.5	5.26	7.37
68.21	Y	C 1	CL	P/S		67	189	GRG	203	84	1	4.04	7.07
68.40	Y	C 1	CA	P/R		60	189	GRG	210	83		3.13	7.29
68.44		S 1	CA	P/S		53	175	GRG	37	88	1	3.61	9.64
68.53		S 1	CA	P/S		62	138	GRG	22	73		7.29	18.75
68.59		S 1	CA	S/S		48	203	GRG	220	73		8.16	18.37
68.60		S 1	CA	S/S		63	189	GRG	207	84		10.00	26.67
68.63		S 1	CLEP	S/S		41	120	GRG	30	50		8.57	20.00
68.64	Y	C 1	CL	P/R		63	181	GRG	207	87	1	9.38	21.88
68.70	Y	C 1	CLEP	P/K		62	195	GRG	207	81	1	4.48	8.96
68.70	Y		EP			38	304	BRC	143	48		4.61	7.89
68.79	Y				N			GRG				4.25	5.66
68.85	Y	C 1	CL	S/R		52	203	GRG	216	74	1	2.78	3.03
69.26		F			N			GRG ONLY LOG FRACT				2.59	3.11
69.36	Y	C 1	CL	I/R		82	157	GRG	8	88	0.5	2.02	2.43
69.69	Y	C 1	CA	P/R		76	175	GRG	194	89	1	1.99	2.33
70.62	Y	C 1	AP	P/S		77	166	GRG	13	88	1	2.35	2.68
70.63	Y	C 1	CA	P/S		73	212	GRG	195	79	0.5	1.95	2.27
71.17	Y	C 1	CL	P/S		62	129	GRG	19	70	1	2.24	2.56
71.80	Y	C 1	FE	C/R		66	175	GRG	24	89	1	2.66	2.84
71.83	Y	C 1		P/R		62	184	GRG	208	86	1	3.28	3.54
72.34		F			N			GRG				2.70	3.43
72.48	Y	C 1	CA	I/R		65	71	GRG	352	67	1	2.25	3.15
72.51	Y	C 1	CL	P/S		68	180	GRG	202	88	1	2.94	4.12
72.60		F			N			GRG				1.87	3.27
72.67	Y	C 1	CL	P/S		85	78	GRG	359	86		1.69	3.37
73.39	Y	C 1	CACL	P/R		55	203	GRG	213	75		1.72	4.02
73.50	Y	C 1	CACL	P/R		42	207	GRG	225	68	1	1.24	3.47
73.97	Y	C 1	CL	P/K		47	251	GRG	197	48		1.03	3.61
74.12		F			N			GRG				1.04	4.15
74.22	Y	C 1	CL	P/S		45	198	GRG	224	75		1.27	4 43
74.53	Y	C 1	CA	P/S		59	186	GRG	211	85	0.5	1.18	3.55
74.54	Y	C 1	FE	IRD		90	186	GRG	180	88	0.5	0.71	3.55
74.60	Y	C 1	CLCA	P/S		59	269	GRG	180	57		0.61	2.44

74.97			F				N							1.28	3.21
75.19			F				N							2.31	3.85
75.38			F				N							1.89	3.03
75.76		Y						67	195	APL	202	82		1.06	1.59
75.78	Y		C	1	QZ	P/S		67	195	APL	202	82	1	1.06	1.06
75.83	Y		C	1	QZ	P/S		78	147	APL	10	84	1	1.05	1.05
75.86		Y								GRG	270	89		1.12	1.35
76.49			F				N			GRG				1.38	1.58
76.85			F				N			GRG				1.79	1.98
77 09			F				N			GRG				1.55	1.94
77.61	Y		C	1	CL	P/K	N			GRG			0.5	1.33	1.89
78.29	Y		C	1	CA	C/R		72	30	GRG	345	82	1	1.73	2.60
78.30	Y		C	1	CA	P/R		75	340	GRG	166	83	1	1.84	2.76
78.41	Y		C	1		P/R		60	238	GRG	197	63	0.5	1.81	2.71
78.50	Y	Y	C	1	CL	P/S		52	9	AND	323	84	0.5	2.45	3.43
78.80	Y		C	1	CL	P/S		41	18	AND	313	76	0.5	2.53	3.37
79 02			F				N			AND				1.81	2.59
79.30			F				N			AND				1.08	1.73
79.65	Y		C	1	CL	C/S		90		AND	180	88	1	1.02	1.63
80.07			F				N			AND				1.02	1.63
80.23			F				N			AND				0.81	1.63
80.72			F				N			AND				1.23	2.05
80.95	Y		C	1	CLCA	S/S		70	20	AND	341	84	0.5	1.38	2.75
81.25	Y		C	1	CLCA	P/S		73	38	AND	347	80	0.5	1.10	3.30
81.48			F	1	CL	C/S	N			AND				1.16	4.07
81.74	Y		C	1		S/S		61	171	AND	29	87	1	1.30	5.19
81.83			F	1			N			AND				1.85	5.56
81.89			F	1			N			AND				1.88	6.02
81.95			F	1			N			AND				1.18	4.14
82.26			F	1			N			AND				1.60	4.49
82.57	Y		C	1	CL	P/S		57	330	AND	150	73	1	0.89	3.55
82.58			F				N			AND				0.83	2.76
83.17			F				N			AND				0.83	2.21
83.30	Y		C	1	CLCA	PSK		59	298	AND	164	61	0.5	0.82	2.19
83.52			F				N			AND				0.93	2.48
83.70			F				N			AND				0.26	1.54
83.76			F				N			AND				0.81	2.15
84.09	Y		C	1	CL	P/R		44	70	AND	342	48		1.20	2.40
84.18	Y		C	1	CL	P/R		63	30	AND	337	77		1.54	2.56
84.53			F				N			AND				1.77	3.03
85.03	Y		C	1	CL	P/S		75	87	AND	0	76	1	1.57	2.69
85.38	Y		C	1	CL	P/S		56	124	AND	21	63	1	1.89	3.30
85.47	Y		C	1	CL	C/S		44	55	AND	331	54	1	1.91	2.97
85.68	Y		C	1	CL	P/S		46	151	AND	40	71	0.5	2.23	2.68
85.99			F			I/R	N			AND				2.27	3.18
86.21	Y		C	1	CLEP	P/S		63	74	AND	353	65	0.5	1.93	2.90
86.54	Y		C	1	CL	P/S		24	199	AND	245	71	0.5	1.43	2.38
86.77			F				N			AND			0.5	0.92	1.83
87.23	Y		F	1		C/S		66	60	AND	336	88		0.78	1.56
87.45			F				N			AND				0.59	1.58
87.57			F				N			AND				0.42	1.26
87.86			F				N			AND				0.22	0.87
87.91		Y						30	198	GRG	302	73		0.00	1.09
88.74	Y		C	1	EPCL	P/R		57	72	GRG	350	59		0.00	0.58
88.92		Y				I/S		72	115	APL	343	87		0.00	0.56
89.06		Y						82	129	GRG	352	89		0.00	1.27
89.07			F				N			GRG				0.00	1.01
89.17		Y				I/R		90		APL	180	88		0.00	1.37

89.35			F			I/R		90		APL	180	88		0.00	0.59
89.44	Y		C	1	CA	P/S		79	180	APL	191	88		0.27	1.09
89.89		Y					N			GRG				0.25	1.51
90.20			F				N			GRG				0.41	1.63
90.61			F				N			GRG				0.42	1.67
90.90	Y		C	1	QZ	P/R		69	170	GRG	21	88	0.5	0.60	1.99
91.06	Y		C	1	CL	P/S		80	0	GRG	170	88		0.65	2.16
91.62	Y		C	1	EP	P/S		70	85	GRG	359	71	0.5	0.64	2.55
91.75			F				N			GRG				0.63	2.51
91.95	Y		C	1	CACLEP	C/R		64	85	GRG	358	65	0.5	0.69	2.78
92.21			F	1	CL	C/S		54	162	GRG	35	81		0.72	2.88
92.55			F	1	CL	PSK		43	120	GRG	29	52		0.73	2.43
93.00			F				N			GRG				0.44	1.77
93.06			F				N			GRG				0.40	1.58
93.14	Y		C	1	QZ	S/R		77	305	GRG	172	78	0.5	0.20	1.22
93.68			F		CACL	P/S		50	190	GRG	220	81		0.24	1.90
94.01			F		CL			73	270	GRG	180	71		0.25	1.51
94.48			F				N			GRG				0.22	1.29
94.66		Y					N			AND				0.66	1.75
94.66	Y		C	2	CL		N			AND				0.75	2.01
94.99			F				N			AND				1.13	2.82
95.38			F				N			AND				1.43	4.29
95.42	Y		C	1	CA	PSD		60	177	AND	210	89	1	1.89	6.06
95.67	Y		C	1	CL	P/S		59	102	AND	8	61	0.5	1.88	6.77
95.78	Y		C	1	CAEP	P/S		60	102	AND	7	62	0.5	2.12	6.78
95.88			F	1	CL	P/S		64	110	AND	10	67		2.05	6.56
95.98	Y		C	2	CL		N			AND			0.5	1.94	6.20
95.99			F	1	CL	P/S		65	229	AND	197	69		1.32	5.30
96.17	Y		C	1	CA	PSD		66	88	AND	0	67		0.99	5.26
96.60			F				N			AND				0.68	5.44
96.71			F				N			AND				1.37	5.48
97.18	Y		C	1	CLCA	P/S		61	140	AND	23	73	0.5	0.99	3.95
97.30			F	1	CA	P/S		72	108	AND	6	74		1.71	4.11
97.35			F	1	CACL	P/S		77	150	AND	12	85		2.43	4.17
97.44	Y		C	1	CA	P/S		65	158	AND	24	82	1	2.92	4.55
97.51			F				N			AND				4.66	6.78
97.63	Y		C	1	CA	P/R		75	200	AND	194	83	1	3.73	5.22
98.04	Y		C	1	CL	S/S		58	225	AND	204	66	1	3.60	4.32
98.25	Y		C	1	CLCA		N			AND			1	3.62	3.62
98.36	Y		C	1	CACL	S/S		58	102	AND	8	60	1	3.36	3.36
98.64			F				N			AND				2.42	2.42
98.74		Y					N			GRG				2.33	2.33
98.82			F				N			GRG				2.09	2.09
99.00	Y		C	1	CA	I/R		78	212	GRG	190	82	1.000	1.51	2.01
99.70			F				N							1.24	1.98
99.76			F				N			GRG				1.12	1.79
100.16	Y		C	1	CLCA	P/R		60	215	GRG	205	71	1.000	1.53	2.18
100.35			F	1	CL	P/K		45	178	GRG	225	89		1.54	2.20
100.66	Y		C	1	CL	P/S		41	160	GRG	47	76	0.500	1.57	2.62
100.97			F				N			GRG				1.81	2.71
101.11	Y		C	1	CL	P/S		90		GRG	180	88	1.000	2.18	3.88
101.27			F				N			GRG				1.74	3.48
101.61	Y		C	1	CLEP	P/S		76	72	GRG	356	77	0.500	1.86	3.26
101.97	Y		C	1	CL	P/S		76	62	GRG	354	78	1.000	1.67	2.87
102.22	Y		C	2	CL		N			GRG			0.500	1.84	2.87
102.65	Y		C	1	CL	P/S		24	120	GRG	48	39	0.500	1.14	2.28
102.81			F				N			GRG				1.18	2.36
103.06		Y					N			GRP				1.07	2.50

103.55	Y	Y	C	1	CL	S/R		22	128	GRG	56	44	1.000	0.60	2.11
104.34			S	1	CL	S/R		55	180	GRG	215	88		0.24	0.81
104.57		Y	F				N			GRP				0.26	1.03
104.77			S	1	CL	I/R		90		GRP	180	88		0.35	1.18
105.53			F	1				0	130	GRP	89	40		0.66	1.58
108.86			F				N			GRP				0.49	1.95
106.71			F					66	208	GRP	202	77		0.65	1.94
107.29	Y	Y	C	1	CLCA	P/S		70	160	AND	19	84	0.500	0.85	2.38
107.35	Y		C	1	CL	S/S		32	240	AND	219	41	1.000	1.04	2.50
107.42			S	1	CL	P/S		29	200	AND	240	71		-4.22	-7.23
107.67	Y		C	1	CACL	P/S		47	84	AND	356	48	0.500	2.35	4.70
107.71	Y		C	1	CACL	PSK		38	145	AND	46	64	0.500	3.15	7.21
107.93			F				N			AND				2.70	7.21
108.03			S	1		P/S		54	165	AND	35	82	1.000	1.68	6.72
108.20			S	1	CL	P/S		90		AND	180	88		1.65	5.79
108.40			S	1	CL	P/S		41	95	AND	7	42		1.64	4.61
108.46			S	1	CL	P/S		42	200	AND	227	73		1.85	4.32
108.61			S	1	CLCA	P/S		25	302	AND	130	39		2.48	4.97
108.88		Y					N			GRP				2.63	5.26
109.23	Y		C	1	CLCA	P/S		25	330	GRP	118	63	1.000	3.60	5.76
109.55	Y			1		PRD		46	120	GRP	26	54	1.000	3.45	4.83
109.64	Y			1		PRD		22	310	GRP	121	44	1.000	3.57	4.29
109.72	Y			1		PRD		24	320	GRP	119	54	1.000	3.44	3.75
109.79	Y		C	1	QZ	P/R		12	320	GRP	104	51	1.000	3.27	3.52
109.91			F				N			GRP				2.97	3.24
110.01			F			P/R		56	282	GRP	171	55		2.42	2.69
110.48	Y		C	1	CL	P/R		16	330	GRP	108	61	0.500	2.46	2.73
111.22	Y		C	1	CAEP	P/R		48	180	GRP	222	88	1.000	1.90	2.72
111.40			F				N			GRP				1.22	2.04
111.50			F				N			GRP				1.61	2.41
111.55	Y		C	1	EP	P/K		17	330	GRP	109	61	1.000	2.05	3.18
111.63	Y		C	1	EP	P/K	N							3.38	4.73
112.36	Y		C	1		P/K		19	112	GRP	47	30	0.500	3.08	5.38
112.50	Y		C	1	CLEP	P/R		48	0	GRP	138	89	1.000	3.02	5.37
112.68	Y		C	1	WF	P/R		19	142	GRP	66	55	0.500	2.97	4.86
112.70	Y		C	1	CL	P/R		15	120	GRP	61	34	1.000	2.49	4.97
112.70	Y		C	1	CL	P/R		23	120	GRP	49	38		4.24	7.63
112.99	Y		C	1		P/R		27	140	GRP	56	56	0.500	4.33	7.09
113.40	Y		C	1	CLFE	PRD		30	142	GRP	54	59	1.000	4.87	7.96
113.44	Y		C	1		P/R		25	180	GRP	245	88		3.82	6.11
113.54	Y		C	1		P/R		20	140	GRP	64	54	0.500	2.65	4.64
113.77	Y		C	1	CLWF	P/R		22	205	GRP	247	65	1.000	3.15	4.72
113.81	Y		C	1	CL	P/R		65	130	GRP	17	72	1.000	2.92	4.17
114.01			F				N			GRP				2.73	3.91
114.21			F				N			GRP				2.61	2.99
114.26			F				N			GRP				2.56	2.56
114.60			F				N			GRP				1.18	1.18
114.72	Y		C	1	CL	P/R	N			GRP			1.000	0.65	0.65
114.88			F				N			GRP				0.39	0.39
114.94			F				N			GRP				0.35	0.35
115.51			F				N			GRP				0.66	0.66
115.55			F				N			GRP				0.93	0.93
116.76			S			P/R		63	140	GRP	22	74		0.63	0.63
117.14			F				N			GRP				0.54	0.54
117.63	Y		C	1		P/R		15	14	GRP			1.000	0.77	0.77
117.96	Y		C	1		P/R		20	20	GRP	292	70	1.000	0.90	1.03
118.05			F				N			GRP				1.49	1.66
118.61			F				N			GRP				1.56	1.74

119.41	Y	C	1	CL	P/R		11	340	GRP	101	70	1.000	1.70	1 89
119.43	Y	C	1		P/R		20	350	GRP	110	80	0.500	1.40	1.60
119.78	Y	C	1	CL	S/R		50	340	GRP	142	76	1.000	1.01	1.21
120.02		F				N			GRP				1.51	2.01
120.28		F				N			GRP				1.86	2.48
120.46		F				N			GRP				1.08	1.62
120.52		F				N			GRP				0.32	0.43
120.60	Y		1		P/S		19	0	GRP	289	89	0.500	1.04	1.39
121.02		F				N			GRP				1.27	2.54
121.28		F				N			GRP				1.50	4.00
124.41		F				N			GRP				1.02	3.40
121.46	Y	C	1	CL	P/R		34	280	GRP	164	34	1.000	0.96	2.88
121.46	Y		1				0	100	GRP	83	10		0.74	2.94
121.46			1				0	185	GRP	270	84		1.40	3.93
121.99		F	1		P/R		23	300	GRP	128	36		-2.34	-7.48
122.68	Y	C	1	CL	P/S		34	330	GRP	127	65	0.500	1.71	4.39
123.06	Y	C	1	CLEP	P/S		43	210	GRP	223	66		1.40	4.19
123.06	Y	C	1	CL	P/S		50	310	GRP	151	59	1.000	1.57	3.54
123.34	Y	C	1	CL	P/S		45	320	GRP	142	62		2.31	4.17
123.51	Y	C	1	EPCL	P/K	N			GRP			1.000	3.19	4.79
123.61	Y	C	1	CK	P/R		58	310	GRP	158	65	0.500	3.42	5.59
124.00	Y	C	1	CL	PKS		28	310	GRP	128	47	1.000	2.85	4.15
124.15	Y	C	1	WF	P/R		58	125	GRP	20	65	1.000	3.11	4.52
124.56	Y	C	1	WF	P/R		28	320	GRP	124	55	1.000	3.33	4.10
124.67	Y	C	1	WF	P/R		34	330	GRP	127	65		-9.02	11.48
124.99		F				N			GRP				2.16	2.52
125.11	Y	C	1	WF	P/R		22	335	GRP	114	67	1.000	2.08	2.64
125.46	Y	C	1	CLWF	P/R		32	320	GRP	128	56	1.000	2.23	3.13
123.00		F				N			GRP				1.78	2.67
126.78	Y		1		P/R		42	280	GRP	168	41	1.000	2.42	3.23
126.80	Y		1		P/R		32	290	GRP	150	36	0.500	2.59	3.30
126.80	Y		1		P/R		42	120	GRP	29	51	0.500	2.45	3.43
126.92		F				N			GRP				1.08	1.51
126.85	Y		1		I/R		18	202	GRP	251	67	0.500	3.70	5.93
127.23	Y	C	1	WF	P/R		28	64	GRP	323	37	1.000	2.47	4.32
127.50	Y		1		I/R		15	48	GRP	294	43	0.500	2.36	3.66
127.63	Y	C	1	WF	P/R		30	53	GRP	316	46	1.000	2.75	3.85
128.13	Y		1		P/R		25	18	GRP	297	73		3.05	4.06
128.42		F				N			GRP				3.99	4.91
128.71	Y		1		P/R		56	286	GRP	169	56	1.000	2.93	3.72
128.74	Y		1		P/R		67	294	GRP	170	67	1.000	2.83	3.30
128.82	Y		1		P/R		45	294	GRP	157	48	1.000	3.42	4.35
128.86	Y		1		I/R	N			GRP			1.000	3.87	4.93
129.38							5	202	GRP	265	67		4.20	5.34
129.75	Y		1		PRD		65	26	GRP	338	80	1.000	3.52	4.93
129.74	Y		1		P/R		37	48	GRP	320	54	0.500	2.78	4.32
129.84	Y	C	1	WF	P/R		35	53	GRP	321	49		2.20	3.85
130.02		F				N			GRP				2.17	4.35
130.16	Y		1		P/R		34	46	GRP	316	53	0.500	3.60	6.40
130.44	Y		1		P/R		20	55	GRP	305	39	0.500	2.35	4.70
130.68	Y		1		P/R		16	253	GRP	227	21	0.500	1.82	3.64
130.99	Y		1		P/R		26	26	GRP	299	66	0.500	1.92	3.21
131.00	Y		1		P/R		45	193	GRP	224	79	1.000	2.45	3.68
131.23		F				N			GRP				2.90	3.62
131.49		F				N			GRP				2.63	3.76
131.58	Y						6	299	AND	100	30		2.61	3.48
131.79	Y	C	1	CL	P/R		14	9	AND	285	80	1.000	1.90	1.90
131.82		F				N			AND	270	89	0.500	1.48	2.22

132.01	Y		C	1	CA	S/R		7	326	AND	98	56		1.77	2.65
132.14			F				N			AND				2.50	3.33
132.58			F				N			AND			0.500	2.61	3.48
132.58	Y		C	1	CL	S/S		32	202	AND	236	69		2.31	3.08
132.62			F				N			AND	270	89		2.00	4.00
132.78	Y		C	1	CLWF	P/S		27	299	AND	135	38	1.000	2.69	3.85
132.94			F				N			AND				4.55	6.06
133.12	Y		C	1	CL	P/S		16	266	AND	192	14	1.000	4.59	6.42
133.26	Y		C	1	CACL		N			AND				5.00	10.00
133.44	Y		C	1	CL	P/R		56	101	AND	8	58	1.000	5.88	10.92
133.57	Y		C	1	CL	S/S		44	175	AND	46	87	1.000	6.67	12.38
133.67	Y		C	1	CL	P/S		17	109	AND	46	26	1.000	6.86	12.75
133.82	Y		C	6	CL	P/S		22	357	AND	112	87	1.000	7.00	13.00
133.97	Y		C	1	CLCA	P/R		70	74	AND	355	72	1.000	7.45	12.77
133.99	Y			1		P/S		20	119	AND	53	36	1.000	7.07	12.12
134.14			F				N			AND				6.31	11.65
134.26	Y		C	1	CL	P/S		48	48	AND	330	60	1.000	3.20	6.40
134.38		Y					N			GRP				2.68	2.98
134.56	Y		C	1	WF	P/R		67	130	GRP	16	74	1.000	1.84	2.83
134.70	Y			1		P/R		0	0	GRP	270	89	0.500	1.53	2.55
135.54		Y						37	152	AND	50	69		1.53	3.06
135.65		Y						44	140	GRP	39	64		1.34	3.23
135.89	Y		F	1			N			GRP				1.69	3.95
136.10	Y		C	1	CL	P/S		20	184	GRP	250	84	0.500	1.23	4.29
136.22			F	1			N			GRP				2.02	7.07
136.24	Y			1		P/S		20	184	GRP	250	84	0.500	2.06	8.25
136.33			F	1			N			GRP			0.500	2.38	8.57
136.33	Y			1		I/R		0	317	GRP	89	47		2.78	10.00
136.53	Y		C	1	CL	I/R		27	317	GRP	124	52	0.500	2.43	8.74
136.62			F	1			N			GRP				2.99	7.69
136.94	Y		C	1	CL	P/S		0	110	GRP	87	20	0.500	2.99	7.69
137.00			F	1			N			GRP				3.10	6.98
137.25	Y		C	1	CL	P/R		0	276	GRP	79	7	0.500	3.67	8.26
137.41	Y		C	1	CAQZ	P/R		28	259	GRP	199	28	1.000	3.74	8.41
137.50	Y		C	1	CL	P/S		25	175	GRP	65	86	0.500	4.94	11.11
137.62	Y		C	1	CLEP	P/R		3	294	GRP	94	24	1.000	5.26	11.84
137.62	Y		C	1	CACL	PRD		42	97	GRP	9	43		8.49	16.98
137.69	Y			1		P/R	N			GRP			0.500	10.00	20.00
137.75				1			N			GRP				9.52	21.43
137.76	Y			1		P/S		55	76	GRP	351	57	0.500	12.86	25.71
137.78	Y			1		P/S		28	106	GRP	28	33	0.500	9.18	18.37
137.86	Y			1		P/R		48	110	GRP	18	52	0.500	5.56	9.88
137.92	Y			1		P/S		70	92	GRP	1	71	0.500	3.77	6.60
137.97	Y		C	1	CL	SSD		60	184	GRP	210	86	1.000	3.54	5.22
138.11	Y		C	1	CL	P/S		43	99	GRP	10	45	1.000	3.01	4.96
138.50			F				N			GRP				3.49	5.15
138.81			F			I/R	N			GRP				3.82	5.34
139.10	Y			1		P/S		11	257	GRP	231	15	0.750	4.23	5.38
139.19	Y			1		S/R		71	112	GRP	8	73		2.98	4.64
139.22	Y		C	1	WFCA	P/R		17	285	GRP	136	22	1.000	3.78	5.88
139.23	Y		C	1	WFCA	P/R		19	289	GRP	134	26	0.750	4.59	7.14
139.27	Y		F	1		P/R		72	92	GRP	1	73	1.000	9.02	13.11
139.62	Y		C	1	WFCL	S/R		23	277	GRP	161	22		5.86	8.64
139.69	Y		C	1	WF	P/R		23	261	GRP	200	23	1.000	5.83	7.78
139.79			F				N			GRP				4.90	7.22
139.71	Y		C	1	WF	C/R		20	295	GRP	128	31	1.000	3.60	5.60
140.00			F				N			GRP				4.08	7.14
140.12	Y		C	1	CL	P/R		19	268	GRP	184	17	0.500	4.74	7.37

140.20	Y		C	1	CL	P/S		56	100	GRP	7	58	0.500	4.65	8.14
140.52	Y		C	1	CL	S/R		22	283	GRP	148	24	0.500	2.56	4.49
140.60	Y			1		P/R		22	256	GRP	211	24	0.500	2.76	4.83
140.64	Y			1		P/R		25	263	GRP	194	24	0.500	2.73	4.86
140.65	Y			1		P/R		19	263	GRP	199	18	0.500	2.51	3.91
141.27		Y				25 222	B	25	222	BRC	239	51		2.67	4.00
141.45	Y	Y	C	1	CA	U/S		27	245	AND	220	34	1.000	2.67	4.00
141.56			F		CA	S/R		53	118	AND	20	59		2.70	4.05
141.99	Y		C	1	CA	U/S		32	254	AND	204	33	1.000	2.98	3.97
142.02		Y				39 313	BRC				139	54		4.79	6.38
142.10	Y		C	1	CL	U/S		44	108	BRC	18	48	0.500	7.35	10.29
142.12	Y			1		P/S		53	104	BRC	11	55	0.500	6.62	10.29
142.16	Y		C	1	CL	P/S		51	91	BRC	2	52	1.000	14.52	22.58
142.21	Y			1		P/S		39	104	BRC	17	42	0.500	10.29	17.65
142.13	Y			1		P/S		40	113	BRC	25	46	0.500	10.61	18.18
142.24	Y			1		P/S		35	109	BRC	25	40	0.500	7.00	12.00
142.30			F				N			BRC				4.11	8.22
142.36			F				N			BRC				2.94	7.35
142.43		Y								GRP	270	89		1.67	5.56
142.62				1		I/?		51	32	GRP	326	71	0.500	1.14	4.55
142.89			S	1	CL	P/R		68	41	GRP	344	76		1.42	3.77
142.89		Y					N			AND				1.96	4.90
143.03			S	1	CL	PSK		38	261	AND	191	37		1.69	4.24
143.12		Y					N			GRP				1.59	4.76
143.36	Y			1		IRK		55	27	GRP	329	75	1.000	1.38	5.50
143.38	Y			1		P/S		18	308	GRP	116	41	0.500	1.68	5.04
143.61		Y			1	12 I		12	286		123	19		1.90	6.67
143.88			S	1	CL	P/S		20	322	AND	114	54		1.74	6.09
143.98			S	1	CLCA	S/S		49	263	AND	186	47		1.56	6.25
144.08	Y		C	1	CLCA			14	313	AND	109	45	0.500	0.81	6.50
144.08			S	1	CL	P/S		0	263	AND	283	6		0.83	6.67
144.27		Y		1		P/R		24	295	GRP	134	33		0.75	6.02
144.64			F	1			N			GRP				0.69	4.86
144.61			F	1			N			GRP				0.67	4.03
144.81	Y		C	1	CLEP	P/R		54	95	GRP	4	55	0.500	0.30	3.64
145.21			F			I/R	N			GRP				0.32	3.82
145.42			F				N			GRP				0.71	4.26
145.57			F				N			GRP				1.10	3.30
145.73	Y			1		P/R		64	116	GRP	13	68		1.10	3.31
145.84	Y		F	1		I/R		43	218	GRP	220	61		0.86	2.87
146.05	Y			1		P/S		62	204	GRP	206	77	0.500	0.90	3.59
146.43	Y		C	1	WH?	P/S		33	225	GRP	228	52	1.000	1.16	4.05
146.62			F	1		P/S		55	218	GRP	209	67		1.40	4.49
146.95		Y				C/S		25	290	AND	141	31		1.75	4.68
147.09			S	1	CLEP	P/S		63	64	AND	348	67		2.53	5.06
147.30			S	1	CLEPCA	C/R		50	82	AND	354	51	0.500	2.92	5.84
147.51			S	1	CL	S/S		75	86	AND	359	76	0.500	2.76	6.30
147.55			S	1	CL	S/S		75	86	AND	192	81	0.500	4.05	7.21
147.63	Y		C	1	CL	P/R		32	77	AND	342	35	1.000	5.15	9.28
147.80	Y		C	1	CL	IRD		63	73	AND	352	65	0.500	5.62	10.11
147.89	Y		C	1	CL	S/S		63	204	AND	205	77	0.500	6.87	11.25
148.06	Y			1		IRD		64	64	AND	349	67	1.000	6.33	11.39
148.06	Y			!		IRD		55	222	AND	208	65	0.500	5.62	8.99
148.19	Y		C	.	CLCA	P/S		65	36	AND	340	76		5.56	11.11
148.31	Y		C	1	CLWH	P/S		33	36	AND	310	60	1.000	5.22	11.94
148.34	Y		C	1	CL	P/S	N			AND				4.69	10.94
148.52			F				N			AND			0.500	2.70	9.46
148.52	Y		C	1	CLCA	S/S		28	172	AND	62	84		2.22	7.78

148.56	Y	S	1	CL	P/S		70	27	AND	342	82		2.50	7.50
148.70		F				N			AND				0.95	4.76
148.80		S	1	CLCA	P/R		62	104	AND	8	64		0.93	4.63
149.09	Y	C	1	CL	P/R		23	163	AND	66	75	0.500	0.45	5.36
149.11		F				N			AND				0.40	4.80
149.39		F				N			AND				0.41	4.92
149.60		S	1		S/S		57	168	AND	33	85		0.36	4.35
149.64		F	1		I/R		63	118	AND	14	67		0.44	4.39
149.81		S	1	CL	P/R		66	14	AND	337	85		0.00	3.94
149.92		S	1	CL	P/R		63	9	AND	334	86		0.00	3.18
150.18		F				N			AND				0.27	3.23
150.23		F				N			AND				0.27	3.19
150.38	Y	C	1	CL	P/S		70	154	AND	18	82		0.28	2.82
150.96		F			S/S		60	245	AND	194	61		0.53	2.65
151.46	Y		1		P/S		73	200	AND	196	82	0.500	0.65	2.17
151.52	Y	S	1	CLCA	P/S		57	41	AND	335	69		0.67	2.67
151.58		F				N			AND				0.90	3.14
151.81	Y	C	1	CACL	P/S		56	147	AND	30	73	0.500	1.10	3.85
152.48	Y	C	1	CL	P/S		22	236	AND	235	38	0.500	1.61	5.16
152.48	Y	C	1	CL	P/S		60	54	AND	342	67		1.89	5.03
152.61	Y	C	1	CLCA	S/S		48	192	AND	222	80	0.500	1.64	3.83
152.78		S	1	CL	P/S		71	165	AND	19	86		1.56	4.17
153.01	Y	C	1	CL	P/S		63	116	AND	13	67	0.500	1.87	5.97
153.11	Y	C	1	CLCA	P/R		61	41	AND	338	72	1.000	1.64	5.26
153.41		F				N			AND				1.95	5.19
153.73		S	1	CLCA	P/R		75	54	AND	351	79		1.79	4.76
153.82		S	1	CLCA	P/R		71	242	AND	189	71		2.03	4.73
154.00	Y	C	1	CA	S/S		66	220	AND	199	73	0.500	1.64	3.95
154.15	Y	C	1	CLCA	P/S		68	30	AND	341	80	0.500		
154.46	Y	C	1	CLCA	P/S		58	85	AND	358	59	0.500		
154.49	Y				I/R	N								
154.63	END													

APPENDIX C Geochemical Analyses

Notes regarding acronyms used in Tables

SIV	indicates number of times the sampling cavity was flushed prior to sampling
Temp degC	Temperature in °C measured in a surface flow cell. Samples were collected between August and November and thus showed a large variation in temperature.

APPENDIX C

GEOCHEMICAL DATA FROM NSCRV B NICK SARGENT

Sample interval and number
all depths in metres

TEST TOOL CONFIGURATION:
3/=3/16" Sampling tube.
4/=1/4" Sampling tube.
Three digit number cavity length in cms.
Last letter W=run on wireline R=run on rods

Top	Btm.	SAMPLE MID DEPTH	Samp #	Test tool config.	SIV's	Temp degC	ISOTOPE DATA 18O per.mil.	2H per.mil.
			STD					
			STD					
			STD					
17.71	19.82	18.77	11(17)	3/211R	1.70	n/a	-8.215	-56.77
18.61	21.77	20.19	1a	4/316R	1.59	17.6		
18.61	21.77	20.19	1b	4/316R	2.23	17.6		
18.61	21.77	20.19	1b(19)	4/316R	2.23	17.6		
18.61	21.77	20.19	1c	4/316R	5.37	17.6		
55.75	57.86	56.81	10(2)	3/211R	8.50	n/a	-8.311	
55.75	57.86	56.81	7a(10)	3/211R	1.61	n/a	-8.454	
55.75	57.86	56.81	7b(12)	3/211R	2.10	n/a	-8.271	-55.39
68.58	70.69	69.64	6a(6)	3/211R	2.89	n/a	-8.213	
68.58	70.69	69.64	+6a	3/211R	2.89	n/a		
68.58	70.69	69.64	8(5)	3/211R	8.32	0.7	-8.337	
70.59	72.70	71.65	5a(9)	3/211R	3.70	17.1	-8.209	
70.59	72.70	71.65	5b(14)	3/211R	6.05	17.1	-8.361	
70.59	72.70	71.65	5c(1)	3/211R	9.44	17.1	(?)-8.036	-58.19
73.62	76.20	74.91	2a	3/248W	1.18	20.4		
73.62	76.20	74.91	2b	3/248W	3.80	20.4		
73.62	76.20	74.91	2b(11)	3/248W	3.80	20.4		
73.62	76.20	74.91	2c	3/248W	7.46	20.4		
73.62	76.20	74.91	2d	3/248W	9.85	20.4	-8.33	-60.31
73.62	76.20	74.91	+2d	3/248W	9.85	20.4		
76.35	78.46	77.41	9(4)	3/211R	1.43	2		
76.35	78.46	77.41	9(18)	3/211R	1.43	2		
95.58	97.69	96.64	4a	3/211R	1.00	n/a	-8.424	
95.58	97.69	96.64	4b(15)	3/211R	6.34	7.3	-8.598	
95.58	97.69	96.64	4c(3)	3/211R	8.01	7.3	-8.481	-58.03
96.17	98.65	97.41	3a(7)	3/248W	1.00	6.9	-8.306	
96.17	98.65	97.41	3b(13)	3/248W	2.00	6.9	-8.366	
96.17	98.65	97.41	3c(8)	3/248W	6.80	6.9	-8.407	
96.17	98.65	97.41	3d(16)	3/248W	9.00	6.9	-8.572	-60.89

FINAL SAMPLE VALUES

all depths in metres

lld Top >	Btm.	mid.	Samp #	Test tool config	SIV's	Temp degC	18O per.mil.	2H per.mil.
17.71	19.82	18.77	11(17)	3/211R	1.70	n/a	-8.215	-56.77
55.75	57.86	56.81	10(2)	3/211R	8.50	n/a	-8.311	
68.58	70.69	69.64	8(5)	3/211R	8.32	0.7	-8.337	-55.39
70.59	72.70	71.65	5c(1)	3/211R	9.44	17.1	-8.361*	-58.19
73.62	76.20	74.91	2d	3/248W	9.85	20.4	-8.330	-60.31
76.35	78.46	77.41	9(4)	3/211R	1.43	2		
95.58	97.69	96.64	4c(3)	3/211R	8.01	7.3	-8.424	-58.03
96.17	98.65	97.41	3d(16)	3/248W	9.00	6.9	-8.572	-60.89

DILUTED SEAWATER (CONCEPTION BAY) — *sample 5b(14)

Diluted Seawater Cl normalised (see section 4.1.3) — see Table 4.4

SAMPLE MID DEPTH	Eh mV	pE (calculated)	Alk ppm [hco3-]	Alk mequiv [hco3-]	pH	Conductivity micro.S
18.77	n/a	n/a	115.7	1.9	7.50	n/a
20.19	n/a	n/a	138.9	2.3	7.22	425
20.19	n/a	n/a	131.2	2.2	7.25	430
20.19	n/a	n/a	131.2	2.2	7.25	430
20.19	n/a	n/a	138.9	2.3	7.54	430
56.81	n/a	n/a	138.9	2.3	8.22	590
56.81	n/a	n/a	n/a	n/a	n/a	570
56.81	n/a	n/a	n/a	n/a	n/a	565
69.64			n/a	n/a	n/a	630
69.64			n/a	n/a	n/a	630
69.64	543	10.01	92.6	1.5	7.70	560
71.65	337	5.86	138.9	2.3	n/a	n/a
71.65	337	5.86	n/a	n/a	n/a	630
71.65	337	5.86	n/a	n/a	8.43	660
74.91	148	2.55	123.5	2.0	9.08	615
74.91	148	2.55	123.5	2.0	8.91	630
74.91	148	2.55	123.5	2.0	8.91	630
74.91	148	2.55	131.2	2.2	8.84	620
74.91	148	2.55	131.2	2.2	8.80	630
74.91	148	2.55	131.2	2.2	8.80	630
77.41		0.00	123.5	2.0	8.76	700
77.41		0.00	123.5	2.0	8.76	700
96.64	n/a	n/a	108.0	1.8	n/a	n/a
96.64	252	4.54	115.7	1.9	9.05	840
96.64	252	4.54	108.0	1.8	9.05	820
97.41	205	3.70	n/a	n/a	9.8	790
97.41	205	3.70	n/a	n/a	9.89	840
97.41	205	3.70	n/a	n/a	9.87	920
97.41	205	3.70	84.9	1.4	9.61	920

mid.	Eh(corr) mV	pE	Alk ppm [hco3-]	Alk mequiv [hco3-]	pH	Cond. micro.S
18.77	n/a	n/a	115.7	1.9	7.50	n/a
56.81	n/a	n/a	138.9	2.3	8.22	590
69.64	543	10.01	92.6	1.5	7.70	560
71.65	337	5.86	n/a	n/a	8.43	660
74.91	148	2.55	131.2	2.2	8.80	630
77.41		0.00	123.5	2.0	8.76	700
96.64	252	4.54	108.0	1.8	9.05	820
97.41	205	3.70	84.9	1.4	9.61	920

MAJOR IONS - negative results indicate analyte concentration below that in blank

Ion notation:

@ AA analysis
* ICP-MS analysis
+ HPLC analysis
corr corrected with data from USGS stds

SAMPLE MID DEPTH	Analysis Date for ICP-MS (not including Lithium)	Ca@ mg/kg	Mg@ mg/kg	Fe@ mg/kg	K@ mg/kg	Na@ mg/kg	Al@ mg/kg	Si@ mg/kg
18.77	28/2/90	32.9	2.44	0.07	2.03	71.9	0	3.9
20.19	27/9/89	41.80	2.87	n/a	1.19	43.10	0.30	4.20
20.19	27/9/89	41.90	2.85	n/a	1.13	42.80	0.00	4.40
20.19	28/2/90	40.8	2.86	0.3	1.17	43.8	0	3.5
20.19	27/9/89	41.50	2.88	n/a	1.03	45.30	0.00	4.00
56.81	28/2/90	28	2.36	0	1.69	83.1	0	2.7
56.81	28/2/90	27.7	2.33	0	1.71	84.6	0	3.1
56.81	28/2/90	27.7	2.35	0	1.69	85.3	0	3
69.64	28/2/90	29.2	2.42	0	1.7	86.1	0	3.2
69.64	28/2/90							
69.64	28/2/90	29.8	2.47	0	1.73	84.6	0	3.3
71.65	28/2/90	21.7	1.81	0	1.49	94.9	0	3.2
71.65	28/2/90	20.5	1.72	0	1.57	98.7	0	3.7
71.65	28/2/90	21.3	1.71	0	1.46	96.4	0	3
74.91	27/9/89	6.80	0.96	n/a	2.04	123.10	0.50	5.20
74.91	27/9/89	8.80	0.95	n/a	1.52	119.10	0.60	4.80
74.91	28/2/90	9	0.98	0.3	1.64	119.4	0.4	4.7
74.91	27/9/89	9.60	0.86	n/a	1.34	117.60	0.40	4.10
74.91	27/9/89	10.00	0.81	n/a	1.46	115.00	0.30	4.60
74.91	27/9/89	10.10	0.80	n/a	1.46	116.10	0.30	4.40
77.41	28/2/90	19.2	1.44	0	1.27	110.5	0	3.5
77.41	28/2/90	18.9	1.42	0	1.23	110.5	0	3.8
96.64	22/8/90	n/a	n/a	n/a	n/a	n/a	n/a	n/a
96.64	28/2/90	5.3	0.22	0	0.92	135.8	0	4.6
96.64	28/2/90	5.4	0.23	0	0.9	135.8	0	4.3
97.41	28/2/90	4.6	0.46	0.7	2.19	147.6	1.2	8.1
97.41	28/2/90	4.6	0.39	0.6	2.17	158	0.9	8.2
97.41	28/2/90	4.9	0.24	0.2	1.77	167.7	0.5	7
97.41	28/2/90	4.7	0.22	0.3	2.11	169.1	0.5	7.2

mid.	Analysis Date for ICP-MS(-dd/mm/yy	Ca@ mg/kg	Mg@ mg/kg	Fe@ mg/kg	K@ mg/kg	Na@ mg/kg	Al@ mg/kg	Si@ mg/kg
18.77	28/2/90	32.9	2.44	0.07	2.03	71.9	0	3.9
56.81	28/2/90	28	2.36	0	1.69	83.1	0	2.7
69.64	28/2/90	29.8	2.47	0	1.73	84.6	0	3.3
71.65	28/2/90	21.3	1.71	0	1.46	96.4	0	3
74.91	27/9/89	10.00	0.81	n/a	1.46	115.00	0.30	4.60
77.41	28/2/90	19.2	1.44	0	1.27	110.5	0	3.5
96.64	28/2/90	5.4	0.23	0	0.9	135.8	0	4.3
97.41	28/2/90	4.7	0.22	0.3	2.11	169.1	0.5	7.2
Dil.Sea	22/8/90				1.88053	53.2983	<krauskopf	
Norm.Sea					380	10770	<krauskopf	

SAMPLE MID DEPTH	Ba* ug/kg	La* ug/kg	Pb* ug/kg	U* ug/kg	Fe* ug/kg	Fe(corr) ug/kg	Ni* ug/kg	Cu* ug/kg
	-0.08	0.00	3.71	0.01	8.39	9.80	0.21	3.13
	-0.08	0.00	3.93	0.00	5.57	6.51	0.23	3.24
	-0.07	0.00	4.01	0.00	3.49	4.07	0.16	3.28
18.77	165.56	0.09	0.18	22.27	56.81	66.37	0.16	10.29
20.19	272.31	1.13	1.08	13.75	342.69	400.34	1.62	7.71
20.19	270.12	1.00	0.64	14.08	162.69	190.06	0.14	3.33
20.19	270.81	0.99	0.52	13.89	188.82	220.58	0.39	6.40
20.19	276.17	0.27	0.07	11.02	174.34	203.67	-0.07	0.62
56.81	74.49	0.16	0.21	35.88	-11.02	-12.88	0.10	2.86
56.81	73.25	0.22	0.38	36.54	1.19	1.39	0.23	8.68
56.81	73.21	0.19	0.19	37.72	12.85	15.01	0.19	4.79
69.64	81.45	0.29	0.18	36.95	-5.81	-6.79	0.03	3.55
69.64	79.13	0.29	0.18	35.52	24.45	28.57	-0.01	3.38
69.64	83.72	0.22	0.19	36.53	-12.48	-14.58	0.07	4.35
71.65	73.79	0.32	0.72	30.69	15.52	18.13	0.19	9.44
71.65	71.24	0.22	1.26	30.47	4.87	5.69	0.46	23.31
71.65	71.01	0.25	1.91	31.10	-9.64	-11.26	0.14	4.78
74.91	19.32	0.43	10.49	36.34	260.80	304.67	0.62	41.59
74.91	15.65	0.30	1.29	30.81	164.60	192.29	0.87	21.42
74.91	17.61	0.32	1.08	30.74	191.77	224.03	0.84	20.16
74.91	13.89	0.36	1.32	28.12	94.39	110.27	0.54	14.25
74.91	12.50	0.13	0.51	27.87	52.99	61.90	0.05	5.15
74.91	12.61	0.21	0.56	27.33	64.02	74.79	0.35	6.14
77.41	68.59	0.18	0.25	25.59	5.90	6.89	0.08	3.60
77.41	67.73	0.02	-0.02	23.52	-10.14	-11.85	-0.08	0.95
96.64	20.66	0.23	0.35	11.97	6.74	7.88	0.24	6.89
96.64	24.43	0.08	0.35	14.15	7.95	9.29	0.17	7.58
96.64	25.58	0.12	0.26	14.71	6.25	7.31	0.21	7.26
97.41	51.14	0.53	4.94	16.34	570.66	666.66	0.41	13.41
97.41	50.55	0.43	4.37	17.02	452.36	528.46	0.20	9.42
97.41	42.19	0.16	3.04	15.09	200.48	234.20	1.17	10.55
97.41	39.25	0.32	1.93	15.13	208.12	243.13	0.42	8.99

mid.	Ba* ppb	La* ppb	Pb* ppb	U* ppb	Fe* ppb	Fe(corr) ppb	Ni* ppb	Cu* ppb
	0.12	0.00	0.06	0.02	14.33		0.13	0.11
18.77	165.56	0.09	0.18	22.27	56.81	66.37	0.16	10.29
56.81	74.49	0.16	0.21	35.88	-11.02	-12.88	0.10	2.86
69.64	83.72	0.22	0.19	36.53	-12.48	-14.58	0.07	4.35
71.65	71.01	0.25	1.91	31.10	-9.64	-11.26	0.14	4.78
74.91	12.50	0.13	0.51	27.87	52.99	61.90	0.05	5.15
77.41	68.59	0.18	0.25	25.59	5.90	6.89	0.08	3.60
96.64	25.58	0.12	0.26	14.71	6.25	7.31	0.21	7.26
97.41	39.25	0.32	1.93	15.13	208.12	243.13	0.42	8.99
Dil.Sea	-0.10	0.04	0.36	0.03	23.87	27.89	1.08	1.50
Norm.Se	-21.02	8.28	72.14	6.47	4823.62	5635.07	218.24	303.71

SAMPLE MID DEPTH	Zn* ug/kg	As* ug/kg	Br* ug/kg	Rb* ug/kg	Sr* ug/kg	Mo* ug/kg	Cd* ug/kg	*I ug/kg
	3.54	-0.06	9.05	0.19	0.44	0.04	0.03	12.36
	3.78	0.04	13.42	0.19	0.45	0.07	0.04	18.76
	3.31	0.04	8.98	0.18	0.42	0.05	0.03	14.80
18.77	94.60	0.54	138.69	1.79	248.12	35.27	0.29	537.22
20.19	157.53	0.70	84.47	1.51	200.58	13.44	0.25	0.00
20.19	110.04	0.76	85.79	1.48	199.89	13.17	0.24	0.00
20.19	105.33	0.51	105.03	1.43	192.27	12.89	0.24	14.34
20.19	84.40	0.88	81.34	1.47	199.04	13.49	0.18	0.00
56.81	37.17	0.48	138.46	1.70	323.20	41.37	0.20	220.15
56.81	143.83	0.43	145.88	1.71	317.54	43.63	0.32	224.41
56.81	102.91	0.66	144.39	1.70	320.73	43.41	0.26	216.54
69.64	289.83	0.57	146.97	1.70	315.02	41.15	0.28	159.94
69.64	281.24	0.52	148.14	1.73	316.27	41.66	0.30	152.06
69.64	63.07	0.62	145.42	1.81	324.64	40.81	0.24	229.52
71.65	331.13	0.58	152.68	1.19	276.07	43.24	0.31	245.96
71.65	251.61	0.68	148.97	1.32	260.37	43.52	0.38	241.91
71.65	199.97	0.59	146.10	1.26	258.67	42.28	0.25	237.30
74.91	204.38	1.16	161.50	2.19	75.35	67.75	0.46	1510.48
74.91	114.46	1.41	151.76	1.94	104.30	62.82	0.45	857.00
74.91	115.13	1.07	176.00	2.05	108.01	61.37	0.40	388.83
74.91	93.34	1.36	148.55	1.67	124.59	61.08	0.37	873.55
74.91	89.10	1.30	145.93	1.52	138.08	61.99	0.29	1385.45
74.91	87.78	1.25	150.16	1.58	138.43	61.16	0.27	1410.49
77.41	53.32	0.72	172.47	1.07	261.80	48.54	0.23	286.49
77.41	34.31	0.75	175.76	1.04	264.34	51.33	0.23	475.93
96.64	92.14	0.87	226.11	0.88	112.01	72.10	0.38	213.98
96.64	107.03	0.62	189.85	0.64	83.77	75.12	0.29	274.01
96.64	102.46	0.79	189.67	0.64	86.70	73.64	0.31	323.20
97.41	334.87	1.69	212.47	2.74	59.13	133.33	0.51	543.57
97.41	248.63	1.90	224.55	2.51	58.20	130.02	0.43	504.55
97.41	166.67	2.23	245.40	1.81	59.71	116.97	0.53	385.67
97.41	93.79	2.26	239.42	1.74	59.31	112.47	0.42	456.92

mid.	Zn* ppb	As* ppb	Br* ppb	Rb* ppb	Sr* ppb	Mo* ppb	Cd* ppb	*I ppb
	0.28	0.09	1.21	0.01	0.00	0.02	0.05	68.34
18.77	94.60	0.54	138.69	1.79	248.12	35.27	0.29	537.22
56.81	37.17	0.48	138.46	1.70	323.20	41.37	0.20	220.15
69.64	63.07	0.62	145.42	1.81	324.64	40.81	0.24	229.52
71.65	199.97	0.59	146.10	1.26	258.67	42.28	0.25	237.30
74.91	89.10	1.30	145.93	1.52	138.08	61.99	0.29	1385.45
77.41	53.32	0.72	172.47	1.07	261.80	48.54	0.23	286.49
96.64	102.46	0.79	189.67	0.64	86.70	73.64	0.31	323.20
97.41	93.79	2.26	239.42	1.74	59.31	112.47	0.42	456.92
Dil.Sea	-0.70	0.42	331.17	0.97	38.15	0.33	-0.03	-0.09
Norm.Sea	-141.25	85.68	*******	196.82	7707.97	66.48	-5.66	-17.98

SAMPLE MID DEPTH	*Li ug/kg	B* ug/kg	Mg* ug/kg	Al* ug/kg	Si* ug/kg	P* ug/kg	S* ug/kg
		5.77	4.09	1.22	27.63	19.28	75167.64
		4.99	6.82	4.03	33.83	13.57	79172.84
		6.39	4.36	1.23	27.33	6.59	77337.25
18.77		20.71	2300.32	6.99	3432.79	-5.42	5435.92
20.19		17.66	3082.79	12.45	4173.82	19.16	5991.00
20.19		16.94	3153.01	8.56	4236.13	44.02	6083.00
20.19		15.24	2744.93	9.87	3785.87	4.87	4619.02
20.19	7.09	12.51	3121.44	2.31	4381.25	9.95	6132.00
56.81		20.69	2400.94	24.03	3121.25	3.47	5851.29
56.81		21.15	2168.33	16.99	3039.66	25.97	6377.83
56.81		22.31	2246.71	22.58	3163.04	3.95	6133.59
69.64		18.98	2602.40	9.08	3172.11	7.41	7104.02
69.64		19.02	2345.09	8.56	3158.13	3.06	7119.68
69.64	15.61	20.01	2672.18	8.07	3022.34	2.89	6689.32
71.65		25.74	1673.37	19.50	3408.11	14.01	6151.38
71.65		26.26	1630.87	25.55	3500.35	3.75	6126.76
71.65	17.23	27.01	1680.38	22.40	3491.96	15.76	5762.06
74.91		65.89	789.45	331.05	4352.06	0.00	5333.00
74.91		55.60	767.45	214.12	3759.99	0.00	4680.00
74.91		59.81	914.57	386.98	4660.33	19.88	7511.42
74.91		48.85	730.52	155.38	3861.78	0.00	5633.00
74.91	22.55	57.35	716.33	99.92	3715.05	0.00	5767.00
74.91		51.82	718.42	107.68	3706.40	0.00	5956.00
77.41		40.97	1480.18	13.53	3563.81	12.06	7335.82
77.41		41.44	1348.98	8.91	3817.27	-21.82	7134.74
96.64		105.65	254.12	22.31	4097.09	8.77	14614.19
96.64		106.10	209.64	22.85	4409.27	9.38	11797.83
96.64	31.90	117.38	234.79	23.44	4471.69	20.01	12389.43
97.41		215.46	488.01	1418.20	7996.78	18.21	28189.78
97.41		232.10	365.68	1151.64	7772.54	15.81	29694.80
97.41		252.18	214.89	584.69	6947.10	81.63	31321.39
97.41	55.56	220.09	210.08	589.76	6868.68	17.21	30581.46

mid.	*Li ppb	B* ppb	Mg* ppb	Al* ppb	Si* ppb	P* ppb	S* ppb
		6.29	0.68	1.93	20.47	117.00	2540.00
18.77		20.71	2300.32	6.99	3432.79	-5.42	5435.92
56.81		20.69	2400.94	24.03	3121.25	3.47	5851.29
69.64	15.61	20.01	2672.18	8.07	3022.34	2.89	6689.32
71.65	17.23	27.01	1680.38	22.40	3491.96	15.76	5762.06
74.91	22.55	57.35	716.33	99.92	3715.05	0.00	5767.00
77.41		40.97	1480.18	13.53	3563.81	12.06	7335.82
96.64	31.90	117.38	234.79	23.44	4471.69	20.01	12389.43
97.41	55.56	220.09	210.08	589.76	6868.68	17.21	30581.46
Dil.Sea	1.01	660.86	6460.71	16.06	81.03	12.13	9881.43
Norm.Sea	203.60	133539.07	1305516.60	3245.25	16373.74	2451.11	1996741.98

SAMPLE MID DEPTH	[SO4]* ug/kg	[SO4]corr ug/kg	[SO4]+ mg/kg	Cl+ mg/kg	Cl* ug/kg	F+ mg/kg
					93043.00	
					96380.00	
					96151.00	
18.77	16287.41	19229.52	13.25	97.17	101321.00	2.07
20.19	17950.58	21193.12			77548.00	
20.19	18226.23	21518.57			77051.00	
20.19	13839.78	16339.76			77842.00	
20.19	18373.05	21691.91	7.87	71.50	75769.00	1.28
56.81	17531.96	20698.89			101973.00	
56.81	19109.61	22561.52	20.62	94.27	105974.00	2.70
56.81	18377.82	21697.54	34.38	95.46	105251.00	2.64
69.64	21285.48	25130.44	25.28	104.17	112899.00	2.40
69.64	21332.39	25185.82			110771.00	
69.64	20042.92	23663.43	16.55	98.49	110132.00	1.75
71.65	18431.11	21760.46	23.37	107.17	112550.00	2.30
71.65	18357.35	21673.37	22.87	96.01	111322.00	2.08
71.65	17264.60	20383.24	8.91	109.23	109715.00	2.78
74.91	15979.04	18865.45			111077.00	
74.91	14022.48	16555.47			106411.00	
74.91	22506.16	26571.62			130812.00	
74.91	16877.92	19926.70			111008.00	
74.91	17279.41	20400.73	23.11	110.46	109769.00	2.62
74.91	17845.71	21069.31			109449.00	
77.41	21980.01	25950.43			131570.00	
77.41	21377.52	25239.10			130056.00	
96.64	41964.51	49544.88			154803.00	
96.64	35349.33	41734.75	27.92	131.26	143678.00	3.83
96.64	37121.93	43827.54	30.01	130.50	143485.00	4.64
97.41	84463.82	99721.16	70.86	153.53	156122.00	5.68
97.41	88973.25	105045.16	77.74	152.02	162800.00	6.74
97.41	93846.93	110799.21	104.50	169.63	177559.00	7.18
97.41	91629.91	108181.71	72.56	159.81	178183.00	6.16

mid.	[SO4]* ppb	[SO4]corr ppb	[SO4]+ ppm	Cl+ ppm	Cl* ppb	F+ ppm
	7293.59				97.76	
18.77	16287.41	19229.52	13.25	97.17	101321.00	2.07
56.81	17531.96	20698.89			101973.00	
69.64	20042.92	23663.43	16.55	98.49	110132.00	1.75
71.65	17264.60	20383.24	8.91	109.23	109715.00	2.78
74.91	17279.41	20400.73	23.11	110.46	109769.00	2.62
77.41	21980.01	25950.43			131570.00	
96.64	37121.93	43827.54	30.01	130.50	143485.00	4.64
97.41	91629.91	108181.71	72.56	159.81	178183.00	6.16
Dil.Sea	29607.30	34955.49			93037.00	
Norm.Sea	5982752.18	7063461.85	0.00	0.00	18800000.00	0.00

SAMPLE MID DEPTH	Ca* ug/kg	Ti* ug/kg	V* ug/kg	Mn* ug/kg	Br/Cl
	287.38	5.01	0.09	0.03	
	289.35	5.85	0.12	0.01	
	722.53	5.44	0.19	0.00	
18.77	31363.09	0.58	0.88	527.87	0.00137
20.19	40838.00	4.37	0.71	1214.43	0.00109
20.19	41035.00	4.26	0.66	1210.15	0.00111
20.19	39738.24	0.87	0.42	1180.29	0.00135
20.19	41734.00	4.31	0.63	1232.65	0.00107
56.81	27558.70	0.91	1.39	40.18	0.00136
56.81	26599.92	1.03	1.05	39.25	0.00138
56.81	26875.01	0.91	1.42	40.60	0.00137
69.64	29518.05	1.17	1.42	26.45	0.00130
69.64	28297.49	0.92	1.42	25.87	0.00134
69.64	29901.69	0.99	1.42	21.63	0.00132
71.65	20671.28	0.73	1.37	46.66	0.00136
71.65	19236.45	1.29	1.37	45.10	0.00134
71.65	20392.70	1.31	1.20	42.66	0.00133
74.91	6097.00	14.04	3.99	28.40	0.00145
74.91	7609.00	9.10	3.46	27.92	0.00143
74.91	8571.09	11.47	3.42	29.20	0.00135
74.91	8920.00	5.77	3.17	30.16	0.00134
74.91	9394.00	5.01	2.79	33.25	0.00133
74.91	9504.00	5.65	2.83	33.79	0.00137
77.41	19039.11	1.33	1.84	32.92	0.00131
77.41	18401.20	0.73	1.66	25.67	0.00135
96.64	6250.04	-0.45	5.29	30.66	0.00146
96.64	5171.70	1.39	1.79	14.77	0.00132
96.64	5473.40	1.52	1.67	14.44	0.00132
97.41	4415.35	21.17	7.35	35.35	0.00136
97.41	4170.72	19.26	7.44	28.68	0.00138
97.41	4624.32	10.29	6.26	14.58	0.00138
97.41	4334.02	9.95	5.39	15.78	0.00134

mid.	Ca* ppb	Ti* ppb	V* ppb	Mn* ppb	Br/Cl
	999.83	0.18	0.07	0.05	
18.77	31363.09	0.58	0.88	527.87	0.00137
56.81	27558.70	0.91	1.39	40.18	0.00136
69.64	29901.69	0.99	1.42	21.63	0.00132
71.65	20392.70	1.31	1.20	42.66	0.00133
74.91	9394.00	5.01	2.79	33.25	0.00133
77.41	19039.11	1.33	1.84	32.92	0.00131
96.64	5473.40	1.52	1.67	14.44	0.00132
97.41	4334.02	9.95	5.39	15.78	0.00134
Dil.Sea	1940.95	0.39	2.41	0.30	0.00356
Norm.Sea	392208.05	79.21	486.58	60.22	0.00356

CHARGE BALANCE

SAMPLE MID DEPTH	charge balance for: ICP %	ICP+AA %	ICP+ HPLC %	AA+HPLC %	charge sums: cations ICP-MS	cations AA	anions ICP-MS	anions HPLC
18.77	-1.773	-1.375	-1.069	-0.670	0.005	0.005	-0.005	-0.0050
20.19	-6.555	-6.597	n/a	n/a	0.004	0.004	-0.005	
20.19	-5.223	-5.712	n/a	n/a	0.004	0.004	-0.005	
20.19	-5.150	-5.063	n/a	n/a	0.004	0.004	-0.005	
20.19	-4.576	-5.609	-1.664	-3.172	0.004	0.004	-0.005	-0.0045
56.81	-2.914	-3.482	n/a	n/a	0.005	0.005	-0.006	
56.81	n/a	n/a	n/a	n/a	0.005	0.005	-0.003	-0.0032
56.81	n/a	n/a	n/a	n/a	0.005	0.005	-0.003	-0.0035
69.64	n/a	n/a	n/a	n/a	0.005	0.005	-0.004	-0.0035
69.64	n/a	n/a	n/a	n/a	0.002	n/a	-0.004	
69.64	3.525	2.554	6.677	5.940	0.005	0.005	-0.005	-0.0047
71.65	-4.569	-4.436	-5.181	-4.962	0.005	0.005	-0.006	-0.0059
71.65	n/a	n/a	n/a	n/a	0.005	0.005	-0.004	-0.0032
71.65	n/a	n/a	n/a	n/a	0.005	0.005	-0.003	-0.0034
74.91	2.652	3.120	n/a	n/a	0.006	0.006	-0.006	
74.91	3.218	4.126	n/a	n/a	0.006	0.006	-0.005	
74.91	-3.449	-3.276	n/a	n/a	0.006	0.006	-0.006	
74.91	0.212	0.725	n/a	n/a	0.006	0.006	-0.006	
74.91	-0.441	0.025	-2.862	-2.306	0.006	0.006	-0.006	-0.0058
74.91	0.037	0.495	n/a	n/a	0.006	0.006	-0.006	0
77.41	-2.424	-2.688	n/a	n/a	0.006	0.006	-0.006	0
77.41	-2.366	-2.407	n/a	n/a	0.006	0.006	-0.006	0
96.64								
96.64	-3.612	-3.342	-1.293	-1.141	0.006	0.006	-0.007	-0.0063
96.64	-2.702	-2.462	-1.153	-1.099	0.006	0.006	-0.007	-0.0063
97.41	5.881	6.263	6.347	6.521	0.007	0.007	-0.006	-0.0061
97.41	6.429	6.920	7.862	8.133	0.007	0.007	-0.006	-0.0062
97.41	4.982	5.533	2.358	2.629	0.008	0.008	-0.007	-0.0073
97.41	-3.666	-3.142	0.011	0.380	0.008	0.008	-0.008	-0.0077
	-1.022	-0.901	0.912	0.932	<<AVERAGE			
	3.785	3.998	4.101	4.094	<<STD.DEVn.			
mid.								
18.77	-1.773	-1.375	-1.069	-0.670	0.005	0.005	-0.005	-0.0050
56.81	-2.914	-3.482	n/a	n/a	0.005	0.005	-0.006	
69.64	3.525	2.554	6.677	5.940	0.005	0.005	-0.005	-0.0047
71.65	n/a	n/a	n/a	n/a	0.005	0.005	-0.003	-0.0034
74.91	-0.441	0.025	-2.862	-2.306	0.006	0.006	-0.006	-0.0058
77.41	-2.424	-2.688	n/a	n/a	0.006	0.006	-0.006	0
96.64	-2.702	-2.462	-1.153	-1.099	0.006	0.006	-0.007	-0.0063
97.41	-3.666	-3.142	0.011	0.380	0.008	0.008	-0.008	-0.0077
Dil.Sea	-1.485	-1.510	0.321	0.369	<<AVERAGE			
Norm.Se	2.250	1.991	3.308	2.913	<<STD.DEVn.			

APPENDIX D Thermodynamic Data Base Review

APPENDIX D: Thermodynamic Data Base Review

INTRODUCTION

The PHREEQE thermodynamic data base originally provided with the program[1] contains information about the composition of minerals of interest and thermodynamic constants characterizing those minerals. Any mineral composition is stored as a dissociation reaction for that mineral to part of a set of previously defined possible components; either elements or complex species. The dissociation reaction stored in the data base is a string of stoichiometric constants, each one associated with a component of the reaction. Components with positive sign appear on the right side of the dissociation reaction and negatively signed components appear on the left of the reaction, as does the mineral itself. However, the chemical composition of the mineral itself is not stored explicitly in the data base; it can only be derived by summing the stoichiometric constants multiplied by the formulae of their respective components. The dissociation reaction is balanced for both mass and charge.

The thermodynamic information for each mineral dissociation reaction is stored as two thermodynamic constants at 25°C. The thermodynamic parameters stored are the enthalpy of the dissociation reaction ($\Delta H^{\circ}_{dissoc.}$) and the log of the equilibrium constant of the dissociation reaction ($LogK_{dissoc.}$). For comparison of thermodynamic

---

[1] This version of PHREEQE was provided by Colorado State University and included a variant of the MINTEQ data base

parameters in the database, with published parameters for minerals, it is convenient to transform the database constants to thermodynamic values for the mineral only. Initially only the $LogK_{dissoc}$ values have been reviewed.

$LogK_{dissoc}$ was transposed to $\Delta G^{\circ}_{dissoc.}$ using equation (1) recast as (1a)

$$\Delta G^{\circ}_{dissoc.} = -RT\ LnK_{dissoc.} \qquad (1)$$

$$\Delta G^{\circ} = LogK/1.364 \qquad (1a)$$

A value for the Gibb's standard free energy of formation (ΔG°_{f}), for the mineral was than back calculated using equation (2).

$$\Delta G^{\circ}_{dissoc.} = \Sigma\Delta G^{\circ}_{f}(products)-\Sigma\Delta G^{\circ}_{f}(reactants) \qquad (2)$$

The only unknown in equation (2) is $\Delta G^{\circ}_{f mineral}$ and is contained in $\Sigma\Delta G^{\circ}_{f}$(reactants).

SCRUTINY OF DATABASE

Prior to scrutiny of the database attempts were made to develop mineral stability diagrams for some of the sodium minerals, using the database data. These initial attempts produced spurious results because of inconsistent thermodynamic data in the database; the pyrophyllite-Halloysite (syn kaolinite)boundary occurring at a lower concentration of H_4SiO_4 than the Gibbsite-Halloysite boundary. The problem of inconsistent thermodynamic data is discussed by Nordstrom and Munoz (1985), with the case of inconsistency in published **ΔG°**'s for pyrophyllite specifically addressed to highlight the problem.

Method of database scrutiny.

Initial speciation calculations were made for the NSCRV water analyses using PHREEQE with the original unchecked data base. From these initial runs minerals with a Log Saturation Index greater than -1 were extracted as being of possible interest, it is the thermodynamic and compositional data for these minerals which has been scrutinized.

The thermodynamic and compositional constants were entered into a Lotus work sheet and the relevant calculations performed to arrive at a ΔG°_r for each mineral. All values used for ΔG°_r for the mineral components (required for the back calculation of ΔG°_{f} from $LogK_{dissoc}$) were from Robie (1978). Published thermodynamic data was then scoured for values of ΔG°_{f} for the minerals. Where thermodynamic data was available it was entered into the worksheet. The sources of thermodynamic data used to date are Robie et al (1978), Helgeson et al (1978) and Hemingway et al (1982). Some values have also been found in Nriagu (1975). As yet, no extensive listing has been discovered of thermodynamic data for the clay minerals, some values of clays were published by Helgeson (1969). It will be shown that thermodynamic values published by Helgeson (1969) and Helgeson et al (1978) are thermodynamically consistent for the minerals of interest.

Because of the lack of thermodynamic data for clay minerals a theoretical value for ΔG°_{f} for the clay minerals was calculated. The method used to calculate mineral ΔG°_{f}'s is analogous to methods described in physical chemistry texts for calculating ΔG°_{f} of compounds, from component species and or elements. For calculation of $\Delta G^{\circ}_{f(clay)}$ the method of Nriagu (1975) was followed. Nriagu assumed that the clay was formed by combination of metal hydroxides and silicon hydroxide of known thermodynamic values as published by Nriagu (1975) and that an empirical correction term can be applied to the calculations. The calculated ΔG°_{f}'s were then compared to ΔG°_{f}'s back calculated from the database.

Overview of the thermodynamic data reviewed to date.

A few examples of thermodynamic calculations follow to show the inadvisability of mixing thermodynamic data from different workers along with problems of inconsistent data sets published by some authors:

Pyrophyllite and Halloysite.

As noted above, early attempts to compose mineral stability diagrams using the thermodynamic data, from the database, were unsatisfactory and pointed to problems with the value of LogK for pyrophyllite stored in MINTEC; Minor inconsistencies in values of LogK for minerals having common ions may lead to miscalculation of mineral stability boundaries, due to the extremely low ΔG°_r of many mineral reactions.

The ΔG°_r value for pyrophyllite originally stored in the database approximates the value published by Hemingway et al (1982). Changing the sign of the stored value for LogK, which was believed to be the problem, resulted in a back calculated value for Pyrophyllite which was close to the value published by Helgeson et al (1978). However, the value for $\Delta G^\circ_{f(pyrophyllite)}$ published by Helgeson et al (1978) is unlikely to be the required value, as none of the other thermodynamic data in the database appears to be derived from Helgeson et al (1978).

Nordstrom and Munoz (1985) state that there is a systematic error in the thermodynamic calculations of Helgeson et al (1978), first noticed by Hemingway et al (1982). The error in the data of Helgeson et al (1978) is attributed to an error in $\Delta G^{\circ}_{kaolinite}$, used as a secondary reference phase, which ties together the free energy values obtained in different sets of experiments. Table 1, below, is a synopsis of results for calculations of ΔG°_{r}, LogK and the position of mineral stability boundaries (Log[Si]) with respect to $[H_2SiO_4]$ for the reactions Gibbsite-Halloysite (4) and Halloysite-Pyrophyllite (5).

$$2Al(OH)_3 + 2H_4SiO_4 \rightarrow Al_2Si_2O_5(OH)_4 + 5H_2O \quad (4)$$

$$Al_2Si_2O_5(OH)_4 + 2H_4SiO_4 \rightarrow Al_2Si_4O_{10}(OH)_2 + 5H_2O \quad (5)$$

The values of ΔG°_{f} used for the non mineral species, involved in reactions, were taken from Robie et al(1978). The back calculated value for $\Delta G^{\circ}_{f(gibbsite)}$ from the database was used in all the calculations for Table1. $Al_2Si_2O_5(OH)_4$ is referred to as halloysite. No value for ΔG°_{f} halloysite is listed by Helgeson et al (1978) and kaolinite, of the same chemical formula, has been substituted in these calculations.

The thermodynamic data for Gibbsite/Halloysite/pyrophyllite of Hemingway et al (1982) is in error as pyrophyllite appears to precipitate at lower concentrations of

H_4SiO_4 than halloysite. These calculations highlight the problem of attempting to mix thermodynamic data form unrelated groups of workers (NOTE:Hemingway et al (1982) and Robie et al (1978) are both USGS groups and their data is generally consistent.)

Table 1. Comparison of mineral stability boundaries calculated using different thermodynamic data sources for Al2Si2O5(OH)4 and pyrophyllite. **ΔG°f(gibbsite)** is back calculated from MINTEC. These values represent a mixed thermodynamic source. Note that the Log[Si] shown for the Gibbsite-Halloysite boundary for Hlg/Hlg and Hlg/Hem data are the same as they are calculated using the same data

DATA SOURCE	Gibbsite-Halloysite			Halloysite-Pyrophyllite		
	ΔG°_r	LogK	Log[Si]	**ΔG°_r**	LogK	Log[Si]
Hem/Hlg	-11.599	8.504	-4.252	-10.617	7.784	-3.892
Hlg/Hlg	-13.682	10.0312	-5.0156	-8.5342	6.25681	-3.128
Hem/Hem	-9.5313	6.98766	-3.4939	-13.733	10.069	-5.034
Hlg/Hem	-13.682	10.0312	-5.0156	-11.650	8.54	-4.29

The above calculations are now repeated using supposedly consistent thermodynamic data, for reactions (4) and (5) for both halloysite and kaolinite. All data referred to as Hemingways is a combination of Hemingway et al (1982) and Robie et al (1978).

Table 1a Reactions (4) and (5) using kaolinite

DATA SOURCE	Gibbsite-Kaolinite			Kaolinite-Pyrophyllite		
	ΔG°_r	LogK	Log[Si]	ΔG°_r	LogK	Log[Si]
DB	-16.109	11.810	-5.905	-9.998	7.330	-3.665
Heming	-14.130	10.359	-5.179	-9.135	6.697	-3.349
Helg	-11.429	8.379	-4.190	-8.534	6.257	-3.128

Table 1b Reactions (4) and (5) using Halloysite.

DATA SOURCE	Gibbsite-Halloysite			Halloysite-Pyrophyllite		
	ΔG°_r	LogK	Log[Si]	ΔG°_r	LogK	Log[Si]
DB	-11.662	8.550	-4.275	-14.445	10.590	-5.295
Heming	-9.531	6.988	-3.494	-13.734	10.069	-5.034

N.B. **DB** indicates the database supplied with the Colorado version of PHREEQE

The data in Tables 1, 1a and 1b show the quite large differences that will arise in thermodynamic calculations when different data sets are used. The tables also point to errors in the ΔG°_f values for halloysite, published by Hemingway et al (1982) and highlight the errors that will result when incompatible data is mixed.

Calculations were also made to construct mineral stability diagrams for Log[K]/[H] vs Log[H_2SiO_4] space and the mineral assemblage gibbsite-kaolinite-muscovite-microcline-pyrophyllite, using the three data sets. The results of these calculations are shown on Figure 5.3. Only the data of Helgeson et al (1978) is entirely consistent. The thermodynamic data from Hemingway/Robie and from MINTEC is inconsistent, as revealed by the kaolinite-pyrophyllite-muscovite-microcline junctions of Figure 5.3. For the databse and Hemingway/Robie data sets it also appears that four phases may be equilibrium at one point, this contradicts the Gibb's phase rule which, for a system of three components (K^+, H^+, and $H_2SiO_4^O$) predicts that the maximum number of phases at equilibrium together (zero degrees of freedom) is 3. Figure 5.3 also reveals the large disparity in thermodynamic data generally: Water compositions plotting in the muscovite stability field defined by Helgeson et al (1982) would still be in the kaolinite stability fields defined by the other thermodynamic data sets. The mineral stability diagram derived using data from MINTEC, but with Log$\mathbf{K}_{dissoc}$ for pyrophyllite reversed, reveals little except that data which appears to be consistent on the basis of a particular component space, may not be.

Clay minerals

Table 2 shows the values for $\mathbf{\Delta G^\circ_f}$ in kcal/mol, for some clay minerals, calculated by the method outlined by Nriagu (1975), back calculated from the database, and as listed by Nriagu (1975) from other workers. All $\mathbf{\Delta G^\circ_f}$ values calculated by the Nriagu method are in good agreement with the PHREEQE database and published $\mathbf{\Delta G^\circ_f}$ values.

Table 2. $\Delta G^\circ f$ values in kcal/mol as calculated by the method of Nriagu (1975), back calculated from the PHREEQE thermodynamic data base and as listed by Nriagu (1975)

	Nriagu Calculated	PHREEQE Back Calc.	Nriagu published
NA-NONTR	-1399.84	-1399.84	
K-NONTRO	-1403.80	-1403.81	
CA-NONTR	-1065.09	-1065.45	
MG-NONTR	-1063.09	-1063.81	
MONT	-1280.83	-1279.26	-1278.80
ILLITE	-1302.05	-1301.00	-1301.00

Construction of stability diagrams.

Attempts were made to construct mineral stability diagrams, with ordinates Log[Na]/[H], Log[K]/[H], Log[Ca]/$[H]^2$ and Log[Mg]/$[H]^2$ vs Log [H_2SiO_4], using thermodynamic data from the database. The diagrams constructed were in error with some of the calculated mineral boundaries contradicting both Le Chatelier's principal and Gibb's phase rule.

As noted earlier the PHREEQE database has apparently been assembled from the Hemingway/Robie thermodynamic data set; however, the $\Delta G^\circ_{gibbsite}$ value in the database differs by approx 1kcal/mol from the Hemingway/Robie value. The value for $\Delta G^\circ_{gibbsite}$ in the database was replaced by the correct figure and halloysite struck from the data base. The mineral stability diagram constructed from these calculations for Na still contradicted Gibb's phase rule. Furthermore, the formula stored for Na-Nontronite, due to the inclusion of Fe^{3+}, precludes the Na-Nontronite stability field from intersecting Log[Na]/[H], [H_2SiO_4] space. This observation holds true for all the nontronites and the other stability spaces studied here. Except for the case of Gibbsite-Halloysite-Pyrophyllite, where the published ΔG°_{f} for halloysite is in error, it is not known if the source of the inconsistency in thermodynamic data is a result of the approximations within the database or if the Hemingway/Robie data set is truly inconsistent.

The only mineral data set which was successfully used to construct stability diagrams bearing some resemblance to those published by Nesbitt (1983) or Aagard and Helgeson (1983), was that of Helgeson et al (1978), in conjunction with the Beidellite data of Helgeson (1969). However, the thermodynamic data for K-beidellite was not consistent with the other potassium minerals and K-beidellite has been left off the Log[K]/[H] vs Log[H_2SiO_4] stability diagram. Noticeably, K-montmorillonite is also missing from the diagrams of Nesbitt (1983). As pointed out previously the Hemingway/Robie data set does appear to have some inconsistencies, despite claims to the contrary by Nordstrom and Munoz (1985).

CONCLUSIONS

If one compares the back calculated values for $\Delta G°_f$ in the PHREEQE database, with published values, it seems that the data set has, wherever possible, been assembled from the values of Robie et al (1978) with substitutions of data of from Hemingway et al (1983) where applicable.

The PHREEQE thermodynamic data cannot be corrected by substituting $\Delta G°_{f(halloysite)}$ with a value for kaolinite and correcting the value for gibbsite. Because of the inconsistency of the gibbsite-halloysite-pyrophyllite data, found in the Hemingway/Robie data set, all the thermodynamic values from Helgeson et al (1978) for the minerals falling in the spaces Log[Na]/[H], Log[K]/[H], Log[Ca]/[H]^2 and Log[Mg]/[H]^2 vs Log [H_2SiO_4] have been substituted into the database, halloysite deleted and the new data base renamed HELGTHEM.

The thermodynamic data for the Nontronite clays, whose thermodynamic source is unknown, has been deleted and replace with Na, K, Ca, Mg -Beidellites from Helgeson (1969) in the data base HELGTHEM: The data of Helgeson et al (1978) combined with that of Helgeson (1969) appears to be the most internally consistent data set available. Nordstrom and Munoz (1985), despite their criticism of the data set of Helgeson et al (1978), used the Helgeson data set to construct mineral stability diagrams in their publication as did Aagard and Helgeson (1983). Both publications appeared after the publication of the thermodynamic data of Hemingway et al (1982).

Within the PHREEQE database only halloysite has been deleted; all other thermodynamic data remain untouched. Both data sets were run for comparison.

NOTE:A third data base, Helhem.dat, is also available in which the Nontronites are replaced by Beidellites from Helgeson (1969). Any minerals with thermodynamic data published by Helgeson or Hemingway/Robie have had their thermodynamic data altered to reflect published thermodynamic values. Where one mineral has values published by both groups, the data of Helgeson is used. All changed values are annotated in the data base, see comments at the end of Helhem.dat

REFERENCES

AAGARD, P. and HELGESON, H.C. 1983. Activity/Composition relations among silicates and aqueous solutions: II. Chemical and thermodynamic consequences of ideal mixing of atoms on homological sites in montmorillonites, illites, and mixed layer clays. Clays and Clay Mins. v31 No.3 pp207-217

HELGESON, H.C. 1969. Thermodynamics of hydrothermal systems at elevated temperatures and pressures. Am.J.Sci. **v267** pp729-804.

HELGESON, H.C., DELANY, J.M. NESBITT, H.W. and BIRD, D.K. 1978. Summary and critique of the thermodynamic properties of rock forming minerals. Am.J.Sci. **v278a**

HEMINGWAY, B.S, HAAS, J.L. and ROBINSON, G.R. 1982. Thermodynamic properties of selected minerals in the system Al_2O_3-CaO-SiO_2-H_2O at 298.15 K and 1 bar (10^5 Pascals) pressure and at higher temperatures. USGS Bull. No1544 70pp

NESBITT, H.W. 1983. Equilibrium diagrams displaying chemical speciation and mineral stabilities in aqueous solutions.MAC Environmental shortcourse. **v10.** FLEET, M.E. Ed. pp1-44

NORDSTROM, D.K. and MUNOZ, J.L. 1985. Geochemical Thermodynamics. Benjamin/Cumming. pp477

NRIAGU, J.O. 1975.Thermochemical approximations for clay minerals. Am.Min. **v60** pp834-839

ROBIE, R.A. and HEMINGWAY, B.S. and FISHER, J.R. 1978. Thermodynamic properties of minerals and related substances at 298.15 K and 1 bar (10^5 Pascals) pressure and at higher temperatures. USGS Bull. No1452 456pp

APPENDIX E HELGTHEM thermodynamic Data Base Used with PHREEQE

HELGTHEM DATA BASE

```
ELEMENTS
AG      4    107.8680   AG
AL      5     26.9815   AL
AS      6    141.9431   H3ASO4
B       7     61.8331   H3BO3
BA      8    137.3400   BA
BR      9     79.9040   BR
C      10     60.0094   CO3
CA     11     40.0800   CA
CD     12    112.3994   CD
CL     13     35.4530   CL
CS     14    132.9050   CS
CU     15     63.5460   CU+2
F      16     18.9984   F
FE     17     55.8470   FE+2
I      18    126.9044   I
K      19     39.1020   K
LI     20      6.9390   LI
MG     21     24.3120   MG
MN     22     54.9380   MN+2
N      23     62.0049   NO3
NA     24     22.9898   NA
NI     25     58.7100   NI
P      26     94.9714   PO4
PB     27    207.1899   PB
RB     28     85.4699   RB
S      29     96.0616   SO4
SI     30     96.1155   H4SIO4
SR     31     87.6200   SR
U      32    270.0278   UO2+2
V      33     82.9390   VO2+1
ZN     34     65.3699   ZN
MO     35    159.9376   MOO4-2
ND     36    144.24     ND+3

SPECIES
  1
H+        100   1.000   0.000   0.000   9.000   0.000   0.000
    0.000   0.000
  1  1.000
  2
E-        100  -1.000  -1.000   0.000   0.000   0.000   0.000
    0.000   0.000
  2  1.000
  3
H2O       100   0.000   0.000   0.000   0.000   0.000   0.000
    0.000   0.000
  3  1.000
  4
AG+       100   1.000   0.000   0.000   0.000   0.000   0.000
    0.000   0.000
  4  1.000
  5
AL 3+     100   3.000   0.000   0.000   9.000   0.000   0.000
    0.000   0.000
  5  1.000
  6
H3ASO4    100   0.000   5.000   0.000   0.000   0.000   0.000
```

```
    0.000     0.000
  6  1.000
  7
H3BO3     100    0.000    0.000    0.000    0.000    0.000    0.000
    0.000     0.000
  7  1.000
  8
BA 2+     100    2.000    0.000    0.000    5.000    0.000    0.000
    0.000     0.000
  8  1.000
  9
BR-       100   -1.000    0.000    0.000    4.000    0.000    0.000
    0.000     0.000
  9  1.000
 10
CO3 2-    100   -2.000    4.000    0.000    5.400    0.000    2.000
    0.000     0.000
 10  1.000
 11
CA 2+     101    2.000    0.000    0.000    6.000    0.165    0.000
    0.000     0.000
 11  1.000
 12
CD 2+     100    2.000    0.000    0.000    0.000    0.000    0.000
    0.000     0.000
 12  1.000
 13
CL-       101   -1.000    0.000    0.000    3.000    0.015    0.000
    0.000     0.000
 13  1.000
 14
CS+       100    1.000    0.000    0.000    0.000    0.000    0.000
    0.000     0.000
 14  1.000
 15
CU 2+     100    2.000    2.000    0.000    6.000    0.000    0.000
    0.000     0.000
 15  1.000
 16
F-        100   -1.000    0.000    0.000    3.500    0.000    0.000
    0.000     0.000
 16  1.000
 17
FE 2+     100    2.000    2.000    6.000    0.000    0.000    0.000
    0.000     0.000
 17  1.000
 18
I-        100   -1.000    0.000    0.000    0.000    0.000    0.000
    0.000     0.000
 18  1.000
 19
K+        101    1.000    0.000    0.000    3.000    0.015    0.000
    0.000     0.000
 19  1.000
 20
LI+       100    1.000    0.000    0.000    6.000    0.000    0.000
    0.000     0.000
 20  1.000
```

```
21
MG 2+     101   2.000   0.000   0.000   6.500   0.200   0.000
   0.000   0.000
21  1.000
22
MN 2+     100   2.000   2.000   0.000   6.000   0.000   0.000
   0.000   0.000
22  1.000
23
NO3 -     100  -1.000   5.000   0.000   3.000   0.000   0.000
   0.000   0.000
23  1.000
24
NA+       101   1.000   0.000   0.000   4.000   0.075   0.000
   0.000   0.000
24  1.000
25
NI 2+     100   2.000   0.000   0.000   0.000   0.000   0.000
   0.000   0.000
25  1.000
26
PO4 3-    100  -3.000   0.000   0.000   5.000   0.000   2.000
   0.000   0.000
26  1.000
27
PB 2+     100   2.000   0.000   0.000   0.000   0.000   0.000
   0.000   0.000
27  1.000
28
RB+       100   1.000   0.000   0.000   0.000   0.000   0.000
   0.000   0.000
28  1.000
29
SO4 2-    101  -2.000   6.000   0.000   4.000  -0.040   0.000
   0.000   0.000
29  1.000
30
H4SIO4    100   0.000   0.000   0.000   0.000   0.000   0.000
   0.000   0.000
30  1.000
31
SR 2+     100   2.000   0.000   0.000   5.000   0.000   0.000
   0.000   0.000
31  1.000
32
UO2 2+    100   2.000   6.000   0.000   0.000   0.000   0.000
   0.000   0.000
32  1.000
33
VO2 1+    100   1.000   5.000   0.000   0.000   0.000   0.000
   0.000   0.000
33  1.000
34
ZN 2+     100   2.000   0.000   0.000   6.000   0.000   0.000
   0.000   0.000
34  1.000
35
MOO4 2-   100  -2.0     0.0     4.5                     0.0
```

0.0 0.0
35 1.0
36
ND 3+ 100 3.0 0.0 0.0 0.0
0.0 0.0
36 1.0
51
H3ASO3 400 0.000 3.000 0.000 0.000 0.000 0.000
19.444 -30.015
6 1.000 2 2.000 1 2.000 3 -1.000
52
CU+ 200 1.000 1.000 0.000 2.500 0.000 0.000
2.720 1.650
15 1.000 2 1.000
53
FE 3+ 200 3.000 3.000 9.000 0.000 0.000 0.000
-13.032 10.000
17 1.000 2 -1.000
54
MN 3+ 200 3.000 3.000 0.000 9.000 0.000 0.000
-25.507 25.760
22 1.000 2 -1.000
55
NH4 + 400 1.000 -3.000 0.000 2.500 0.000 0.000
119.077 -187.055
23 1.000 3 -3.000 1 10.000 2 8.000
56
NO2 - 400 -1.000 3.000 0.000 0.000 0.000 0.000
28.570 -43.760
23 1.000 1 2.000 2 2.000 3 -1.000
57
HS- 400 -1.000 -2.000 0.000 3.500 0.000 1.000
33.660 -60.140
29 1.000 1 9.000 2 8.000 3 -4.000
58
SO3 2- 400 -2.000 4.000 0.000 0.000 0.000 0.000
-3.650 -2.900
29 1.000 1 2.000 2 2.000 3 -1.000
59
U 3+ 400 3.000 3.000 0.000 0.000 0.000 0.000
0.420 -10.030
32 1.000 2 3.000 1 4.000 3 -2.000
60
U 4+ 400 4.000 4.000 0.000 0.000 0.000 0.000
9.216 -34.430
32 1.000 2 2.000 1 4.000 3 -2.000
61
UO2 + 200 1.000 5.000 0.000 0.000 0.000 0.000
2.785 -3.300
32 1.000 2 1.000
62

V 2+ 400 2.000 2.000 0.000 0.000 0.000 0.000
18.380 -35.330
33 1.000 2 3.000 1 4.000 3 -2.000
63
V 3+ 400 3.000 3.000 0.000 0.000 0.000 0.000
22.610 -44.230
33 1.000 2 2.000 1 4.000 3 -2.000
64
VO 2+ 400 2.000 4.000 0.000 0.000 0.000 0.000
16.930 -29.320
33 1.000 2 1.000 1 2.000 3 -1.000
65
OH- 200 -1.000 0.000 0.000 3.500 0.000 1.000
-13.998 13.345
3 1.000 1 -1.000
66
H3SIO4 - 210 -1.000 0.000 0.000 4.000 0.000 1.000
-9.930 8.935 6.368 -0.016346 -3405.9
30 1.000 1 -1.000
67
H2SIO4-- 210 -2.000 0.000 0.000 5.400 0.000 2.000
-21.619 29.714 39.478 -0.065927 -12355.1
30 1.000 1 -2.000
68
SIF6 2- 400 -2.000 0.000 0.000 5.000 0.000 0.000
30.180 -16.260
30 1.000 16 6.000 1 4.000 3 -4.000
69
H2BO3 - 200 -1.000 0.000 0.000 2.500 0.000 1.000
-9.240 3.224
7 1.000 1 -1.000
70
BF(OH)3- 200 -1.000 0.000 0.000 2.500 0.000 0.000
-0.399 1.850
7 1.000 16 1.000
71
BF2(OH)2 400 -1.000 0.000 0.000 2.500 0.000 0.000
7.630 1.635
7 1.000 16 2.000 3 -1.000 1 1.000
72
BF3OH - 400 -1.000 0.000 0.000 2.500 0.000 0.000
13.667 -1.580
7 1.000 16 3.000 3 -2.000 1 2.000
73
BF4 - 400 -1.000 0.000 0.000 2.500 0.000 0.000
20.274 -1.795
7 1.000 16 4.000 3 -3.000 1 3.000
74
NH3 AQ 410 0.000 -3.000 0.000 0.000 0.000 0.000
109.825 -174.575 0.6322 -0.001225 -2835.76
1 9.000 23 1.000 3 -3.000 2 8.000
75
NH4SO4 - 500 -1.000 3.000 0.000 5.000 0.000 0.000
120.187 -187.055
29 1.000 23 1.000 3 -3.000 1 10.000 2 8.000
76
MGOH + 310 1.000 0.000 0.000 6.500 0.000 0.000
-11.790 15.935 -3.53 0.00513 -2917.1

21 1.000 3 1.000 1 -1.000
77
MGF + 200 1.000 0.000 0.000 4.500 0.000 0.000
1.820 4.674
21 1.000 16 1.000
78
MGCO3 AQ 210 0.000 4.000 0.000 0.000 0.600 2.000
2.980 2.022 0.991 0.00667
21 1.000 10 1.000
79
MGHCO3 + 310 1.000 4.000 0.000 4.000 0.000 1.000
11.400 -2.430 -4.179 0.012734 2902.39 2.29812E-05
21 1.000 10 1.000 1 1.000
80
MGSO4 AQ 200 0.000 6.000 0.000 0.000 0.000 0.000
2.250 1.399
21 1.000 29 1.000
81
MGPO4 - 200 -1.000 0.000 0.000 5.400 0.000 0.000
6.589 3.100
21 1.000 26 1.000
82
MGH2PO4 300 1.000 0.000 0.000 5.400 0.000 0.000
21.066 -1.120
21 1.000 26 1.000 1 2.000
83
MGHPO4 A 300 0.000 0.000 0.000 0.000 0.000 0.000
15.220 -0.230
21 1.000 26 1.000 1 1.000
84
CAOH + 300 1.000 0.000 0.000 6.000 0.000 0.000
-12.598 14.535
11 1.000 3 1.000 1 -1.000
85
CAHCO3 + 310 1.000 4.000 0.000 6.000 0.000 1.000
11.330 1.790 -9.448 0.03709 2902.39
11 1.000 10 1.000 1 1.000
86
CACO3 AQ 210 0.000 4.000 0.000 0.000 0.000 2.000
3.150 4.030 -27.393 0.05617 4114.0
11 1.000 10 1.000
87
CASO4 AQ 200 0.000 6.000 0.000 0.000 0.000 0.000
2.309 1.470
11 1.000 29 1.000
88
CAHPO4 A 300 0.000 0.000 0.000 0.000 0.000 0.000
15.085 -0.230
11 1.000 26 1.000 1 1.000
89
CAPO4 - 200 -1.000 0.000 0.000 5.400 0.000 0.000
6.459 3.100
11 1.000 26 1.000
90
CAH2PO4 300 1.000 0.000 0.000 5.400 0.000 0.000
20.960 -1.120
11 1.000 26 1.000 1 2.000
91

CAF + 200 1.000 0.000 0.000 5.000 0.000 0.000
0.940 3.798
11 1.000 16 1.000
92
NACO3 - 200 -1.000 4.000 0.000 5.400 0.000 2.000
1.268 8.911
24 1.000 10 1.000
93
NAHCO3 A 300 0.000 4.000 0.000 0.000 0.000 1.000
10.080 0.000
24 1.000 10 1.000 1 1.000
94
NASO4 - 200 -1.000 6.000 0.000 5.400 0.000 0.000
0.700 1.120
24 1.000 29 1.000
95
NAHPO4 - 300 -1.000 5.000 0.000 5.400 0.000 0.000
12.636 0.000
24 1.000 26 1.000 1 1.000
96
NAF AQ 200 0.000 0.000 0.000 0.000 0.000 0.000
-0.790 0.000
24 1.000 16 1.000
97
KSO4 - 210 -1.000 6.000 0.000 5.400 0.000 0.000
0.850 2.250 3.106 0.0 -673.6
19 1.000 29 1.000
98
KHPO4 - 300 -1.000 0.000 0.000 5.400 0.000 0.000
12.640 0.000
19 1.000 26 1.000 1 1.000
99
ALOH 2+ 300 2.000 0.000 0.000 5.400 0.000 0.000
-4.990 11.899
5 1.000 3 1.000 1 -1.000
100
AL(OH)2+ 300 1.000 0.000 0.000 5.400 0.000 0.000
-10.100 0.000
5 1.000 3 2.000 1 -2.000
101
AL(OH)4- 300 -1.000 0.000 0.000 4.500 0.000 1.000
-23.000 44.060
5 1.000 3 4.000 1 -4.000
102
ALF 2+ 200 2.000 0.000 0.000 5.400 0.000 0.000
7.010 0.000
5 1.000 16 1.000
103
ALF2 + 200 1.000 0.000 0.000 5.400 0.000 0.000
12.750 20.000
5 1.000 16 2.000
104
ALF3 AQ 200 0.000 0.000 0.000 0.000 0.000 0.000
17.020 2.500
5 1.000 16 3.000
105
ALF4 - 200 -1.000 0.000 0.000 4.500 0.000 0.000
19.720 0.000

```
 5  1.000 16  4.000
106
ALSO4 +     200    1.000    6.000    0.000    4.500    0.000    0.000
    3.020     2.150
 5  1.000 29  1.000
107
AL(SO4)2    200   -1.000   12.000    0.000    4.500    0.000    0.000
    4.920     2.840
 5  1.000 29  2.000
108
AL(OH)3     300    0.000    0.000    0.000    0.000    0.000    0.000
  -16.000     0.000
 5  1.000  3  3.000  1 -3.000
109
FEOH +      300    1.000    2.000    0.000    0.000    0.000    1.000
   -9.500    13.199
17  1.000  3  1.000  1 -1.000
110
FEOH3 -1    300   -1.000    2.000    0.000    0.000    0.000    3.000
  -31.000    30.300
17  1.000  3  3.000  1 -3.000
111
FESO4 AQ    200    0.000    8.000    0.000    0.000    0.000    0.000
    2.250     3.230
17  1.000 29  1.000
112
FEH2PO4     300    1.000    2.000    0.000    0.000    0.000    0.000
   22.253    -4.520
17  1.000 26  1.000  1  2.000
113
FEOH2 AQ    300    0.000    2.000    0.000    0.000    0.000    0.000
  -20.570    28.565
17  1.000  3  2.000  1 -2.000
114
FEHPO4 A    300    0.000    2.000    0.000    0.000    0.000    1.000
   15.946    -3.530
17  1.000 26  1.000  1  1.000
115
FE(HS)2     500    0.000   -2.000    0.000    0.000    0.000    2.000
   76.270  -120.280
17  1.000 29  2.000  1 18.000  2 16.000  3 -8.000
116
FE(HS)3     500   -1.000   -4.000    0.000    0.000    0.000    3.000
  111.937  -180.420
17  1.000 29  3.000  1 27.000  2 24.000  3-12.000
117
FEOH 2+     400    2.000    3.000    0.000    0.000    0.000    0.000
  -15.222    20.399
 3  1.000  1 -1.000 17  1.000  2 -1.000
118
FEHPO4 +    400    1.000    3.000    0.000    0.000    0.000    0.000
    4.748    12.230
26  1.000  1  1.000 17  1.000  2 -1.000
119
FESO4 +     300    1.000    9.000    0.000    0.000    0.000    0.000
   -9.112    13.910
29  1.000 17  1.000  2 -1.000
120
```

```
FECL 2+      300     2.000     3.000     0.000     5.000     0.000     0.000
   -11.552     15.600
  13  1.000 17  1.000  2 -1.000
121
FECL2 +      300     1.000     3.000     0.000     0.000     0.000     0.000
   -10.902     10.000
  13  2.000 17  1.000  2 -1.000
122
FECL3 AQ     300     0.000     3.000     0.000     0.000     0.000     0.000
   -11.902     10.000
  13  3.000 17  1.000  2 -1.000
123
FEOH2 +      400     1.000     3.000     0.000     0.000     0.000     0.000
   -18.702     26.900
   3  2.000  1 -2.000 17  1.000  2 -1.000
124
FEOH3 AQ     400     0.000     3.000     0.000     0.000     0.000     1.000
   -26.632     37.000
   3  3.000  1 -3.000 17  1.000  2 -1.000
125
FEOH4 -      400    -1.000     3.000     0.000     0.000     0.000     2.000
   -34.632     42.500
   3  4.000  1 -4.000 17  1.000  2 -1.000
126
FEH2PO4      400     2.000     3.000     0.000     5.400     0.000     0.000
    11.948      5.480
  26  1.000  1  2.000 17  1.000  2 -1.000
127
FEF 2+       300     2.000     3.000     0.000     0.000     0.000     0.000
    -6.833     12.699
  16  1.000 17  1.000  2 -1.000
128
FEF2 +       300     1.000     3.000     0.000     0.000     0.000     0.000
    -2.232     14.800
  16  2.000 17  1.000  2 -1.000
129
FEF3 AQ      300     0.000     3.000     0.000     0.000     0.000     0.000
     0.968     15.399
  16  3.000 17  1 000  2 -1.000
130
FE(SO4)2     300    -1.000    15.000     0.000     0.000     0.000     0.000
    -7.612     14.600
  29  2.000 17  1.000  2 -1.000
131
FE2(OH)2     400     4.000     6.000     0.000     0.000     0.000     0.000
   -29.014     33.500
   3  2.000  1 -2.000 17  2.000  2 -2.000
132
FE3(OH)4     400     5.000     9.000     0.000     0.000     0.000     0.000
   -45.396     44.300
   3  4.000  1 -4.000 17  3.000  2 -3.000
133
LISO4 -      200    -1.000     6.000     0.000     5.000     0.000     0.000
     0.640      0.000
  20  1.000 29  1.000
134
SROH +       300     1.000     0.000     0.000     5.000     0.000     0.000
   -13.178     14.495
```

31 1.000 3 1.000 1 -1.000
135
BAOH + 300 1.000 0.000 0.000 5.000 0.000 0.000
-13.358 15.095
8 1.000 3 1.000 1 -1.000
136
MNCL + 200 1.000 2.000 0.000 5.000 0.000 0.000
0.607 0.000
22 1.000 13 1.000
137
MNCL2 AQ 200 0.000 2.000 0.000 0.000 0.000 0.000
0.041 0.000
22 1.000 13 2.000
138
MNCL3 - 200 -1.000 2.000 0.000 5.000 0.000 0.000
-0.305 0.000
22 1.000 13 3.000
139
MNOH + 300 1.000 2.000 0.000 5.000 0.000 0.000
-10.590 14.399
22 1.000 3 1.000 1 -1.000
140
MN(OH)3 300 -1.000 2.000 0.000 5.000 0.000 0.000
-34.800 0.000
22 1.000 3 3.000 1 -3.000
141
MNF + 200 1.000 2.000 0.000 5.000 0.000 0.000
0.850 0.000
22 1.000 16 1.000
142
MNSO4 AQ 200 0.000 8.000 0.000 0.000 0.000 0.000
2.260 2.170
22 1.000 29 1.000
143
MN(NO3)2 200 0.000 12.000 0.000 0.000 0.000 0.000
0.600 -0.396
22 1.000 23 2.000
144
MNHCO3 + 300 1.000 6.000 0.000 5.000 0.000 1.000
11.600 0.000
22 1.000 10 1.000 1 1.000
145
CUCL2 - 300 -1.000 1.000 0.000 4.000 0.000 0.000
8.220 1.230
13 2.000 15 1.000 2 1.000
146
CUCL3 2- 300 -2.000 1.000 0.000 5.000 0.000 0.000
8.420 1.910
13 3.000 15 1.000 2 1.000
147
CUCO3 AQ 200 0.000 6.000 0.000 0.000 0.000 2.000
6.730 0.000
15 1.000 10 1.000
148
CU(CO3)2 200 -2.000 10.000 0.000 0.000 0.000 4.000
9.830 0.000
15 1.000 10 2.000
149

```
CUCL +      200   1.000   2.000   0.000   4.000   0.000   0.000
   0.430    8.650
 15  1.000 13  1.000
150
CUCL2 AQ    200   0.000   2.000   0.000   0.000   0.000   0.000
   0.160   10.560
 15  1.000 13  2.000
151
CUCL3 -     200  -1.000   2.000   0.000   4.000   0.000   0.000
  -2.290   13.690
 15  1.000 13  3.000
152
CUCL4 2-    200  -2.000   2.000   0.000   5.000   0.000   0.000
  -4.590   17.780
 15  1.000 13  4.000
153
CUF +       200   1.000   2.000   0.000   0.000   0.000   0.000
   1.260    1.620
 15  1.000 16  1.000
154
CUOH +      300   1.000   2.000   0.000   4.000   0.000   0.000
  -8.000    0.000
 15  1.000  3  1.000  1 -1.000
155
CU(OH)2     300   0.000   2.000   0.000   0.000   0.000   0.000
 -13.680    0.000
 15  1.000  3  2.000  1 -2.000
156
CU(OH)3     300  -1.000   2.000   0.000   0.000   0.000   0.000
 -26.899    0.000
 15  1.000  3  3.000  1 -3.000
157
CU(OH)4     300  -2.000   2.000   0.000   0.000   0.000   0.000
 -39.600    0.000
 15  1.000  3  4.000  1 -4.000
158
CU2(OH)2    310   2.000   4.000   0.000   0.000   0.000   0.000   C
 -10.359   17.539    2.497    0.0    -3833.0
 15  2.000  3  2.000  1 -2.000
159
CUSO4 AQ    200   0.000   8.000   0.000   0.000   0.000   0.000
   2.310    1.220
 15  1.000 29  1.000
160
CU(HS)3     500  -1.000  -4.000   0.000   0.000   0.000   0.000
 126.879 -180.420
 15  1.000 29  3.000  1 27.000  2 24.000  3-12.000
161
CUHCO3 +    300   1.000   6.000   0.000   0.000   0.000   1.000
  13.000    0.000
 15  1.000 10  1.000  1  1.000
162
ZNCL +      200   1.000   0.000   0.000   4.000   0.000   0.000
   0.430    7.790
 34  1.000 13  1.000
163
ZNCL2 AQ    200   0.000   0.000   0.000   0.000   0.000   0.000
   0.450    8.500
```

```
 34  1.000 13  2.000
164
ZNCL3 -      200   -1.000    0.000    0.000    4.000    0.000    0.000
    0.500     9.560
 34  1.000 13  3.000
165
ZNCL4 2-     200   -2.000    0.000    0.000    5.000    0.000    0.000
    0.199    10.960
 34  1.000 13  4.000
166
ZNF +        200    1.000    0.000    0.000    0.000    0.000    0.000
    1.150     2.220
 34  1.000 16  1.000
167
ZNOH +       300    1.000    0.000    0.000    0.000    0.000    0.000
   -8.980    13.399
 34  1.000  3  1.000  1 -1.000
168
ZN(OH)2      300    0.000    0.000    0.000    0.000    0.000    0.000
  -16.899    20.800
 34  1.000  3  2.000  1 -2.000
169
ZN(OH)3      300   -1.000    0.000    0.000    0.000    0.000    0.000
  -28.399    29.300
 34  1.000  3  3.000  1 -3.000
170
ZN(OH)4      300   -2.000    0.000    0.000    0.000    0.000    0.000
  -41.199    43.700
 34  1.000  3  4.000  1 -4.000
171
ZNOHCL A     400    0.000    0.000    0.000    0.000    0.000    0.000
   -7.480     0.000
 34  1.000  3  1.000  1 -1.000 13  1.000
172
ZN(HS)2      500    0.000   -4.000    0.000    0.000    0.000    0.000
   82.260  -120.280
 34  1.000 29  2.000  1 18.000  2 16.000  3 -8.000
173
ZN(HS)3      500   -1.000   -6.000    0.000    0.000    0.000    0.000
  117.080  -180.420
 34  1.000 29  3.000  1 27.000  2 24.000  3-12.000
174
ZNSO4 AQ     200    0.000    6.000    0.000    0.000    0.000    0.000
    2.370     1.360
 34  1.000 29  1.000
175
ZN(SO4)2     200   -2.000   12.000    0.000    0.000    0.000    0.000
    3.280     0.000
 34  1.000 29  2.000
176
ZNBR +       200    1.000    0.000    0.000    0.000    0.000    0.000
   -0.580     0.000
 34  1.000  9  1.000
177
ZNBR2 AQ     200    0.000    0.000    0.000    0.000    0.000    0.000
   -0.980     0.000
 34  1.000  9  2.000
178
```

```
ZNI +       200    1.000    0.000    0.000    0.000    0.000    0.000
   -2.910    0.000
 34  1.000 18  1.000
179
ZNI2 AQ     200    0.000    0.000    0.000    0.000    0.000    0.000
   -1.690    0.000
 34  1.000 18  2.000
180
ZNHCO3 +    300    1.000    0.000    0.000    0.000    0.000    0.000
    2.100    0.000
 34  1.000 10  1.000  1  1.000
181
ZNCO3 AQ    200    0.000    0.000    0.000    0.000    0.000    0.000
    5.300    0.000
 34  1.000 10  1.000
182
ZN(CO3)2    200   -2.000    0.000    0.000    0.000    0.000    0.000
    9.630    0.000
 34  1.000 10  2.000
183
CDCL +      200    1.000    0.000    0.000    0.000    0.000    0.000
    1.980    0.590
 12  1.000 13  1.000
184
CDCL2 AQ    200    0.000    0.000    0.000    0.000    0.000    0.000
    2.600    1.240
 12  1.000 13  2.000
185
CDCL3 -     200   -1.000    0.000    0.000    0.000    0.000    0.000
    2.399    3.900
 12  1.000 13  3.000
186
CDF +       200    1.000    0.000    0.000    0.000    0.000    0.000
    1.100    0.000
 12  1.000 16  1.000
187
CDF2 AQ     200    0.000    0.000    0.000    0.000    0.000    0.000
    1.500    0.000
 12  1.000 16  2.000
188
CD(CO3)3    200   -4.000   12.000    0.000    0.000    0.000    6.000
    6.220    0.000
 12  1.000 10  3.000
189
CDOH +      300    1.000    0.000    0.000    0.000    0.000    0.000
  -10.080   13.100
 12  1.000  3  1.000  1 -1.000
190
CD(OH)2     300    0.000    0.000    0.000    0.000    0.000    0.000
  -20.350    0.000
 12  1.000  3  2.000  1 -2.000
191
CD(OH)3     300   -1.000    0.000    0.000    0.000    0.000    0.000
  -33.300    0.000
 12  1.000  3  3.000  1 -3.000
192
CD(OH)4     300   -2.000    0.000    0.000    0.000    0.000    0.000
  -47.350    0.000
```

12 1.000 3 4.000 1 -4.000
193
CD2OH +3 300 3.000 0.000 0.000 0.000 0.000 0.000
-9.390 10.899
12 2.000 3 1.000 1 -1.000
194
CDOHCL A 400 0.000 0.000 0.000 0.000 0.000 0.000
-7.404 4.355
12 1.000 3 1.000 1 -1.000 13 1.000
195
CDNO3 + 200 1.000 5.000 0.000 0.000 0.000 0.000
0.399 -5.200
12 1.000 23 1.000
196
CDSO4 AQ 200 0.000 6.000 0.000 0.000 0.000 0.000
2.460 1.080
12 1.000 29 1.000
197
CDHS + 500 1.000 -2.000 0.000 0.000 0.000 0.000
43.830 -60.140
12 1.000 29 1.000 1 9.000 2 8.000 3 -4.000
198
CD(HS)2 500 0.000 -4.000 0.000 0.000 0.000 0.000
83.850 -120.280
12 1.000 29 2.000 1 18.000 2 16.000 3 -8.000
199
CD(HS)3 500 -1.000 -6.000 0.000 0.000 0.000 0.000
119.690 -180.420
12 1.000 29 3.000 1 27.000 2 24.000 3-12.000
200
CD(HS)4 500 -2.000 -8.000 0.000 0.000 0.000 0.000
155.540 -240.560
12 1.000 29 4.000 1 36.000 2 32.000 3-16.000
201
CDBR + 200 1.000 0.000 0.000 0.000 0.000 0.000
2.170 -0.810
12 1.000 9 1.000
202
CDBR2 AQ 200 0.000 0.000 0.000 0.000 0.000 0.000
2.899 0.000
12 1.000 9 2.000
203
CDI + 200 1.000 0.000 0.000 0.000 0.000 0.000
2.150 -2.370
12 1.000 18 1.000
204
CDI2 AQ 200 0.000 0.000 0.000 0.000 0.000 0.000
3.590 0.000
12 1.000 18 2.000
205
CDHCO3 + 300 1.000 4.000 0.000 0.000 0.000 1.000
12.400 0.000
12 1.000 10 1.000 1 1.000
206
CDCO3 AQ 200 0.000 4.000 0.000 0.000 0.000 2.000
5.399 0.000
12 1.000 10 1.000
207

```
CD(SO4)2    200   -2.000   12.000    0.000    6.000    0.000    0.000
    3.500    0.000
 12  1.000 29  2.000
208
PBCL +      200    1.000    0.000    0.000    0.000    0.000    0.000
    1.600    4.380
 27  1.000 13  1.000
209
PBCL2 AQ    200    0.000    0.000    0.000    0.000    0.000    0.000
    1.800    1.080
 27  1.000 13  2.000
210
PBCL3 -     200   -1.000    0.000    0.000    0.000    0.000    0.000
    1.699    2.170
 27  1.000 13  3.000
211
PBCL4 2-    200   -2.000    0.000    0.000    0.000    0.000    0.000
    1.380    3.530
 27  1.000 13  4.000
212
PB(CO3)2    200   -2.000    8.000    0.000    0.000    0.000   -4.000
   10.640    0.000
 27  1.000 10  2.000
213
PBF +       200    1.000    0.000    0.000    0.000    0.000    0.000
    1.250    0.000
 27  1.000 16  1.000
214
PBF2 AQ     200    0.000    0.000    0.000    0.000    0.000    0.000
    2.560    0.000
 27  1.000 16  2.000
215
PBF3 -      200   -1.000    0.000    0.000    0.000    0.000    0.000
    3.420    0.000
 27  1.000 16  3.000
216
PBF4 2-     200   -2.000    0.000    0.000    0.000    0.000    0.000
    3.100    0.000
 27  1.000 16  4.000
217
PBOH +      300    1.000    0.000    0.000    0.000    0.000    0.000
   -7.710    0.000
 27  1.000  3  1.000  1 -1.000
218
PB(OH)2     300    0.000    0.000    0.000    0.000    0.000    0.000
  -17.120    0.000
 27  1.000  3  2.000  1 -2.000
219
PB(OH)3     300   -1.000    0.000    0.000    0.000    0.000    0.000
  -28.060    0.000
 27  1.000  3  3.000  1 -3.000
220
PB2OH +3    300    3.000    0.000    0.000    0.000    0.000    0.000
   -6.360    0.000
 27  2.000  3  1.000  1 -1.000
221
PBNO3 +     200    1.000    5.000    0.000    0.000    0.000    0.000
    1.170    0.000
```

```
27 1.000 23 1.000
222
PBSO4 AQ    200    0.000    6.000    0.000    0.000    0.000    0.000
   2.750    0.000
27 1.000 29 1.000
223
PB(HS)2    500    0.000   -4.000    0.000    0.000    0.000    0.000
  82.590  -120.280
27 1.000 29 2.000  1 18.000  2 16.000  3 -8.000
224
PB(HS)3    500   -1.000   -6.000    0.000    0.000    0.000    0.000
 117.550  -180.420
27 1.000 29 3.000  1 27.000  2 24.000  3-12.000
225
PB3(OH)4    300    2.000    0.000    0.000    0.000    0.000    0.000
 -23.880   26.500
27 3.000  3 4.000  1 -4.000
226
PBBR +    200    1.000    0.000    0.000    0.000    0.000    0.000
   1.770    2.880
27 1.000  9 1.000
227
PBBR2 AQ    200    0.000    0.000    0.000    0.000    0.000    0.000
   1.440    0.000
27 1.000  9 2.000
228
PBI +    200    1.000    0.000    0.000    0.000    0.000    0.000
   1.940    0.000
27 1.000 18 1.000
229
PBI2 AQ    200    0.000    0.000    0.000    0.000    0.000    0.000
   3.199    0.000
27 1.000 18 2.000
230
PBCO3 AQ    200    0.000    4.000    0.000    0.000    0.000    2.000
   7.240    0.000
27 1.000 10 1.000
231
PB(OH)4    300   -2.000    0.000    0.000    0.000    0.000    0.000
 -39.699    0.000
27 1.000  3 4.000  1 -4.000
232
PB(SO4)2    200   -2.000   12.000    0.000    0.000    0.000    0.000
   3.470    0.000
27 1.000 29 2.000
233
PBHCO3 +    300    1.000   -4.000    0.000    0.000    0.000    1.000
  13.200    0.000
27 1.000 10 1.000  1 1.000
234
NIBR +    200    1.000    0.000    0.000    0.000    0.000    0.000
   0.500    0.000
25 1.000  9 1.000
235
NICL +    200    1.000    0.000    0.000    0.000    0.000    0.000
   0.399    0.000
25 1.000 13 1.000
236
```

```
NIF +      200   1.000   0.000   0.000   0.000   0.000   0.000
    1.300    0.000
 25  1.000 16  1.000
237
NIOH +     300   1.000   0.000   0.000   0.000   0.000   0.000
   -9.860   12.420
 25  1.000  3  1.000  1 -1.000
238
NI(OH)2    300   0.000   0.000   0.000   0.000   0.000   0.000
  -19.000    0.000
 25  1.000  3  2.000  1 -2.000
239
NI(OH)3    300  -1.000   0.000   0.000   0.000   0.000   0.000
  -30.000    0.000
 25  1.000  3  3.000  1 -3.000
240
NISO4 AQ   200   0.000   6.000   0.000   0.000   0.000   0.000
    2.290    1.520
 25  1.000 29  1.000
241
NICL2 AQ   200   0.000   0.000   0.000   0.000   0.000   0.000
    0.960    0.000
 25  1.000 13  2.000
242
NIHCO3 +   300   1.000   4.000   0.000   0.000   0.000   1.000
   12.470    0.000
 25  1.000 10  1.000  1  1.000
243
NICO3 AQ   200   0.000   4.000   0.000   0.000   0.000   2.000
    6.870    0.000
 25  1.000 10  1.000
244
NI(CO3)2   200  -2.000   8.000   0.000   0.000   0.000   4.000
   10.110    0.000
 25  1.000 10  2.000
245
NI(SO4)2   200  -2.000  12.000   0.000   0.000   0.000   0.000
    1.020    0.000
 25  1.000 29  2.000
246
AGBR AQ    200   0.000   0.000   0.000   0.000   0.000   0.000
    4.240    0.000
  4  1.000  9  1.000
247
AGBR2 -    200  -1.000   0.000   0.000   0.000   0.000   0.000
    7.280    0.000
  4  1.000  9  2.000
248
AGCL AQ    200   0.000   0.000   0.000   0.000   0.000   0.000
    3.270   -2.680
  4  1.000 13  1.000
249
AGCL2 -    200  -1.000   0.000   0.000   0.000   0.000   0.000
    5.270   -3.930
  4  1.000 13  2.000
250
AGCL3 2-   200  -2.000   0.000   0.000   0.000   0.000   0.000
    5.290    0.000
```

4 1.000 13 3.000
251
AGCL4 -3 200 -3.000 0.000 0.000 0.000 0.000 0.000
5.510 0.000
4 1.000 13 4.000
252
AGF AQ 200 0.000 0.000 0.000 0.000 0.000 0.000
0.360 -2.830
4 1.000 16 1.000
253
AGHS AQ 500 0.000 -2.000 0.000 0.000 0.000 0.000
47.710 -60.140
4 1.000 29 1.000 1 9.000 2 8.000 3 -4.000
254
AG(HS)2 500 -1.000 -4.000 0.000 0.000 0.000 0.000
85.770 -120.280
4 1.000 29 2.000 1 18.000 2 16.000 3 -8.000
255
AGI AQ 200 0.000 0.000 0.000 0.000 0.000 0.000
6.600 0.000
4 1.000 18 1.000
256
AGI2 - 200 -1.000 0.000 0.000 0.000 0.000 0.000
10.680 0.000
4 1.000 18 2.000
257
AGOH AQ 300 0.000 0.000 0.000 0.000 0.000 0.000
-12.000 0.000
4 1.000 3 1.000 1 -1.000
258
AG(OH)2 300 -1.000 0.000 0.000 0.000 0.000 0.000
-24.000 0.000
4 1.000 3 2.000 1 -2.000
259
AGSO4 - 200 -1.000 6.000 0.000 0.000 0.000 0.000
1.290 1.490
4 1.000 29 1.000
260
AGNO3 AQ 200 0.000 5.000 0.000 0.000 0.000 0.000
-0.290 0.000
4 1.000 23 1.000
261
AG(NO2)2 500 -1.000 6.000 0.000 0.000 0.000 0.000
59.360 -87.520
4 1.000 23 2.000 1 4.000 2 4.000 3 -2.000
262
AGBR3 2- 200 -2.000 0.000 0.000 0.000 0.000 0.000
8.710 0.000
4 1.000 9 3.000
263
AGI3 2- 200 -2.000 0.000 0.000 0.000 0.000 0.000
13.370 -27.030
4 1.000 18 3.000
264
AGI4 -3 200 -3.000 0.000 0.000 0.000 0.000 0.000
14.080 0.000
4 1.000 18 4.000
265

```
H2ASO3 -    400   -1.000    3.000   0.000    0.000    0.000    0.000
   10.216   -23.455
 1  1.000  6  1.000  2  2.000  3 -1.000
266
HASO3 2-    300   -2.000    3.000   0.000    0.000    0.000    0.000
   -1.886   -15.816
 6  1.000  2  2.000  3 -1.000
267
ASO3 -3     400   -3.000    3.000   0.000    0.000    0.000    0.000
  -15.300    -9.765
 1 -1.000  6  1.000  2  2.000  3 -1.000
268
H4ASO3 +    400    1.000    3.000   0.000    0.000    0.000    0.000
   19.139   -30.015
 1  3.000  6  1.000  2  2.000  3 -1.000
269
H2ASO4 -    200   -1.000    5.000   0.000    0.000    0.000    0.000
   -2.243    -1.690
 6  1.000  1 -1.000
270
HASO4 2-    200   -2.000    5.000   0.000    0.000    0.000    0.000
   -9.001    -0.920
 6  1.000  1 -2.000
271
ASO4 -3     200   -3.000    5.000   0.000    0.000    0.000    0.000
  -20.597     3.430
 6  1.000  1 -3.000
272
HCO3 -      210   -1.000    4.000   0.000    5.400    0.000    1.000
   10.330    -3.617    -6.498   0.02379    2902.39
 10  1.000  1  1.000
273
H2CO3 AQ    210    0.000    4.000   0.000    0.000    0.000    0.000
   16.681    -2.247   -21.3415   0.05657    6307.1
 10  1.000  1  2.000
274
HSO4 -      210   -1.000    6.000   0.000    4.500    0.000    0.000
    1.987     4.910   -5.3505  0.0183412   557.2461
 29  1.000  1  1.000
275
HF AQ       200    0.000    0.000   0.000    0.000    0.000    0.000
    3.169     3.460
 16  1.000  1  1.000
276
HF2 -       200   -1.000    0.000   0.000    3.500    0.000    0.000
    3.749     4.550
 16  2.000  1  1.000
277
H2F2 AQ     200    0.000    0.000   0.000    0.000    0.000    0.000
    6.768     0.000
 16  2.000  1  2.000
278
HPO4 2-     200   -2.000    0.000   0.000    5.000    0.000    1.000
   12.346    -3.530
 25  1.000  1  1.000
279
H2PO4 -     200   -1.000    0.000   0.000    5.400    0.000    0.000
   19.553    -4.520
```

26 1.000 1 2.000
280
H3PO4 AQ 200 0.000 0.000 0.000 0.000 0.000 0.000
21.700 -2.620
26 1.000 1 3.000
281
H2S AQ 400 0.000 -2.000 0.000 0.000 0.000 0.000
40.654 -65.440
1 10.000 29 1.000 2 8.000 3 -4.000
282
S 2- 400 -2.000 -2.000 0.000 5.000 0.000 2.000
20.742 -48.040
1 8.000 29 1.000 2 8.000 3 -4.000
283
UOH +3 400 3.000 4.000 0.000 0.000 0.000 0.000
8.560 -22.715
3 -1.000 1 3.000 32 1.000 2 2.000
284
U(OH)2 + 300 2.000 4.000 0.000 0.000 0.000 0.000
6.946 -16.700
1 2.000 32 1.000 2 2.000
285
U(OH)3 + 400 1.000 4.000 0.000 0.000 0.000 0.000
4.281 -11.785
3 1.000 1 1.000 32 1.000 2 2.000
286
U(OH)4 A 300 0.000 4.000 0.000 0.000 0.000 0.000
0.718 -9.670
3 2.000 32 1.000 2 2.000
287
U(OH)5 - 400 -1.000 4.000 0.000 0.000 0.000 0.000
-3.904 -6.855
3 3.000 1 -1.000 32 1.000 2 2.000
288
UF +3 500 3.000 4.000 0.000 0.000 0.000 0.000
17.875 -29.380
16 1.000 32 1.000 2 2.000 1 4.000 3 -2.000
289
UF2 2+ 500 2.000 4.000 0.000 0.000 0.000 0.000
23.673 -27.230
16 2.000 32 1.000 2 2.000 1 4.000 3 -2.000
290
UF3 +1 500 1.000 4.000 0.000 0.000 0.000 0.000
28.331 -27.280
16 3.000 32 1.000 2 2.000 1 4.000 3 -2.000
291
UF4 AQ 500 0.000 4.000 0.000 0.000 0.000 0.000
32.856 -29.830
16 4.000 32 1.000 2 2.000 1 4.000 3 -2.000
292
UF5 -1 500 -1.000 4.000 0.000 0.000 0.000 0.000
34.454 -29.580
16 5.000 32 1.000 2 2.000 1 4.000 3 -2.000
293
UF6 2- 500 -2.000 4.000 0.000 0.000 0.000 0.000
36.934 -31.130
16 6.000 32 1.000 2 2.000 1 4.000 3 -2.000
294

```
UCL +3      500    3.000    4.000    0.000    0.000    0.000    0.000
   10.554  -24.497
 13  1.000 32  1.000  2  2.000  1  4.000  3 -2.000
295
USO4 2+     500    2.000   10.000    0.000    0.000    0.000    0.000
   14.677  -30.730
 29  1.000 32  1.000  2  2.000  1  4.000  3 -2.000
296
U(SO4)2     500    0.000   16.000    0.000    0.000    0.000    0.000
   18.965  -26.830
 29  2.000 32  1.000  2  2.000  1  4.000  3 -2.000
297
UHPO4 2+    500    2.000    4.000    0.000    0.000    0.000    0.000
   33.659  -26.930
 26  1.000  1  5.000 32  1.000  2  2.000  3 -2.000
298
U(HPO4)2    500    0.000    4.000    0.000    0.000    0.000    0.000
   56.049  -32.730
 26  2.000  1  6.000 32  1.000  2  2.000  3 -2.000
299
U(HPO4)3    500   -2.000    4.000    0.000    0.000    0.000    0.000
   76.780  -42.230
 26  3.000  1  7.000 32  1.000  2  2.000  3 -2.000
300
U(HPO4)4    500   -4.000    4.000    0.000    0.000    0.000    0.000
   97.699  -60.930
 26  4.000  1  8.000 32  1.000  2  2.000  3 -2.000
301
UO2OH +1    300    1.000    6.000    0.000    0.000    0.000    0.000
   -5.090   10.216
 32  1.000  3  1.000  1 -1.000
302
UO2)2OH2    300    2.000   12.000    0.000    0.000    0.000    0.000
   -5.645   10.220
 32  2.000  3  2.000  1 -2.000
303
UO2)3OH5    300    1.000   18.000    0.000    0.000    0.000    0.000
  -15.593   25.075
 32  3.000  3  5.000  1 -5.000
304
UO2CO3 A    210    0.000   10.000    0.000    0.000    0.000    2.000
   10.071    0.840    -9.56   0.03434    2809.0
 32  1.000 10  1.000
305
UO2CO3)2    210   -2.000   14.000    0.000    0.000    0.000    4.000
   17.008    3.480    14.14   0.0096
 32  1.000 10  2.000
306
UO2CO3)3    200   -4.000   18.000    0.000    0.000    0.000    6.000
   21.384   -8.780
 32  1.000 10  3.000
307
UO2F +1     200    1.000    6.000    0.000    0.000    0.000    0.000
    5.105   -0.450
 32  1.000 16  1.000
308
UO2F2 AQ    200    0.000    6.000    0.000    0.000    0.000    0.000
    8.920   -0.900
```

```
32  1.000 16  2.000
309
UO2F3 -1     200    -1.000    6.000    0.000    0.000    0.000    0.000
   11.364    -0.850
32  1.000 16  3.000
310
UO2F4 2-     200    -2.000    6.000    0.000    0.000    0.000    0.000
   12.607    -1.100
32  1.000 16  4.000
311
UO2CL +1     200     1.000    6.000    0.000    0.000    0.000    0.000
   0.220     1.233
32  1.000 13  1.000
312
UO2SO4 A     210     0.000   12.000    0.000    0.000    0.000    0.000
   2.709    5.100    11.384   -0.07088     0.0     1.40277E-04
32  1.000 29  1.000
313
UO2SO4)2     210    -2.000   18.000    0.000    0.000    0.000    0.000
   4.183    6.100    12.130  -0.068297     0.0     1.3987E-04
32  1.000 29  2.000
314
UO2HPO4      300     0.000    6.000    0.000    0.000    0.000    0.000
   20.814    -2.100
32  1.000 26  1.000  1  1.000
315
UO2HPO4)     300    -2.000    6.000    0.000    0.000    0.000    0.000
   42.988   -11.399
32  1.000 26  2.000  1  2.000
316
UO2H2PO4     300     1.000    6.000    0.000    0.000    0.000    0.000
   22.643    -3.700
32  1.000 26  1.000  1  2.000
317
UO2H2PO4     300     0.000    6.000    0.000    0.000    0.000    0.000
   44.700   -16.500
32  1.000 26  2.000  1  4.000
318
UO2H2PO4     300    -1.000    6.000    0.000    0.000    0.000    0.000
   66.245   -28.600
32  1.000 26  3.000  1  6.000
319
UO2H3SIO     300     1.000    6.000    0.000    0.000    0.000    0.000
   -2.400     0.000
32  1.000 30  1.000  1 -1.000
320
VOH +        400     1.000    2.000    0.000    0.000    0.000    0.000
   12.740   -35.330
3 -1.000  1  3.000 33  1.000  2  3.000
321
VOH 2+       400     2.000    3.000    0.000    0.000    0.000    0.000
   20.310   -34.880
3 -1.000  1  3.000 33  1.000  2  2.000
322
V(OH)2 +     300     1.000    3.000    0.000    0.000    0.000    0.000
   16.780   -44.230
1  2.000 33  1.000  2  2.000
323
```

V(OH)3 A 400 0.000 3.000 0.000 0.000 0.000 0.000
11.590 -44.230
3 1.000 1 1.000 33 1.000 2 2.000
324
VSO4 +1 500 1.000 9.000 0.000 0.000 0.000 0.000
24.050 -44.230
29 1.000 33 1.000 2 2.000 1 4.000 3 -2.000
325
V2(OH)3 400 3.000 6.000 0.000 0.000 0.000 0.000
37.720 -88.460
3 -1.000 1 5.000 33 2.000 2 4.000
326
V2(OH)2 400 4.000 6.000 0.000 0.000 0.000 0.000
41.470 -88.460
3 -2.000 1 6.000 33 2.000 2 4.000
327
V(OH)3 + 400 1.000 4.000 0.000 0.000 0.000 0.000
11.260 -29.320
3 1.000 1 1.000 33 1.000 2 1.000
328
H2V2O4 + 300 2.000 8.000 0.000 0.000 0.000 0.000
27.420 -58.640
1 2.000 33 2.000 2 2.000
329
VOF + 500 1.000 4.000 0.000 0.000 0.000 0.000
20.270 -27.420
16 1.000 33 1.000 2 1.000 1 2.000 3 -1.000
330
VOF2 AQ 500 0.000 4.000 0.000 0.000 0.000 0.000
22.670 -25.820
16 2.000 33 1.000 2 1.000 1 2.000 3 -1.000
331
VOF3 -1 500 -1.000 4.000 0.000 0.000 0.000 0.000
24.230 -24.420
16 3.000 33 1.000 2 1.000 1 2.000 3 -1.000
332
VOF4 2- 500 -2.000 4.000 0.000 0.000 0.000 0.000
25.040 -22.920
16 4.000 33 1.000 2 1.000 1 2.000 3 -1.000
333
VOSO4 AQ 500 0.000 10.000 0.000 0.000 0.000 0.000
19.380 -25.600
29 1.000 33 1.000 2 1.000 1 2.000 3 -1.000
334
VOCL +1 500 1.000 4.000 0.000 0.000 0.000 0.000
16.950 -29.320
13 1.000 33 1.000 2 1.000 1 2.000 3 -1.000
335
H3VO4 AQ 300 0.000 5.000 0.000 0.000 0.000 0.000
-3.300 10.630
33 1.000 3 2.000 1 -1.000
336
H2VO4 -1 300 -1.000 5.000 0.000 0.000 0.000 0.000
-7.090 11.330
33 1.000 3 2.000 1 -2.000
337
HVO4 2- 300 -2.000 5.000 0.000 0.000 0.000 0.000
-15.150 14.930

33 1.000 3 2.000 1 -3.000
338
VO4 -3 300 -3.000 5.000 0.000 0.000 0.000 0.000
-28.400 19.530
33 1.000 3 2.000 1 -4.000
339
V2O7 -4 300 -4.000 10.000 0.000 0.000 0.000 0.000
-29.080 0.000
33 2.000 3 3.000 1 -6.000
340
HV2O7 -3 300 -3.000 10.000 0.000 0.000 0.000 0.000
-16.320 0.000
33 2.000 3 3.000 1 -5.000
341
H3V2O7 - 300 -1.000 10.000 0.000 0.000 0.000 0.000
-3.790 0.000
33 2.000 3 3.000 1 -3.000
342
V3O9 -3 300 -3.000 15.000 0.000 0.000 0.000 0.000
-15.880 0.000
33 3.000 3 3.000 1 -6.000
343
V4O12 -4 300 -4.000 20.000 0.000 0.000 0.000 0.000
-20.790 0.000
33 4.000 3 4.000 1 -8.000
344
V10O28 - 300 -6.000 50.000 0.000 0.000 0.000 0.000
-17.530 0.000
33 10.000 3 8.000 1-16.000
345
HV10O28 300 -5.000 50.000 0.000 0.000 0.000 0.000
-11.350 21.520
33 10.000 3 8.000 1-15.000
346
H2V10O28 300 -4.000 50.000 0.000 0.000 0.000 0.000
-7.710 0.000
33 10.000 3 8.000 1-14.000
347
VO2F AQ 200 0.000 5.000 0.000 0.000 0.000 0.000
3.120 0.000
33 1.000 16 1.000
348
VO2F2 -1 200 -1.000 5.000 0.000 0.000 0.000 0.000
5.670 0.000
33 1.000 16 2.000
349
VO2F3 2- 200 -2.000 5.000 0.000 0.000 0.000 0.000
6.970 0.000
33 1.000 16 3.000
350
VO2F4 -3 200 -3.000 5.000 0.000 0.000 0.000 0.000
7.070 0.000
33 1.000 16 4.000
351
VO2SO4 - 200 -1.000 11.000 0.000 0.000 0.000 0.000
1.710 0.000
33 1.000 29 1.000
352

```
VO2NO3 A    200    0.000    10.000    0.000    0.000    0.000    0.000
   -0.430    0.000
 33  1.000 23  1.000
353
HSO3-       400   -1.000    4.000    0.000    0.000    0.000    0.000
    3.570   -1.620
  1  3.000 29  1.000  2  2.000  3 -1.000
354
H2SO3 AQ    400    0.000    4.000    0.000    0.000    0.000    0.000
    5.340    3.990
  1  4.000 29  1.000  2  2.000  3 -1.000
355
CUSO3-      500   -1.000    5.000    0.000    0.000    0.000    0.000
    6.880   -1.250
 29  1.000  1  2.000  2  3.000  3 -1.000 15  1.000
356
CU(SO3)2    500   -3.000    9.000    0.000    0.000    0.000    0.000
    4.030   -4.150
 15  1.000  2  5.000 29  2.000  1  4.000  3 -2.000
357
CU(SO3)3    500   -5.000   13.000    0.000    0.000    0.000    0.000
    1.120   -7.050
 15  1.000  2  7.000 29  3.000  1  6.000  3 -3.000
358
AGSO3-      500   -1.000    4.000    0.000    0.000    0.000    0.000
    1.950   -2.900
  4  1.000 29  1.000  1  2.000  2  2.000  3 -1.000
359
AGSO3)2-    500   -3.000    8.000    0.000    0.000    0.000    0.000
    1.380   -5.800
  4  1.000 29  2.000  1  4.000  2  4.000  3 -2.000
360
AGSO3)3-    500   -5.000   12.000    0.000    0.000    0.000    0.000
   -1.950   -8.700
  4  1.000 29  3.000  1  6.000  2  6.000  3 -3.000
361
AG2SO3)     500    0.000    4.000    0.000    0.000    0.000    0.000
    4.960   -2.900
  4  2.000 29  1.000  1  2.000  2  2.000  3 -1.000
362
O2 AQ       300     .000    4.000     .000     .000     .000     .000
  -86.080  134.790  .00000E+00  .00000E+00  .00000E+00  .00000E+00  .00000E+00
  3  2.000  1 -4.000  2 -4.000

LOOK MIN
URANINIT   2     4.00   -13.92    15.80    0          0.000    URANI
 32     1.000  2      2.000
UO2  (AM   2     4.00    -8.28     8.20    0          0.000    UO2
 32     1.000  2      2.000
U4O9 (C)   4    18.00   -40.25    36.49    0          0.000    U4O9
  1    -2.000  2      6.000  3     1.000  32     4.000
U3O8 (C)   4    16.00    -6.54   -12.73    0          0.000    U3O8
  1    -4.000  2      2.000  3     2.000  32     3.000
USIO4 (C   4     4.00   -16.84    19.88    0          0.000    USIO4
 30     1.000 32      1.000  2     2.000   3    -2.000
UF4  (C)   5     4.00   -27.82    15.53    0          0.000    UF4
 16     4.000 32      1.000  2     2.000   1     4.000  3    -2.000
UF4.2.5H   5     4.00   -36.79    33.84    0          0.000    UF4.2
```

16 4.000 3 0.500 32 1.000 2 2.000 1 4.000
UHPO4)2, 5 4.00 -60.80 38.27 0 0.000 UHPO4
26 2.000 1 6.000 3 2.000 32 1.000 2 2.000
NINGYOIT 5 4.00 -63.12 32.16 0 0.000 NINGY
11 1.000 26 2.000 32 1.000 2 2.000 1 4.000
UO3 (C) 3 6.00 7.72 -19.32 0 0.000 UO3 (
1 -2.000 32 1.000 3 1.000
GUMMITE 3 6.00 10.40 -23.01 0 0.000 GUMMI
1 -2.000 32 1.000 3 1.000
B-UO2(OH 3 6.00 5.54 -13.73 0 0.000 B-UO2
1 -2.000 32 1.000 3 2.000
SCHOEPIT 3 6.00 5.40 -12.05 0 0.000 SCHOE
1 -2.000 32 1.000 3 3.000
RUTHERFO 2 10.00 -14.44 -1.44 1 0.000 RUTHE
32 1.000 10 1.000
4.54 -0.03318 -2716.0
(UO2)3(P 2 18.00 -49.04 94.90 0 0.000 (UO2)
32 3.000 26 2.000
H-AUTUNI 3 12.00 -47.93 -3.60 0 0.000 H-AUT
1 2.000 32 2.000 26 2.000
NA-AUTUN 3 12.00 -47.41 -0.46 0 0.000 NA-AU
24 2.000 32 2.000 26 2.000
K-AUTUNI 3 12.00 -48.24 5.86 0 0.000 K-AUT
19 2.000 32 2.000 26 2.000
URAMPHIT 6 6.00 -289.90 383.81 0 0.000 URAMP
32 2.000 26 2.000 23 2.000 3 -6.000 1 20.000
2 16.000
SALEEITE 3 12.00 -43.65 -20.18 0 0.000 SALEE
32 2.000 21 1.000 26 2.000
AUTUNITE 3 12.00 -43.93 -14.34 0 0.000 AUTUN
32 2.000 11 1.000 26 2.000
SR-AUTUN 3 12.00 -44.46 -13.05 0 0.000 SR-AU
32 2.000 31 1.000 26 2.000
URANOCIR 3 12.00 -44.63 -10.10 0 0.000 URANO
32 2.000 8 1.000 26 2.000
BASSETIT 3 14.00 -44.49 -19.90 0 0.000 BASSE
32 2.000 17 1.000 26 2.000
TORBERNI 3 14.00 -45.28 -15.90 0 0.000 TORBE
32 2.000 15 1.000 26 2.000
PRZHEVAL 3 12.00 -44.37 -11.00 0 0.000 PRZHE
32 2.000 27 1.000 26 2.000
URANOPHA 4 12.00 17.49 0.00 0 0.000 URANO
1 -6.000 32 2.000 11 1.000 30 2.000
ALOH3(A) 3 0.00 10.38 -27.05 0 0.000 ALOH3
5 1.000 3 3.000 1 -3.000
ALOHSO4 4 6.00 -3.23 0.00 0 0.000 ALOHS
1 -1.000 5 1.000 29 1.000 3 1.000
AL4(OH)1 4 6.00 22.70 0.00 0 0.000 AL4(O
1 -10.000 5 4.000 29 1.000 3 10.000
ALUM K 4 12.00 -5.17 7.22 0 0.000 ALUM
19 1.000 5 1.000 29 2.000 3 12.000
ALUNITE 5 12.00 -1.35 3.92 0 0.000 ALUNI
19 1.000 5 3.000 29 2.000 3 6.000 1 -6.000
ANHYDRIT 2 6.00 -4.64 -3.77 0 0.000 ANHYD
11 1.000 29 1.000
ARAGONIT 2 4.00 -8.36 -2.62 1 0.000 ARAGO
11 1.000 10 1.000
-10.21 0.0217 0.0 -5.17E-05

```
ARTINITE  4      4.00    9.60    -28.74    0          0.000   ARTIN
 1   -2.000  21    2.000  10    1.000   3    5.000
BAF2      2      0.00    -5.76    1.00     0          0.000   BAF2
 8    1.000  16    2.000
BARITE    2      6.00    -9.98    6.28     0          0.000   BARIT
 8    1.000  29    1.000
BOEHMITE  3      0.00    8.58    -28.13    0          0.000   BOEHM
 1   -3.000   5    1.000   3    2.000
BRUCITE   3      0.00    16.79   -25.84    0          0.000   BRUCI
 21   1.000   3    2.000   1   -2.000
CALCITE   2      4.00    -8.48   -2.59     1          0.000   CALCI
 11   1.000  10    1.000
 13.543    -0.0401    -3000.0
CELESTIT  2      6.00    -6.47   -0.47     0          0.000   CELES
 31   1.000  29    1.000
CHALCEDO  2      0.00    -3.52    4.61     0          0.000   CHALC
 3   -2.000  30    1.000
CHRYSOTI  4      0.00    32.19   -52.49    0          0.000   CHRYS
 1   -6.000  21    3.000  30    2.000   3    1.000
CLINOENS  4      0.00    11.34   -20.01    0          0.000   CLINO
 3   -1.000  21    1.000  30    1.000   1   -2.000
CRISTOBA  2      0.00    -3.59    5.50     0          0.000   CRIST
 3   -2.000  30    1.000
DIASPORE  3      0.00    6.87    -24.63    0          0.000   DIASP
 1   -3.000   5    1.000   3    2.000
DIOPSIDE  5      0.00    19.89   -32.28    0          0.000   DIOPS
 3   -2.000  11    1.000  21    1.000  30    2.000   1   -4.000
DOLOMITE  3      8.00    -17.09  -8.29     0          0.000   DOLOM
 11   1.000  21    1.000  10    2.000
EPSOMITE  3      6.00    -2.14    2.82     0          0.000   EPSOM
 21   1.000  29    1.000   3    7.000
SEPIOLIT  4      0.00    15.91   -27.27    0          0.000   SEPIO
 3   -0.500  21    2.000  30    3.000   1   -4.000
FERRIHYD  4      3.00    17.92   -10.00    0          0.000   FERRI
 1   -3.000   3    3.000  17    1.000   2   -1.000
FE3(OH)8  4      8.00    46.29   -20.00    0          0.000   FE3(O
 1   -8.000  17    3.000   3    8.000   2   -2.000
FEOH)2.7  5      3.00    9.99    -10.00    0          0.000   FEOH)
 1   -2.700   3    2.700  13    0.300  17    1.000   2   -1.000
FES PPT   5      0.00    -37.58   60.14    0          0.000   FES P
 1    8.000  17    1.000  29    1.000   2    8.000   3   -4.000
FE2(SO4)  3      24.00   29.64   -79.12    0          0.000   FE2(S
 29   3.000  17    2.000   2   -2.000
FCO3APAT  5      4.80   -114.40   39.39    0          0.000   FCO3A
 11   9.496  21    0.144  26    4.800  10    1.200  16    2.480
FLUORITE  2      0.00    -10.96   4.71     0          0.000   FLUOR
 11   1.000  16    2.000
FORSTERI  3      0.00    28.30   -48.51    0          0.000   FORST
 1   -4.000  21    2.000  30    1.000
Gibbsite  3      0.00    7.94    -22.79    0          0.000   GIBBS
 1   -3.000   5    1.000   3    3.000
GOETHITE  4      3.00    13.53   -24.48    0          0.000   GOETH
 1   -3.000   3    2.000  17    1.000   2   -1.000
GREENALI  4      6.00    20.81    0.00     0          0.000   GREEN
 1   -6.000  17    3.000  30    2.000   3    1.000
GREIGITE  5      0.00   -153.61  220.56    0          0.000   GREIG
 1   32.000  17    3.000   2   30.000  29    4.000   3  -16.000
GYPSUM    3      6.00    -4.85    0.26     0          0.000   GYPSU
```

```
 11     1.000  29      1.000   3      2.000
HALITE    2          0.00     1.58     0.92     0            0.000    HALIT
 24     1.000  13      1.000
HEMATITE  4          6.00     22.06    -50.85    0            0.000    HEMAT
 1     -6.000   3      3.000  17      2.000   2     -2.000
HUNTITE   3         16.00    -29.97    -25.76    0            0.000    HUNTI
 21     3.000  11      1.000  10      4.000
HYDRMAGN  4         16.00    -8.77    -52.21    0            0.000    HYDRM
 21     5.000  10      4.000   1     -2.000   3      6.000
JAROSITE  6         21.00    27.90    -66.18    0            0.000    JAROS
 1     -6.000  24      1.000  29      2.000   3      6.000  17      3.000
 2     -3.000
JAROSITE  6         21.00    24.30    -61.28    0            0.000    JAROS
 1     -6.000  19      1.000  29      2.000   3      6.000  17      3.000
 2     -3.000
JAROSITE  5         21.00    27.00    -85.15    0            0.000    JAROS
 1     -5.000  29      2.000   3      7.000  17      3.000   2     -3.000
MACKINAW  5          0.00    -38.31    60.14    0            0.000    MACKI
 1      8.000  17      1.000  29      1.000   2      8.000   3     -4.000
MAGADIIT  4          0.00    -14.30     0.00    0            0.000    MAGAD
 1     -1.000   3     -9.000  24      1.000  30      7.000
MAGHEMIT  4          6.00     32.45   -20.00    0            0.000    MAGHE
 1     -6.000   3      3.000  17      2.000   2     -2.000
MAGNESIT  2          4.00     -8.03    -6.17    0            0.000    MAGNE
 21     1.000  10      1.000
MAGNETIT  4          8.00     29.80   -70.46    0            0.000    MAGNE
 1     -8.000  17      3.000   3      4.000   2     -2.000
MELANTER  3          8.00     -2.47     2.86    0            0.000    MELAN
 17     1.000  29      1.000   3      7.000
MIRABILI  3          6.00     -1.11    18.99    0            0.000    MIRAB
 24     2.000  29      1.000   3     10.000
NATRON    3          4.00     -1.31    15.74    0            0.000    NATRO
 24     2.000  10      1.000   3     10.000
NESQUEHO  3          4.00     -5.62    -5.79    0            0.000    NESQU
 21     1.000  10      1.000   3      3.000
PHLOGOPI  5          0.00     66.30   -86.36    0            0.000    PHLOG
 1    -10.000  19      1.000  21      3.000   5      1.000  30      3.000
PYRITE    5          0.00    -85.80   131.58    0            0.000    PYRIT
 1     16.000   2     14.000  17      1.000  29      2.000   3     -8.000
QUARTZ    2          0.00     -4.01     6.22    0            0.000    QUART
 3     -2.000  30      1.000
SEPIOLIT  4          0.00     18.78     0.00    0            0.000    SEPIO
 3     -0.500  21      2.000  30      3.000   1     -4.000
SIDERITE  2          6.00    -10.55    -5.33    0            0.000    SIDER
 17     1.000  10      1.000
SIO2(A,G  2          0.00     -3.02     4.44    1            0.000    SIO2(
 3     -2.000  30      1.000
 0.3380     -0.0007889  -840.1
SIO2(A,P  2          0.00     -2.71     3.91    1            0.000    SIO2(
 3     -2.000  30      1.000
0.3380      -0.0007889  -840.1
SRF2      2          0.00     -8.54     1.25    0            0.000    SRF2
 31     1.000  16      2.000
STRENGIT  4          3.00    -13.37   -12.03    0            0.000    STREN
 26     1.000   3      2.000  17      1.000   2     -1.000
STRONTIA  2          4.00     -9.25    -0.69    0            0.000    STRON
 31     1.000  10      1.000
TALC      4          0.00     23.06   -35.01    0            0.000    TALC
```

```
 3    -4.000  21     3.000  30     4.000   1     -6.000
THENARDI   2       6.00    -0.18     -0.57     0            0.000    THENA
 24     2.000  29     1.000
THERMONA   3       4.00     0.13     -2.80     0            0.000    THERM
 24     2.000  10     1.000   3     1.000
TREMOLIT   5       0.00    56.55    -96.61     0            0.000    TREMO
 3    -8.000  11     2.000  21     5.000  30     8.000   1   -14.000
VIVIANIT   3       6.00   -36.00      0.00     0            0.000    VIVIA
 17     3.000  26     2.000   3     8.000
WITHERIT   2       4.00    -8.59      0.36     0            0.000    WITHE
 8     1.000  10     1.000
PYROLUSI   4       4.00    41.37    -54.94     0            0.000    PYROL
 1    -4.000   2    -2.000   3     2.000  22     1.000
BIRNESSI   4       4.00    43.60    -25.76     0            0.000    BIRNE
 1    -4.000   2    -2.000   3     2.000  22     1.000
NSUTITE    4       4.00    43.01    -25.76     0            0.000    NSUTI
 1    -4.000   2    -2.000   3     2.000  22     1.000
BIXBYITE   4       6.00    50.40    -66.76     0            0.000    BIXBY
 1    -6.000   3     3.000  22     2.000   2     -2.000
HAUSMANN   4       8.00    61.54    -80.14     0            0.000    HAUSM
 1    -8.000   2    -2.000  22     3.000   3     4.000
PYROCROI   3       2.00    15.09    -22.59     0            0.000    PYROC
 1    -2.000  22     1.000   3     2.000
MANGANIT   4       3.00    25.27    -25.76     0            0.000    MANGA
 1    -3.000   3     2.000  22     1.000   2     -1.000
RHODOCHR   2       6.00   -10.41     -2.08     0            0.000    RHODO
 22     1.000  10     1.000
MNCL2, 4   3       2.00     2.71     17.38     0            0.000    MNCL2
 22     1.000  13     2.000   3     4.000
MNS GREE   5       0.00   -29.86     54.35     0            0.000    MNS G
 1     8.000  22     1.000  29     1.000   2     8.000   3    -4.000
MNSO4      2       8.00     2.67    -15.48     0            0.000    MNSO4
 22     1.000  29     1.000
MN2(SO4)   3      24.00    45.30    -90.58     0            0.000    MN2(S
 29     3.000  22     2.000   2    -2.000
MN3(PO4)   2       6.00   -23.83      2.12     0            0.000    MN3(P
 22     3.000  26     2.000
CU METAL   2       0.00   -11.48     15.48     0            0.000    CU ME
 2     2.000  15     1.000
NANTOKIT   3       1.00    -9.48      8.33     0            0.000    NANTO
 13     1.000  15     1.000   2     1.000
CUF        3       1.00     4.36    -14.02     0            0.000    CUF
 16     1.000  15     1.000   2     1.000
CUPRITE    4       2.00    -6.99      2.94     0            0.000    CUPRI
 1    -2.000   3     1.000  15     2.000   2     2.000
CHALCOCI   5       0.00   -73.72    106.19     0            0.000    CHALC
 1     8.000  15     2.000   2    10.000  29     1.000   3    -4.000
DJURLEIT   5       0.00   -72.66    104.94     0            0.000    DJURL
 1     8.000  15     1.934   2     9.868  29     1.000   3    -4.000
ANILITE    5       0.00   -69.62    101.20     0            0.000    ANILI
 1     8.000  15     1.750   2     9.500  29     1.000   3    -4.000
BLAUBLEI   5       0.00   -63.12     58.82     0            0.000    BLAUB
 1     8.000  15     1.400   2     8.800  29     1.000   3    -4.000
BLAUBLEI   5       0.00   -58.37     59.81     0            0.000    BLAUB
 1     8.000  15     1.100   2     8.200  29     1.000   3    -4.000
COVELLIT   5       0.00   -56.70     84.15     0            0.000    COVEL
 1     8.000  15     1.000  29     1.000   2     8.000   3    -4.000
CU2SO4     3       8.00    -7.39     -7.86     0            0.000    CU2SO
```

```
 29      1.000  15     2.000   2      2.000
CUPROUSF   4        4.00     1.39    -15.45      0           0.000    CUPRO
  1    -4.000   3     2.000  15     1.000  17       1.000
MELANOTH   2         2.00     3.73    -12.32     0           0.000    MELAN
 15      1.000  13     2.000
CUCO3      2        6.00    -9.63      0.00      0           0.000    CUCO3
 15      1.000  10     1.000
CUF2       2        2.00    -0.62    -13.32      0           0.000    CUF2
 15      1.000  16     2.000
CUF2, 2H   3        2.00    -4.55     -3.65      0           0.000    CUF2,
 15      1.000  16     2.000   3      2.000
CU(OH)2    3        2.00     8.64    -15.25      0           0.000    CU(OH
  1    -2.000  15     1.000   3      2.000
ATACAMIT   4        4.00     7.34    -18.69      0           0.000    ATACA
  1    -3.000  15     2.000   3      3.000  13       1.000
CU2(OH)3   4        9.00     9.24    -17.35      0           0.000    CU2(O
  1    -3.000  15     2.000   3      3.000  23       1.000
ANTLERIT   4       12.00     8.29      0.00      0           0.000    ANTLE
  1    -4.000  15     3.000   3      4.000  29       1.000
BROCHANT   4       14.00    15.34      0.00      0           0.000    BROCH
  1    -6.000  15     4.000   3      6.000  29       1.000
LANGITE    4       14.00    16.79    -39.61      0           0.000    LANGI
  1    -6.000  15     4.000   3      7.000  29       1.000
TENORITE   3        2.00     7.62    -15.24      0           0.000    TENOR
  1    -2.000  15     1.000   3      1.000
CUOCUSO4   4       10.00    11.53    -35.58      0           0.000    CUOCU
  1    -2.000  15     2.000   3      1.000  29       1.000
CU3(PO4)   2        6.00   -36.85      0.00      0           0.000    CU3(P
 15      3.000  26     2.000
CU3(PO4)   3        6.00   -35.12      0.00      0           0.000    CU3(P
 15      3.000  26     2.000   3      3.000
CUSO4      2        8.00     3.01    -18.14      0           0.000    CUSO4
 15      1.000  29     1.000
CHALCANT   3        8.00    -2.64      1.44      0           0.000    CHALC
 15      1.000  29     1.000   3      5.000
DIOPTASE   3        2.00     6.50     -8.96      0           0.000    DIOPT
  1    -2.000  15     1.000  30      1.000
CUPRICFE   5        8.00    31.94    -58.69      0           0.000    CUPRI
  1    -8.000  15     1.000   3      4.000  17       2.000   2     -2.000
CHALCOPY   6        0.00  -102.59    155.76      0           0.000    CHALC
  1    16.000  15     1.000  17      1.000  29       2.000   2     16.000
  3    -8.000
CUBR       3        1.00   -10.93     11.43      0           0.000    CUBR
  9      1.000  15     1.000   2      1.000
CUI        3        1.00   -14.61     18.49      0           0.000    CUI
 18      1.000  15     1.000   2      1.000
ZN METAL   2       -2.00    25.76    -36.78      0           0.000    ZN ME
 34      1.000   2     2.000
ZNCL2      2        0.00     7.03    -17.48      0           0.000    ZNCL2
 34      1.000  13     2.000
SMITHSON   2        4.00   -10.00     -4.36      0           0.000    SMITH
 34      1.000  10     1.000
ZNCO3, 1   3        4.00   -10.26      0.00      0           0.000    ZNCO3
 34      1.000  10     1.000   3      1.000
ZNF2       2        0.00    -1.52    -13.08      0           0.000    ZNF2
 34      1.000  16     2.000
ZN(OH)2    3        0.00    12.45      0.00      0     [illegible]    ZN(OH
  1    -2.000  34     1.000   3      2.000
```

```
ZN(OH)2    3      0.00   12.20    0.00    0        0.000   ZN(OH
 1    -2.000  34    1.000  3    2.000
ZN(OH)2    3      0.00   11.75    0.00    0        0.000   ZN(OH
 1    -2.000  34    1.000  3    2.000
ZN(OH)2    3      0.00   11.71    0.00    0        0.000   ZN(OH
 1    -2.000  34    1.000  3    2.000
ZN(OH)2    3      0.00   11.50    0.00    0        0.000   ZN(OH
 1    -2.000  34    1.000  3    2.000
ZN2(OH)3   4      0.00   15.20    0.00    0        0.000   ZN2(O
 1    -3.000  34    2.000  3    3.000  13    1.000
ZN5(OH)8   4      0.00   38.50    0.00    0        0.000   ZN5(O
 1    -8.000  34    5.000  3    8.000  13    2.000
ZN2(OH)2   4      6.00    7.50    0.00    0        0.000   ZN2(O
 1    -2.000  34    2.000  3    2.000  29    1.000
ZN4(OH)6   4      6.00   28.40    0.00    0        0.000   ZN4(O
 1    -6.000  34    4.000  3    6.000  29    1.000
ZNNO3)2,   3     10.00    3.44    5.51    0        0.000   ZNNO3
 34    1.000  23    2.000  3    6.000
ZNO(ACTI   3      0.00   11.31    0.00    0        0.000   ZNO(A
 1    -2.000  34    1.000  3    1.000
ZINCITE    3      0.00   11.14  -21.86    0        0.000   ZINCI
 1    -2.000  34    1.000  3    1.000
ZN3O(SO4   4     12.00   19.02  -62.00    0        0.000   ZN3O(
 1    -2.000  34    3.000  29    2.000  3    1.000
ZN3(PO4)   3      0.00  -32.04    0.00    0        0.000   ZN3(P
 34    3.000  26    2.000  3    4.000
ZNS (A)    5     -2.00  -42.71   63.81    0        0.000   ZNS (
 1     8.000  34    1.000  29    1.000  2    8.000  3   -4.000
SPHALERI   5     -2.00  -45.28   68.39    0        0.000   SPHAL
 1     8.300  34    1.000  29    1.000  2    8.000  3   -4.000
WURTZITE   5     -2.00  -43.34   65.20    0        0.000   WURTZ
 1     8.000  34    1.000  29    1.000  2    8.000  3   -4.000
ZNSIO3     4      0.00    2.93  -18.27    0        0.000   ZNSIO
 1    -2.000  3    -1.000  34    1.000  30    1.000
WILLEMIT   3      0.00   15.33  -33.37    0        0.000   WILLE
 1    -4.000  34    2.000  30    1.000
ZINCOSIT   2      6.00    3.01  -19.20    0        0.000   ZINCO
 34    1.000  29    1.000
ZNSO4, 1   3      6.00   -0.57  -10.64    0        0.000   ZNSO4
 34    1.000  29    1.000  3    1.000
BIANCHIT   3      6.00   -1.76   -0.16    0        0.000   BIANC
 34    1.000  29    1.000  3    6.000
GOSLARIT   3      6.00   -1.96    3.30    0        0.000   GOSLA
 34    1.000  29    1.000  3    7.000
ZNBR2, 2   3      0.00    5.21   -7.51    0        0.000   ZNBR2
 34    1.000  9     2.000  3    2.000
ZNI2       2      0.00    7.23  -13.44    0        0.000   ZNI2
 34    1.000  18    2.000
CD METAL   2     -2.00   13.49  -18.00    0        0.000   CD ME
 12    1.000  2     2.000
GAMMA CD   2     -2.00   13.59  -18.14    0        0.000   GAMMA
 12    1.000  2     2.000
OTAVITE    2      4.00  -13.74   -0.58    0        0.000   OTAVI
 12    1.000  10    1.000
CDCL2      2      0.00   -0.68   -4.47    0        0.000   CDCL2
 12    1.000  13    2.000
CDCL2, 1   3      0.00   -1.71   -1.82    0        0.000   CDCL2
 12    1.000  13    2.000  3    1.000
```

```
CDCL2,2.   3        0.00    -1.94     1.71    0          0.000    CDCL2
 12    1.000  13     2.000   3      2.500
CDF2       2       0.00    -2.98    -9.72    0          0.000    CDF2
 12    1.000  16     2.000
CD(OH)2    3        0.00   13.73   -20.77    0          0.000    CD(OH
 1    -2.000  12     1.000   3      2.000
CD(OH)2    3        0.00   13.65     0.00    0          0.000    CD(OH
 1    -2.000  12     1.000   3      2.000
CDOHCL     4        0.00    3.52    -7.41    0          0.000    CDOHC
 1    -1.000  12     1.000   3      1.000  13     1.000
CD3(OH)4   4        6.00   22.56     0.00    0          0.000    CD3(O
 1    -4.000  12     3.000   3      4.000  29     1.000
CD3OH2(S   4       12.00    6.71     0.00    0          0.000    CD3OH
 1    -2.000  12     3.000   3      2.000  29     2.000
CD4(OH)6   4        6.00   28.40     0.00    0          0.000    CD4(O
 1    -6.000  12     4.000   3      6.000  29     1.000
MONTEPON   3        0.00   15.12   -24.76    0          0.000    MONTE
 1    -2.000  12     1.000   3      1.000
CD3(PO4)   2       0.00   -32.60     0.00    0          0.000    CD3(P
 12    3.000  26     2.000
CDSIO3     4       0.00     9.06   -16.63    0          0.000    CDSIO
 3    -1.000  12     1.000  30      1.000   1    -2.000
CDSO4      2       6.00    -0.10   -14.74    0          0.000    CDSO4
 12    1.000  29     1.000
CDSO4, 1   3       6.00    -1.66    -7.52    0          0.000    CDSO4
 12    1.000  29     1.000   3      1.000
CDSO4,2.   3       6.00    -1.87    -4.30    0          0.000    CDSO4
 12    1.000  29     1.000   3      2.670
GREENOCK   5       -2.00  -49.59    76.50    0          0.000    GREEN
 1     8.000  12     1.000  29      1.000   2     8.000   3    -4.000
CDBR2, 4   3       0.00    -2.42     7.23    0          0.000    CDBR2
 12    1.000   9     2.000   3      4.000
CDI2       2       0.00    -3.61     4.08    0          0.000    CDI2
 12    1.000  18     2.000
PB METAL   2       -2.00    4.27     0.40    0          0.000    PB ME
 27    1.000   2     2.000
COTUNNIT   2        0.00   -4.77     5.60    0          0.000    COTUN
 27    1.000  13     2.000
MATLOCKI   3        0.00   -9.43     7.95    0          0.000    MATLO
 27    1.000  13     1.000  16      1.000
PHOSGENI   3        4.00  -19.81     0.00    0          0.000    PHOSG
 27    2.000  13     2.000  10      1.000
CERRUSIT   2        4.00  -13.13     4.86    0          0.000    CERRU
 27    1.000  10     1.000
PBF2       2       0.00    -7.44    -0.70    0          0.000    PBF2
 27    1.000  16     2.000
MASSICOT   3        0.00   12.91   -16.78    0          0.000    MASSI
 1    -2.000  27     1.000   3      1.000
LITHARGE   3        0.00   12.72   -16.38    0          0.000    LITHA
 1    -2.000  27     1.000   3      1.000
PBO, .3H   3       0.00    12.98     0.00    0          0.000    PBO,
 1    -2.000  27     1.000   3      1.330
PB2OCO3    4        4.00   -0.50   -11.46    0          0.000    PB2OC
 1    -2.000  27     2.000   3      1.000  10     1.000
LARNAKIT   4        6.00   -0.28    -6.44    0          0.000    LARNA
 1    -2.000  27     2.000  29      1.000   3     1.000
PB3O2SO4   4        6.00   10.40   -20.75    0          0.000    PB3O2
 1    -4.000  27     3.000  29      1.000   3     2.000
```

PB4O3SO4 4 6.00 22.10 -35.07 0 0.000 PB4O3
1 -6.000 27 4.000 29 1.000 3 3.000
CLPYROMO 3 0.00 -84.43 0.00 0 0.000 CLPYR
27 5.000 26 3.000 13 1.000
HXYPYROM 4 0.00 -62.79 0.00 0 0.000 HXYPY
1 -1.000 27 5.000 26 3.000 3 1.000
PB3O2CO3 4 4.00 11.02 -26.43 0 0.000 PB3O2
1 -4.000 27 3.000 10 1.000 3 2.000
PLUMBGUM 5 0.00 -32.79 0.00 0 0.000 PLUMB
1 -5.000 27 1.000 5 3.000 26 2.000 3 6.000
HINSDALI 6 6.00 -2.50 0.00 0 0.000 HINSD
1 -6.000 27 1.000 5 3.000 26 1.000 29 1.000
3 6.000
TSUMEBIT 5 2.00 -9.79 0.00 0 0.000 TSUME
1 -3.000 27 2.000 15 1.000 26 1.000 3 6.000
PBSIO3 4 0.00 7.32 -9.26 0 0.000 PBSIO
3 -1.000 1 -2.000 27 1.000 30 1.000
PB2SIO4 3 0.00 19.76 -26.00 0 0.000 PB2SI
1 -4.000 27 2.000 30 1.000
ANGLESIT 2 6.00 -7.79 2.15 0 0.000 ANGLE
27 1.000 29 1.000
GALENA 5 -2.00 -48.79 79.54 0 0.000 GALEN
1 8.000 27 1.000 29 1.000 2 8.000 3 -4.000
PLATTNER 4 2.00 49.30 -70.73 0 0.000 PLATT
1 -4.000 2 -2.000 27 1.000 3 2.000
PB2O3 4 2.00 61.04 0.00 0 0.000 PB2O3
1 -6.000 2 -2.000 27 2.000 3 3.000
MINIUM 4 2.00 73.69 -102.76 0 0.000 MINIU
1 -8.000 2 -2.000 27 3.000 3 4.000
PB(OH)2 3 0.00 8.15 -13.99 0 0.000 PB(OH
1 -2.000 27 1.000 3 2.000
LAURIONI 4 0.00 0.62 0.00 0 0.000 LAURI
1 -1.000 27 1.000 13 1.000 3 1.000
PB2(OH)3 4 0.00 8.79 0.00 0 0.000 PB2(O
1 -3.000 27 2.000 3 3.000 13 1.000
HYDCERRU 4 8.00 -17.46 0.00 0 0.000 HYDCE
1 -2.000 27 3.000 10 2.000 3 2.000
PB2O(OH) 3 0.00 26.20 0.00 0 0.000 PB2O(
1 -4.000 27 2.000 3 3.000
PBBR2 2 0.00 -5.18 8.10 0 0.000 PBBR2
27 1.000 9 2.000
PBBRF 3 0.00 -8.49 0.00 0 0.000 PBBRF
27 1.000 9 1.000 16 1.000
PBI2 2 0.00 -8.07 15.16 0 0.000 PBI2
27 1.000 18 2.000
PB4(OH)6 4 6.00 21.10 0.00 0 0.000 PB4(O
1 -6.000 27 4.000 29 1.000 3 6.000
NICO3 2 4.00 -6.84 -9.94 0 0.000 NICO3
25 1.000 10 1.000
NI(OH)2 3 0.00 10.80 30.45 0 0.000 NI(OH
1 -2.000 25 1.000 3 2.000
NI4(OH)6 4 6.00 32.00 0.00 0 0.000 NI4(O
1 -6.000 25 4.000 29 1.000 3 6.000
BUNSENIT 3 0.00 12.45 -23.92 0 0.000 BUNSE
1 -2.000 25 1.000 3 1.000
NI3(PO4) 2 0.00 -31.30 0.00 0 0.000 NI3(P
25 3.000 26 2.000
MILLERIT 5 -2.00 -41.70 62.64 0 0.000 MILLE

```
1   8.000 25   1.000 29   1.000  2   8.000  3  -4.000
RETGERSI  3   6.00  -2.04   1.10   0   0.000  RETGE
25   1.000 29   1.000  3   6.000
MORENOSI  3   6.00  -2.36   2.94   0   0.000  MOREN
25   1.000 29   1.000  3   7.000
NI2SIO4  3   0.00  14.54  -33.36   0   0.000  NI2SI
1  -4.000 25   2.000 30   1.000
AG METAL  2  -1.00  -13.51  25.23   0   0.000  AG ME
4   1.000  2   1.000
BROMYRIT  2   0.00  -12.27  20.17   0   0.000  BROMY
4   1.000  9   1.000
CERARGYR  2   0.00  -9.75  15.65   0   0.000  CERAR
4   1.000 13   1.000
AG2CO3  2   4.00  -11.07   9.53   0   0.000  AG2CO
4   2.000 10   1.000
AGF.4H2O  3   0.00   0.55   4.27   0   0.000  AGF.4
4   1.000 16   1.000  3   4.000
IODYRITE  2   0.00  -16.07  26.82   0   0.000  IODYR
4   1.000 18   1.000
AG2O  3   0.00  12.58  -10.43   0   0.000  AG2O
1  -2.000  4   2.000  3   1.000
AG3PO4  2   0.00  -17.55   0.00   0   0.000  AG3PO
4   3.000 26   1.000
ACANTHIT  5  -2.00  -69.71  113.44   0   0.000  ACANT
1   8.000  4   2.000 29   1.000  2   8.000  3  -4.000
AG2SO4  2   6.00  -4.92   4.25   0   0.000  AG2SO
4   2.000 29   1.000
ANALCIME  5   0.00   6.72  -22.84   0   0.000  ANALC
24   1.000  5   1.000 30   2.000  3  -1.000  1  -4.000
Kaolinit  4   0.00   7.51  -37.81   0   0.000  KAOLI
5   2.000 30   2.000  3   1.000  1  -6.000
LEONHARD  5   0.00  16.49  -85.36   0   0.000  LEONH
3  -1.000  1  -16.000 11   2.000 30   8.000  5   4.000
Low albi  5   0.00   3.23  -18.25   0   0.000  LOW A
24   1.000  5   1.000 30   3.000  1  -4.000  3  -4.000
ANALBITE  5   0.00   3.51  -20.00   0   0.000  ANALB
24   1.000  5   1.000 30   3.000  1  -4.000  3  -4.000
Muscovit  4   0.00  14.65  -60.44   0   0.000  MUSCO
19   1.000  5   3.000 30   3.000  1  -10.000
ANNITE  5   6.00  23.29  -65.72   0   0.000  ANNIT
19   1.000 17   3.000  5   1.000 30   3.000  1  -10.000
Anorthit  4   0.00  27.26  -73.69   0   0.000  ANORT
11   1.000  5   2.000 30   2.000  1  -8.000
Pyrophyl  4   0.00   1.25  -31.04   0   0.000  PYROP
5   2.000 30   4.000  3  -4.000  1  -6.000
LAUMONTI  4   0.00  14.46  -50.45   0   0.000  LAUMO
11   1.000  5   2.000 30   4.000  1  -8.000
WAIRAKIT  5   0.00  18.87  -63.15   0   0.000  WAIRA
11   1.000  5   2.000 30   4.000  1  -8.000  3  -2.000
MALACHIT  4   8.00  -5.18  -15.61   0   0.000  MALAC
15   2.000  3   2.000 10   1.000  1  -2.000
AZURITE  4  14.00  -16.92  -23.77   0   0.000  AZURI
15   3.000  3   2.000 10   2.000  1  -2.000
ARSENOLI  4  12.00  -80.58  134.39   0   0.000  ARSEN
3  -10.000  6   4.000  2   8.000  1   8.000
CLAUDETI  4  12.00  -80.84  133.35   0   0.000  CLAUD
3  -10.000  6   4.000  2   8.000  1   8.000
ASI3  5   3.00  -15.29  31.89   0   0.000  ASI3
```

```
 18     3.000   1     5.000   3    -4.000   6     1.000   2     2.000
ORIPMENT   5      0.00  -200.84   323.34    0          0.000   ORIPM
 1   34.000   3   -20.000   6    2.000   2    28.000  29     3.000
REALGAR    5      0.00   -72.85   120.70    0          0.000   REALG
 1   13.000   2    11.000   3    -8.000   6     1.000  29     1.000
AS2O5      2     10.00     6.70    -5.41    0          0.000   AS2O5
 6    2.000   3    -3.000
ZN(BO2)2   4      0.00     8.29     0.00    0          0.000   ZN(BO
 3   -2.000   1    -2.000  34     1.000   7     2.000
CD(BO2)2   4      0.00     9.84     0.00    0          0.000   CD(BO
 3   -2.000   1    -2.000  12     1.000   7     2.000
PB(BO2)2   4      0.00     7.61    -5.80    0          0.000   PB(BO
 3   -2.000   1    -2.000  27     1.000   7     2.000
MNHPO4(C   3      2.00   -25.40     0.00    0          0.000   MNHPO
 22    1.000  26     1.000   1     1.000
PBHPO4     3      0.00   -23.90     0.00    0          0.000   PBHPO
 27    1.000  26     1.000   1     1.000
PB3(PO4)   2      0.00   -44.50     0.00    0          0.000   PB3(P
 27    3.000  26     2.000
SULFUR     4      0.00   -35.77    55.94    0          0.000   SULFU
 1    8.000   2     6.000  29     1.000   3    -4.000
ALASO4.2   4      5.00     4.80     0.00    0          0.000   ALASO
 5    1.000   6     1.000   3     2.000   1    -3.000
CA3(ASO4   4     10.00    22.30     0.00    0          0.000   CA3(A
 11    3.000   6     2.000   3     4.000   1    -6.000
CU3(ASO4   4     16.00     6.10     0.00    0          0.000   CU3(A
 15    3.000   6     2.000   3     2.000   1    -6.000
FEASO4.2   5      8.00    13.43   -10.00    0          0.000   FEASO
 6    1.000   3     2.000   1    -3.000  17     1.000   2    -1.000
MN3ASO42   4     16.00    12.50     0.00    0          0.000   MN3AS
 22    3.000   6     2.000   3     8.000   1    -6.000
NI3(ASO4   4     10.00    15.70     0.00    0          0.000   NI3(A
 25    3.000   6     2.000   3     8.000   1    -6.000
PB3(ASO4   3     10.00     5.80     0.00    0          0.000   PB3(A
 27    3.000   6     2.000   1    -6.000
ZN3ASO42   4     10.00    13.65     0.00    0          0.000   ZN3AS
 34    3.000   6     2.000   3     2.500   1    -6.000
BA(ASO4)   3     10.00    -8.91     2.64    0          0.000   BA(AS
 8    3.000   6     2.000   1    -6.000
V METAL    4      0.00    19.74   -18.67    0          0.000   V MET
 2    5.000  33     1.000   1     4.000   3    -2.000
VO         4      2.00    -9.53    16.21    0          0.000   VO
 1    2.000   3    -1.000   2     3.000  33     1.000
VCL2       5      2.00    -4.64     8.43    0          0.000   VCL2
 13    2.000   2     3.000  33     1.000   1     4.000   3    -2.000
V2O3       4      3.00   -17.71    24.51    0          0.000   V2O3
 1    1.000   3    -0.500  33     1.000   2     2.000
V(OH)3     4      3.00   -14.96    44.23    0          0.000   V(OH)
 1    1.000   3     1.000  33     1.000   2     2.000
VCL3       5      3.00    -0.88     0.27    0          0.000   VCL3
 13    3.000  33     1.000   2     2.000   1     4.000   3    -2.000
VOCL       5      3.00   -13.20    18.06    0          0.000   VOCL
 13    1.000   3    -1.000   1     2.000  33     1.000   2     2.000
V2O4       2      4.00   -12.66    15.25    0          0.000   V2O4
 33    1.000   2     1.000
VO(OH)2    3      4.00   -11.08    29.32    0          0.000   VO(OH
 3    1.000  33     1.000   2     1.000
VF4        5      4.00    -2.00   -18.27    0          0.000   VF4
```

```
3    -2.000  16     4.000   1     4.000  33     1.000   2     1.000
VOSO4 (C   5      10.00   -13.36     8.60    0              0.000     VOSO4
29     1.000  33     1.000   2     1.000   1     2.000   3    -1.000
(VO)3(PO   5      4.00   -25.30     29.32    0              0.000     (VO)3
26   0.666667  33     1.000   2     1.000   1     2.000   3    -1.000
VOCL2      5      4.00    -4.14      1.12    0              0.000     VOCL2
13     2.000  33     1.000   2     1.000   1     2.000   3    -1.000
V2O5       3      5.00    -0.72     -4.16    0              0.000     V2O5
1    -1.000  33     1.000   3     0.500
TYUYAMUN   5      11.00     2.04    -18.30    0              0.000     TYUYA
1    -4.000  11     0.500  32     1.000  33     1.000   3     2.000
CA-VANAD   4      5.00      2.83    -10.13    0              0.000     CA-VA
1    -2.000  11     0.500  33     1.000   3     1.000
CA3(VO4)   4      5.00     19.48    -35.07    0              0.000     CA3(V
1    -4.000  11     1.500  33     1.000   3     2.000
CA2V2O7    4      5.00      8.75    -19.06    0              0.000     CA2V2
1    -3.000  11     1.000  33     1.000   3     1.500
FE-VANAD   4      6.00     -1.86     -7.37    0              0.000     FE-VA
1    -2.000  17     0.500  33     1.000   3     1.000
MG-VANAD   4      5.00      5.64    -16.33    0              0.000     MG-VA
1    -2.000  21     0.500  33     1.000   3     1.000
MG2V2O7    4      5.00     13.18    -30.50    0              0.000     MG2V2
1    -3.000  21     1.000  33     1.000   3     1.500
MN-VANAD   4      6.00      2.45    -11.05    0              0.000     MN-VA
1    -2.000  22     0.500  33     1.000   3     1.000
NH4VO3     5      2.00   -116.39    183.28    0              0.000     NH4VO
1     8.000  33     1.000   3    -2.000  23     1.000   2     8.000
NA-VANAD   4      5.00      3.71     -7.01    0              0.000     NA-VA
1    -2.000  24     1.000  33     1.000   3     1.000
NA3VO4     4      5.00     36.94    -44.42    0              0.000     NA3VO
1    -4.000  24     3.000  33     1.000   3     2.000
NA4V2O7    4      5.00     18.70    -24.03    0              0.000     NA4V2
1    -3.000  24     2.000  33     1.000   3     1.500
PB3(VO4)   4      5.00      3.07     -8.68    0              0.000     PB3(V
1    -4.000  27     1.500  33     1.000   3     2.000
PB2V2O7    4      5.00     -0.95     -3.22    0              0.000     PB2V2
1    -3.000  27     1.000  33     1.000   3     1.500
CARNOTIT   5      11.00     0.23     -8.70    0              0.000     CARNO
1    -4.000  19     1.000  32     1.000  33     1.000   3     2.000
AG-VANAD   4      5.00      0.77      0.00    0              0.000     AG-VA
1    -2.000   4     1.000  33     1.000   3     1.000
AG2HVO4    4      5.00      1.48      0.00    0              0.000     AG2HV
1    -3.000   4     2.000  33     1.000   3     2.000
AG3H2VO5   4      5.00      5.18      0.00    0              0.000     AG3H2
1    -4.000   4     3.000  33     1.000   3     3.000
VO2CL      2      5.00      2.81     -9.65    0              0.000     VO2CL
33     1.000  13     1.000
V3O5       4      10.00   -48.92     64.43    0              0.000     V3O5
1     2.000   3    -1.000   2     5.000  33     3.000
V4O7       4      14.00   -60.58     78.13    0              0.000     V4O7
1     2.000   3    -1.000   2     6.000  33     4.000
V6O13      4      26.00   -60.86     64.89    0              0.000     V6O13
1    -2.000  33     6.000   3     1.000   2     4.000
LIME       3      0.00     32.80    -46.26    0              0.000     LIME
1    -2.000  11     1.000   3     1.000
PORTLAND   3      0.00     22.67    -30.69    0              0.000     PORTL
1    -2.000  11     1.000   3     2.000
WUSTITE    4      1.89     11.69    -24.85    0              0.000     WUSTI
```

```
 1    -2.000  17     0.947   3     1.000   2     -0.106
PERICLAS   3     0.00    21.51   -36.13    0          0.000    PERIC
 1    -2.000  21     1.000   3     1.000
HERCYNIT   4     2.00    27.16   -78.36    0          0.000    HERCY
 1    -8.000  17     1.000   5     2.000   3     4.000
SPINEL     4     0.00    36.33   -89.09    0          0.000    SPINE
 1    -8.000  21     1.000   5     2.000   3     4.000
MAG-FERR   5     6.00    42.83   -86.64    0          0.000    MAG-F
 1    -8.000  21     1.000   3     4.000  17     2.000   2    -2.000
CRYOLITE   3     0.00   -31.49    10.90    0          0.000    CRYOL
 5     1.000  24     3.000  16     6.000
WOLLASTO   4     0.00    13.00   -19.50    0          0.000    WOLLA
 3    -1.000   1    -2.000  30     1.000  11     1.000
P-WOLLST   4     0.00    13.85   -21.07    0          0.000    P-WOL
 3    -1.000   1    -2.000  30     1.000  11     1.000
CA-OLIVI   3     0.00    37.65   -54.69    0          0.000    CA-OL
 1    -4.000  30     1.000  11     2.000
LARNITE    3     0.00    39.14   -57.24    0          0.000    LARNI
 1    -4.000  30     1.000  11     2.000
CA3SIO5    4     0.00    73.87  -106.33    0          0.000    CA3SI
 1    -6.000  30     1.000  11     3.000   3     1.000
MONTICEL   4     0.00    30.27   -49.42    0          0.000    MONTI
 1    -4.000  30     1.000  11     1.000  21     1.000
AKERMINI   5     0.00    47.47   -76.44    0          0.000    AKERM
 3    -1.000   1    -6.000  30     2.000  11     2.000  21     1.000
MERWINIT   4     0.00    68.54  -107.11    0          0.000    MERWI
 1    -8.000  30     2.000  21     1.000  11     3.000
KALSILIT   4     0.00    12.84   -28.92    0          0.000    KALSI
 1    -4.000  30     1.000   5     1.000  19     1.000
LEUCITE    5     0.00     6.42   -22.08    0          0.000    LEUCI
 3    -2.000   1    -4.000  30     2.000   5     1.000  19     1.000
Microcli   5     0.00     0.19   -11.58    0          0.000    MICRO
 3    -4.000   1    -4.000  30     3.000   5     1.000  19     1.000
H SANIDI   5     0.00     1.06   -14.25    0          0.000    H SAN
 3    -4.000   1    -4.000  30     3.000   5     1.000  19     1.000
NEPHELIN   4     0.00    14.22   -33.20    0          0.000    NEPHE
 1    -4.000  30     1.000   5     1.000  24     1.000
GEHLENIT   5     0.00    56.82  -116.13    0          0.000    GEHLE
 1   -10.000   5     2.000  30     1.000  11     2.000   3     3.000
LEPIDOCR   4     3.00    14.40   -10.00    0          0.000    LEPID
 1    -3.000   3     2.000  17     1.000   2    -1.000
Na-beid    5     0.00     8.20   -45.77    0          0.000    Na-be
 1    -7.332   3    -2.667   5     2.333  24     0.333  30     3.670

K-beid     5     0.00     8.06   -44.63    0          0.000    K-bei
 1    -7.332   3    -2.667   5     2.333  19     0.333  30     3.670
 1    -7.320   3    -2.680   5     0.330  19     0.330  30     3.670
Ca-beid    5     0.00     8.03   -47.17    0          0.000    Ca-be
 1    -7.333   3    -2.667   5     2.333  11     0.167  30     3.670
 1    -7.320   3    -2.680   5     0.330  11     0.165  30     3.670
Mg-beid    5     0.00     8.00   -47.98    0          0.000    Mk-be
 1    -7.333   3    -2.667   5     2.333  21     0.167  30     3.670
FE(OH)3S   4     3.00    15.70   -10.00    0          0.000    FE(OH
 3     3.000   1    -3.000  17     1.000   2    -1.000
HYDROXYA   4     0.00   -39.38   -38.92    0          0.000    HYDRO
 11    5.000  26     3.000   3     1.000   1    -1.000
FLUORAPA   3     0.00   -61.30   -14.77    0          0.000    FLUOR
 11    5.000  26     3.000  16     1.000
```

```
PREHNITE  4      0.00    33.63   -78.04    0          0.000   PREHN
 11    2.000  5    2.000  30    3.000  1    -10.000
PHILLIPS  6      0.00    1.95    0.00    0          0.000   PHILL
 24    0.500  19    0.500  5    1.000  30    3.000  1    -4.000
 3   -3.000
ILLITE    6      0.00    12.12   -49.79    0          0.000   ILLIT
 19    0.600  21    0.250  5    2.300  30    3.500  1    -8.000
 3   -2.000
MONTMORI  5      0.00    8.62   -47.99    0          0.000   MONTM
 11    0.170  5    2.330  30    3.670  1    -7.330  3    -2.670
Chlorite  5      0.00    73.72  -158.62    0          0.000   CHLOR
 21    5.000  5    2.000  30    3.000  3    6.000  1   -16.000
NA2SO3    5      4.00    4.95    -2.96    0          0.000   NA2SO
 24    2.000  29    1.000  1    2.000  2    2.000  3    -1.000
K2S03     5      4.00    8.21    -2.18    0          0.000   K2S03
 19    2.000  29    1.000  1    2.000  2    2.000  3    -1.000
CAS03.2H  5      4.00    -3.48    3.05    0          0.000   CAS03
 11    1.000  3    1.000  29    1.000  1    2.000  2    2.000
CASO3.5H  5      4.00    -3.14    -0.40    0          0.000   CASO3
 11    1.000  3    -0.500  29    1.000  1    2.000  2    2.000
MGSO3     5      4.00    6.50   -18.41    0          0.000   MGSO3
 21    1.000  29    1.000  1    2.000  2    2.000  3    -1.000
BASO3     5      4.00    -5.37    4.40    0          0.000   BASO3
 8    1.000  29    1.000  1    2.000  2    2.000  3    -1.000
AG2SO3    5      4.00   -10.18    18.77    0          0.000   AG2SO
 4    2.000  29    1.000  1    2.000  2    2.000  3    -1.000
CH4(GAS)  4      -4.00   -41.08    61.00    0          0.000   CH4(G
 10    1.000  2    8.000  1    10.000  3    -3.000
CO2(GAS)  3      4.00   -18.16    0.53    0          0.000   CO2(G
 10    1.000  1    2.000  3    -1.000
O2(GAS)   3      4.00    83.12  -136.63    0          0.000   O2(GA
 3    2.000  1    -4.000  2    -4.000
ND(OH)3S  3      0.0     18.87    0.0    0
 36    1.0    1    -3.0    3    3.0
ND(OH)3R  3      0.0     15.59   -11.66    0
 36    1.0    1    -3.0    3    3.0
ND2CO3)3  2      4.0    -33.0    0.0    0
 36    2.0    10    3.0
CAMOO4    2      0.0     -7.72    0.7    0
 11    1.0    35    1.0
BAMOO4    2      0.0     -7.46    3.0    0
 8    1.0    35    1.0

END
```

Modified data base Nick Sargent MUN 09/Dec/1990

NEW DATA BASE REFERRED TO AS HELGTHM.DAT

LOOK MIN data modified from original MINTEC data base stored as phrtherm.dat

•Halloysite struck original data follows:

```
HALLOYSI  4      0.00    8.99   -39.73    0          0.000   HALLO
 5    2.000  30    2.000  3    1.000  1    -6.000
```

•All modified data is from Helgeson (69) and Helgeson et al (1978) and is denoted by an upper case first letter followed by lower case letters i.e(Kaolinit as opposed to KAOLINIT)

•Generally modification was by replacement only. However, the original MINTEC Nontronites were completely replaced by the equivalent Beidellites.

•CHLOR-M and CHLOR-F are struck from this data base.

•All thermodynamic values of ionic species, used to back calculate thermodynamic

constants for mineral dissociations, abstracted from Robie et al (1978).

APPENDIX F Results of Mass Balance Calculations

APPENDIX F: RESULTS OF MASS BALANCE CALCULATIONS

See Appendix G for explanations of derivation of results

N_A

MODEL RUN

Anorth	Alb	Kaol	Calc	Mix1	Mix2	P PHASES		
Ca	TC	Si	Na	Cl	Mix	K "ELEMENTS"		
DEPTH	18.77	56.81	69.64	71.65	74.91	77.41	96.64	97.41
Anorth	-1.3151	-1.6587	-0.9165	-1.6904	-1.9208	-1.5658	-1.6092	-1.1063
Alb	0.6751	1.1465	1.0142	1.5376	2.3453	1.6219	2.4340	3.0426
Kaol	0.3634	-0.0056	-0.5512	-0.5540	-1.5313	-0.8039	-1.9624	-3.3357
Calc	2.0438	2.2921	1.6040	2.1409	2.0968	1.9709	1.6695	1.1197
Mix1	0.9949	0.9949	0.9945	0.9945	0.9945	0.9934	0.9928	0.9911
Mix2	0.0051	0.0051	0.0055	0.0055	0.0055	0.0066	0.0072	0.0089

DEPTH

MMOLES OF P PHASES
LOST OR ADDED TO GROUNDWATER

N_B

Anorth	Alb	Qtz	Calc	Mix1	Mix2			
Ca	TC	Si	Na	Cl	Mix			
	18.7650	56.8050	69.6350	71.6450	74.9100	77.4050	96.6350	97.4100
Anorth	-1.3151	-1.6587	-0.9165	-1.6904	-1.9208	-1.5658	-1.6092	-1.1063
Alb	0.6751	1.1465	1.0142	1.5376	2.3453	1.6219	2.4340	3.0426
Qtz	0.7269	-0.0112	-1.1024	-1.1080	-3.0626	-1.6078	-3.9249	-6.6714
Calc	2.0438	2.2921	1.6040	2.1409	2.0968	1.9709	1.6695	1.1197
Mix1	0.9949	0.9949	0.9945	0.9945	0.9945	0.9934	0.9928	0.9911
Mix2	0.0051	0.0051	0.0055	0.0055	0.0055	0.0066	0.0072	0.0089

N_C

Anorth	Micro	Qtz	Calc	Mix1	Mix2			
Ca	TC	Si	K	Cl	Mix			
DEPTH	18.7650	56.8050	69.6350	71.6450	74.9100	77.4050	96.6350	97.4100
Anorth	-1.3151	-1.6587	-0.9165	-1.6904	-1.9208	-1.5658	-1.6092	-1.1063
Micro	-0.0015	-0.0106	-0.0138	-0.0205	-0.0206	-0.0369	-0.0527	-0.0400
Qtz	2.7567	3.4599	1.9818	3.5663	4.0350	3.3687	3.5351	2.5766
Calc	2.0438	2.2921	1.6040	2.1409	2.0968	1.9709	1.6695	1.1197
Mix1	0.9949	0.9949	0.9945	0.9945	0.9945	0.9934	0.9928	0.9911
Mix2	0.0051	0.0051	0.0055	0.0055	0.0055	0.0066	0.0072	0.0089

N_D

Anorth	Micro	Qtz	Chlor	Calc	Mix1	Mix2		
Ca	TC	Si	Mg	K	Cl	Mix		
DEPTH	18.7650	56.8050	69.6350	71.6450	74.9100	77.4050	96.6350	97.4100
Anorth	-1.3151	-1.6587	-0.9165	-1.6904	-1.9208	-1.5658	-1.6092	-1.1063
Micro	-0.0015	-0.0106	-0.0138	-0.0205	-0.0206	-0.0369	-0.0527	-0.0400
Qtz	2.8669	3.5687	2.0974	3.7057	4.1983	3.5490	3.7658	2.8650
Chlor	-0.0367	-0.0363	-0.0385	-0.0464	-0.0544	-0.0601	-0.0769	-0.0961
Calc	2.0438	2.2921	1.6040	2.1409	2.0968	1.9709	1.6695	1.1197
Mix1	0.9949	0.9949	0.9945	0.9945	0.9945	0.9934	0.9928	0.9911
Mix2	0.0051	0.0051	0.0055	0.0055	0.0055	0.0066	0.0072	0.0089

N_E

Anorth	Micro	Qtz	Chlor	Calc	Mix1	Mix2		
Ca	TC	Si	Mg	K	Cl	Mix		
DEPTH	18.7650	56.8050	69.6350	71.6450	74.9100	77.4050	96.6350	97.4100
Anorth	-1.3151	-1.6587	-0.9165	-1.6904	-1.9208	-1.5658	-1.6092	-1.1063
Micro	-0.0015	-0.0106	-0.0138	-0.0205	-0.0206	-0.0369	-0.0527	-0.0400
Qtz	2.8669	3.5687	2.0974	3.7057	4.1983	3.5490	3.7658	2.8650
Chlor	-0.0367	-0.0363	-0.0385	-0.0464	-0.0544	-0.0601	-0.0769	-0.0961
Calc	2.0438	2.2921	1.6040	2.1409	2.0968	1.9709	1.6695	1.1197
Mix1	0.9949	0.9949	0.9945	0.9945	0.9945	0.9934	0.9928	0.9911
Mix2	0.0051	0.0051	0.0055	0.0055	0.0055	0.0066	0.0072	0.0089

N_F

Qtz	Alb	Kaol	Calc	Mont	Mix1	Mix2		
Ca	TC	Si	Na	Cl	Al	Mix		
DEPTH	18.7650	56.8050	69.6350	71.6450	74.9100	77.4050	96.6350	97.4100
Qtz	9.1378	10.8916	5.3030	10.3724	10.5776	9.2242	7.9743	2.8572
Alb	0.6751	1.1465	1.0142	1.5376	2.3453	1.6219	2.4340	3.0426
Kaol	8.6751	10.7944	5.7740	10.8159	11.9920	9.9195	9.8114	6.0712
Calc	2.0438	2.2921	1.6040	2.1409	2.0968	1.9709	1.6695	1.1197
Mont	-7.7[illegible]	-9.7572	-5.3914	-9.9436	-11.2986	-9.2105	-9.4660	-6.5078
Mix1	0.9949	0.9949	0.9945	0.9945	0.9945	0.9934	0.9928	0.9911
Mix2	0.0051	0.0051	0.0055	0.0055	0.0055	0.0066	0.0072	0.0089

N_G

Qtz Alb Kaol Calc Mont Mix1 Mix2

Ca TC Si Na Cl Al Mix

DEPTH	18.7650	56.8050	69.6350	71.6450	74.9100	77.4050	96.6350	97.4100
Qtz	9.1378	10.8916	5.3030	10.3724	10.5776	9.2242	7.9743	2.8572
Alb	0.6751	1.1465	1.0142	1.5376	2.3453	1.6219	2.4340	3.0426
Kaol	8.6751	10.7944	5.7740	10.8159	11.9920	9.9195	9.8114	6.0712
Calc	2.0438	2.2921	1.6040	2.1409	2.0968	1.9709	1.6695	1.1197
Mont	-7.7361	-9.7572	-5.3914	-9.9436	-11.2986	-9.2105	-9.4660	-6.5078
Mix1	0.9949	0.9949	0.9945	0.9945	0.9945	0.9934	0.9928	0.9911
Mix2	0.0051	0.0051	0.0055	0.0055	0.0055	0.0066	0.0072	0.0089

N_H

Qtz Alb An Calc Illite CO2 Mix1 Mix2

Ca TC Si Na Cl K@ Al Mix

DEPTH	18.7650	56.8050	69.6350	71.6450	74.9100	77.4050	96.6350	97.4100
Qtz	-1.2251	-2.1595	-1.8906	-2.9062	-4.5166	-3.0355	-4.5926	-5.7738
Alb	0.6751	1.1465	1.0142	1.5376	2.3453	1.6219	2.4340	3.0426
An	-0.3344	-0.5523	-0.4801	-0.7285	-1.1309	-0.7390	-1.1143	-1.4327
Calc	1.0635	1.1886	1.1715	1.1848	1.3127	1.1546	1.1895	1.4574
Illite	-0.0025	-0.0176	-0.0231	-0.0342	-0.0343	-0.0615	-0.0878	-0.0667
CO2	0.9804	1.1036	0.4327	0.9563	0.7842	0.8165	0.4802	-0.3375
Mix1	0.9949	0.9949	0.9945	0.9945	0.9945	0.9934	0.9928	0.9911
Mix2	0.0051	0.0051	0.0055	0.0055	0.0055	0.0066	0.0072	0.0089

N_I

Qtz	Alb	Micro	Calc	Mont	CO2	Mix1	Mix2	
Ca	TC	Si	Na	Cl	K@	Al	Mix	
DEPTH	18.7650	56.8050	69.6350	71.6450	74.9100	77.4050	96.6350	97.4100
Qtz	-0.8383	-1.5092	-1.3187	-2.0390	-3.1865	-2.1328	-3.2358	-4.0689
Alb	0.6751	1.1465	1.0142	1.5376	2.3453	1.6219	2.4340	3.0426
Micro	-0.0015	-0.0106	-0.0138	-0.0205	-0.0206	-0.0369	-0.0527	-0.0400
Calc	0.7778	0.7162	0.7605	0.5611	0.3454	0.5207	0.2340	0.2309
Mont	-0.2890	-0.4871	-0.4292	-0.6507	-0.9962	-0.6800	-1.0217	-1.2793
CO2	1.2660	1.5759	0.8436	1.5798	1.7514	1.4502	1.4355	0.8858
Mix1	0.9949	0.9949	0.9945	0.9945	0.9945	0.9934	0.9928	0.9911
Mix2	0.0051	0.0051	0.0055	0.0055	0.0055	0.0066	0.0072	0.0089

N_J

Qtz	Alb	Micro	Calc	Chlor	CO2	Mix1	Mix2	
Ca	TC	Si	Na	Cl	K@	Al	Mix	
DEPTH	18.7650	56.8050	69.6350	71.6450	74.9100	77.4050	96.6350	97.4100
Qtz	-0.8889	-1.5944	-1.3938	-2.1529	-3.3608	-2.2518	-3.4146	-4.2928
Alb	0.6751	1.1465	1.0142	1.5376	2.3453	1.6219	2.4340	3.0426
Micro	-0.0015	-0.0106	-0.0138	-0.0205	-0.0206	-0.0369	-0.0527	-0.0400
Calc	0.7287	0.6334	0.6875	0.4505	0.1760	0.4051	0.0603	0.0134
Chlor	-0.3366	-0.5675	-0.5000	-0.7581	-1.1605	-0.7922	-1.1902	-1.4904
CO2	1.3151	1.6587	0.9165	1.6904	1.9208	1.5658	1.6092	1.1063
Mix1	0.9949	0.9949	0.9945	0.9945	0.9945	0.9934	0.9928	0.9911
Mix2	0.0051	0.0051	0.0055	0.0055	0.0055	0.0066	0.0072	0.0089

N_K

Qtz	Alb	Micro	Calc	Chlor	illite	CO2	Mix1	Mix2
Ca	TC	Si	Na	Mg	Cl	K@	Al	Mix
DEPTH	18.7650	56.8050	69.6350	71.6450	74.9100	77.4050	96.6350	97.4100
Qtz	-1.2075	-2.1589	-1.8842	-2.9090	-4.5361	-3.0298	-4.5976	-5.7742
Alb	0.6751	1.1465	1.0142	1.5376	2.3453	1.6219	2.4340	3.0426
Micro	0.2234	0.3879	0.3323	0.5132	0.8090	0.5122	0.7823	1.0056
Calc	0.7287	0.6334	0.6875	0.4505	0.1760	0.4051	0.0603	0.0134
Chlor	-0.0180	-0.0031	-0.0097	-0.0020	0.0147	-0.0143	-0.0073	-0.0090
illite	-0.3749	-0.6640	-0.5769	-0.8896	-1.3827	-0.9152	-1.3917	-1.7428
CO2	1.3151	1.6587	0.9165	1.6904	1.9208	1.5658	1.6092	1.1063
Mix1	0.9949	0.9949	0.9945	0.9945	0.9945	0.9934	0.9928	0.9911
Mix2	0.0051	0.0051	0.0055	0.0055	0.0055	0.0066	0.0072	0.0089

R_A

Qtz	Alb	Calc	CO2	Mix1	Mix2			
Ca	Si	Na	Cl	RS	Mix			
DEPTH	18.7650	56.8050	69.6350	71.6450	74.9100	77.4050	96.6350	97.4100
Qtz	-1.9034	-3.3286	-2.9355	-4.4888	-6.9041	-4.7393	-7.1433	-8.8840
Alb	0.6751	1.1465	1.0142	1.5376	2.3453	1.6219	2.4340	3.0426
Calc	0.7287	0.6334	0.6875	0.4505	0.1760	0.4051	0.0603	0.0134
CO2	1.3994	1.7592	0.9329	1.7663	1.2942	0.9782	1.9708	0.8522
Mix1	0.9949	0.9949	0.9945	0.9945	0.9945	0.9934	0.9928	0.9911
Mix2	0.0051	0.0051	0.0055	0.0055	0.0055	0.0066	0.0072	0.0089

R_B

Qtz	Alb	Calc	CO2	kaol	Mix1	Mix2		
Ca	Si	Na	Cl	Al	RS	Mix		
DEPTH	18.7650	56.8050	69.6350	71.6450	74.9100	77.4050	96.6350	97.4100
Qtz	-1.2286	-2.1831	-1.9215	-2.9521	-4.5625	-3.1179	-4.7102	-5.8632
Alb	0.6751	1.1465	1.0142	1.5376	2.3453	1.6219	2.4340	3.0426
Calc	0.7287	0.6334	0.6875	0.4505	0.1760	0.4051	0.0603	0.0134
CO2	1.3994	1.7592	0.9329	1.7663	1.2942	0.9782	1.9708	0.8522
kaol	-0.3374	-0.5728	-0.5070	-0.7684	-1.1708	-0.8107	-1.2166	-1.5104
Mix1	0.9949	0.9949	0.9945	0.9945	0.9945	0.9934	0.9928	0.9911
Mix2	0.0051	0.0051	0.0055	0.0055	0.0055	0.0066	0.0072	0.0089

R_C

Qtz	Alb	Calc	CO2	kaol	CH2O	Mix1	Mix2	
Ca	Si	Na	Cl	Al	C	RS	Mix	
DEPTH	18.7650	56.8050	69.6350	71.6450	74.9100	77.4050	96.6350	97.4100
Qtz	-1.2286	-2.1831	-1.9215	-2.9521	-4.5625	-3.1179	-4.7102	-5.8632
Alb	0.6751	1.1465	1.0142	1.5376	2.3453	1.6219	2.4340	3.0426
Calc	0.7287	0.6334	0.6875	0.4505	0.1760	0.4051	0.0603	0.0134
CO2	1.3994	1.7592	0.9329	1.7663	1.2942	0.9782	1.9708	0.8522
kaol	-0.3374	-0.5728	-0.5070	-0.7684	-1.1708	-0.8107	-1.2166	-1.5104
CH2O	-0.0841	-0.1003	-0.0162	-0.0757	0.6268	0.5878	-0.3614	0.2543
Mix1	0.9949	0.9949	0.9945	0.9945	0.9945	0.9934	0.9928	0.9911
Mix2	0.0051	0.0051	0.0055	0.0055	0.0055	0.0066	0.0072	0.0089

R_D

Qtz	Alb	Micro	Calc	CO2	kaol	CH2O	Mix1	Mix2
Ca	Si	Na	Cl	Al	K	C	RS	Mix
DEPTH	18.7650	56.8050	69.6350	71.6450	74.9100	77.4050	96.6350	97.4100
Qtz	-1.2255	-2.1619	-1.8939	-2.9110	-4.5214	-3.0441	-4.6049	-5.7832
Alb	0.6751	1.1465	1.0142	1.5376	2.3453	1.6219	2.4340	3.0426
Micro	-0.0015	-0.0106	-0.0138	-0.0205	-0.0206	-0.0369	-0.0527	-0.0400
Calc	0.7287	0.6334	0.6875	0.4505	0.1760	0.4051	0.0603	0.0134
CO2	1.3994	1.7592	0.9329	1.7663	1.2942	0.9782	1.9708	0.8522
kaol	-0.3366	-0.5675	-0.5000	-0.7581	-1.1605	-0.7922	-1.1902	-1.4904
CH2O	-0.0843	-0.1005	-0.0164	-0.0759	0.6266	0.5876	-0.3616	0.2542
Mix1	0.9949	0.9949	0.9945	0.9945	0.9945	0.9934	0.9928	0.9911
Mix2	0.0051	0.0051	0.0055	0.0055	0.0055	0.0066	0.0072	0.0089

R_E

Calc	CO2	CH2O	Mix1	Mix2				
Ca	Cl	C	RS	Mix				
DEPTH	18.7650	56.8050	69.6350	71.6450	74.9100	77.4050	96.6350	97.4100
Calc	0.7287	0.6334	0.6875	0.4505	0.1760	0.4051	0.0603	0.0134
CO2	1.3996	1.7594	0.9331	1.7665	1.2943	0.9784	1.9710	0.8523
CH2O	-0.0843	-0.1005	-0.0164	-0.0759	0.6266	0.5876	-0.3616	0.2542
Mix1	0.9949	0.9949	0.9945	0.9945	0.9945	0.9934	0.9928	0.9911
Mix2	0.0051	0.0051	0.0055	0.0055	0.0055	0.0066	0.0072	0.0089

R_G

Calc	CO2	Mix1	Mix2					
Ca	Cl	C	Mix					
DEPTH	18.7650	56.8050	69.6350	71.6450	74.9100	77.4050	96.6350	97.4100
Calc	0.7287	0.6334	0.6875	0.4505	0.1760	0.4051	0.0603	0.0134
CO2	1.3151	1.6587	0.9165	1.6904	1.9208	1.5658	1.6092	1.1063
Mix1	0.9949	0.9949	0.9945	0.9945	0.9945	0.9934	0.9928	0.9911
Mix2	0.0051	0.0051	0.0055	0.0055	0.0055	0.0066	0.0072	0.0089

R_H

Calc	CO2	Anorth	Mix1	Mix2				
Ca	Cl	Si	C	Mix				
DEPTH	18.7650	56.8050	69.6350	71.6450	74.9100	77.4050	96.6350	97.4100
Calc	0.6677	0.5780	0.6339	0.3885	0.1101	0.3419	-0.0190	-0.1085
CO2	1.3760	1.7141	0.9701	1.7524	1.9867	1.6290	1.6886	1.2283
Anorth	0.0609	0.0554	0.0536	0.0620	0.0659	0.0632	0.0793	0.1219
Mix1	0.9949	0.9949	0.9945	0.9945	0.9945	0.9934	0.9928	0.9911
Mix2	0.0051	0.0051	0.0055	0.0055	0.0055	0.0066	0.0072	0.0089

R_I

Calc	qtz	Anorth	Mix1	Mix2				
Ca	Cl	Si	C	Mix				
DEPTH	18.7650	56.8050	69.6350	71.6450	74.9100	77.4050	96.6350	97.4100
Calc	2.0438	2.2921	1.6040	2.1409	2.0968	1.9709	1.6695	1.1197
qtz	2.7521	3.4282	1.9403	3.5047	3.9734	3.2580	3.3771	2.4565
Anorth	-1.3151	-1.6587	-0.9165	-1.6904	-1.9208	-1.5658	-1.6092	-1.1063
Mix1	0.9949	0.9949	0.9945	0.9945	0.9945	0.9934	0.9928	0.9911
Mix2	0.0051	0.0051	0.0055	0.0055	0.0055	0.0066	0.0072	0.0089

R_J

Calc	qtz	Anorth	micr	Mix1	Mix2			
Ca	Cl	Si	K	C	Mix			
DEPTH	18.7650	56.8050	69.6350	71.6450	74.9100	77.4050	96.6350	97.4100
Calc	2.0438	2.2921	1.6040	2.1409	2.0968	1.9709	1.6695	1.1197
qtz	2.7567	3.4599	1.9818	3.5663	4.0350	3.3687	3.5351	2.5766
Anorth	-1.3151	-1.6587	-0.9165	-1.6904	-1.9208	-1.5658	-1.6092	-1.1063
micr	-0.0015	-0.0106	-0.0138	-0.0205	-0.0206	-0.0369	-0.0527	-0.0400
Mix1	0.9949	0.9949	0.9945	0.9945	0.9945	0.9934	0.9928	0.9911
Mix2	0.0051	0.0051	0.0055	0.0055	0.0055	0.0066	0.0072	0.0089

R_K

Calc	qtz	Anorth	micr	Albite	Mix1	Mix2		
Ca	Cl	Si	K	Na	C	Mix		
DEPTH	18.7650	56.8050	69.6350	71.6450	74.9100	77.4050	96.6350	97.4100
Calc	2.0438	2.2921	1.6040	2.1409	2.0968	1.9709	1.6695	1.1197
qtz	0.7315	0.0205	-1.0608	-1.0464	-3.0009	-1.4970	-3.7669	-6.5513
Anorth	-1.3151	-1.6587	-0.9165	-1.6904	-1.9208	-1.5658	-1.6092	-1.1063
micr	-0.0015	-0.0106	-0.0138	-0.0205	-0.0206	-0.0369	-0.0527	-0.0400
Albite	0.6751	1.1465	1.0142	1.5376	2.3453	1.6219	2.4340	3.0426
Mix1	0.9949	0.9949	0.9945	0.9945	0.9945	0.9934	0.9928	0.9911
Mix2	0.0051	0.0051	0.0055	0.0055	0.0055	0.0066	0.0072	0.0089

R_L

Calc	qtz	Anorth	micr	Chlor	Mix1	Mix2		
Ca	Cl	Si	K	Mg	C	Mix		
DEPTH	18.7650	56.8050	69.6350	71.6450	74.9100	77.4050	96.6350	97.4100
Calc	2.0438	2.2921	1.6040	2.1409	2.0968	1.9709	1.6695	1.1197
qtz	2.8669	3.5687	2.0974	3.7057	4.1983	3.5490	3.7658	2.8650
Anorth	-1.3151	-1.6587	-0.9165	-1.6904	-1.9208	-1.5658	-1.6092	-1.1063
micr	-0.0015	-0.0106	-0.0138	-0.0205	-0.0206	-0.0369	-0.0527	-0.0400
Chlor	-0.0367	-0.0363	-0.0385	-0.0464	-0.0544	-0.0601	-0.0769	-0.0961
Mix1	0.9949	0.9949	0.9945	0.9945	0.9945	0.9934	0.9928	0.9911
Mix2	0.0051	0.0051	0.0055	0.0055	0.0055	0.0066	0.0072	0.0089

R_M

Calc qtz Anorth micr Kaol Mix1 Mix2

Ca Cl Si K Al C Mix

DEPTH	18.7650	56.8050	69.6350	71.6450	74.9100	77.4050	96.6350	97.4100
Calc	2.0438	2.2921	1.6040	2.1409	2.0968	1.9709	1.6695	1.1197
qtz	-2.5074	-3.1979	-1.7126	-3.2380	-3.6965	-2.9693	-3.0089	-1.9725
Anorth	-1.3151	-1.6587	-0.9165	-1.6904	-1.9208	-1.5658	-1.6092	-1.1063
micr	-0.0015	-0.0106	-0.0138	-0.0205	-0.0206	-0.0369	-0.0527	-0.0400
Kaol	2.6320	3.3289	1.8472	3.4022	3.8658	3.1690	3.2720	2.2745
Mix1	0.9949	0.9949	0.9945	0.9945	0.9945	0.9934	0.9928	0.9911
Mix2	0.0051	0.0051	0.0055	0.0055	0.0055	0.0066	0.0072	0.0089

R_N

Calc qtz Anorth micr illite Kaol Mix1 Mix2

Ca Cl Si K Al Mg C Mix

DEPTH	18.7650	56.8050	69.6350	71.6450	74.9100	77.4050	96.6350	97.4100
Calc	2.0438	2.2921	1.6040	2.1409	2.0968	1.9709	1.6695	1.1197
qtz	-3.7563	-4.4308	-3.0221	-4.8171	-5.5462	-5.0125	-5.6230	-5.2415
Anorth	-1.3151	-1.6587	-0.9165	-1.6904	-1.9208	-1.5658	-1.6092	-1.1063
micr	0.4393	0.4246	0.4483	0.5368	0.6323	0.6842	0.8700	1.1138
illite	-0.7346	-0.7252	-0.7703	-0.9289	-1.0881	-1.2019	-1.5377	-1.9230
Kaol	3.8809	4.5618	3.1567	4.9813	5.7155	5.2122	5.8861	5.5436
Mix1	0.9949	0.9949	0.9945	0.9945	0.9945	0.9934	0.9928	0.9911
Mix2	0.0051	0.0051	0.0055	0.0055	0.0055	0.0066	0.0072	0.0089

R_P

Calc	CO2	Anorth	Mix1	Mix2				
Ca	Cl	Si	C	Mix				
DEPTH	18.7650	56.8050	69.6350	71.6450	74.9100	77.4050	96.6350	97.4100
Calc	0.6677	0.5780	0.6339	0.3885	0.1101	0.3419	-0.0190	-0.1085
CO2	1.3760	1.7141	0.9701	1.7524	1.9867	1.6290	1.6886	1.2283
Anorth	0.0609	0.0554	0.0536	0.0620	0.0659	0.0632	0.0793	0.1219
Mix1	0.9949	0.9949	0.9945	0.9945	0.9945	0.9934	0.9928	0.9911
Mix2	0.0051	0.0051	0.0055	0.0055	0.0055	0.0066	0.0072	0.0089

R_Q

Calc	CO2	Anorth	micr	Mix1	Mix2			
Ca	Cl	Si	K	C	Mix			
DEPTH	18.7650	56.8050	69.6350	71.6450	74.9100	77.4050	96.6350	97.4100
Calc	0.6654	0.5622	0.6131	0.3577	0.0793	0.2865	-0.0980	-0.1686
CO2	1.3783	1.7299	0.9909	1.7832	2.0175	1.6844	1.7676	1.2883
Anorth	0.0632	0.0712	0.0744	0.0928	0.0968	0.1186	0.1583	0.1820
micr	-0.0015	-0.0106	-0.0138	-0.0205	-0.0206	-0.0369	-0.0527	-0.0400
Mix1	0.9949	0.9949	0.9945	0.9945	0.9945	0.9934	0.9928	0.9911
Mix2	0.0051	0.0051	0.0055	0.0055	0.0055	0.0066	0.0072	0.0089

R_S

Calc	CO2	Anorth	micr	Chlor	Mix1	Mix2		
Ca	Cl	Si	K	Mg	C	Mix		
DEPTH	18.7650	56.8050	69.6350	71.6450	74.9100	77.4050	96.6350	97.4100
Calc	0.6103	0.5078	0.5554	0.2881	-0.0023	0.1964	-0.2134	-0.3128
CO2	1.4334	1.7843	1.0487	1.8528	2.0991	1.7745	1.8829	1.4325
Anorth	0.1183	0.1256	0.1321	0.1624	0.1784	0.2087	0.2737	0.3262
micr	-0.0015	-0.0106	-0.0138	-0.0205	-0.0206	-0.0369	-0.0527	-0.0400
Chlor	-0.0367	-0.0363	-0 0385	-0.0464	-0.0544	-0.0601	-0.0769	-0.0961
Mix1	0.9949	0.9949	0.9945	0.9945	0.9945	0.9934	0.9928	0.9911
Mix2	0.0051	0.0051	0.0055	0.0055	0.0055	0.0066	0.0072	0.0089

R_T

Calc	CO2	Anorth	micr	Kaol	Mix1	Mix2		
Ca	Cl	Si	K	Al	C	Mix		
DEPTH	18.7650	56.8050	69.6350	71.6450	74.9100	77.4050	96.6350	97.4100
Calc	0.7901	0.6931	0.7477	0.5219	0.2485	0.4862	0.1651	0.1335
CO2	1.2537	1.5990	0.8563	1.6190	1.8483	1.4846	1.5044	0.9862
Anorth	-0.0614	-0.0598	-0.0602	-0.0714	-0.0725	-0.0812	-0.1048	-0.1201
micr	-0.0015	-0.0106	-0.0138	-0.0205	-0.0206	-0.0369	-0.0527	-0.0400
Kaol	0.1246	0.1310	0.1346	0.1641	0.1693	0.1997	0.2631	0.3021
Mix1	0.9949	0.9949	0.9945	0.9945	0.9945	0.9934	0.9928	0.9911
Mix2	0.0051	0.0051	0.0055	0.0055	0.0055	0.0066	0.0072	0.0089

R_U

Calc	CO2	Anorth	micr	Illite	Kaol	Mix1	Mix2	
Ca	Cl	Si	K	Al	Mg	C	Mix	
DEPTH	18.7650	56.8050	69.6350	71.6450	74.9100	77.4050	96.6350	97.4100
Calc	0.1656	0.0767	0.0930	-0.2677	-0.6763	-0.5354	-1.1420	-1.5010
CO2	1.8781	2.2154	1.5110	2.4086	2.7731	2.5063	2.8115	2.6208
Anorth	0.5630	0.5567	0.5945	0.7181	0.8524	0.9405	1.2023	1.5145
micr	0.4393	0.4246	0.4483	0.5368	0.6323	0.6842	0.8700	1.1138
Illite	-0.7346	-0.7252	-0.7703	-0.9289	-1.0881	-1.2019	-1.5377	-1.9230
Kaol	0.1246	0.1310	0.1346	0.1641	0.1693	0.1997	0.2631	0.3021
Mix1	0.9949	0.9949	0.9945	0.9945	0.9945	0.9934	0.9928	0.9911
Mix2	0.0051	0.0051	0.0055	0.0055	0.0055	0.0066	0.0072	0.0089

R_V

Calc	CO2	Anorth	micr	chlor	mont	Kaol	Mix1	Mix2
Ca	Cl	Si	K	Al	Na	Mg	C	Mix
DEPTH	18.7650	56.8050	69.6350	71.6450	74.9100	77.4050	96.6350	97.4100
Calc	2.7373	4.0132	3.6816	4.9757	7.0503	5.1788	7.2139	8.9448
CO2	-0.6936	-1.7211	-2.0776	-2.8348	-4.9536	-3.2079	-5.5444	-7.8251
Anorth	-2.0087	-3.3798	-2.9941	-4.5252	-6.8743	-4.7737	-7.1536	-8.9314
micr	-0.0015	-0.0106	-0.0138	-0.0205	-0.0206	-0.0369	-0.0527	-0.0400
chlor	-0.0367	-0.0363	-0.0385	-0.0464	-0.0544	-0.0601	-0.0769	-0.0961
mont	3.9710	6.7438	5.9660	9.0446	13.7960	9.5406	14.3176	17.8978
Kaol	-5.1598	-8.8695	-7.8213	-11.9091	-18.2630	-12.5246	-18.8456	-23.5848
Mix1	0.9949	0.9949	0.9945	0.9945	0.9945	0.9934	0.9928	0.9911
Mix2	0.0051	0.0051	0.0055	0.0055	0.0055	0.0066	0.0072	0.0089

R_W

Calc	CO2	Anorth	micr	alb	ill	Kaol	Mix1	Mix2
Ca	Cl	Si	K	Al	Na	Mg	C	Mix
DEPTH	18.7650	56.8050	69.6350	71.6450	74.9100	77.4050	96.6350	97.4100
Calc	1.5377	1.4530	1.5783	1.2086	0.8006	1.2288	0.7757	0.8931
CO2	0.5169	0.8499	0.0375	0.9439	1.3078	0.7560	0.9090	0.2455
Anorth	-0.7551	-0.7654	-0.8322	-0.6998	-0.5662	-0.7538	-0.6392	-0.7850
micr	-1.1944	-1.2196	-1.3274	-1.2322	-1.1376	-1.4371	-1.4435	-1.7592
alb	0.6751	1.1465	1.0142	1.5376	2.3453	1.6219	2.4340	3.0426
ill	0.3785	0.3951	0.4397	0.2765	0.1179	0.2436	0.0386	0.0346
Kaol	-1.2255	-2.1619	-1.8939	-2.9110	-4.5214	-3.0441	-4.6049	-5.7832
Mix1	0.9949	0.9949	0.9945	0.9945	0.9945	0.9934	0.9928	0.9911
Mix2	0.0051	0.0051	0.0055	0.0055	0.0055	0.0066	0.0072	0.0089

R_X

Calc	qtz	Anorth	micr	alb	ill	Kaol	Mix1	Mix2
Ca	Cl	Si	K	Al	Na	Mg	C	Mix
DEPTH	18.7650	56.8050	69.6350	71.6450	74.9100	77.4050	96.6350	97.4100
Calc	2.0438	2.2921	1.6040	2.1409	2.0968	1.9709	1.6695	1.1197
qtz	-4.4314	-5.5773	-4.0363	-6.3547	-7.8916	-6.6344	-8.0570	-8.2842
Anorth	-1.3151	-1.6587	-0.9165	-1.6904	-1.9208	-1.5658	-1.6092	-1.1063
micr	0.4393	0.4246	0.4483	0.5368	0.6323	0.6842	0.8700	1.1138
alb	0.6751	1.1465	1.0142	1.5376	2.3453	1.6219	2.4340	3.0426
ill	-0.7346	-0.7252	-0.7703	-0.9289	-1.0881	-1.2019	-1.5377	-1.9230
Kaol	3.2059	3.4154	2.1424	3.4437	3.3702	3.5903	3.4521	2.5010
Mix1	0.9949	0.9949	0.9945	0.9945	0.9945	0.9934	0.9928	0.9911
Mix2	0.0051	0.0051	0.0055	0.0055	0.0055	0.0066	0.0072	0.0089

R_Y

Calc	CO2	Anorth	micr	Xna/Mg	ill	Kaol	Mix1	Mix2
Ca	Cl	Si	K	Al	Na	Mg	C	Mix
DEPTH	18.7650	56.8050	69.6350	71.6450	74.9100	77.4050	96.6350	97.4100
Calc	1.3086	2.0255	1.8182	2.3506	3.3151	2.2333	3.0144	3.6818
CO2	0.7460	0.2775	-0.2025	-0.1981	-1.2067	-0.2484	-1.3297	-2.5432
Anorth	-0.6069	-1.4192	-1.1600	-1.9293	-3.1683	-1.8632	-2.9923	-3.7159
micr	-0.3904	-0.9709	-0.7900	-1.3295	-2.2033	-1.2875	-2.0786	-2.5718
Xna/Mg	-0.3375	-0.5732	-0.5071	-0.7688	-1.1727	-0.8110	-1.2170	-1.5213
ill	0.6520	1.6044	1.2979	2.1858	3.6421	2.0893	3.3820	4.2265
Kaol	0.1246	0.1310	0.1346	0.1641	0.1693	0.1997	0.2631	0.3021
Mix1	0.9949	0.9949	0.9945	0.9945	0.9945	0.9934	0.9928	0.9911
Mix2	0.0051	0.0051	0.0055	0.0055	0.0055	0.0066	0.0072	0.0089

S_F

Anorth	Alb	Micr	Calc	Musc	NaCl	Mix1	Mix2	
Ca	TC	Si	Na	K	Al	Cl	Mix	
DEPTH	18.7650	56.8050	69.6350	71.6450	74.9100	77.4050	96.6350	97.4100
Anorth	-1.3476	-1.6596	-0.8694	-1.6439	-1.7875	-1.4993	-1.4420	-0.8154
Alb	0.9807	1.1550	0.5710	1.1003	1.0914	0.9964	0.8600	0.3052
Micr	-0.9201	-1.1001	-0.5173	-1.0386	-1.0268	-0.9332	-0.7804	-0.1929
Calc	2.0357	2.2919	1.6158	2.1525	2.1300	1.9874	1.7112	1.1922
Musc	0.8783	1.0884	0.5618	1.0757	1.1714	0.9786	0.9351	0.5135
NaCl	-2.1529	-0.0604	3.1224	3.0798	8.8325	4.4061	11.0870	19.2823
Mix1	0.9911	0.9948	1.0000	1.0000	1.0101	1.0012	1.0124	1.0252
Mix2	0.0089	0.0052	0.0000	0.0000	-0.0101	-0.0012	-0.0124	-0.0252

S_G

Anorth Alb CO2 Calc NaCl Mix1 Mix2

Ca TC Si Na Al Cl Mix

DEPTH	18.7650	56.8050	69.6350	71.6450	74.9100	77.4050	96.6350	97.4100
Anorth	-0.0304	-0.0273	-0.0268	-0.0307	-0.0307	-0.0316	-0.0396	-0.0452
Alb	0.0611	0.0554	0.0539	0.0622	0.0651	0.0637	0.0800	0.1124
CO2	1.2195	1.5155	0.7877	1.5029	1.6477	1.3686	1.3195	0.7497
Calc	0.8406	0.8055	0.8418	0.6770	0.5094	0.6435	0.4123	0.4476
NaCl	4.3250	7.6851	6.7645	10.3924	16.0616	10.9762	16.5816	20.6407
Mix1	1.0026	1.0085	1.0065	1.0129	1.0229	1.0128	1.0222	1.0276
Mix2	-0.0026	-0.0085	-0.0065	-0.0129	-0.0229	-0.0128	-0.0222	-0.0276

S_H

Anorth Alb CO2 Calc NaCl Illite Mix1 Mix2

Ca TC Si Na Al Mg Cl Mix

DEPTH	18.7650	56.8050	69.6350	71.6450	74.9100	77.4050	96.6350	97.4100
Anorth	1.2209	2.9607	2.4294	4.0781	6.7773	4.0171	6.4429	8.0124
Alb	0.9438	2.1632	1.7866	2.9607	4.8678	2.9198	4.6530	5.7966
CO2	2.5646	4.7274	3.4281	5.9198	8.9662	5.7208	8.2879	9.4114
Calc	-0.5280	-2.4622	-1.8445	-3.8165	-6.9362	-3.7843	-6.6772	-8.3646
NaCl	-1.8931	-7.1622	-5.4408	-10.0247	-17.7684	-9.1420	-15.6305	-19.3989
Illite	-1.4719	-3.5146	-2.8892	-4.8331	-8.0082	-4.7624	-7.6252	-9.4781
Mix1	0.9916	0.9823	0.9849	0.9768	0.9631	0.9773	0.9652	0.9568
Mix2	0.0084	0.0177	0.0151	0.0232	0.0369	0.0227	0.0348	0.0432

S_I

Anorth	Alb	CO2	Calc	NaCl	Micr	Illite	Mix1	Mix2
Ca	TC	Si	Na	Al	Mg	K	Cl	Mix
DEPTH	18.7650	56.8050	69.6350	71.6450	74.9100	77.4050	96.6350	97.4100
Anorth	-1.0507	-2.3123	-1.9138	-3.1480	-5.1739	-3.0954	-4.9126	-6.1723
Alb	-0.0303	-0.0978	-0.0758	-0.1378	-0.2569	-0.1301	-0.2163	-0.2859
CO2	0.1895	-0.7858	-1.1131	-1.6357	-3.5297	-1.7158	-3.5851	-5.4197
Calc	1.8730	3.1109	2.7460	3.8209	5.6954	3.7331	5.3247	6.6275
NaCl	4.9683	8.7647	7.6779	11.8016	18.3301	12.3411	18.6686	23.4456
Micr	-0.6288	-1.4596	-1.2023	-2.0003	-3.3083	-1.9688	-3.1434	-3.9265
Illite	1.2003	2.6883	2.2200	3.6674	6.0508	3.6045	5.7330	7.2082
Mix1	1.0037	1.0104	1.0081	1.0154	1.0269	1.0153	1.0258	1.0326
Mix2	-0.0037	-0.0104	-0.0081	-0.0154	-0.0269	-0.0153	-0.0258	-0.0326

S_J

Anorth	Alb	CO2	Calc	NaCl	Micr	Mont	Illite	Mix1	Mix2
Ca	TC	Si	Na	Al	Mg	K	RS	Cl	Mix
DEPTH	18.7650	56.8050	69.6350	71.6450	74.9100	77.4050	96.6350	97.4100	
Anorth	1.8787	2.5550	1.9034	3.0353	-0.2121	-0.7882	6.3754	3.5872	
Alb	0.8292	1.3303	1.0442	1.6764	1.1989	0.5469	3.0956	2.5776	
CO2	3.0207	3.9184	2.5763	4.3406	1.2659	0.5141	7.3248	4.0129	
Calc	-0.9810	-1.6312	-0.9730	-2.2034	0.8612	1.4852	-5.6729	-2.8809	
NaCl	-1.0859	-1.2947	-0.2113	-0.9777	8.0754	7.5727	-4.6605	3.2755	
Micr	0.6727	0.7029	0.4937	0.7470	-1.1037	-0.9437	1.8719	0.4096	
Mont	-1.1144	-1.8517	-1.4522	-2.3524	-1.8877	-0.8778	-4.2944	-3.7129	
Illite	-1.1575	-1.2295	-0.8525	-1.3096	2.0570	1.7473	-3.3528	-0.6473	
Mix1	0.9930	0.9926	0.9941	0.9928	1.0088	1.0068	0.9846	0.9969	
Mix2	0.0070	0.0074	0.0059	0.0072	-0.0088	-0.0068	0.0154	0.0031	

S_K

Anorth	Alb	CO2	Calc	NaCl	Micr	Na-Beid	Mix1	Mix2
Ca	TC	Si	Na	Al	Mg	K	Cl	Mix
DEPTH	18.7650	56.8050	69.6350	71.6450	74.9100	77.4050	96.6350	97.4100
Anorth	0.9059	2.0696	1.7048	2.8299	4.6889	2.7799	4.4322	5.5772
Alb	0.7829	1.7233	1.4281	2.3466	3.8421	2.3117	3.6674	4.5972
CO2	2.1925	3.7002	2.5915	4.4843	6.5676	4.2992	5.9819	6.6090
Calc	-0.1417	-1.4011	-0.9800	-2.3345	-4.4603	-2.3167	-4.2975	-5.4707
NaCl	1.8863	1.8622	1.9777	2.3850	2.7938	3.0861	3.9483	4.9376
Micr	0.0337	0.0243	0.0231	0.0241	0.0317	0.0208	0.0212	0.0523
Na-Beid	-1.1279	-2.5261	-2.0861	-3.4462	-5.6858	-3.3870	-5.3872	-6.7734
Mix1	0.9983	0.9982	0.9980	0.9987	0.9995	0.9989	0.9998	0.9998
Mix2	0.0017	0.0018	0.0020	0.0013	0.0005	0.0011	0.0002	0.0002

S_L

Anorth	Alb	CO2	Calc	NaCl	Micr	Na-Beid	Mix1	Mix2
Ca	TC	Si	Na	Al	Mg	K	Cl	Mix
DEPTH	18.7650	56.8050	69.6350	71.6450	74.9100	77.4050	96.6350	97.4100
Anorth	0.9059	2.0696	1.7048	2.8299	4.6889	2.7799	4.4322	5.5772
Alb	0.7829	1.7233	1.4281	2.3466	3.8421	2.3117	3.6674	4.5972
CO2	2.1925	3.7002	2.5915	4.4843	6.5676	4.2992	5.9819	6.6090
Calc	-0.1417	-1.4011	-0.9800	-2.3345	-4.4603	-2.3167	-4.2975	-5.4707
NaCl	1.8863	1.8622	1.9777	2.3850	2.7938	3.0861	3.9483	4.9376
Micr	0.0337	0.0243	0.0231	0.0241	0.0317	0.0208	0.0212	0.0523
Na-Beid	-1.1279	-2.5261	-2.0861	-3.4462	-5.6858	-3.3870	-5.3872	-6.7734
Mix1	0.9983	0.9982	0.9980	0.9987	0.9995	0.9989	0.9998	0.9998
Mix2	0.0017	0.0018	0.0020	0.0013	0.0005	0.0011	0.0002	0.0002

S_M

Anorth	Alb	Calc	NaCl	qtz	Na-Beid	Mix1	Mix2	
Ca	TC	Si	Na	Al	Mg	Cl	Mix	
DEPTH	18.7650	56.8050	69.6350	71.6450	74.9100	77.4050	96.6350	97.4100
Anorth	-1.2867	-1.6306	-0.8867	-1.6544	-1.8786	-1.5192	-1.5497	-1.0318
Alb	0.0460	0.4852	0.5600	0.8470	1.6465	0.8744	1.6689	2.3844
Calc	2.0509	2.2991	1.6115	2.1499	2.1073	1.9825	1.6843	1.1383
NaCl	1.8863	1.8622	1.9777	2.3850	2.7938	3.0861	3.9483	4.9376
qtz	-1.4239	-2.4574	-1.7108	-2.9870	-4.3805	-2.8674	-4.0026	-4.3742
Na-Beid	1.0848	1.1918	0.5209	1.0569	0.9075	0.9290	0.6143	-0.1283
Mix1	0.9983	0.9982	0.9980	0.9987	0.9995	0.9989	0.9998	0.9998
Mix2	0.0017	0.0018	0.0020	0.0013	0.0005	0.0011	0.0002	0.0002

S_N

Anorth	Alb	CO2	Calc	NaCl	Na-Beid	Mix1	Mix2	
Ca	TC	Si	Na	Al	Mg	Cl	Mix	
DEPTH	18.7650	56.8050	69.6350	71.6450	74.9100	77.4050	96.6350	97.4100
Anorth	0.8227	2.0099	1.6478	2.7706	4.6109	2.7287	4.3801	5.4484
Alb	0.7495	1.6993	1.4053	2.3228	3.8108	2.2911	3.6465	4.5455
CO2	2.1094	3.6405	2.5345	4.4251	6.4895	4.2480	5.9297	6.4802
Calc	-0.0585	-1.3414	-0.9231	-2.2752	-4.3822	-2.2655	-4.2454	-5.3419
NaCl	1.8863	1.8622	1.9777	2.3850	2.7938	3.0861	3.9483	4.9376
Na-Beid	-1.0278	-2.4541	-2.0174	-3.3748	-5.5918	-3.3254	-5.3244	-6.6182
Mix1	0.9983	0.9982	0.9980	0.9987	0.9995	0.9989	0.9998	0.9998
Mix2	0.0017	0.0018	0.0020	0.0013	0.0005	0.0011	0.0002	0.0002

S_O

qtz Alb CO2 Calc NaCl Na-Beid Mix1 Mix2

Ca TC Si Na Al Mg Cl Mix

DEPTH	18.7650	56.8050	69.6350	71.6450	74.9100	77.4050	96.6350	97.4100
qtz	-0.5554	-1.3567	-1.1123	-1.8702	-3.1124	-1.8419	-2.9566	-3.6777
Alb	0.4751	1.0290	0.8557	1.3988	2.2730	1.3811	2.1857	2.7285
CO2	1.2867	1.6306	0.8867	1.6544	1.8786	1.5192	1.5497	1.0318
Calc	0.7642	0.6685	0.7248	0.4954	0.2287	0.4632	0.1347	0.1065
NaCl	1.8863	1.8622	1.9777	2.3850	2.7938	3.0861	3.9483	4.9376
Na-Beid	-0.2038	-0.4413	-0.3671	-0.6000	-0.9740	-0.5925	-0.9377	-1.1616
Mix1	0.9983	0.9982	0.9980	0.9987	0.9995	0.9989	0.9998	0.9998
Mix2	0.0017	0.0018	0.0020	0.0013	0.0005	0.0011	0.0002	0.0002

T_A

Anorth Alb CO2 Calc NaCl Micr S-min Na-Beid Mix1 Mix2

Ca TC Si Na Al Mg RS SO4 Cl Mix

DEPTH	18.7650	56.8050	69.6350	71.6450	74.9100	77.4050	96.6350	97.4100
Anorth	0.7699	0.6689	0.6127	0.4931	-0.4762	-0.2416	0.1260	-1.4470
Alb	0.7283	1.1613	0.9900	1.4090	1.7698	1.0994	1.9397	1.7791
CO2	2.0566	2.2995	1.4994	2.1476	1.4024	1.2776	1.6756	-0.4151
Calc	-0.0057	-0.0004	0.1121	0.0023	0.7049	0.7048	0.0087	1.5534
NaCl	1.8863	1.8622	1.9777	2.3850	2.7938	3.0861	3.9483	4.9376
Micr	-0.0214	-0.5445	-0.4203	-0.9247	-2.0655	-1.2060	-1.7273	-2.7997
S-min	0.1499	0.1630	0.1880	0.1755	0.1967	0.2378	0.4511	1.1216
Na-Beid	-0.9642	-0.8385	-0.7703	-0.6308	0.5373	0.2533	-0.1990	1.6894
Mix1	0.9983	0.9982	0.9980	0.9987	0.9995	0.9989	0.9998	0.9998
Mix2	0.0017	0.0018	0.0020	0.0013	0.0005	0.0011	0.0002	0.0002

T_B

Anorth	Alb	CO2	Calc	NaCl	Musc	Micr	S-min	Na-Beid	Mix1	Mix2
Ca	TC	Si	Na	Al	Mg	K	RS	SO4	Cl	Mix
DEPTH	18.7650	56.8050	69.6350	71.6450	74.9100	77.4050	96.6350	97.4100		
Anorth	-1.7051	-2.0493	-1.3058	-2.0719	-2.2946	-1.9364	-1.9648	-1.4470		
Alb	-2.8599	-2.2667	-1.9688	-1.5384	-0.5628	-0.6788	0.7195	2.8262		
CO2	-0.4185	-0.4186	-0.4191	-0.4175	-0.4160	-0.4172	-0.4152	-0.4151		
Calc	2.4693	2.7177	2.0305	2.5673	2.5232	2.3996	2.0995	1.5534		
NaCl	4.0545	4.0120	3.8974	4.3164	4.7237	4.4010	4.9271	4.9376		
Musc	-0.7096	-0.3118	-0.4477	0.0216	0.5431	0.3600	0.9928	1.7400		
Micr	0.7096	0.3118	0.4477	-0.0216	-0.5431	-0.3600	-0.9928	-1.7400		
S-min	1.0759	1.0737	1.0678	1.0895	1.1105	1.0938	1.1211	1.1216		
Na-Beid	3.3003	2.9999	2.3503	2.4205	1.7465	1.6447	0.5260	-1.4551		
Mix1	0.9983	0.9982	0.9980	0.9987	0.9995	0.9989	0.9998	0.9998		
Mix2	0.0017	0.0018	0.0020	0.0013	0.0005	0.0011	0.0002	0.0002		

T_C

Anorth	Alb	CO2	Calc	NaCl	Micr	S-min	Qtz	Na-Beid	Mix1	Mix2
Ca	TC	Si	Na	Al	Mg	K	RS	SO4	Cl	Mix
DEPTH	18.7650	56.8050	69.6350	71.6450	74.9100	77.4050	96.6350	97.4100		
Anorth	0.7699	0.6689	0.6127	0.4931	-0.4762	-0.2416	0.1260	-1.4470		
Alb	0.7376	1.2562	1.0639	1.5673	2.1195	1.3040	2.2313	2.2546		
CO2	2.0566	2.2995	1.4994	2.1476	1.4024	1.2776	1.6756	-0.4151		
Calc	-0.0057	-0.0004	0.1121	0.0023	0.7049	0.7048	0.0087	1.5534		
NaCl	1.8863	1.8622	1.9777	2.3850	2.7938	3.0861	3.9483	4.9376		
Micr	0.0337	0.0243	0.0231	0.0241	0.0317	0.0208	0.0212	0.0523		
S-min	0.1499	0.1630	0.1880	0.1755	0.1967	0.2378	0.4511	1.1216		
Qtz	-0.0917	-0.9455	-0.7372	-1.5773	-3.4865	-2.0396	-2.9067	-4.7414		
Na-Beid	-0.9918	-1.1233	-0.9923	-1.1059	-0.5129	-0.3610	-1.0745	0.2613		
Mix1	0.9983	0.9982	0.9980	0.9987	0.9995	0.9989	0.9998	0.9998		
Mix2	0.0017	0.0018	0.0020	0.0013	0.0005	0.0011	0.0002	0.0002		

T_D

Anorth	Alb	CO2	Calc	NaCl	Micr	S-min	Kao	Na-Beid	Mix1	Mix2
Ca	TC	Si	Na	Al	Mg	K	RS	SO4	Cl	Mix

DEPTH	18.7650	56.8050	69.6350	71.6450	74.9100	77.4050	96.6350	97.4100
Anorth	0.7699	0.6689	0.6127	0.4931	-0.4762	-0.2416	0.1260	-1.4470
Alb	0.7829	1.7233	1.4281	2.3466	3.8421	2.3117	3.6674	4.5972
CO2	2.0566	2.2995	1.4994	2.1476	1.4024	1.2776	1.6756	-0.4151
Calc	-0.0057	-0.0004	0.1121	0.0023	0.7049	0.7048	0.0087	1.5534
NaCl	1.8863	1.8622	1.9777	2.3850	2.7938	3.0861	3.9483	4.9376
Micr	0.0337	0.0243	0.0231	0.0241	0.0317	0.0208	0.0212	0.0523
S-min	0.1499	0.1630	0.1880	0.1755	0.1967	0.2378	0.4511	1.1216
Kao	0.1359	1.4007	1.0921	2.3368	5.1652	3.0215	4.3062	7.0242
Na-Beid	-1.1279	-2.5261	-2.0861	-3.4462	-5.6858	-3.3870	-5.3872	-6.7734
Mix1	0.9983	0.9982	0.9980	0.9987	0.9995	0.9989	0.9998	0.9998
Mix2	0.0017	0.0018	0.0020	0.0013	0.0005	0.0011	0.0002	0.0002

F-25

T_E										
Anorth	Alb	CO2	Calc	NaCl	Micr	S-min	Mont	Na-Beid	Mix1	Mix2
Ca	TC	Si	Na	Al	Mg	K	RS	SO4	Cl	Mix
DEPTH	18.7650	56.8050	69.6350	71.6450	74.9100	77.4050	96.6350	97.4100		
Anorth	0.7933	0.9094	0.8002	0.8943	0.4106	0.2772	0.8653	-0.2410		
Alb	0.6920	0.7867	0.6979	0.7841	0.3885	0.2914	0.7881	-0.0994		
CO2	2.0566	2.2995	1.4994	2.1476	1.4024	1.2776	1.6756	-0.4151		
Calc	-0.0057	-0.0004	0.1121	0.0023	0.7049	0.7048	0.0087	1.5534		
NaCl	1.8863	1.8622	1.9777	2.3850	2.7938	3.0861	3.9483	4.9376		
Micr	0.0337	0.0243	0.0231	0.0241	0.0317	0.0208	0.0212	0.0523		
S-min	0.1499	0.1630	0.1880	0.1755	0.1967	0.2378	0.4511	1.1216		
Mont	-0.1373	-1.4146	-1.1030	-2.3600	-5.2166	-3.0516	-4.3491	-7.0940		
Na-Beid	-0.8550	0.2864	0.1068	1.2459	4.6854	2.6799	3.2593	7.3305		
Mix1	0.9983	0.9982	0.9980	0.9987	0.9995	0.9989	0.9998	0.9998		
Mix2	0.0017	0.0018	0.0020	0.0013	0.0005	0.0011	0.0002	0.0002		

T_F										
Anorth	Alb	CO2	Calc	NaCl	Micr	S-min	illite	Na-Beid	Mix1	Mix2
Ca	TC	Si	Na	Al	Mg	K	RS	SO4	Cl	Mix
DEPTH	18.7650	56.8050	69.6350	71.6450	74.9100	77.4050	96.6350	97.4100		
Anorth	0.7739	0.7093	0.6442	0.5605	-0.3272	-0.1544	0.2502	-1.2444		
Alb	0.7280	1.1579	0.9873	1.4034	1.7574	1.0922	1.9294	1.7622		
CO2	2.0574	2.3076	1.5057	2.1610	1.4322	1.2951	1.7005	-0.3746		
Calc	-0.0057	-0.0004	0.1121	0.0023	0.7048	0.7048	0.0086	1.5533		
NaCl	2.0942	4.0049	3.6484	5.9597	10.6954	7.7083	10.5359	15.6830		
Micr	-0.0110	-0.4364	-0.3360	-0.7444	-1.6670	-0.9729	-1.3950	-2.2577		
S-min	0.1607	0.2738	0.2744	0.3604	0.6054	0.4769	0.7918	1.6774		
illite	0.0810	0.8345	0.6507	1.3922	3.0774	1.8002	2.5656	4.1849		
Na-Beid	-1.0518	-1.7419	-1.4747	-2.1379	-2.7941	-1.6954	-2.9763	-2.8409		
Mix1	0.9986	1.0020	1.0010	1.0051	1.0134	1.0071	1.0115	1.0188		
Mix2	0.0014	-0.0020	-0.0010	-0.0051	-0.0134	-0.0071	-0.0115	-0.0188		

T_G

Anorth	Alb	CO2	Calc	NaCl	Micr	S-min	Chlor	Na-Beid	Mix1	Mix2
Ca	TC	Si	Na	Al	Mg	K	RS	SO4	Cl	Mix
DEPTH	18.7650	56.8050	69.6350	71.6450	74.9100	77.4050	96.6350	97.4100		
Anorth	0.7781	0.7532	0.6784	0.6338	-0.1653	-0.0597	0.3852	-1.0242		
Alb	0.6726	0.5866	0.5419	0.4503	-0.3494	-0.1402	0.1730	-1.1028		
CO2	2.0582	2.3164	1.5125	2.1757	1.4645	1.3140	1.7275	-0.3306		
Calc	-0.0057	-0.0005	0.1120	0.0022	0.7047	0.7047	0.0085	1.5532		
NaCl	2.3202	6.3334	5.4639	9.8443	19.2818	12.7312	17.6944	27.3597		
Micr	0.0419	0.1079	0.0883	0.1635	0.3400	0.2011	0.2782	0.4716		
S-min	0.1724	0.3943	0.3683	0.5613	1.0495	0.7367	1.1621	2.2813		
Chlor	0.0084	0.0871	0.0679	0.1453	0.3211	0.1878	0.2677	0.4366		
Na-Beid	-0.9817	-1.0190	-0.9110	-0.9318	-0.1281	-0.1359	-0.7537	0.7846		
Mix1	0.9990	1.0061	1.0042	1.0119	1.0286	1.0159	1.0241	1.0395		
Mix2	0.0010	-0.0061	-0.0042	-0.0119	-0.0286	-0.0159	-0.0241	-0.0395		

APPENDIX G Method of Mass Balance Calculation

APPENDIX G: The Spreadsheet Approach to hydrogeochemical mass balance modelling

INTRODUCTION

An explanation of the concepts behind mass balance modelling of changes in groundwater chemistry, and the linear algebra required to solve mass balance problems is provided by Parkhurst et al (1982) and Plummer et al (1983).

Included in Parkhurst et al (1982) is a FORTRAN code (BALANCE) for solving groundwater (or any other), mass balance calculations. However, with the advent of PC's and spreadsheet programs it is now easier to make these calculations using the matrix multiplication and inversion features found in modern spreadsheet programs, in combination with their increasingly powerful macro features. This approach was selected for the mass balance modelling in this work. The spreadsheet approach to mass balance modelling has not been seen published in any articles by this author. Because of its simplicity, and flexibility, with the additional benefit that input and output are seen on the same screen, that graphing features of the spreadsheet program can immediately be used once a calculation is made, the flexible requirements for the input format (rather than the relatively rigid requirements for FORTRAN input format) and the ease with which data can be moved between differing spreadsheets, this approach is worthy of note.

REVIEW OF MASS BALANCE MODELLING

In brief, if the groundwater chemistry at two points along a flow path is known then by selection of phases (typically minerals gases or mixing end-members) which are likely to be precipitating or dissolving (in the aquifer of interest) the net transfer of these minerals into (dissolving) or out of the groundwater (precipitating) can be calculated, assuming the stoichiometry of the plausible phases is known, and the net change in the concentration of the elements composing the plausible phases is also known. For J plausible phases selected then J elements (each element must be contained in at least one of the plausible phases) must be selected. The element mass balance equation is given by Parkhurst et al (1982):

(Equation G-1)

$$\sum_{p=1}^{P} \alpha_p B_p, k = m_{T,k(final)} - m_{T,k(initial)} = \Delta m_{T,k}$$

For each element k = 1 to J

where the notation is as follows:

P - number of total reactant and product phases in the net reaction,

α_p - is the calculated mass transfer of the p^{th} phase,

$b_{p,k}$ - denotes the stoichiometric coefficient of the k^{th} element in the p^{th} phase,

$m_{T,k}$ - is the total molality of the kth element in solution, and

J - is the number of elements included in the calculation.

In problems with only element mass balance equations (no redox or mixing) P = J.

For problems where mixing of two end members is involved P = J - 1, two of the phases are replaced by the end members with the compositions of the end members reflected in the stoichiometries of the elements of interest, for each end member. An equation is included (with the loss of an element) of the form:

$$\alpha_1 + \alpha_2 = 1 \qquad \textbf{(Equation G.2)}$$

where α_1 and α_2 are respectively the mixing fractions of the two end-members which combine, along with mineral reactions, to give the composition of the final solution.

These two simple types of mass balance equations can be further embellished to allow for redox reactions and isotope calculations, as explained in Parkhurst et al (1982).

THE SPREADSHEET APPROACH TO MASS BALANCE MODELLING

A partial mass balance spreadsheet, designed for the particular problem at NSCRV is shown in Table G.1. Not shown on Table G.1 is the macro (which runs the calculations) or the inverted matrix of [A] ($[A]^{-1}$) which is multiplied with matrix

[B] to give matrix [C]. In all cases the example is for data from a depth of 97.41. Some other data, which will be discussed later, is also not seen but would typically be included on a mass balance spreadsheet.

Matrix [A] is the matrix expression of the linear equations provided by the summed part of Equation G.1 for the p phases and k elements of the mass balance model S_K. In matrix terminology it is the coefficient matrix. Matrix [B] shows the molar concentrations of the k elements of interest (expressed in mmoles) for the particular problem i.e the difference in concentration for a particular element between the initial and final solutions, with the value in the final row derived from the mixing equation, equation G.2.

From matrix algebra a solution for the p unknown phase (in this case the mmoles of the plausible phases added or lost from the groundwater) and the relative mixing fractions of the end-members, can be found by inverting [A] and multiplying it by [B] to provide C:

$$[A]^{-1}[B] = [C] \qquad \textbf{(Equation G.3)}$$

Proof of equation G.3 can be found in most linear algebra textbooks. As matrix inversion and multiplication are both features of spreadsheets it is a simple problem to calculate [C]. Table G.2 shows the macro which powers this mass balance spreadsheet (in Lotus macro language); however, once the method is understood the compiling of a macro to meet particular data requirements is relatively simple. Spreadsheet range names, and locations of blank rows and columns, must conform to the macro shown, and thus it may not be possible to simply copy the macro. This particular macro inverts [A] (with $[A]^{-1}$ not shown) and successively replaces the first six rows of [B] (by importing the groundwater data from a matrix not shown in Table G.1) and multiplies $[A]^{-1}$ by [B] and generating [C] at the appropriate position on the spreadsheet.

For the purposes of deriving data for input into PHREEQE, the original input molarities of the elements (i.e the analyzed data) can be recalculated by equation G4·

$$[A][B] = [D] \qquad \textbf{(Equation G.4)}$$

The matrix [D] contains exactly the same values as the input molarities used to construct [B], with the addition of a row for the mixing equation. This step only really checks the veracity of the solution. The k element contributions from the rock mass can be calculated using equation G.5:

$$d_k - C.S_k = R_k$$ **(Equation G.5)**

Where;

d_k - is the total contribution of element k (from both the rock mass and the seawater component) to the groundwater,

C - is the calculated mixing fraction of seawater,

S_k - is the molar concentration of element k in seawater,

R_k - moles of element k contributed from the rock mass

REFERENCES

SEE MAIN REFERENCE LIST

TABLE G.1 Output of the mass balance spreadsheet

MINERALS & ELEMENTS

Anorth	Alb	CO2	Calc	NaCl	Micr	Na-Beid	Mix1	Mix2
Ca	TC	Si	Na	Al	Mg	K	Cl	Mix

ROWS 9

COLS 9

	Anorth	Alb	CO2	Calc	NaCl	Micr	Na-Beid	Mix1	Mix2	Sample Point
				MTX [A]				Mix1*	NORDSEA	97.41
Ca	1	0	0	1	0	0	0	0.0E+00	10.662	0.106
TC	0	0	1	1	0	0	0	1.8E-04	2.126	1.139
Si	2	3	0	0	0	3	3.67	0.0E+00	0.074	0.245
Na	0	1	0	0	1	0	0.333	0.0E+00	485.44	7.355
Al	2	1	0	0	0	1	2.33	0.0E+00	0.000	0.022
Mg	0	0	0	0	0	0	0	0.0E+00	55.086	0.009
K	0	0	0	0	0	1	0	0.0E+00	10.579	0.054
Cl	0	0	0	0	1	0	0	0.0E+00	565.76	5.026
Mix	0	0	0	0	0	0	0	1.0E+00	1.000	1.000

MTX [B]

DEPTH	18.77	56.81	69.64	71.65	74.91	77.41	96.64	97.41	
Anorth	0.9059	2.0696	1.7048	2.8299	4.6889	2.7799	4.4322	5.5772	
Alb	0.7829	1.7233	1.4281	2.3466	3.8421	2.3117	3.6674	4.5972	
CO2	2.1925	3.7002	2.5915	4.4843	6.5676	4.2992	5.9819	6.6090	
Calc	-0.142	-1.401	-0.980	-2.334	-4.460	-2.317	-4.298	-5.471	
NaCl	1.8863	1.8622	1.9777	2.3850	2.7938	3.0861	3.9483	4.9376	MTX [C]
Micr	0.0337	0.0243	0.0231	0.0241	0.0317	0.0208	0.0212	0.0523	
Na-Beid	-1.128	-2.526	-2.086	-3.446	-5.686	-3.387	-5.387	-6.773	
Mix1	0.9983	0.9982	0.9980	0.9987	0.9995	0.9989	0.9998	0.9998	
Mix2	0.0017	0.0018	0.0020	0.0013	0.0005	0.0011	0.0002	0.0002	= C

TOTAL (mmoles of elements)

	18.77	56.81	69.64	71.65	74.91	77.41	96.64	97.41	
Ca	0.7825	0.6876	0.7461	0.5088	0.2344	0.4750	0.1366	0.1081	
TC	2.0547	2.3031	1.6159	2.1527	2.1086	1.9850	1.6849	1.1388	
Si	0.1222	0.1111	0.1076	0.1243	0.1323	0.1269	0.1592	0.2445	
Na	3.1274	3.6146	3.6799	4.1931	5.0022	4.8064	5.9069	7.3554	
Al	0.0003	0.0009	0.0003	0.0008	0.0037	0.0005	0.0009	0.0219	MTX [D]
Mg	0.0946	0.0988	0.1099	0.0691	0.0295	0.0609	0.0097	0.0086	
K	0.0519	0.0432	0.0442	0.0373	0.0373	0.0325	0.0230	0.0540	
Cl	2.8581	2.8765	3.1067	3.0949	3.0964	3.7114	4.0475	5.0263	
Mix	n/a	n/a	n/a	n/a	n/a	n/a	n/a	n/a	

ELEMENT CONTRIBUTION FROM ROCK MATRIX (mmoles)

	18.77	56.81	69.64	71.65	74.91	77.41	96.64	97.41
Ca	0.7642	0.6685	0.7248	0.4954	0.2287	0.4632	0.1347	0.1065
TC	2.0510	2.2993	1.6117	2.1500	2.1075	1.9826	1.6845	1.1385
Si	0.1221	0.1110	0.1074	0.1242	0.1322	0.1268	0.1592	0.2445
Na	2.2936	2.7443	2.7112	3.5840	4.7425	4.2699	5.8218	7.2792
Al	0.0003	0.0009	0.0003	0.0008	0.0037	0.0005	0.0009	0.0219
Mg	-4E-18	-4E-18	5E-18	3E-18	-2E-18	1E-18	1E-20	2E-19
K	0.0337	0.0243	0.0231	0.0241	0.0317	0.0208	0.0212	0.0523
Cl	1.8863	1.8622	1.9777	2.3850	2.7938	3.0861	3.9483	4.9376
Mix 2	0.0017	0.0018	0.0020	0.0013	0.0005	0.0011	0.0002	0.0002

TABLE G.2 Spreadsheet Macros

```
ALT_M:  {GOTO}mtx~
        /re.{END}{D}{END}{R}~
        {GOTO}out~
        /re.{END}{R}{END}{D}~
        {GOTO}phr~
        /re.{END}{D}{END}{R}~
        {GOTO}inp~
        /rncput~{END}{R}{L}{END}{D}~
        /dmiput~mtx~
        {GOTO}dep~
        {GOTO}mtx~
        /rncmtot~.{END}{D}{END}{R}~
        {GOTO}dep~
        {GOTO}inn~
        /rncaug~{ESC}{ESC}aug~{ESC}{D}.{END}{D}~
        {GOTO}dep~
        {\C}
        /dmmmtot~aug~out~
        {R}
        {\C}
        /dmm~~{R}~
        {R}
        {\C}
        /dmm~~{R}~
        {R}
        {\C}
        /dmm~~{R}~
        {R}
        {\C}
        /dmm~~{R}~
        {R}
        {\C}
        /dmm~~{R}~
        {R}
        {\C}
        /dmm~~{R}~
        {R}
        {\C}
        /dmm~~{R}~
        /rndaug~
        /rndmtot~
        {GOTO}PHR~
        /CELS~{L}~
        {GOTO}OUT~
        {U}
        /RNCPDEP~.{END}{R}~
        {GOTO}PHR~
        /CPDEP~{U}~
        /RNDPDEP~
        {GOTO}OUT~
        /RNCOUT1~.{END}{D}~
        {GOTO}PHR~
        /DMMPUT~OUT1~PHR~
        /DMM~{ESC}{R}.{END}{D}~{R}~
        {R}
        /DMM~{ESC}{R}.{END}{D}~{R}~
        {R}
        /DMM~{ESC}{R}.{END}{D}~{R}~
        {R}
        /DMM~{ESC}{R}.{END}{D}~{R}~
        {R}
        /DMM~{ESC}{R}.{END}{D}~{R}~
        {R}
        /DMM~{ESC}{R}.{END}{D}~{R}~
        {R}
        /DMM~{ESC}{R}.{END}{D}~{R}~
        /RNDPUT~
        /RNDOUT1~
        {\F}

ALT_F:  /REHEAD~
        {GOTO}HEAD3~
        /C.{END}{R}{L}~HEAD1~
        /RT.{END}{R}{L}~HEAD5~
        {GOTO}HEAD4~
        /RT.{END}{D}~HEAD2~
        /C.{END}{D}~HEAD6~

ALT_C:  /C.{END}{D}~INN~
```